Ev-K^2-CNR
ITALIAN EXPEDITION TO THE KARAKORUM 1988
Prof. A. DESIO Leader

GEODESY, GEOPHYSICS AND GEOLOGY OF THE UPPER SHAKSGAM VALLEY (NORTH-EAST KARAKORUM) AND SOUTH SINKIANG

Ev-K^2-CNR

ITALIAN EXPEDITION TO THE KARAKORUM 1988

Prof. ARDITO DESIO Leader

SCIENTIFIC REPORTS

GEODESY, GEOPHYSICS AND GEOLOGY OF THE UPPER SHAKSGAM VALLEY (NORTH-EAST KARAKORUM) AND SOUTH SINKIANG

by

ARDITO DESIO

ALESSANDRO CAPORALI
GUIDO GOSSO
UGO POGNANTE
MAURIZIO GAETANI
FRANCESCO PALMIERI
LUIGI RAMPINI

Consiglio Nazionale delle Ricerche - MILANO (ITALY) - Via Ampère, 56 -
1991

To the memory of Sven Hedin
the great explorer of Central Asia

FINMECCANICA
MILANO

FOREWORD (1)

The volume which it is my pleasure to present here, contains the scientific reports on the 1988 Ev-K^2-CNR (2) expedition, drawn by the heads of the teams, i.e.: Prof. Alessandro Caporali of the Department of Physics of the University of Bari for the geophysical, geodetical, topographycal fields, and Prof. Maurizio Gaetani, of the Department of Earth Sciences of the University of Milano with regard to the geological field. These reports are introduced by a brief note added by me, essentially of a historical nature.

The two main chapters have also benefited from the cooperation of Prof. Francesco Marzari of the Department of Physics of the University of Padova, and Dr. Francesco Palmieri, with regard to the geodetic and geophysical part; and of Arch. Luigi Rampini of the Region of Lombardia for the topographical part. Prof. Guido Gosso of the Department of Earth Sciences of the University of Milano, and Prof. Ugo Pognante of the Department of Earth Sciences of the University of Torino have contributed for the geological part.

The purpose of this volume is chiefly to make the public of scholars interested in the Himalayan region acquainted with what the Ev-K^2-CNR expedition of 1988 has been able to do in the scientific field. And it has been written in english to make it easier to divulge in international circles.

The territory dealt is one of the lesser known ones in Central Asia from a scientific viewpoint. I am therefore confident that the investigations carried out by the expedition will prove to be an important contribution to its knowledge with regard to the sciences of the earth. I should also like to point out that the territory had been

---

(1) Ardito DESIO, *Università di Milano, Dipartimento di Scienze della Terra, Via Mangiagalli, 34, 20133 Milano; Comitato Ev-K^2-CNR, Via Ampère 56, 20131 Milano.*

(2) These initials are formed by the first syllable of the word Everest (Ev), the place-name of the second highest mountain in the world, (K^2) and by the initials of the Consiglio Nazionale delle Richerche (CNR = National Research Council).

studied in past times by Italian scholars as well, with regard both to the geodetical-geophysical aspects and to the geological one, as can be easily inferred from the reports that follow.

I must add that these reports are just a stage in the scientific research programme for the areas considered. As a matter of fact, in the years that followed, other Ev-K^2-CNR expeditions have operated in Central Asia and are still working according to the programmes of the Committee which heads the scientific activities of the Ev-K^2-CNR Project.

It operates under the patronage of the Italian Ministry of Foreign Affairs as well as the Ministry of University and Scientific and Technical Research. It is also backed by the European Economic Commission of Bruxelles, which is largely responsable for financing the expedition, jointly with the Italian National Council of Research.

Ardito Desio

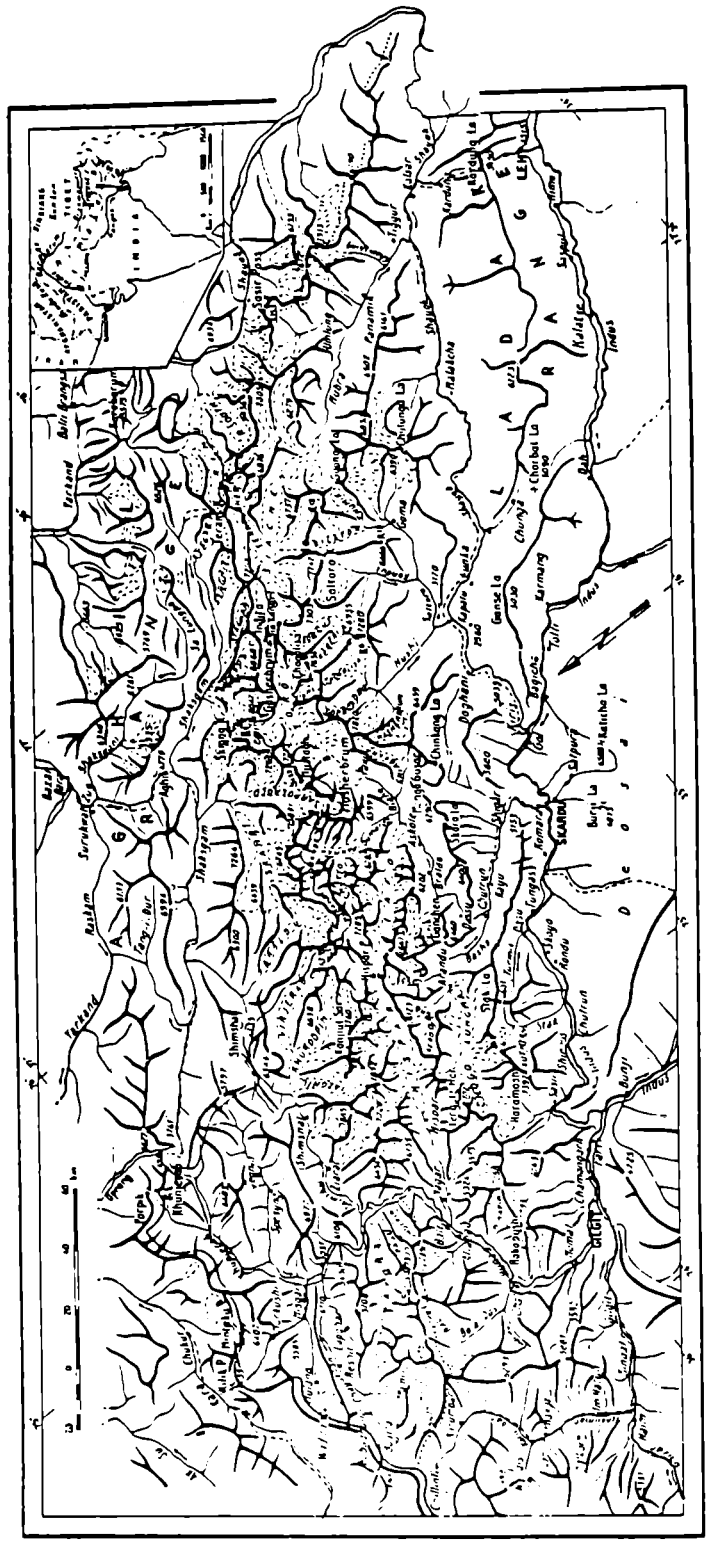

Fig. 1. Orographic sketch-map of the Karakorum.

studied in past times by Italian scholars as well, with regard both to the geodetical-geophysical aspects and to the geological one, as can be easily inferred from the reports that follow.

I must add that these reports are just a stage in the scientific research programme for the areas considered. As a matter of fact, in the years that followed, other Ev-K^2-CNR expeditions have operated in Central Asia and are still working according to the programmes of the Committee which heads the scientific activities of the Ev-K^2-CNR Project.

It operates under the patronage of the Italian Ministry of Foreign Affairs as well as the Ministry of University and Scientific and Technical Research. It is also backed by the European Economic Commission of Bruxelles, which is largely responsable for financing the expedition, jointly with the Italian National Council of Research.

Ardito Desio

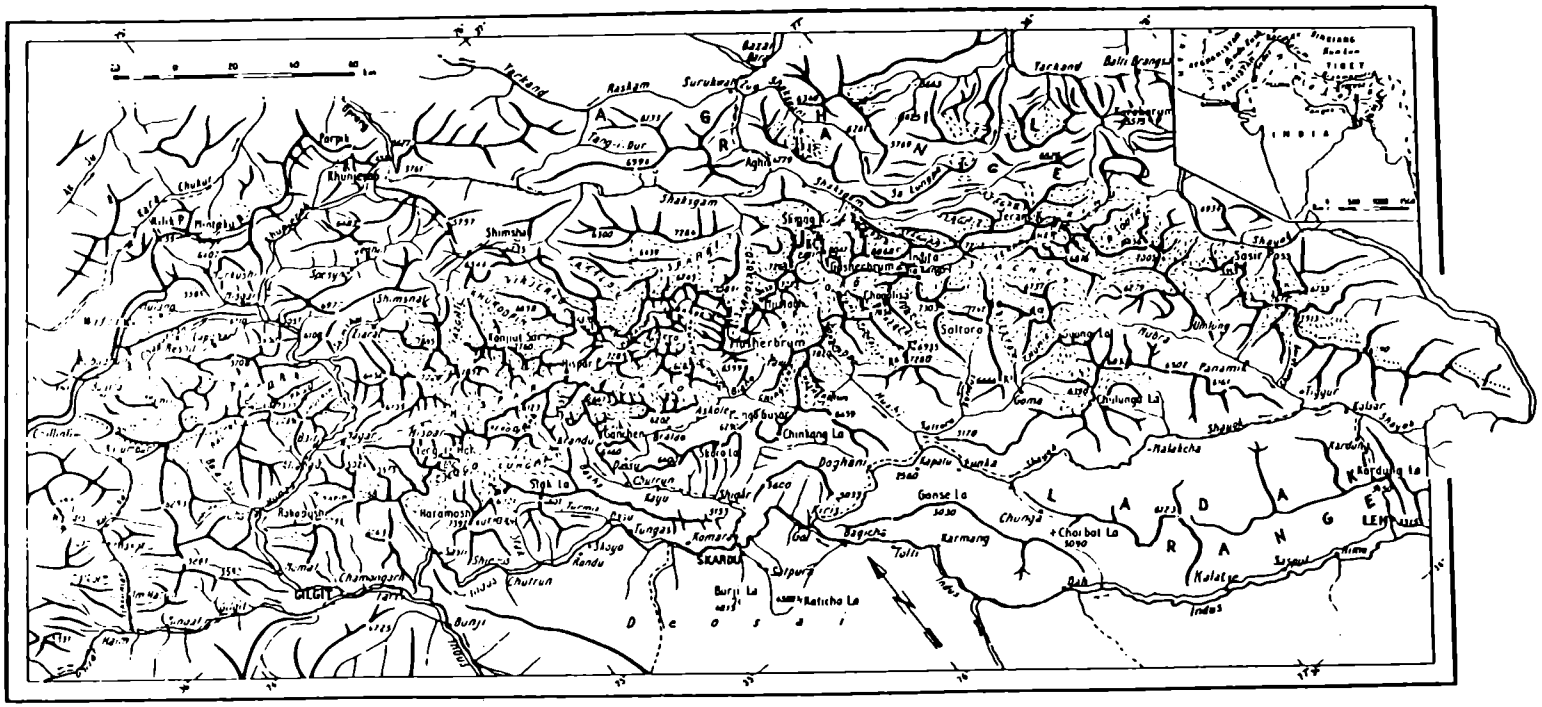

Fig. 1. Orographic sketch-map of the Karakorum.

CONTENTS

I. INTRODUCTION (1)

1. The 1987 Expedition to the Everest and K^2 Areas

On March 7th 1987 the "New York Times", and then on the 8th the radio, the television and the major Italian newspapers announced that K^2 was the highest mountain in the world, 8,859 m, 11m higher than Mt. Everest.

This sensational announcement was originated by the measurements carried out by prof. George Wallerstein, an astronomer of the University of Washington, who determined them with the most modern equipment which uses signals broadcast from the Navy Navigation Satellite System (NNSS) of U.S.A.

On April 11th, during a meeting with Prof. Luigi Rossi Bernardi, the chairman of the Italian National Research Council (CNR), I proposed to him the financing of an expedition aimed to remeasure, in situ and with recent and more precise satellite receivers, the height of K^2 and Everest, proposal that was immediately accepted.

I concerned myself at once with organizing the new expedition.

After one week I began constructive co-operation with Agostino Da Polenza, the first Italian alpinist who climbed the K^2 along the northen slope with the "Santon Expedition" in 1983, and we started the preparation of the new expedition. There wasn't too much time since the survey had to be carried out during the summer, the researchers couldn't operate for long periods and the budget was limited.

It must be remembered that the accepted heights of K^2 8,611 m and Mt. Everest, 8,848 m, were obtained with the traditional instruments and measurements system by the researchers of the Survey of India in the middle of the last century, when more precise measurements couldn't have been carried out.

On April 27th I handed to the CNR chairman a note with the draft programme of the expedition and after a while the funds were at my disposal.

---

(1) Ardito DESIO. *Università di Milano. Dipartimento di Scienze della Terra.*

As far as the measurements are concerned, it was necessary to use equipment of a more recent generation than those used by Wallerstein.

To trace it was not an easy task, nevertheless by the beginning of June I was able to find a private group from Padua, the only one in Italy which, at that time, had two operating GPS (Global Positioning System) receivers, and which also had at its disposal trained personnel.

While the Company's technicians, directed by Prof. Alessandro Caporali of the University of Padua, went to the Dolomites for training with the equipment, Agostino Da Polenza got in touch with the Pakistan authorities in order to use two military helicopters, on duty on the border, to reach in a short time the camp base of K^2 on Baltoro glacier at 4,300 m of altitude.

It is to be remembered that the temporary border between Pakistan and India, which is still debated and protected by troops lies on a mountain crest. In these overtures we were helped by General Omar Alì Mirza, Chairman of the Pakistan Alpine Club, who joined the expedition.

As far as the Everest measurement is concerned, the alpinist Renato Moro informed me that it was possible to reach the base camp at 5,300 m of altitude by motor-vehicle from the Tibetan slope near the Rongbuk Monastery, and offered to guide the expedition.

I decided then to give priority to the Everest measurements.

The expedition was totally made up by volunteers: Prof. Alessandro Caporali geodesist; Ing. Lionello Lavarini, Ing. Claudio Pigato Caporali's assistants; Dr. Attilio Bernini Doctor; Dr. Mino Damato journalist; Agostino Da Polenza alpine guide and head of logistics; Kurt Diemberger film-maker; Renato Moro alpinist and head of logistics for Mt. Everest with Da Polenza; Soro Dorotei alpine guide, Da Polenza assistant for the K^2. For my part, I intended to intervene only if my presence was necessary, and this occured during the operations in Pakistan.

On July 28th the expedition departed from Milan and the next day it arrived at Kathmandu, the capital of Nepal. From there it proceeded partly by motorvehicles and partly on foot to Tibet, crossing the border at Kodari, from where it went to Nyalam and Tingri. At this point the expedition left the main road to climb up the Rong Chu valley, and set up camp near the Rongbuck Monastery at 5,100 m of altitude.

Notwithstanding the bad weather, during the days after the arrival at the base camp, the sky cleared, making it possible for the researchers to proceed immediately with the Mt. Everest measurements.

After the departure of the expedition from Kathmandu, I didn't receive any

news until August 10th, when they informed me that the measurement of Mt. Everest height had been carried qut and that the members of the expedition were ready to leave for Pakistan.

So, on August 15th, the expedition landed in Islamabad, capital of Pakistan, and proceeded by motor-vehicle to the oasis of Skardu. Because of bad weather they had some problems to take off with the military helicopters towards Concordia base camp, on the Baltoro glacier; finally, one of them was able to carry the researchers only near Urdukas, from where they proceeded by foot to Concordia. Here, thanks to the perfect weather, Caporali's team was able to measure the height of K^2 and of Falchan Kangri (Broad Pk.) and Gasherbrum IV in just four days. Then, the expeditions members returned to Skardu, and from there, on August 29th, moved on to Islamabad, where I had been for a few days.

On that same day the President of Pakistan, Zia Ul Haq, who was in Karachi for a few days, went back to Rawalpindi and received the expedition members at his mansion. During the night the whole expedition left Pakistan and in the late afternoon of August 30th landed in Milan. The journey was concluded in about a month with the complete achievement of the expedition's objective.

The expedition operational phase was now over, and it was time to process the collected data and carry out all the necessary checks in order to obtain the greatest accuracy from the results of the measurements.

As I said at the beginning, the official heights of K^2 and Everest were respectively 8,611 m and 8,848 m. Since then, other surveys have been carried out, but they didn't justify substancial rectifications in the above mentioned values. The innovation of the measurements carried out by our expedition consists in the fact that for the first time the height of the two mountains, situated 1,200 km apart, was determined almost simultaneously with the same measuring instruments which – as I said – were the best available in 1987.

The two mountain heights, other than the Falchan Kangri (Broad Peak) and Gasherbrum IV visible from Concordia, were measured respectively to the same reference surface defined indipendently from sea level and known as WGS84 (World Geodetic System 84), and a global model of the geoid was used to convert ellipsoidal heights into orthometric heights so the three mountain heights are directly and strictly comparable.

The instruments used were an electronic distance-meter, a theodolite and two satellite receivers GPS.

Measurements were carried out in two phases: first the base camp was determined in relation to the reference surface by satellite observation, then the height of

the mountain top was determined through collimation from different points.

As far as the K^2 is concerned, the top height resulted to be 8,616 m, give or take 7 m. So the height was only 5 m higher than the one obtained by Col. Montgomerie more than a century ago.

Here are the heights we obtained and, next to them, the official ones:

- Falchan Kangri (Broad Peak) 8,060 m (8,051 m)
- Gasherbrum IV 7,929 m (7,925 m)

Also Falchan Kangri proved to be 9 m higher, whereas for Gasherbrum IV the difference is 4 m only.

We will see later the meaning which can be attributed to these differences.

As far as Mt. Everest is concerned, the height resultant from our measurements was 8,872 m, give or take 20 m; 24 m higher than the height formerly considered the most valid one. All the heights we obtained were higher than the traditional ones with differences ranging from 24 m for the Everest, to 9 m for the Falchan Kangri, 5 m for the K^2 and 4 m for the Gasherbrum IV.

How to explain such differences?

There are two reasonable hypothesis. Either the mountains raised during the last century, or the measurement taken were not exact, and they will be checked in any case. That the Karakorum (and not only K^2) is in a phase of low raising is well known, and I have affirmed this several times myself.

The same can be said for Mt. Everest. If we admitted that there were no errors in measurements, the K^2 area would have raised 6 cm per year and the Everest area 18 cm. But also the extent of the hypotetical raising of the two areas we measured seems to be eccessive, since normally one talks of a few millimeters per year.

Do we have to ascribe the differences to some deficiency in the present and old measurements? The most logical conclusion seems to be that of assigning the differences in part to one factor, in part to the other. But can we really exclude that the raising was a lot more intense than it was estimated until now?

Well, it is possible to find a negative evidence in the vicinity. Some years ago, during an excursion through Southern Tibet with some Chinese colleagues, a little below the Yagru Shonh pass (5,122 m), at 4,950 m, they showed me, in the recent cuts in the road, some bone fragments embedded in a sandy layer of lacustrine origin. They were fossile bones of *Hipparion*, a horse progenitor, some remains of which are known also on the southern Himalayan slope only a thousand meters above sea level.

What does that mean?

It means that in the last 2 million years that area has risen by 4,000 m, that is 2

mm per year. This figure seems to me very significant and we can take it as a comparison for the interpretation of the results of our measurements of the Everest.

2. The 1988 Expedition to the Southern Sinkiang and the Shaksgam Valley

2.1. ORGANIZATION OF THE EXPEDITION

The Ev-K^2-CNR 1987 expedition is in the first place to be credited with answering a query as to the real height of the world's two highest mountains. However a more thorough analysis of the results of the expedition also shows that for the first time the operative feasibility of a systematic series of geodetic measumerents via satellite, thus meeting the requirement for data and scientific surveys which conventional technologies were unable to provide.

The magnificence of the geophysical and geological events which have taken place in the Himalaya, Karakorum and Hindu Kush mountains chains, as well as their high impact on the current structure and evolution of the Indo-Chinese territory, have already been outlined also thanks to the ample contribution of Italian scholars for over more than a century's activity in these regions.

The 1988 expedition represents the continuation of earlier research in the sense that the geodetical exploration of 1987 was supposed to be followed up and developed according to the most advanced technologies by large-scale geodetical and geophysical investigation. Some hitherto unsolved problems on the structure and geological composition of some key areas for the interpretation of research from which current configuration of these territories has originated, still remain to be cleared up.

Before proceeding to the plans of the expedition, it must be remembered that four scientists had been called upon to give advice to the expedition in the preparation of the geodetical-geophysical programme, namely: Prof. Gen. Giuseppe Birardi of the Institute of Topography of the "La Sapienza" University of Rome; Prof. Michele Caputo of the Institute of Physics of the same University, Gen. Dr. Rolando Chiggio, Vice Commander of the Military Geographical Institute of Florence, Prof. Dr. Fernando Sansò of the Institute of Topography of the Milan Engineering School.

During a number of joint meetings the general research guidelines of the expedition within the above context were discussed and defined. With regard to the geological area, my own extended and direct familiarity with the chief area to be visited made any action by other scholars superfluous.

At the beginning the programme, presented on January 23rd to the CNR, called

for the execution of researches starting from the Everest area and proceeding then to that of K^2. After establishing contact with the operative representatives of Pakistan and China, I encountered difficulties in programming the two operations in a continuous way, and therefore it became necessary to conduct them in two different times, starting with the Karakorum, where the route had been opened by our two logistic operators, Agostino Da Polenza and Renato Moro, and postponing researches in the Everest area to the year after.

The expedition was made up, with regard to the topographical geodetic-geophysical area, of Prof. Alessandro Caporali (team leader), Mr. Daniele Benasciutti and Dr. Francesco Marzari of the Padua University, Dr. Francesco Palmieri of the University of Trieste and Arch. Luigi Rampini, land surveyor, of the Region of Lombardy as topographical assistant.

The geological team was formed by Prof. Maurizio Gaetani of the Milan University (team leader), who had already conducted research on the southern slopes of Karakorum and in Zanskar area, by Prof. Guido Gosso of the University of Palermo and Dr. Ugo Pognante of the University of Turin.

The logistic group was represented by the alpine guide Gianni Calcagno, assisted by Marino Giacometti and Kurt Diemberger, the latter acting as cinema operator. They were joined by Dr. Giovanna Gaffuri, mountaineer and physician of the expedition, and Massimo Zamorani, reporter.

2.2. ITINERARIES

The expedition left Italy by plane on the last day of August with all its members and after landing in Islamabad, proceeded northwards by motor vehicle (Fig.1.1). After crossing the Kunjerab pass (4,950 m a.s.l.) on 6th September, it reached Kashgar in Sinkiang, whence it proceeded, after a brief stopover, again by motor vehicles, but not without logistic difficulties, for Bazar Dara in the Yarkand valley, where it arrived on the 10th. The next day, left the motor-vehicles, they continued to Ilik and further on camel back. After crossing the Aghil pass (4,779 m), it finally entered the Shaksgam valley at Durbin Jangal on the 14th. While the logistic caravan was waiting in Durbin Jangal oasis, the team of scientists and mountaineers climbed upwards to the foot of the Gasherbrum glacier's lateral moraine where it set up the base camp.

The weather was often bad, with frequent snow falls and road hold-ups due to landslips and, in the Shaksgam valley, also flooded rivers had to be forded.

At this point both the geodetical-geophysical and the geological team split up

and conducted measurements and surveys separately in the sorrounding areas, especially in the Urdok valley. The same had been done by some of the mountaineers, who carried out a set of explorations.

The expedition left the base camp of the Gasherbrum moraine on 27th September for Durbin Jangal once more, and proceeded thence along the valley bottom as far as the Tek-ri hillock, where the Shaksgam is joined by the Sarpo Laggo river, which was reached on the last day of September.

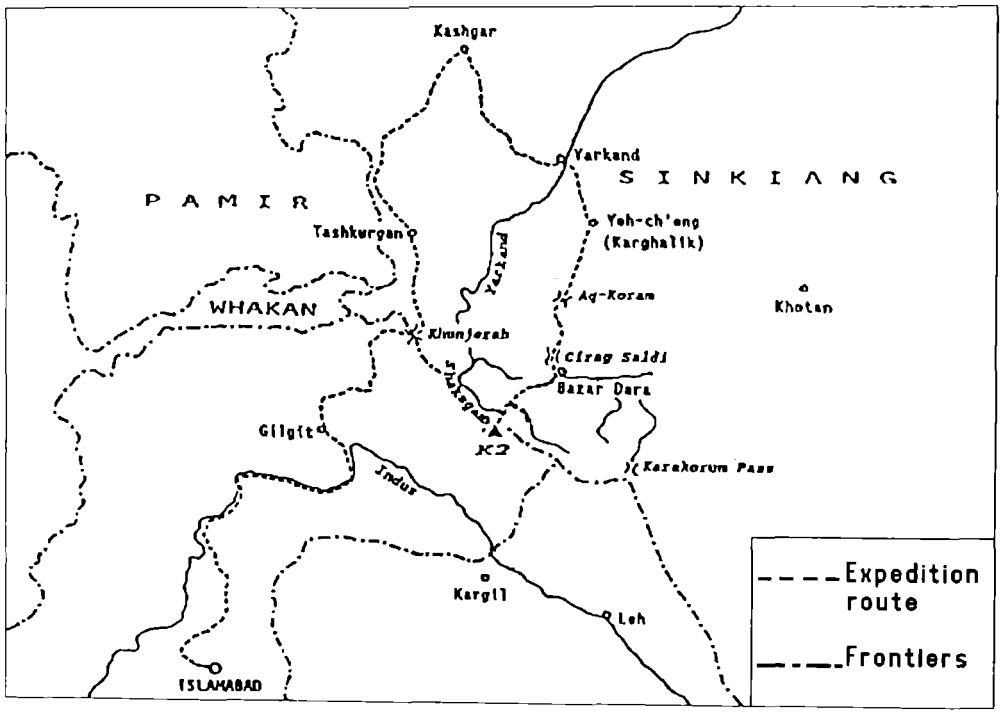

Fig. 1.1. The route followed by the 1988 expedition to the Shaksgam Valley.

In the following days the two teams of researchers proceeded along the Sarpo Laggo valley as far as the Sughet Jangal oasis, where they scouted the neighbourhood. On October 4th all the members of the expedition met at Sughet Jangal and the next day made their way back on camel to Durbin Jangal. On October 8th the

entire expedition climbed up the Aghil pass which was covered by one metre of snow, in very cold weather. The march proceeded along the route followed earlier and Bazar Dara was reached on the 9 th. The expedition drove on to Kashgar and after crossing the Kunjerab pass it finally reached Islamabad on the 17th, and then Rome, on the 19th.

Concluding, I may safely say that, despite logistic difficulties and the adverse weather conditions, the expedition's schedule has been followed to a large extent. Owing to weather conditions, however, it was not possibile to measure the height of K^2 and the other 8,000 m peaks.

2.3. EARLIER AVAILABLE DATA

The Shaksgam valley was all but geographically unknown until 1887. In that year the British diplomat Francis Younghusband, who was travelling with a caravan from Peking, entered it via the Aghil pass and left it via the Eastern Muztagh pass. Before that, this route had been followed in both directions only by native mountaineers from China and India, who plied their wares as itinerant salesmen.

I do not know whether any other expeditions with scientific purposes had travelled Younghusband's route in Sinkiang, between the Kun Lun mountain chain and that of Aghil, before 1926. In that year the northern slopes of the Aghil were explored by Kenneth Mason's expedition. He had attempted unsuccessfully to cross the Kyagar glacier for reaching the upper Shaksgam valley. Therefore the stretch of valley between this glacier and the Urdok glacier (explored by Younghusband in 1889) had remained unexplored until 1929. In that year a small patrol of the Duke of Spoleto's expedition consisting of Umberto Balestreri, myself and eight porters, managed to enter that part of the valley and explored it from a geographical and a geological points of view. Both geological and topographical surveys of the expedition, at a scale of 1:50,000 (published at 1:75,000), were carried out. A report of the exploration was published in a volume in Italian language, written by myself with an introduction by the Duke of Spoleto.

The volume is chiefly of geographical nature, and the sections devoted to geology are therefore very brief. Until 1980, geological data on the Upper Shaksgam valley were very few, and I therefore felt it advisable in that year to illustrate the geology of the valley on the basis of data collected half a century earlier, and hitherto unpublished, in a volume of this series under the title "Geology of the Upper Shaksgam Valley, North-East Karakorum, Xinjan (Sinkiang)". A geological map at the scale 1:200,000 of the entire region is annexed to it.

Since also earlier studies of both geographical and geological nature are illustrated in that volume, it is pointless for me linger on this and I refer the reader to the said volume. More detailed informations on the previous researches concerning the geology of the Upper Shaksgam valley and the surrouding area, are reported in the chapter IV of this volume.

II. GEODETIC AND GEOPHYSICAL REPORT (1)

1. Deflection of the Vertical in the Upper Shaksgam Valley (Northern Karakorum) by Astronomic and GPS Observations

1.1. INTRODUCTION

Astrogeodetic observations in Northern Karakorum have been done in a limited quantity, when compared with the relative abundance of stations established by the Survey of India in the northern part of the Indian subcontinent and along the Great Himalayan Range (Gulatee, 1955). Besides the work of the Survey of India, the von Schlagintweit Expedition (1854-1858) with its extensive program of astronomic positioning and measurement of magnetic declination should be mentioned for the past century. The Italian work was initiated by Prof. G. Abetti and Comm. A. Alessio with the De Filippi Expedition (1913-14) in Karakorum and Chinese Turkestan and was continued by Comm. M. Cugia with the expedition of the Duke of Spoleto in 1929. During the same expedition Prof. A. Desio (Desio, 1930, 1980) explored and surveyed the region of the Shaksgam valley, the same where, some 60 years later and under his leadership, we continued the astrogeodetic work.

This region was visited for the first time by F. E. Younghusband, on the second of his Central Asian journey in 1889 and was, in part, mapped by M. Spender with E. Shipton's Expedition in 1937. A fine description of the region is given by R. C. F. Schomberg (1947). During the Desio's 1954-55 Expeditions in Karakorum and Pamir (Desio, 1977), Prof. A. Marussi and Capt. F. Lombardi established five astronomic stations between Gilgit and Skardu (Pakistan), which were connected to trigonometric points of the Survey of India. Fig. 2. 1 provides a sketch, on the basis

---

(1) Alessandro CAPORALI, *Dipartimento di Fisica, Università di Bari, with the collaboration of* Francesco MARZARI, *Dipartimento di Fisica, Università di Padova*, Francesco PALMIERI, *Istituto di Miniere e Geofisica Applicata, Università di Trieste.*

of data reported by Marussi (1964), of points at which the deflection of the vertical was measured by the Survey of India, the De Filippi and Desio expeditions in the Karakorum area.

The points have been mapped on a geoidal profile constructed with Rapp's gravity field model, complete to degree and order 180, to highlight the approximate behavior of the equipotential surfaces in this region. All stations lie south of the 36° parallel and, for most stations, only the north-south component of the deflection of the vertical has been determined. These stations are indicated in Fig. 2. 1 with a dot (no label). For the labelled stations both components are known. To fill, at least in

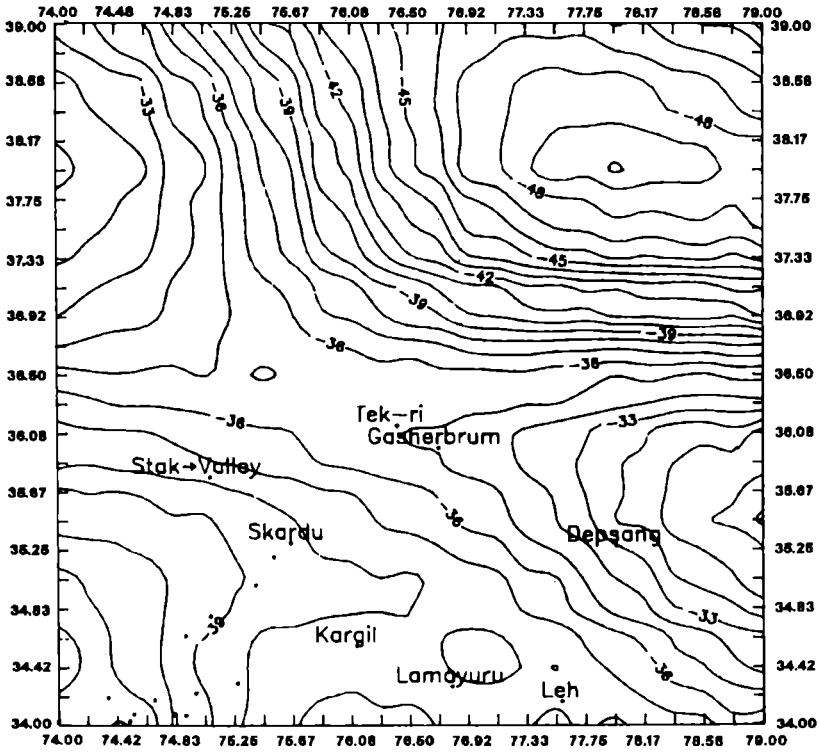

Fig. 2.1. Geoidal profile in northern Karakorum computed with the Rapp model complete to degree and order 180. Contours in meters. Equidistance 1 m. Reference ellipsoid: GRS80 (a=6378137 m; 1/f=298.2572). Labeled sites are stations of known deflection of the vertical both in the meridian and prime vertical plane. At the unlabeled points only the meridian component is known.

part, the gaps existing north of Karakorum it is necessary to establish new astronomic stations at sites of known geodetic coordinates. These, contrary to previous work which had to refer to verteces of local networks, can be readily obtained by means of GPS or Doppler receivers (Birardi, 1977; Ebblin et al., 1983). Several trigonometric verteces of the Survey of India along the Karakorum Highway have recently been re-surveyed as part of the "International Karakorum Project" (Bilham and Simpson, 1980; Crompton, 1980; Chen Jianming et al. 1980). However these trigonometric points are of little relevance for us, as they are confined to the very limited region of Maj. K. Mason's Indo-Russian connection and are located at sites of very difficult access. We originally hoped to establish a number of astronomic GPS stations from Islamabad to Kashgar and down to the Shaksgam valley region. Due to time and logistic constrains we soon realized that it would have been impossibile to systematically establish observing stations along the route, and that we should have confined ourselves to the Kun Lun range and Shaksgam valley. Initially three sites were scheduled: Aghil pass, Gasherbrum glacier and Tek-ri hillock. However base camps were established only at the two latter sites and the planned station at Aghil pass, being just a point of transit, had to be dropped.

1.2. INSTRUMENTATION

The classical method of determination of astronomic latitudes is based on the measurement of the elevation angle at which one, or – preferably – suitable pairs of fundamental stars transit through the meridian of the observer. Longitude cannot be estimated unless a timing device synchronized with the Universal Time Scale UTC is used to precisely time-tag the angle observations. Astronomic positioning by means of a precise theodolite is somewhat cumbersome, as a detailed star program must be prepared in advance, and because the field work is all but automated. Zenith cameras are more commonly used and exist in portable versions (Birardi, 1976). However none was available to us at the time we needed it. In addition, we felt unconfortable with the idea of handling and transporting delicate photographic plates and of not doing a "quick look" data reduction on the field, to check at least the consistency of the data. For these reasons, having really no alternative, we decided to use a precise theodolite. We chose Kern E2 which, besides being light and robust, has the distinctive feature of offering digital readouts of both circles to 0.1 mgon corrected with built-in software for occasional small misalignements relative to the local vertical. A quartz chronometer Casio with 0.01 sec resolution was used for timing. It was synchronized before each observing session using time signals

continuously broadcasted by RWM (Moskow) at 9996 and 14996 kHz and received with a ICOM RE 71 receiver coupled with a 30 feet broadband antenna. Tests on the chronometer indicated a drift smaller than 0.03 sec/hour, making unnecessary the reset during the observing session.

The GPS receivers were two Wild Magnavox WM 101 working with coded C/A signals modulated on the L1 carrier (1575 MHz). Although they do not receive the P code nor the L2 frequency, they have a horizontal precision better than 0".5 which was sufficient for our work. Most importantly, as demonstrated in previous work (Desio, 1988), they are easy to use and have proven robustness and operating capability, even in the hardest environmental conditions, which in fact were experienced during our expedition.

1.3. Determination of Astronomic Coordinates

The basic method adopted for determining the astronomic coordinates consists in timing the instant at which a fundamental star crosses the almucantar with a nominal radius of 30° from zenith. The method is discussed in detail, for example, by Tomelleri (1960), Pericoli (1973) & De Concini and De Florentiis (1983).

Epochs and azimuths were pre-computed, on the basis of approximate site coordinates, for stars of the FK5 System which met the requirements of: a) being of visual magnitude ≤ 5, b) being distributed as uniformly as possible in azimuth and c) being such that the interval between two consecutive stars is not shorter than 4 min, so that 5 to 20 readouts of time and zenith angle could be made for each star. Table 2 .1 summarizes the results of the observing sessions at Gasherbrum glacier and Tek-ri, reporting star names, visual magnitude and coordinates in the true-of date-reference system, azimuth and mean zenith excess δz with r.m.s. (root mean square) about the mean.

At Gasherbrum glacier the station was positioned in the middle of the Shaksgam valley, at an elevated site dominating the Gasherbrum glacier, near a Chinese trigonometric vertex. The site was about 45 min. walk from the camp, so that a small tent had to be set up to permit us to spend the night there without having to reach the base camp in the darkness.

At Tek-ri the station was established at the western side of the camp and an identification brass marker "Ev-K^2-CNR 1988" was hammered in a nearby rock. On both sides we used the standard self-centering Kern tripods well secured to the ground by heavy stones on each leg.

Table 2.1a. Stars observed at the Gasherbrum Astronomic Station.

STAR	MAG	RIGHT ASCENS.	DECLINATION	AZIM.(GON)	18/09/88		19/09/88		26/09/88	
					δz (0.1 mgon)	σ	δz (0.1 mgon)	σ	δz (0.1 mgon)	σ
γ Her	3.8	16h 21m 25.2s	19° 10' 49"	270.859	-4	9	4	5		
ν Cyg	3.9	20 56 46.2	41 07 33	75.835	-102	12	-102	9		
β Her	2.8	16 29 43.9	21 30 54	277.397	-15	10	-15	7		
τ CrB	4.8	16 08 33.2	36 31 17	313.863	-111	12	-104	6	-117	11
σ Cyg	4.2	21 16 59.4	39 20 58	79.791			-99	9	-90	7
ζ Cyg	3.2	21 12 28.4	30 10 57	100.759	-42	12	-46	7	-43	5
α Oph	2.1	17 34 24.8	12 34 06	249.218	46	9	39	10	30	9
51 Her	5.0	16 51 17.2	24 40 35	285.724	-47	19	-37	9	-37	8
ζ Her	2.8	16 40 51.6	31 37 30	302.635	-80	12	-74	7	-69	6
42 Her	4.9	16 38 26.3	48 57 10	341.654	-166	8	-161	8	-182	9
π2 Cyg	4.1	21 46 23.8	49 15 35	57.648	-138	6	-150	6	-138	9
2 Peg	2.4	21 29 27.3	23 35 28	117.077	4	6	-11	12	0	7
14 Peg	3.8	21 49 21.9	30 07 25	100.899	-27	8	-60	16	-53	9
μ Cep	4.3	21 43 11.1	58 43 50	34.487	-183	8	-198	6	-183	9
α Cep	2.4	21 18 20.1	62 32 25	22.666	-200	6	-209	4	-206	8
ι Peg	3.8	22 06 30.4	25 17 31	112.711	-5	6	-39	8	-33	9
ν Cep	4.3	21 45 08.8	61 04 15	27.615	-185	9	-197	6	-194	7
α Lac	3.8	22 30 50.9	50 43 36	55.439	-146	7	-159	8	-156	7
β Aql	3.7	19 54 46.4	06 22 44	213.194	78	6	87	6	83	6
η Peg	2.9	22 42 29.6	30 09 51	100.802	-39	11	-49	5	-51	6
ο And	3.6	23 01 25.4	42 16 03	73.296	-98	8	-111	10	-123	5

Table 2.1a (continued).

STAR	MAG	RIGHT ASCENS	DECLINATION	AZIM.(GON)	18/09/88		19/09/88		26/09/88	
					δz (0.1 mgon)	σ	δz (0.1 mgon)	σ	δz (0.1 mgon)	σ
ζ Aql	3.0	19 04 54.1	13 50 50	253.933	15	9	32	9	32	10
ε Peg	2.4	21 43 39.2	09 49 29	162.522	65	11	54	4	49	9
a Aql	0.8	19 50 14.8	08 50 20	232.360	62	7	53	3	57	4
o Dra	4.7	18 51 02.6	59 22 39	367.326	-221	5	-209	8	-191	8
γ Aql	2.7	19 45 44.3	10 35 11	241.033	42	14	19	7	50	8
x Cep	4.3	22 03 29.4	64 34 30	13.883	-207	4	-212	5	-203	5
k And	4.1	23 39 52.5	44 16 25	68.838	-119	6	-141	6	-127	8
β Lyr	3.5	18 49 40.3	33 21 05	306.640	-85	5	-90	9	-84	10
γ Lyr	3.2	18 58 31.8	32 40 33	305.080	-91	10	-85	4	-83	6
ζ Peg	3.4	22 40 55.3	10 46 28	158.131	58	9	60	7	64	8
δ Sge	3.8	19 46 53.9	18 30 26	268.898	0	8	12	6	13	12
ρ Cas	4.5	23 53 50.6	57 26 21	37.962					-197	6
ι Cyg	3.8	19 29 25.8	51 42 31	347.986					-172	9
θ Cyg	4.5	19 36 08.8	50 11 52	344.494					-167	9
β Del	3.6	20 37 02.1	14 33 26	256.410					30	8
ζ Cas	3.7	00 36 22.0	53 50 13	46.980					-184	7

Table 2.1b. Stars observed at the Tek-ri Astronomical Station.

STAR	MAG	RIGHT ASCENS	DECLINATION	AZIM.(GON)	30/09/88		02/10/88	
					δz (0.1 mgon)	σ	δz (0.1 mgon)	σ
51 Her	5.0	16h 51m 17.0s	24° 40' 35"	285.183	4	8		
ζ Her	2.8	16 40 51.4	31 37 29	302.161	-2	5		
42 Her	4.9	16 38 25.9	48 57 09	341.203	-29	9		
π2 Cyg	4.1	21 46 23.7	49 15 38	58.099	-129	14		
2 Peg	2.4	21 29 27.2	23 35 30	117.651	-95	13		
14 Peg	3.8	21 49 21.8	30 07 27	101.382	-107	11		
μ Cep	4.3	21 43 10.8	58 43 53	35.078	-100	5		
α Cep	2.4	21 18 19.7	62 32 28	23.487	-103	10		
ι Peg	3.8	22 06 30.3	25 17 33	113.242	-84	6		
ν Cep	4.3	21 45 08.5	61 04 19	28.314	-100	9		
α Lac	3.8	22 30 50.8	50 13 40	55.896	-111	7		
β Aql	3.7	19 54 46.3	06 22 44	209.332	-23	7		
η Peg	2.9	22 42 29.6	30 09 54	101.285	-85	12		
ο And	3.6	23 01 25.3	42 16 06	73.732	-96	8		
ζ Aql	3.0	19 04 53.9	13 50 50	253.107	0	7		
ε Peg	2.4	21 43 39.1	09 49 30	163.708	-60	12		
α Aql	0.8	19 50 14.6	08 50 21	230.982	-1	1-		
ο Dra	4.7	18 51 02.1	59 22 40	366.709	-30	9		
γ Aql	2.7	19 45 44.1	10 35 11	239.95	-1	9		
ξ Cep	4.3	22 03 29.1	64 34 34	15.136	-95	7		
κ And	4.1	23 39 52.5	44 16 28	69.273	-99	9	-107	6
β Lyr	3.5	18 49 40.0	33 21 06	306.178	-10	9	2	4
γ Lyr	3.2	18 58 31.6	32 40 34	304.614	-5	3	25	17
ζ Peg	3.4	22 40 55.3	10 46 29	159.191	-63	8	-53	10
δ Sge	3.8	19 46 53.7	18 30 27	268.243	4	10	16	5

Table 2.1b (continued).

STAR	MAG	RIGHT ASCENS	DECLINATION	AZIM.(GON)	30/09/88		02/10/88	
					δz (0.1 mgon)	σ	δz (0.1 mgon)	σ
β Del	3.6	20 37 02.1	14 33 36	255.503	35	8	39	6
ζ Cas	3.7	00 36 22.0	53 50 14	47,471	-107	9	-112	10
μ And	3.9	00 56 09.0	38 26 28	82.264	-93	7	-105	12
α Cas	2.2	00 39 53.5	56 28 41	41.985	-118	8	-110	7
γ Peg	2.8	00 12 40.8	15 07 27	142.439	-63	13	-63	6
η Cas	3.4	00 48 26.6	57 45 30	37.683	-118	11	-109	8
ε Peg	2.4	21 43 39.1	09 49 30	236.392			15	6
γ Cyg	2.2	20 21 50.0	40 13 24	321.718			-2	12
ν Psc	4.8	01 18 52.2	27 12 30	108.445			-88	7
ξ Cep	4.3	22 03 29.1	64 34 34	384.864			-64	19
φ Per	4.1	01 42 58.7	50 38 04	54.964			-111	11
9 Peg	4.3	21 43 59.7	17 18 01	264.585			6	9
β Tri	3.0	02 08 53.7	34 56 14	90.183			-94	10
μ Cep	4.1	21 43 10.8	58 43 53	364.922			-45	10
γ Tri	4.0	02 16 40.0	33 47 54	92.793			-100	8
η Psc	3.6	01 30 54.2	15 17 29	141.876			-54	8
ξ Peg	4.2	22 46 09.1	12 07 03	246.527			18	9
δ Psc	4.4	00 48 07.4	07 31 39	177.836			-32	11
ζ Cep	3.4	22 10 29.0	58 08 56	363.351			-30	7
ε Psc	4.3	01 02 23.0	07 49 59	175.511			-40	6
ε Cep	4.2	22 14 38.2	56 59 26	360.322			-48	11
τ Per	4.0	02 53 28.9	52 43 06	50.125			-103	9
β Per	2.1	03 07 27.4	40 54 53	76.742			-102	9
α Peg	2.5	23 04 13.3	15 08 50	257.638			16	4
1 Lac	4.1	22 15 29.8	37 41 45	316.063			0	8
1 Peg	4.0	22 46 00.5	23 30 33	282.152			15	5
α Lac	3.8	22 30 50.8	50 13 40	344.104			-26	4

The data reduction was made in three steps. In the first step precession, nutation and annual aberration matrices were applied to the coordinates of the observed stars. For each day of observation, we then constructed a set of coordinates referred to the true equinox and equator of date.

In the second step, assuming nominal site coordinates truncated to the minute of arc, the predicted zenith distance of each star was computed for each epoch of observation. This was the lengthiest part of the work because for each star there were approximately 10-20 (z,UT) readouts near z=30°. About 1000 predicted zenith angles were computed using a program stored on a Hewlett Packard 28C hand calculator. By computing, for each pass, the zenith angle averaged over a good number of readouts we hope to have minimized the effects of the "personal equation" in time-tagging the transit of a star through the cross-hairs. A timing bias of a few tenths of a second at the epoch of start of the chronometer cannot, however, be excluded and will affect the estimated longitudes. For this reason it was decided to repeat the measurements at each site more than one night, rather than surveying a larger number of sites.

In the third and last step the average zenith excesses δz were tabulated with the corresponding azimuth A and mean epoch of observation. The data were then least squares fit to the model, easily computable from spherical trigonometry.

$$\delta z = \delta z_0 - \cos(A) \cdot \delta\Phi - \sin(A) \cdot \cos(\Phi) \cdot \delta\Lambda - \sin(A) \cdot \cos(\Phi) \cdot t \cdot df \qquad (1.1)$$

Here the solve-for parameters are:

$\delta\Phi$= correction to be added to the a priori north latitude Φ of the station;

$\delta\Lambda$= correction to be added to the a priori longitude east Λ of the station;

δf= fractional drift of the chronometer;

δz_0= atmospheric zenith bias in the zenith angle near z=30°.

We have indicated with t the mean epoch of observation of each star multiplied by the appropriate dimensional factor.

Because δz and δf may vary from night to night, the partial derivatives of δz_0 relative to these two parameters were time-blocked so that their values were estimated each night anew. Eventually the solution was iterated, but it turned out that convergence was already reached at the first iteration. Table 2.2 summarizes our results.

Table 2.2. Astronomic coordinates. Quoted errors are computed as the product of the formal error (as deduced from the variance covariance matrix) and the root-mean-square spread of the post-fit residuals.

GASHERBRUM ASTRONOMIC STATION

	latitude N	*longitude EG*
a priori coordinates	35° 53′ 00".0	76° 45′ 00".0
least squares corrections	+48".9 ± 1".5	-4".5 ± 1".4
polar motion	+0".1	-0".1
UT1-UTC		+0".5
final coordinates	35° 53′ 49".0 ± 1".5	76° 44′ 55".9 ± 1".4

Auxiliary Parameters:

date	δz	δf
18/09/88	-19".6 ± 1".6	$(-0.1 \pm 2.4) \cdot 10^{-5}$ sec/sec
19/09/88	-21".2 ± 1".6	$(+0.1 \pm 2.4) \cdot 10^{-5}$ sec/sec
26/09/88	-20".7 ± 1".6	$(+1 \pm 2.4) \cdot 10^{-5}$ sec/sec

TEK-RI ASTRONOMIC STATION

	latitude N	*longitude EG*
a priori coordinates	36° 08′ 00".0	76° 24′ 00".0
least squares corrections	+10".5 ± 1".6	20".7 ± 1".6
polar motion	+0".1	-0".0
UT1-UTC		+0".4
final coordinates	36° 08′ 10".6 ± 1".6	76° 24′ 21".1 ± 1".6

Auxiliary Parameters:

date	δz	δf
30/09/88	-16".1 ± 1".4	$(+0.2 \pm 2.2) \cdot 10^{-5}$ sec/sec
02/10/88	-14".1 ± 1".4	$(-1.4 \pm 2.2) \cdot 10^{-5}$ sec/sec

It may be noted that the recovered atmospheric biases have values typical for heights of about 4000 m. The estimated clock drifts are consistent with zero and contain in their error bars the value $\pm 6 \cdot 10^{-6}$ sec/sec (or 15 sec/month) specified by the manufacturer. Fig. 2. 2 shows the distribution of the post-fit residuals for the two solutions. Each point refers to a star and different symbols have been used for the various observing sessions. The relatively smaller number of stars scheduled near $A = 0^g$ and a $A = 200^g$ is due to the fact that these stars follow an apparent path nearly tangent to the *almucantar* so that the exact epoch of transit through the cross-hairs becomes ill-defined. Interesting is the sinusoidal signature for the 30/09 session at Tek-ri with amplitude 5". This is presumably due to an offset relative to UTC of the local time for that particular session.

For completeness, the coordinates in Table 2.2 are corrected for the departure of the instantaneous pole from the mean pole. The appropriate values of the pole coordinates and UT1-UTC provided by the International Earth Rotation Service (Bull. B9 of Nov. 4, 1988) are:

Gasherbrum glacier: x=+0".043 y=+0".143 UT1-UTC=0.033 sec

Tek-ri: x=+0".010 y=+0".132 UT1-UTC=0.023 sec

1.4. Determination of the Ellipsoidal Coordinates

The geocentric coordinates of the center-of-phase of the GPS antenna are, at each instant, determined by passive multilateration to four or more GPS satellites. Multilateration is done by matching the PRN (Pseudo Random Noise) code modulated on the carrier with a replica generated within the receiver and detecting the difference between the epoch (in the GPS time-scale) of transmission and the epoch (in the receiver time-scale) of reception of the wave packet.

By tracking at least four satellites at once, the instantaneous offset of the crystal oscillator internal to the receiver relative to the time kept by atomic oscillators on board the GPS satellites - which is a known function of UTC - is determined simultaneously with the cartesian coordinates of the antenna. Sequential Kalman filtering provides real time, "quick look" update of the coordinates on the receiver's display. Computer post processing of the data stored in cassettes provides geodetic coordinates in the WGS84 system and a more refined solution.

Each satellite continuously broadcasts navigation signals at two carrier frequencies: L1=1575.42 MHz and L2=1227.60 MHz. The L1 wave is BPSK (Binary Phase Shift Keying) modulated by two PRN codes: a P code ranging signal, with bandwidth 10.23 MHz and a C/A code ranging signal. On the L1 carrier, a navigation message

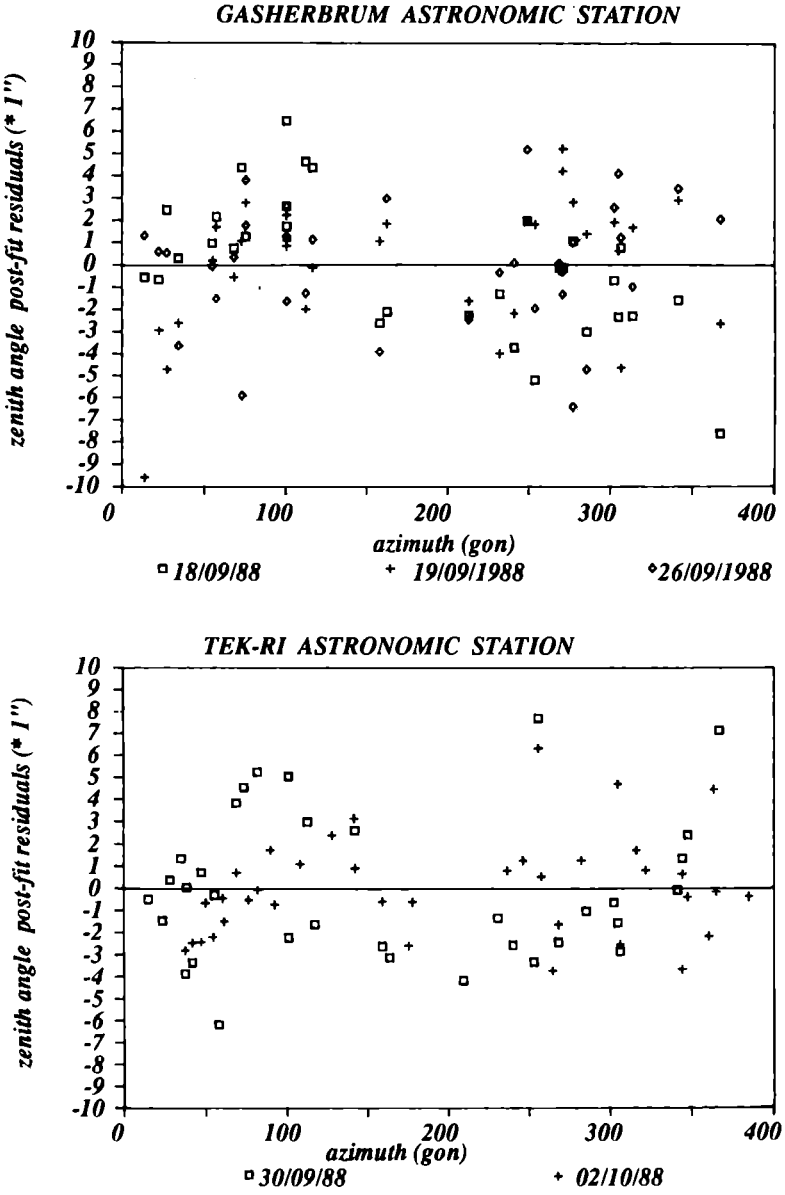

Fig. 2.2. Azimuth distribution of the past-fit residuals of the zenith angle observation at or near 2=30 for the Gasherbrum (above) and Tek-ri (below) astronomic stations. Each point refers the transit of one star. Different symbols are used for the various observing nights.

is modulated at 50 bits/sec to provide satellite ephemeris and clock bias (relative to UTC) information. The L2 carrier is modulated only by the P code.

The receivers we used are designed to decode the C/A sequence at the L1 frequency. If we adopt the "rule of thumb" that the observation resolution is about 1% of the signal wavelength, then the nominal resolution with C/A coded pseudo-ranges (wavelength=300 m) is 3 m (Wells, 1986). The overall system accuracy in absolute positioning is, however, determined by other error sources. The most important are: receiver noise, satellite clock errors, satellite ephemeris errors, multipath, ionospheric and tropospheric effects, earth orientation effects and satellite geometry (King et al., 1985; Caporali and Ciraolo, 1985). Of these the most unpredictable are certainly the ionospheric effects. They produce the largest errors when the satellite is at the horizon, near midday and in periods of maximum sunspot activity.

The Post Processing Software PoPS models the ionospheric zenith delay with a time dependent scale factor consisting of a constant plus, in the interval of 8-20 local time, a cosine bell centered at 2 pm. This delay is mapped to zenith angles $\leq 75°$ by a 1/cos(z) function (Bauersima, 1983) A typical error size may be $\approx$30 m, which should in any case be considered with the due caveats.

Table 2.3 summarizes the ellipsoidal coordinates of the astronomic stations referred to the WGS84 system.

We note that the root mean square repeatibility is better in latitude than in longitude. This is simply due to the ground tracks being, with the actual constellation, more distributed in the North-South direction, causing the solution for longitude be geometrically weacker than for latitude. The reported repeatibility is, in any case, better than predicted on a geometric basis alone. The satellite geometry defines at each instant the Geometric Dilution of Precision GDOP as the scale factor which should be applied to the nominal resolution to estimate the root sum square user's formal position error. As we have consistently scheduled our observing sessions with GDOP ≤ 5 the geometric error is $\approx$ 15 m, or 0".5, if the nominal resolution is 3 m with the C/A code. As to the height, again the repeatibility is remarkably good, but the height estimates are most probably biased by an unknown amount, having no control on the effect of ionospheric refraction on the group delays.

Table 2.3. Results of the determinations of ellipsoidal coordinates using GPS receivers. Quoted errors are defined in terms of the r.m.s. repeatibility about the mean value of the daily determinations. The WSG84 semi major axis and inverse flattening are 6378137 m and 298.257.

GASHERBRUM GLACIER GPS STATION

day	*latitude N*	*longitude EG*	*ellips. height*
18/09/88	35° 53′ 48".48	76° 45′ 12".35	4372 m
19/09/88	.42	.15	4368
20/09/88	.40	.37	4374
21/09/88	.40	.20	4356
22/09/88	.31	.34	4369
23/09/88	.40	.34	4373
25/09/88	.43	.09	4375
Geodetic Coordinates	35° 53′ 48".41	76° 45′ 12".25	4370
(WGS84)	± 0".51	± 0".11	± 7 m

TEK-RI GPS STATION

day	*latitude N*	*longitude EG*	*ellips. height*
01/10/88	36° 08′ 09".12	76° 24′ 36".15	3796 m
02/10/88	.11	.38	3788
03/10/88	.20	.34	3794
04/10/88	.12	.22	3798
Geodetic Coordinates	36° 08′ 09".14	76° 24′ 36".27	3794
	± 0".04	± 0".11	± 4 m

1.5. Discussion on the Curvature of the Plumb Line

By comparing the astronomical and ellipsoidal coordinates in Tables 2.2 and 2.3 respectively we obtain the absolute deflection of the vertical at the two sites:

	ξ	η	H
Tek-ri	1".5 ± 1".5	-12".3 ± 1".3	3794 m
Gasherbrum	0".5 ± 1".5	-13".3 ± 1".1	4382 m

These values refer to the observation points and therefore do not represent the deflection at the geoid. In general, one expects that the field lines will be twisted and curved as they are continued from the observatory down to the corresponding location on the reference surface, an effect known as curvature of the plumb line. To estimate its value requires some assumption. We shall examine here a simple model (Vanicek and Krakiwski, 1986, p. 507) where the vertical gradient of gravity $\frac{\delta g}{\delta H}$ is assumed constant.

Given two nearby points on the earth surface of known relative and mean gravity δg and $\bar{g}$ respectively, distance δS, relative and mean height δH and $\bar{H}$, the deflection of the plumb line on the vertical plane containing the two points is given by the expression:

$$\Delta\varepsilon = \frac{-\bar{H}}{2\cdot\bar{g}} \cdot \left(\frac{\delta g}{\delta S} - \frac{\delta g}{\delta H} \cdot \frac{\delta H}{\delta S} \right) \qquad (1.2)$$

The total (i.e. including topography) surface vertical gradient $\frac{\delta g}{\delta H}$ ranges between the Poincaré value -0.0848 mGal/m and the free-air value -0.3086 mGal/m (see also Chapter 4).

As mentioned earlier, the Gasherbrum Astronomic Station was situated on the crest of a sharp, roof-shaped morene on the side of the Gasherbrum glacier.

Gravity was measured at the astronomic station and at a number of locations nearby, with relative positions accurately determined by theodolite EDM or by GPS in translocation mode. We can thus attempt an estimate of $\Delta\varepsilon$ in two nearly orthogonal directions relative to the astronomic station. We choose the following:

	Az	ΔS	ΔH	Δg
From Gasherbrum GPS1 to Urdok GPS2	173°	2979 m	+ 39 m	- 7.60 mGal
From Gasherbrum GPS1 to Base Camp 7	74°	1017 m	+ 150 m	- 21.85 mGal

As average height and gravity we assume 4250 m and 987429.72 mGal. It follows that:

$$\Delta\varepsilon_{173^\circ} = -0.002152 \cdot (0.003 + \frac{\delta g}{\delta H} \cdot 0.013)$$

$$\Delta\varepsilon_{74'} = -0.002152 \cdot (0.003 + \frac{\delta g}{\delta H} \cdot 0.15)$$

As values of the vertical gradients we take the two extreme values and the intermediate deduced from the tables above. After some trigonometry we find:

$\frac{\delta g}{\delta H}$ (mGal/m)	-0.084	-0.15	-0.19	-0.31
$\Delta\xi$	-0".3	+ 0".7	+ 1".1	+ 2".8
$\Delta\eta$	-3".8	+ 0".5	+ 3".0	+ 10".6

Typical values for the Alps are of the order of a few arcseconds per km of elevation (Kobold and Hunziker, 1962). If similar values apply in Karakorum at an average height of 4 km, then the right of magnitude is found in the last column, which corresponds to a free-air weighting factor for the topographical term in equation (1.2).

1.6. CONCLUSION

Table 2.4 gives the values of the deflection of the vertical at the two sites and, for reference, at other sites in this area, as reported by Marussi (1964).

The first two entries in Table 2.4 are our results and indicate that the direction of the gravity vector remains essentially the same, within the quoted uncertainties, over the 40 km distance. This could well be a pure coincidence as changes of some

Table 2.4. Observed deflections of the vertical. The first two values refer to the WGS84 ellipsoid. All the remaining refer to the Everest ellipsoid (a=6377276 m; 1/f=300.8017)

Site	*height (m)*	*latit.*	*longit.*	ξ	η
Tek-ri	3794	36° 08′	76° 24′	+1".5 ± 1".5	-12".3 ± 1".3
Gasherbrum	4370	35° 54′	76° 45′	+0".5 ± 1".5	-13".3 ± 1".1
Stak valley					
Camp IV		35° 47′	75° 01′	-8".3	-4".8
Camp III	3900	35° 46′	75° 05′	-11".5	+16".2
Skardu	2233	35° 18′	75° 39′	-28".3	+6".3
Depsang	5361	35° 17′	77° 58′	+2".8	+2".3
Kargil	2713	34° 34′	76° 07′	+0".9	+10".7
Lamayuru	3461	34° 17′	76° 48′	-6".3	+10".2
Leh	3519	34° 10′	77° 35′	+14".5	+6".1
Poshkar	2537	34° 02′	74° 30′	-13".8	-9".9
Gogipatri	2363	33° 52′	74° 41′	-3".0	-9".4

arcseconds in few kilometres are common in Himalaya (Gulatee, 1955). From Table 2. 4 it also follows that the azimuth of the gravity vector is approximately 272° at Gasherbrum and 277° at Tek-ri.

However our analysis does not reliably account for the deflection of the plumb-line. As discussed in section 1.5 the effect could ammount to as much as 10" in these mountain areas (Torge, 1980). An additional important effect is due to topography as for gravimetric measurements. For these reasons numerical differences between observed and predicted values of the deflection of the vertical can not be directly interpreted at this stage of the analysis.

Also, an estimate of the uncertainty of geoidal models in these areas is needed, but is far from obvious. The most interesting feature of Table 2.4 is that two more points have been added to a set which, even considering the gravimetric data, is yet unadequate to unveil the high frequency structure of the gravity field of the geoidal undulations in this area. Owing to the impossibility to establish a regular grid of stations, we can expect that future work will add a few more points, yet major gaps will remain. Space borne measurements will really be capable to map the gravity field with a regular sampling. However the gravity field in this area is so structured that the needed resolution can be achieved, for the foreseable future, only by patiently continuing ground based measurements.

2. Triangulation work on K^2

2.1. INTRODUCTION

The southern side of K^2 is well visible all along the Godwin Austen and Upper Baltoro glaciers, but from the Shaksgam valley the intervening Bdongo ridge (see Figure 2.3) does not permit K^2 to be observed. One has to reach the front of the Gasherbrum and Urdok glaciers, from where one also enjoys the magnificent view of the four Gasherbrums and of the Falchan Kangri. Descending the Shaksgam valley, K^2 can be observed from Tek-ri, along the Sarpo Laggo valley.

In 1856 Col. T.G. Montgomerie measured vertical angles of K^2 from the top of Mount Haramukh and estimated for the height a value of 8611 m (Burrard and Hayden, 1933). Recent suggestions that K^2 might be considerably higher (Wallerstein, 1988) have not been confirmed and it rather appears that the original estimates of the Survey of India can be trusted to within some meters (Desio, 1988). We have been unsuccesful in finding evidence in the literature of Chinese triangula-

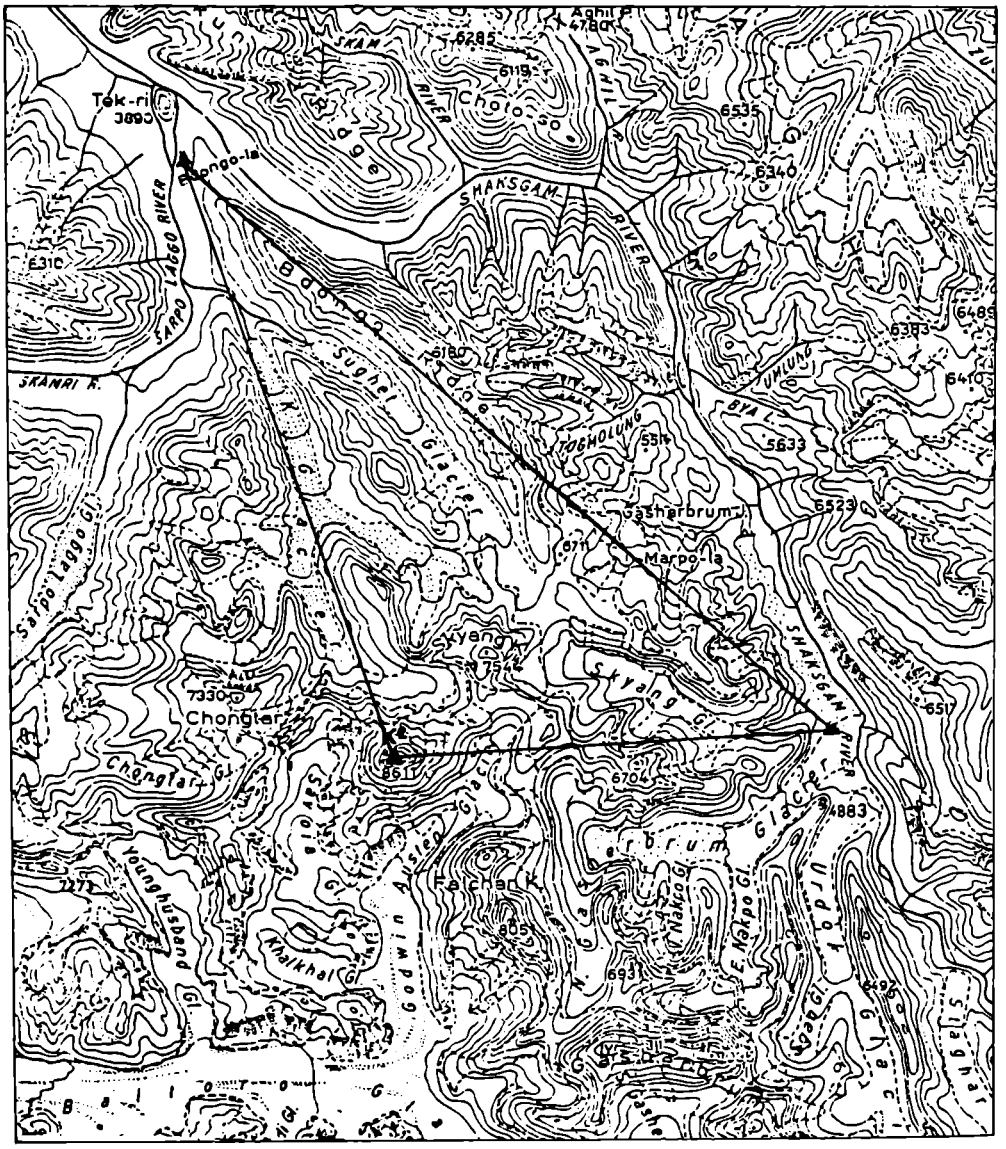

Fig. 2.3. Geodetic triangle used for the triangulation of K^2.

tion work from the northern side of K^2, but we expect that a very accurate work must have been done, having found several trigonometric signals going from Bazar Dara to the Aghil pass and all along the Shaksgam valley.

Because the height of K^2 seems to be reasonably well established, triangulating to K^2 was, in the scientific plans of the Ev-K^2-CNR 1988 expedition, considered very valuable in order to have an independent reference of height for the reduction of the gravimetric data. For this reason horizontal and vertical angles to K^2 were measured at the astrogeodetic stations established on the front of the Gasherbrum glacier and at Tek-ri, where geodetic and astronomic coordinates of the sites had been determined, as well as astronomic azimuths. The angular measurements were made by means of a Kern E2 theodolite.

In the following we report on the analysis of the trigonometric data leading to two results: one is the determination of the geographic coordinates of K^2 in the WGS84 ellipsoid. The other is the determination of the height of the two observing sites.

2.2. Analysis of the Horizontal Angles

The WGS84 coordinates of the observing sites have been determined by repeated GPS measurements at epochs of minimum GDOP, that is when the distribution of satellites over the site has the most favourable geometry. They are:

	Gasherbrum	*Tek-ri*
latitude N	35° 53′ 48".4	36° 08′ 09".1
longitude EG	76° 45′ 12".3	76° 24′ 36".3

and are referred to a geocentric ellipsoid with a= 6378137 $\frac{1}{f} = 298.257$

From here the radius of the local sphere $R = \frac{a\sqrt{1-e^2}}{(1-e^2 \sin^2 \varphi)}$ $(e^2 = 2f - f^2)$ can be computed at the two sites: R=6371415 m at Gasherbrum R=6371585 m at Tek-ri

Inversion of the geodetic coordinates yields the forward and backward azimuths and the distance reduced at the ellipsoid:

From	*to*	*azimuth*	*distance*
Gasherbrum	Tek-ri	310° 42′ 13".2	40764 m
Tek-ri	Gasherbrum	130° 30′ 06".5	40764 m

The astronomic azimuths of K^2 at the two stations were determined by collimating Polaris and using the algorithms and tables in the 1988 Astronomical Almanac. At Gasherbrum the astronomic azimuth of two suitably shaped neraby peacks was first determined and the azimuth of K^2 was then referred to them. The astronomic azimuths of K^2 with the two targets are:

Gasherbrum:

day	*target north*	*target south*
19/09	265° 35′ 38".6	265° 35′ 11".0
26/09	265° 35′ 45".1	265° 35′ 20".8
mean	265° 35′ 41".9	265° 35′ 15".9

These values give an exemple of the systematic, target dependent error which can be introduced in this process. Rather than taking an average azimuth for the two targets, we prefer to carry this 26" difference in the calculations and to estimate its effect in the final results.

At Tek-ri we took only one reference astronomic azimuth and the azimuth of K^2 is: Tek-ri: day 02/10; target north 161° 42′ 59".7.

The relative azimuths are then obtained by difference:

site	*target north*	*target south*
Gasherbrum	45° 06′ 31".5	45° 06′ 57".4
Tek-ri	31° 12′ 53".2	

The plane triangle Gasherbrum–Tek-ri can then be resolved:

quantity	*target north*	*target south*
center angle at K^2	103° 40′ 35".3	103° 40′ 09".4
side Gasherbrum to K^2	21742 m	21742 m
side Tek-ri to K^2	29722 m	29725 m

Finally, the geographic coordinates of K^2 are:

from Gasherbrum	*target north*	*target south*
latitude north	35° 52′ 53".4	35° 52′ 53".3
longitude EG	76° 30′ 48".1	76° 30′ 48".0

from Tek-ri	
latitude north	35° 52′ 53".5
longitude EG	76° 30′ 48".0

The scatter among the various estimates indicates that they should be affected by an uncertainty not exceeding the second of arc. Is is also clear that, due to the large opening of the center-angle, the uncertainty in the reference azimuth of one target does not reflect appreciably in the final coordinates.

2.3. COMPARISON WITH PREVIOUS TRIANGULATIONS

The area of northern Karakorum belongs to the Sheet 52.A (K^2) (International Sheet NI43Q) comprised between 35° and 36° latitude north and 76° and 77° longitude east. It includes K^2 (peak 13/52A), first surveyed in 1861 by H.H. Godwin Austen; Falchan Kangri (Conway's "Broad Peak", peak 16/52A), photogrammetrically surveyed by the expedition of Duke of Abruzzi in 1909 and found to be 8051 m high. In the Gasherbrum range, Gasherbrum I (Conway's "Hidden Peak") and II reach 8068 m and 8035 m respectively. Gasherbrum III and IV fall just short of 8000 m: the former is credited with 7952 m and the latter 7925 m. Recent independent height estimates by GPS and triangulation from the Baltoro glacier confirm the height estimates of K^2, Falchan Kangri (Broad Peak) and Gasherbrum IV to within few meters (8616, 8060 and 7929 m respectively; Desio, 1988). To complete the picture of this 1°x 1° area of the world, there are at least eight peaks above 7500 m and seven triangulated peaks over 7300 m. As mentioned in the explanatory pamphlet of the Survey of India (1922) for sheet 52.A, this area «... probably contains more ice and permanent snow than any other degree sheet outside polar or sub-polar regions...».

Sheet 52.A contains only the geodetic station Nang H.S. (36) with coordinates $\phi = 35° 5' 6".42$, $\lambda = 76° 10' 2".59$, h = 17254 ft (5259 m) and one subsidiary station, Ombartro (locally called Gamat), with coordinates $\phi = 35° 7' 12".67$, $\lambda = 76° 6' 10".43$, h=17201 ft (5243 m). The former was observed by G. Shelverton of the Survey of India in 1858 during the Kashmir series. The latter was observed by W.H. Johnson in the same year as part of the Lower Shyok Triangulation and its coordinates were fixed relative to Nang. Both stations were included in the 1921 adjustment. Additional topographic data were drawn from the explorations of the Duke of Abruzzi in 1909 and Peterkin's triangulation during the Workman's Expedition of 1912.

In this context, K^2 is identified as a Class A (i.e. directly connected to the Indian Triangulation) intersected point with coordinates:
ϕ=35° 52′ 55" λ=76° 30′ 51" h=28250 ft.

It is here assumed that the longitude of Madras is defined so that starting meridian is +75° east of Greenwich. The earlier degree sheet n. 21 of the Survey of

India (1877) gives values for the longitudes shifted by 2'27".18, and K^2 has in fact coordinates: $\phi = 35° 52' 55"$ $\lambda = 76° 33' 18"$.

It was in this system, planimetrically related to the former by Prof. P. Bencini (1954), that Capt. F. Lombardi of the Italian Military Geographic Institute (I.G.M.) estimated the coordinates of K^2 : $\phi = 35° 52' 47".2$ $\lambda = 76° 33' 15".4$ on the basis of photogrammetric work he carried out during the Desio 1954-55 expedition. These are in fact the coordinates published in the 1:12,500 map of K^2 published by the I.G.M.

All these earlier estimates of the coordinates of K^2 were communicated to us during a meeting with Lombardi on February 20, 1989 after we had computed the values reported in sect. 2.2. They clearly indicate that the reference system used in GPS work is very close to the one employed in the 1921 adjustment. The discrepancies of 1 to 2 arcseconds with our determinations are difficult to interpret without further information on the size and orientation of the error ellipse and of the relative orientation of the Everest and WGS84 ellipsoids. They are also caused by the uncertainty associated to the identification of the highest point of the snow cap covering the summit of K^2 and, perhaps, with the definition of the origin meridian.

2.4. Analysis of the Vertical Angles

At Gasherbrum we took the vertical angles in two days:

	19/09	26/09
elevation of K^2	10° 55' 27".1	10° 55' 30".0

We take the mean and add the corrections for refraction and deflection of the vertical:

mean elevation of K^2	10° 55' 28".6
refraction $\frac{kd}{2R}$ ($k = 0.08$; $d = 21742$ m; $R = 6371415$ m)	-28".1
deflection of the vertical ($\xi = 0".5$; $\eta = -13".3$)	-13".2
corrected elevation	10° 54' 47".3

Likewise at Tek-ri we have:

elevation of K^2	9° 03′ 24".1
refraction $\frac{kd}{2R}$	
(k = 0.08; d = 29724 m; R = 6371585 m)	-38".5
deflection of the vertical	
(ξ = 1".5; η = -12".3)	+5".3
corrected elevation	9° 02′ 50".9

Due to the relative closeness of K^2, the precise value of the constant of refraction k (here assumed 0.08) is not critical, if the acceptable uncertainty is of the order of some meters. For example, having chosen k=0.09 at Tek-ri, the most distant station, would have produced a vertical change of 1 m. It is probably more important the fact that we have certainly collimated from the Gasherbrum and Tek-ri stations different spots on the summit of K^2 (a snow cap continuously modified by the winds), which can well be at a relative height of some meters. The values (ξ, η) of the vertical refer to the places of observation. A rigorous procedure would require their reduction to the ellipsoid. This reduction is discussed in section 1.5 where it is concluded that the uncertainty in the vertical gradient of gravity at the reference surface only permits the definition of a range of values for the curvature of the plumb line. Because this correction is unlikely to be larger than 10" and the distances are limited, ignoring this correction will not affect our height estimate more than about 1 meter.

The heights of the observing sites for an assumed height of K^2 of 8611 m are:

Gasherbrum	
assumed height of K^2	8611 m
d/tan (elevation)	-4192 m
curvature correction $\frac{d^2}{2R}$	-37 m
total	4382 m

Tek-ri	
assumed height of K^2	8611 m
d/tan (elevation)	-4733 m
curvature correction $\frac{d^2}{2R}$	-69 m
total	3809 m

2.5. DISCUSSION

Having used a commonly accepted value for the height of K^2, the heights of the two observing stations are thus trigonometrically tied to the geodetic systems of the Survey of India, south of Karakorum. This is an important point in our effort to consistently reduce the gravimetric data (see Chapter 4) without introducing a major bias related to the height system. However it must be noted that the assumed height of K^2 is affected by a non neglegible uncertainty. While for Everest there exists an in-depth analysis by Gulatee (1954) based on a critical re-evaluation of old measurements and on an improved knowledge of refraction and geoidal heights and profiles, a similar analysis for the height of K^2 does not seem to have been yet carried out. Burrard and Hayden (1933) report in their table XII Montgomerie's original height data.

Station of observation	*Year*	*Height of station (Feet)*	*Distance from K^2 (Miles)*	*Raw height* (Feet)*	*Corrected height** (Feet)*
Shangruti	1859	17531	78.9	28640	28246.6
Biachuthusa	1859	16746	99.0	28864	28218.7
Marshala	1858	16906	58.6	28472	28240.0
Kastor	1858	15983	66.0	28560	28261.4
Thurigo	1858	17246	61.8	28515	28254.1
Haramukh	1856	16001	136.5	29300	28293.9
Kanuri-Nar	1857	15437	114.3	28920	28218.4
Barwai	1857	16304	88.0	28666	28258.5
Thalanka	1857	16830	74.7	28613	28322.7
Mean					28253 (8611.144 m)

Range of variation of the values: 828 and 104

*values of height if no correction for refraction be applied

** height as determined by Montgomerie with coefficients of refraction varying from 0.04 to 0.05.

From this table it is clear that the value of 8611 m may be subject to adjustements of several meters, or even more.

It is interesting to compare the values of the observing sites with those independently obtained with the GPS receivers in point positioning mode. The comparison requires the knowledge of the geoidal height at both sites. We will assume the value N=-35 m at both sites, computed from the Rapp model complete to degree and order 180. The minus sign indicates that in this region the geoid is below the

ellipsoid. We have:
at Gasherbrum 4370+ 35 m = 4405 m; at Tek-ri 3794+ 35 m= 3829 m.

The difference of the GPS heights combined with the geoidal undulation and the trigonometric heights is very similar in the two cases: 23 m and 20 m. Taking into account that the GPS measurements were taken at similar periods of the day at both sites, these values are explainable in terms of a ionospheric bias affecting the GPS data, which may, therefore, be temptatively quantified as a -21 m constant term.

3. Evaluation of the Heights of the Gravity Stations

3.1. INTRODUCTION

To detect gravity anomalies from a given set of gravimetric observations, the data must be reduced to the geoid. The knowledge of the orthometric heights of the base stations is one of the most arduous tasks in gravimetry. An uncertainty of 1 m in height maps into 0.3 mgal in the local gravity i.e. a factor of ten worse than the instrumental resolution. For practical and logistical reasons, the determination of such altitudes during the expedition has been made with different methods and instruments. We have considered a correct attitude first to report all the collected data and then to construct, taking into account the different accuracy and reliability of the various measurements, an altimetric profile.

The data set consists of two reference heights determined trigonometrically relative to K^2, of the values of atmospheric pressure, temperature and relative humidity, measured at each gravimetric site with a Pennwalt barometer and a thermohygrometer Delta-Ohm respectively. A pocket Thommen altimeter has been employed to determine the difference in height between two successive gravimetric stations.

At some gravimetric points (Fig. 2.4) it was possible to install also a GPS receiver a Wild Magnavox WM 101, able to estimate the ellipsoidal height of the station point with an accuracy of about ten meters, up to a bias error due to the ionospheric refraction which cannot be estimated with a single frequency receiver. A short series of trigonometric levelling data completes the set of altimetric measurements.

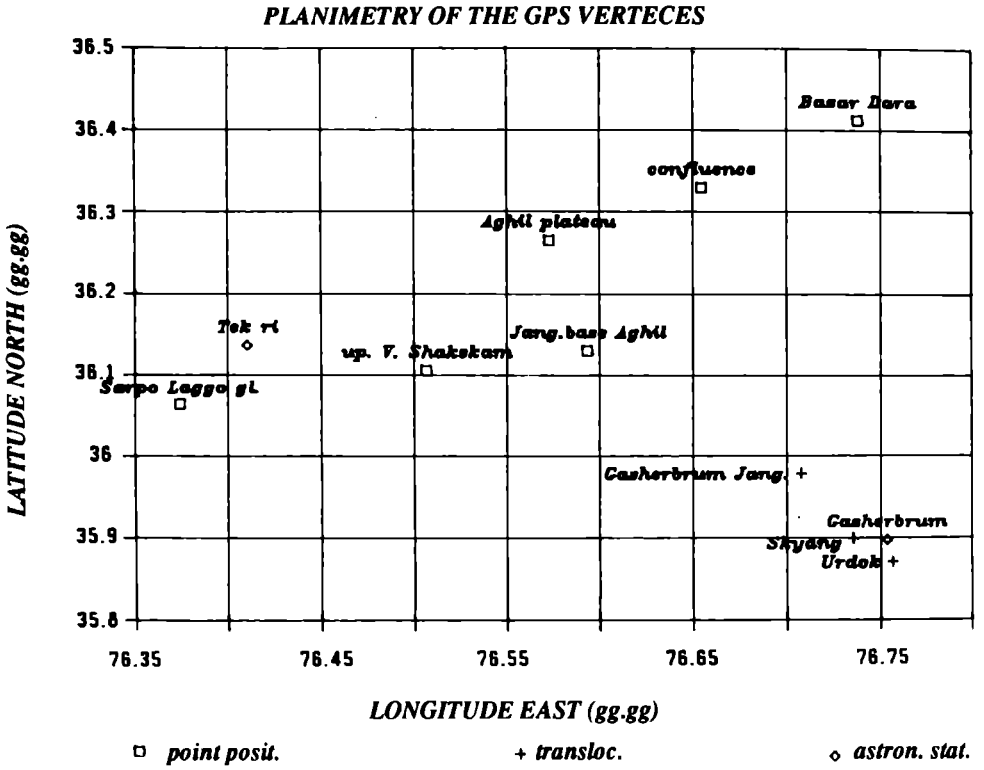

Fig. 2.4. Distribution of the stations occupied by GPS receivers.

3.3. CRITERIA FOR DATA ANALYSIS

Our aim is to estimate from the data collected during the expedition a reasonable height value for each gravimetric site.

We start assuming as reference points the Gasherbrum and Tek-ri astrogeodetic stations. Their orthometric heights *HGasherbrum* and *HTek-ri* have been evaluated trigonometrically (see Chapter 2) relative to K^2, the height of which is known within the trigonometric network of the Survey of India.

At these points we also have GPS height data *hGasherbrum* and *hTek-ri*.

The GPS measurements are biased because of the ionospheric refraction and because they refer to the ellipsoid, not to the geoid, but the relevant corrections can be inferred by comparing the GPS heights values with the trigonometric ones.

We introduce a scale factor $S' = \frac{HGasherbrum - HTek\text{-}ri}{hGasherbrum - hTek\text{-}ri}$ (3.1) to scale all the GPS height differences between one site and the Gasherbrum (or Tek-ri) reference points.

We then assume as reference altitude the *HGasherbrum* (or *HTek-ri)* and use the following relation: $Hi = HGasherbrum + S \cdot \Delta hi,Gasherbrum$ (3.2) with S defined by (3.1) and $\Delta hi,Gasherbrum$ computed by differencing the ellipsoidal heights of the i-th site and Gasherbrum listed in the second column of Table 2.5. Equation (3.2) is thus used to compute from the differences of GPS heights in Table 2.5 an estimate of the orthometric height of the i-th intermediate GPS point. The scaling factor S guarantees the closure of the GPS differences of height between the two reference points provided the effect of ionospheric refraction is constant for each observing session (this hypothesis is highly speculative but not unreasonable as all GPS session took place during the same period of the day).

In Table 2.5 we report the observed GPS heights and the computed (rescaled) values using the equation (3.2).

Table 2.5. Ellipsoidal and orthometric (in the sense of ellipsoidal times a scale factor) heights of the intermediate GPS stations along the gravimetric profile. The adopted scale factor is (4232-3809)/(4220-3794)=0.993.

Trigonometric height	*GPS observed height h (ellipsoidal)*	*Scaled height H (orthometric)*	*Site*
4232	*4220*	*4232*	*Gasherbrum*
	4121	*4134*	*GPS 4 (Gasherbrum jangal)*
	3845	*3860*	*c.b.8 (Upper Shaksgam valley)*
3809	*3794*	*3809*	*Tek-ri*
	3955	*3969*	*Sarpo Laggo*
	4341	*4352*	*Urdok*
	4368	*4379*	*Skyang*
	3924	*3938*	*Jangal base Aghil*
	4103	*4116*	*GPS 3A (Aghil plateau)*
	3634	*3650*	*GPS 2A (confluence)*
	3481	*3498*	*GPS 1A (Bazar Dara)*

To complete our altimetric profile, we now have to compute the altitudes of the gravimetric sites included between two consecutive GPS points using only barometric and thermometric data. We follow the same method used before to compute the heights of the GPS stations. The GPS stations are treated as reference points of known (see Table 2.5) orthometric height and the height differences between two consecutive sites are deduced from the barometric and thermometric data.

To compute from the barometric data the values of the differences in height between i-th and (i+1)-th sites we have followed the approach of Caputo (Marussi, 1964) based on the Laplace formula:

$$\Delta H_{i,i} + 1 = 18400(1.00157 + 0.00367T_m)(1 + 0.377\frac{\varepsilon_m}{P_m})log\ (\frac{P_i}{P_{i+1}}) \qquad (3.3)$$

The term 0.00367 represents the air dilatation coefficient at 1°C, the coefficient 0.377 comes from the difference 1- 0.623, where 0.623 is the water vapour density compared with dry air at the same temperature and pressure. The constant 18400 (barometric constant) takes into account the air density in normal conditions and its CO_2 content. T_m (C°), P_m (millibar), and ε_m (millibar) are respectively the mean values of temperature, pressure and vapour pressure measured at the two considered sites. The relative humidity U_i at the i-th site can be expressed as a function of the water vapour pressure with the following equation:

$$\varepsilon_i = 0.0611 \cdot U_i \cdot 10\ (\frac{7.7T_i}{237.3 + T_i}) \cdot \frac{760}{1013.2} \qquad (3.4)$$

With equation (3.3) we estimate the differences in altitude between two consecutive points. The differences obtained in this way are reported in column 2 (way on) and respectively 3 (way back) of Table 2.6. Consecutive altimetric data with the Thommen altimeter were made at intervals of about one hour and, therefore, ought to be on average not too influenced by major atmospheric changes which rarely were so sudden.

The Thommen data have been differentiated from each other in order to give the height differences listed respectively on column 4 (way on) and column 5 (way back). In the same Table, at the end of each column of the data included between two reference GPS points, we report also the total difference we obtain summing up all the above difference values. This number can vary considerably depending on the instruments and period of observation. In general, to compute the scaling coefficient, we have taken the mean whenever the range of variation of data referring to the same stations but different instruments or epochs is limited. Otherwise Thommen (way back) was selected.

This number divided by the difference of the scaled GPS heights of the two extremal points (Table 2.5, column 3) gives the scale between the barometric data and the rescaled GPS height differences. If the two numbers differ by more than, say, 30%, we suspect that the atmospheric conditions have altered our measurements and the whole column of data is rejected as unreliable.

The short series of trigonometric levelling is reported in column 8 and can be used as a reference term to estimate the quality of the barometric levelling.

The Thommen (way back) data clearly appear in this test to be closest to the levelled height differences. The values reported in column 6 of Table 2.6 are those we consider as more reliable. They are used to evaluate the absolute heights of the j-th gravimetric point between consecutive GPS stations (i,i+1) as follows:

S=(algebraic sum of all intermediate barometric height differences between GPS sites i,i+1) / (H_{GPSi+1} - H_{GPSi})

$H_j = H_{GPSi}+S \cdot$ (algebraic sum of intermediate barometric height differences between sites i and j) $i \leq j \leq i+1$

We insert among the reference points also the gravimetric station established at the Aghil pass whose altitude reported in the map is 4780 m. This is a working hypothesis because we do not know if the given altitude corresponds exactly to our gravimetric point. Making this assumption yields however a stronger constraint to the altimetric and barometric differences.

In Table 2.7 we give the altitudes of the sites measured with the Thommen (way back). The heights labeled "Gilgit Airport" are estimate using again the Laplace formula by comparison of our barometric data with the same quantities measured at the Gilgit Airport (Pakistan), which has a known height, at fixed epochs each day. In Fig. 2.5 we plot the height of the gravimetric points as a discrete function of the site progressive number. The correlation coefficients between the assumed heights (column 3 of Table 2.7) and those listed in columns 1 (barometric heights relative to Gilgit) and 2 (Thommen way back) result: ρ Thommen = 0.99; ρ Barometric = 0.98. showing a statistically significant agreement between the barometric and the assumed heights.

Table 2.6. Barometric differences of height.

STATION POINTS	Pennwalt barometer (m)		Thommen (m)		assumed	scaling coefficient S	trigonometric
	way on	way back	way on	way back			
PON. BAZ. DAR.				-55	-55		
MUR. SOST				-48	-48		
OMET. 01				56	56		
GPS 1A							
OM 02		14		40	40		
1LIV		-2		20	20		19.454
2 LIV		-9		11	11		18.089
3 LIV		-19		4	4		10.922
4 LIV		-16		-55	-55		-63.323
5 LIV		-14		15	15		8.963
6 LIV OM. 03		29		-20	-20		-22.270
OM. 04		19		22	22		
7		19		22	22		
8		43		65	65		
8 EX		-21		-73	-73	S=152/196	
CASA ILICA		-143		-69	-65		
C. B. 2/ILICA		-2		-28	-28		
9		-14		65	65		
10		65		40	40		
11		31		32	32		
12		44		33	33		
13 (GPS) 2A		27		27	27		
DH		51		196	196		
13 (GPS) 2A							
C.B. JANGAL		36		8	8		
14		63		55	59		
C.B.3		75		66	71		
15		106		89	97		
16		40		52	46	S=466/480	
17		115		103	109		
18		41		90	90		
GPS 3A		2		0	0		
DH		478		463	480		

Table 2.6 (continued).

STATION POINTS	Pennwalt barometer (m)		Thommen (m)		assumed	scaling coefficient S	trigonometric
	way on	way back	way on	way back			
GPS 3A							
19	73			25	73		
C.B. OVILE RT	–			20	20		
20 C.B. 4 AND	98			55	78	S=664/765	
21	177			–	177		
22	226			–	226		
23 GR. SASSO	170			132	170		
24 PS. AGHIL	21				21		
DH	765				765		
VERT. CINESE	35						
25		-375		-320	-348		
26 GR. MS		-260		-165	-165		
27 C.B. 5		-235		-193	-214		
ST 41		26		10	18		
C.B. 6 DRB. JN		47		20	20	S=628/659	
ST 40		58		-5	-5		
ST 39		-18		-5	-5		
ST 38		9		20	20		
ST 37		26		15	15		
ST 30 GPS 4		9		5	5		
DH		-714		-670	-659		
ST 30 GPS 4							
ST 31	-78	7			7		
ST 32	17	-13			-12		
ST 33	4	24			23	S=98/100	
ST 34	40	38			37		
ST 36 GPS GAS	18	45			45		
DH	0	100			100		

Table 2.6 (continued).

STATION POINTS	Pennwalt barometer (m)		Thommen (m)		assumed	scaling coefficient S	trigonometric
	way on	way back	way on	way back			
ST 36 GPS GAS							
27 C.B. 5	-180	–	–	–	-180		
ST 42	4	-31	120	-70	-70		
ST 43	44	-5	-15	-10	-10		
ST 44	-35	17	-25	-10	-10		
ST 45	-16	-49	-20	-40	-45	S=372/389	
ST 46	-29	-58	-20	-5	-5		
ST 47	-27	-47	-20	-40	-44		
C.B. 8	-119	16	-85	-25	-25		
DH	-357	-336	-65	-380	-389		
C.B. 8							
ST 48	-31	-28	-15	-10	-13		
ST 49	-7	-19	-15	-30	-23		
ST 50	-0	-15	-10	-22	-16		
ST 51	-7	-24	-20	-18	-19,	S=51/68	
ST52	7	-39	-15				
ST 53	-37	-0	0	2	1		
C.B. 9 GPS	37	48	20	15	17		
DH	-38	-77	-55	-78	-68		
C.B. 9 GPS							
ST 54	17		10		13		
ST 55	39		15		27		
C.B. 9							
ST 56			80	58	69		
ST 57			15	30	23		
ST 58			15	15	15	S=160/152	
ST 59			10	-175	-175		
C.B.10 GPS			10	220	220		
DH			130	148	152		
C.B. 10 GPS							
ST 60	–	–	140	10	10		
ST 61	–	–	40	25	33		
ST 61 B	–	–	15	10	13		
ST 62	–	–	25	25	25		
ST 63	–	–	80	85	53		
ST 64	–	–	130	–	130		
DH			430	155	264		

Table 2.7. Final values of the heights of the gravimetric stations of the Shaksgam valley profile (last column) compared with corresponding values computed with the Laplace formula and simultaneous Gilgit airport data (column 2) and read on the pocket altimeter Thommen on the way on and back (column 3 and 4 respectively).

STATION POINT	PENNWALT (GILGIT AIRPORT) (m)	THOMMEN WAY ON (m)	THOMMEN WAY BACK (m)	ADOPTED VALUES OF HEIGHT (m)
PON. BAZ. DAR	3607	3380	3595	3545
MUR SOST	3585	3320	3540	3490
OMET. 01	3495	3300	3492	3442
0 LIV. GPS	3486	3500	3548	3498
OMET 02	3620	3300	3540	3529
1 LIV	3633	_	3560	3545
2 LIV	3622	_	3571	3553
3 LIV	3615	_	_	3556
4 LIV	3589	3370	3520	3513
5 LIV	3566	3385	3535	3525
6 LIV OM. 03	3609	3280	3515	3517
OM. 04	3535	3340	3568	3558
7	3646	3390	3590	3576
8	3691	3440	3655	3626
8 EX	3659	3390	3582	3569
CASA ILICA	3532	3320	3513	3519
C.B. 2/ILICA	3549	3280	3485	3497
9	3528	3355	3550	3548
10	3588	3440	3590	3579
11	3596	3500	3622	3603
12	3619	3510	3655	3629
13 (GPS) 2A	3649	3540	3682	3650
C.B. JANGAL	3661	_	3657	
14	3784	3525	3745	3715
C.B. 3	3856	3580	3811	3784
15	3943	3680	3900	3878
16	3972	3750	3952	3923
17	4088	3855	4055	4029
18	4114	3945	4145	4116

Table 2.7 (continued).

STATION POINT	PENNWALT (GILGIT AIRPORT) (m)	THOMMEN WAY ON (M)	THOMMEN WAY BACK (m)	ADOPTED VALUES OF HEIGHT (m)
GPS 3A	4139	_	4145	4116
19	4181	4000	4180	4179
C.B. OVILE RT	4170	_	4220	4197
20 C.B. 4 AND	4340	4050	4275	4264
21	_	4180	_	4418
22	_	4420	_	4614
23 GR. SASSO	4836	4590	4810	4762
24 PS. AGHIL	_	4600	_	4780
VERT. CINESE	_	4675	_	4815
25	4464	4360	4490	4430
26 GR. MS	4266	4110	4215	4273
27 C.B. 5	4076	3920	4050	4069
ST 41	4060	_	4060	4086
C.B. 6 DRB. JN	4113	_	4080	4105
ST 40	4168	_	4105	4100
ST 39	4127	_	4100	4095
ST 38	4161	_	4120	4114
ST 37	4144	_	4135	4129
ST 30 GPS 4	4128	4110	4140	4134
ST 31	4125	_	4165	4140
ST 32	4142	_	4170	4129
ST 33	4123	_	4180	4151
ST 34	4135	_	4195	4187
ST36 GPS GAS	4121	_	4214	4232
27 C.B. 5	4076	3920	4050	4060
ST 42	3929	4040	3980	3992
ST 43	3959	4025	3970	3983
ST 44	4026	4000	3960	3974
ST 45	3973	3980	3920	3931

Table 2.7 (continued).

STATION POINT	PENNWALT (GILGIT AIRPORT) (m)	THOMMEN WAY ON (m)	THOMMEN WAY BACK (m)	ADOPTED VALUES OF HEIGHT (m)
ST 46	3926	3960	3915	3926
ST 47	3883	3940	3875	3884
C.B. 8	339	3855	3850	3860
ST 48	3875	3840	3840	3850
ST 49	3867	3825	3810	3833
ST 50	3820	3815	3788	3821
ST 51	3777	3795	3770	3806
ST 52	3771	3780	3768	3795
ST 53	3736	3780	3770	3796
C.B. 9 GPS	3766	3800	3785	3809
ST 54	–	3820	–	3822
ST 55	–	3835	–	3849
ST 56	–	3845	–	3868
C.B.9	3766	3800	3785	3809
ST 56	–	3920	3915	3881
ST 57	–	3935	3945	3906
ST 58	–	3950	3960	3921
ST 59	–	3960	3785	3737
C.B.10 GPS	–	3970	4005	3969
ST 60	–	4000	4015	3979
ST 61	–	4040	4040	4012
ST 61 B	–	4055	4050	4025
ST 62	–	4080	4075	4050
ST 63	–	4160	4160	4103
ST 64	–	4290	–	4233

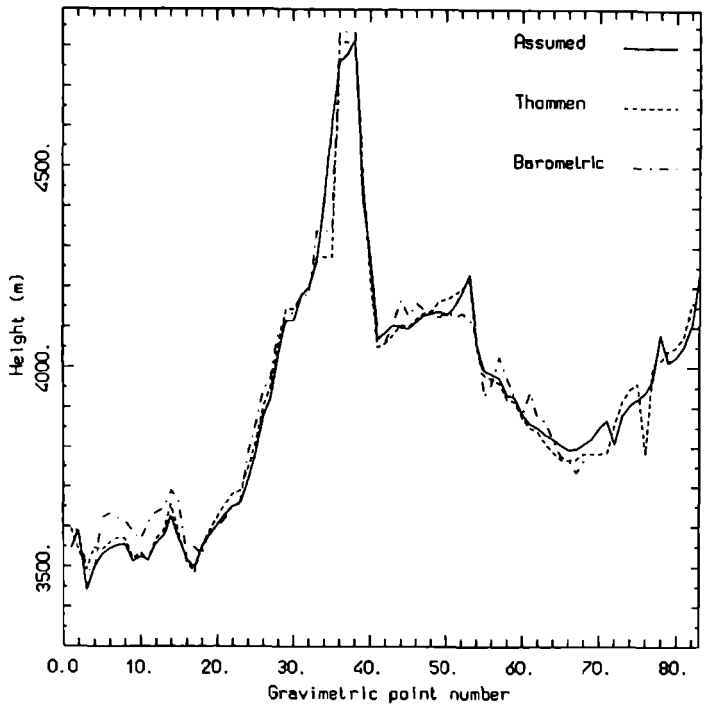

Fig. 2.5. Comparison of barometric height estimates of the gravimetric sites determined with a pocket Thommen altimeter a precise barometer. Also shown in the curve judged to represent the more reliable values of the heights.

4. Gravimetry

4.1 THE IGSN71 SYSTEM

The scientific program of the geodetic-geophysical Expedition Ev-K^2-CNR 1988 includes the measurements of the gravity field along the profiles shown in Fig. 2.6 and 4.22. This chapter is devoted to the discussion of instrumentation used, of the definition of the reference datum and of the data reduction. The gravity prospection has been performed with the Lacoste-Romberg (LCR) mod. G-297, courtesy of dr. P. Squarci, director of Istituto Internazionale per le Ricerche Geotermiche - CNR Pisa, and dr. Rossi, research scientist of the same Institute.

A primary topic of fundamental importance for the geodetic metrology concerns

the problem of defining the gravity datum. In order to standardize all gravity measurements and surveys, they must be referred to a global reference system. From 1909 to 1971 the Potsdam System served as the international reference system. It was based on a reversible pendulum measurement at the Geodetic Institute at Potsdam (Kuhnen-Furtwangler 1898-1904). More recent absolute gravity determinations showed that the value of Potsdam is roughly 14 mGal too large. Therefore between 1950 to 1971 approximately 24000 relative measurements have been collected with gravity meters, 1200 with relative pendulum apparatus, 10 with absolute, related to 1854 points (500 primary stations).

The adjustment of this worldwide net led to the definition of a new global reference gravity system: the International Gravity Standardisation Net 71 (IGSN71) (Morelli et al. 1974). The standard errors of this resulting net are less than .100 mGal over the gravity range of the earth. Therefore the tie to the IGSN71 is of primary importance both from the metrologic (definition of the standardized gravity datum) and from the geophysical points of view since all the gravity observations can refer to a common reference system. This is of peculiar importance if a merging of all the gravity data observed in these last years will be performed. Nowadays this problem could be solved by means of modern transportable absolute gravimeters which enable the measurement of the gravity acceleration with an accuracy of few parts in 10^9, thus allowing the definition of the gravity datum with an accuracy higher than the IGSN71 system itself.

In the area of our interest there are no IGSN71 base stations, the nearest ones being Dehra Dun (13708 A) and Amristar (13714 J) (Morelli et al., 1974). The fundamental station of the prospection (Rawalpindi–Pearl Continental Hotel) has been connected to the IGSN71 station in Trieste (17953 A) through the following tie: Trieste–Roma–Rawalpindi–Lahore–Karachi–Roma–Trieste. The closure error resulted equal to 0.70 mGal. The gravity profile has been thus measured along the road Rawalpindi–Gilgit, observing also four intermediate stations (Fig. 2.6).

The observation at Gilgit performed at the base station established by A. Marussi (1954) has given the opportunity to compare once again the Potsdam (used by Marussi) and IGSN71 (used by us) reference systems. The difference resulted equal to -13.81 mGal, a value well comparable with the observations performed in Europe. The observation of the gravity value in this fundamental site allows us to refer to the IGSN71 system all the gravity data collected by Italian expeditions (Fig. 2.6) and therefore provides a valuable tool for the homogenization of the observations. Gilgit has been the starting point for the gravity profile which has been performed along the KKH (Karakorum Highway). This procedure has allowed us to

determine the gravity datum in 14 base stations from Gilgit to the bridge of Bazar Dara (Fig. 2.6). Pictures and station descriptions are also available in the Appendix B. The bridge of Bazar Dara site is the starting base station for the gravity profiles shown in Fig. 4.22.

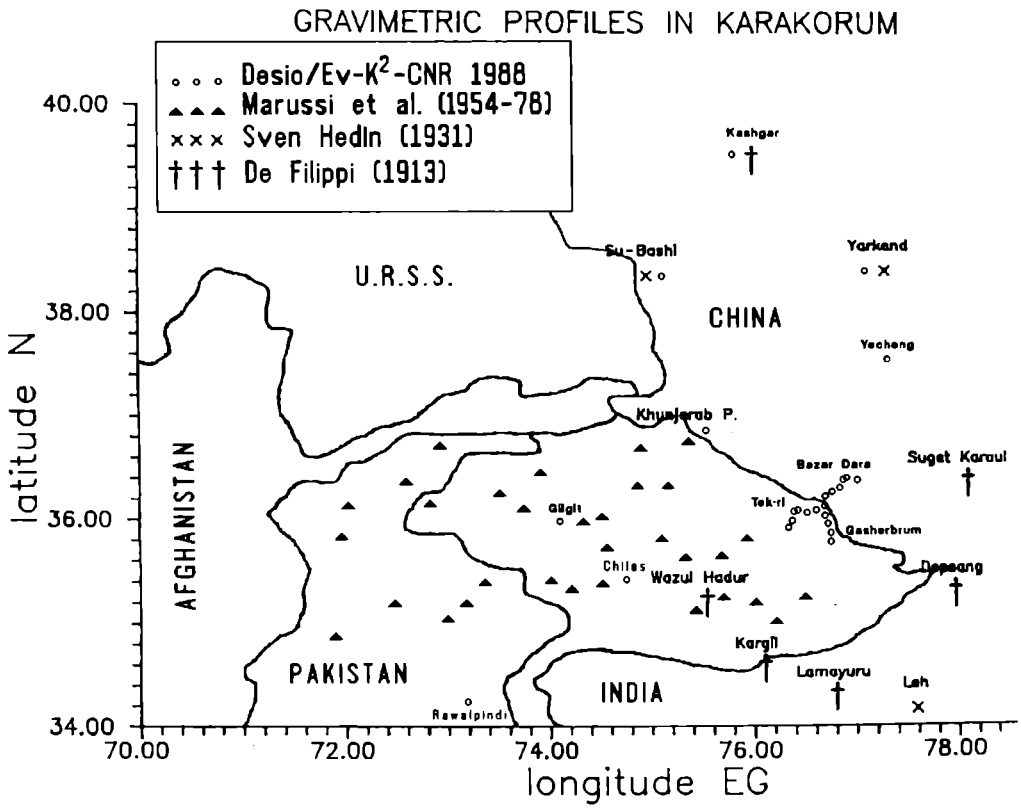

Fig. 2.6. The more important gravimetric profiles in Northern Pakistan and Sinkiang are shown. The profiles across the border line between Kunjerab Pass and Depsang belong to the 1988 work are described with more detail in fig. 4.22.

The gravity observations have been performed on 73 sites, spaced about 1,5-2 km. A number of 32 stations have been occupied twice, which has shown an average discrepancy of g's equal to 0.20 mGal. The gravity observations were taken on 5 sites where height was measured with GPS, 67 sites where the height was measured by means of altimetric-barometric technique and 2 by trigonometric methods. The positions and coordinates of the stations were determined on the map 1:75,000 of the Italian expedition (Desio 1929) and on the satellitezed spots with a scale of 1:100,000. The errors in latitude determinations of the various stations are negligible in the determination of the normal gravity, which was taken, according to the IGSN71 system, from Moritz (1980) and computed by means of the formula:

$$g_t = g_e (1 + A\sin^2 \phi + B\sin^4 \phi + C\sin^6 \phi + D\sin^8 \phi)$$

where: g_e = 978032.677 normal gravity value at equator, A= 0.0052790414, B= 0.0000232718, C= 0.0000001262, D= 0.0000000007.

This formula has a relative error corresponding to 10^{-4} mGal.

4.2. THE LACOSTE-ROMBERG

The most stable and widely used gravity field instrument is the Lacoste-Romberg. Basically it is a long period seismograph which utilizes a "zero-length" spring. This spring is characterised by a stress-strain curve that is a straight line passing through the origin so that the initial length, corresponding to zero force, is zero: this means that the force (according to Hooke's law) is directly proportional to the length of the spring. This condition is obtained by prestressing the spring in winding so that a initial force is required before the coils begin to separate. As a result of this feature it is possible to design an instrument with a period theoretically infinite. To describe this important feature see Fig. 2.7, in which the gravitational torque is given by

$$T_g = Mgd \cdot \sin(\theta) = Mgd \cdot \cos(\alpha) \qquad (4.2)$$

and the torque from the spring is given by

$$T_s = k \cdot s \cdot r \quad s = \frac{b \cdot \cos(\alpha)}{\sin(\beta)} \quad r = a \cdot \sin(\beta)$$

At equilibrium

$$T_g - T_s = 0 \quad Mgd \cdot \cos(\alpha) = k \cdot b \cdot a \cdot \cos(\alpha) \quad Mgd = k \cdot b \cdot a$$

so the instrument is insensitive to the angles α, β, θ.

Thus the beam can be in equilibrium over a small range of angles and consequently its period can be nearly infinite. In the Lacoste-Romberg the period is

adjusted to 15 secs which, in practice, results in a sensitivity to $\delta g/g$ of the order of 0.001 ppm. A schematic drawing is given in Fig. 2.8.

The meter-housing carries the levelling screws, levelling bubbles, temperature probe to verify that the instrument is at its operating temperature (52°), an arrestment knob which permits the beam to be clamped during the transportation and the dial connected to the counter. In the same housing there is the beam, with the beam weight at one end held horizontally by a main spring of "zero length", made of a special alloy of the elinvar type. The upper end of the spring is connected to a micrometer screw which, by means of the beam, is brought to the zero position. Thus the LCR has a zero system of readings which ensures linearity of scale.

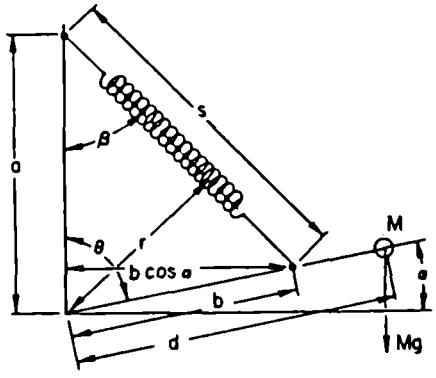

Fig. 2.7. Schematic diagram of "zero lenght" spring theory.

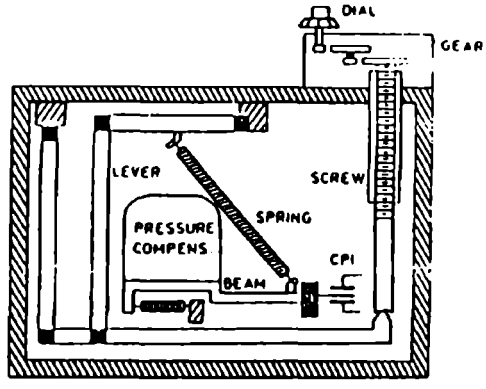

Fig. 2.8. Semplified diagram of Lacoste-Romberg meter.

A recent version of this instrument adopts an electronic readout which consists of a set of capacitor plates installed above and below the beam and a nulling meter. As the beam moves between these plates, the change in capacitance is recorded on the nulling meter installed on the top of the meter housing. This nulling meter is then adjusted so when the beam is in the null position the nulling meter will be in its center. The sensitive device, situated in a sealed chamber, is thermostatically controlled to make the meter insensitive to changes in the outside temperature, a hollow (buoyancy compensating) cell is attached to the moving system to make the meter insensitive to changes in atmospheric pressure. The system has a shock assorbing spring that forms a floating pivot thus eliminating any friction in the moving system. The lever system and measuring screw are accurately calibrated over the entire range:

calibration factors depend only on the quality of the measuring screw and the lever system. The meter is powered by rechargeable batteries to ensure the on-heat of the instrument.

The Lacoste-Romberg manufactures the widely used land gravity meter mod. G, which is a relative gravity meter designed to be utilized anywhere on the land surface of the earth. To satisfy this requirement it was designed to have a measuring range of approximately 7 Gal (977 to 984 Gal) with resulting resolution of .010 mGal. With very careful measurements it is possible to have a precision of .005 mGal. The drift rate is of the order of 1 mGal/year and depends on the age, the means and manner of transportation and on environmental conditions. To check the behaviour of Lacoste-Romberg, some loops have been carried out, on the same day, following the procedure abcd..dcba. The drift curve, obtained after the application of the earth tide correction, shows the great stability of the instrument, the ininfluence of the manner of transportation and environmental conditions, although a very weak correlation between temperature and readings seems to exist (Fig. 2.9).

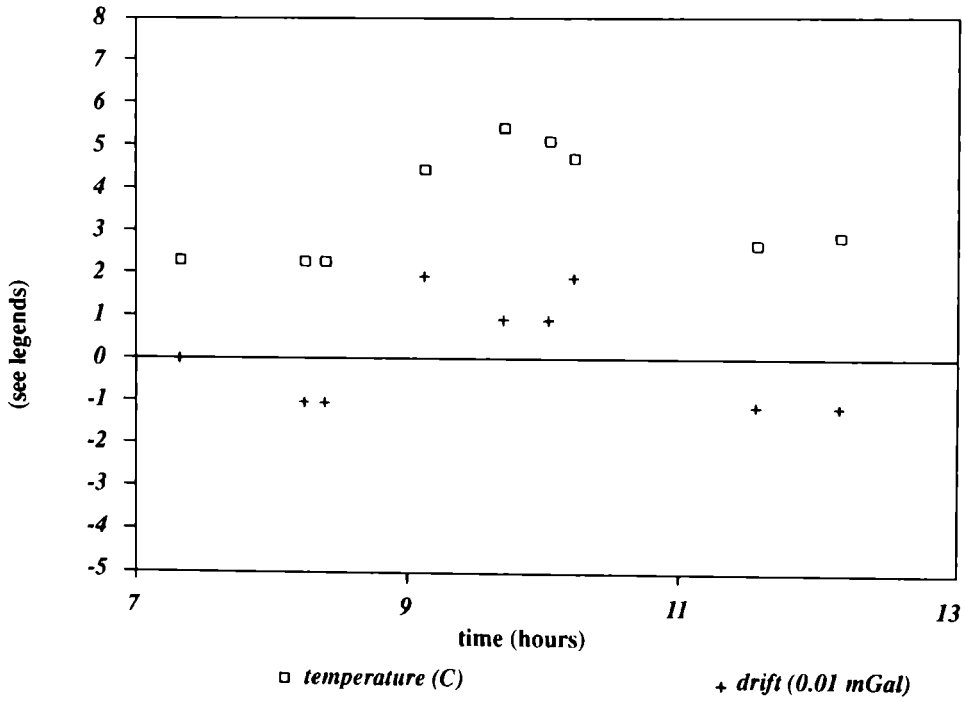

Fig. 2.9. Drift curve of the LCR - G 297 correlated in time with atmospheric temperature.

4.3. DATA REDUCTION

4.3.1. *GENERALITIES ON GRAVITY ANOMALIES*

A relative gravity survey consists of a certain number of base stations, covering the area to be studied, which are connected by relative ties. The density of the stations depends on the depth of the geological features to be investigated. Relative surveys are connected to a reference point where the value of gravity is known and they are usually organised as series of closed loops in order to control the propagation of errors and the instrumental drift. Reading differences are converted into gravity differences using the instrument calibration table. The data must also be corrected for the gravity tidal effects, due to the moon and sun (Longman, 1959). Only after the application of the drift correction the value of gravity for each point can be calculated. To produce a map or a profile of the anomaly gravity it is necessary to know the elevation and the position of each gravimetric point.

The observed gravity values reflect the local and regional irregular distribution of masses. Therefore, the first step, called gravity reduction, is to remove from the data these extraneous disturbances and reduce the values to a reference surface. Very briefly (for more detailed see Dobrin 1976, Grant and West 1965, Mironov 1977, Morelli 1968, Nettleton 1976, Sazhina- Grushinsky 1971, Telford et al. 1976) they are:

1) *Free air correction.* This reduction takes into account that the attraction of the earth at a point decreases with height, according to the inverse square of its distance from the center of the earth: its magnitude is obtained from the expression F-H where F is the mean gravity gradient of the earth (.3086 mGal/m) and H is the height of the point from the datum surface. The free air correction is positive for positive elevations.

2) *Bouguer correction.* This reduction accounts for the material between the station and the datum plane, that was ignored in the free air correction. It is derived by assuming a slab with infinite horizontal extent. Its magnitude is obtained from the expression $B \cdot \rho \cdot H$, where B is a factor equal to 0.4193, ρ is the density slab, H has the same meaning of the free air reduction. It is negative because the gravity values has been increased by the effect of this slab. Two assumptions are made in the formulation of this reduction: the first assumption is that the slab has uniform density, the second assumption is that it has infinite horizontal extent. Neither is true. In order to modify the first assumption one would need a good knowledge of local geology as to the rock types and densities; the second assumption is the object of the next reduction.

3) *Terrain correction*. This correction allows for surface irregularities on the Bouguer slab. The topographic undulations (hills and valleys) affect the gravity value in the same sense reducing the readings because of upward attraction (hills) or lack of downward attraction (valleys). Hence this correction is always added to the station measurement. The usual procedure is to divide the geographical area into compartments on a uniform grid and calculate the average elevation. From the coordinates of the point and its elevation the distance and elevation difference to each unit of topography are determined and the effects calculated and summed. In order to avoid a laborious process by means of templates, suitable algorithms for digital computers have been suggested by several authors (Bott 1959, Nagy 1966, Banerjee et al. 1977).
4) *Isostatic correction*. This correction is necessary to regularize the earth's crust according to some model of isostasy (usually Airy-Heiskanen system): the topographic masses are not completely removed, as in the Bouguer correction, but are shifted into the interior of the geoid in order to make up the mass deficiencies that exist beneath the continents. The final result is, ideally, a homogeneous crust of density 2.67 $\frac{gr}{cm^3}$ and varying thickness.

The resulting gravity value $g_{cor} = g_{obs}$+(1)-(2)+(3)+(4) is then compared with the theoretical value g_t, obtained from the standards formulas of gravity (Moritz 1980). The difference g_{cor}-g_t is the gravity anomaly, due to lateral subsurface density variation, that represents the downward component of the force of attraction produced by underground features.

4.3.2. *COMPUTATION OF THE ANOMALIES*

The free air correction was calculated with the formula (Kertz W., 1969)

$$Cf = 0.002 \cdot \frac{g_t}{R^2} H + 0.000006 \cdot \frac{g_t}{R} \cdot H^2 \qquad (4.4)$$

where g_t = theoretical gravity, R = radius of the earth for the latitude station in km, H = height of the station in m.

The Bouguer correction was calculated using the Cassini's formula for a finite spherical cap (Bouguer calotte) with a radius of 166,736 km and a density of 2.67 $\frac{gr}{cm^3}$.

The parameters of this complex formula are the thickness H of the spherical cap equal to the height of the station and the geographic latitude of the station to calculate the local radius. The difference, considering all stations, between the Bouguer correction with Cassini's formula and the classic formula, which neglects the earth's

curvature, varies from -6.54 to -6.90 mGal. In order to perform the terrain correction, an area of 80x130 km was subdivided into rectangular prisms with various dimension (varying from 1 to 4 km). The mean height of each prism was computed "weighting" the values found in it and was read off several maps, due to the lack of an homogeneous cartography, of different scale: maps 1:500,000 of Government of Pakistan, maps 1:250,000 of US. Army Maps, map 1:100,000 of the Baltoro glacier by prof. A. Desio and Italian Military Geographic Institute. With this data base the terrain effects have been calculated up to 20 km of distance from the stations. For the outside region, up to 166,736 km, the correction was done using the digitized topography ETOPO5 provided by NOAA, on a square grid with a nominal grid spacing of 5'x5'.

To the estimation of terrain correction effect, with density of 2.67, the algorithm suggested by Banerjee et al. (1977) was used.

This equation was chosen for the high flexibility and simplicity:

$$g_t = \gamma \cdot \rho \left[x \cdot \ln\left(y+\sqrt{x^2+y^2+z^2}\right) + y \cdot \ln\left(x+\sqrt{x^2+y^2+z^2}\right) - z \cdot \tan^{-1}\frac{xy}{z\sqrt{x^2+y^2+z^2}} \right]_{x_1}^{x_2} \Bigg|_{y_1}^{y_2} \Bigg|_{z_1}^{z_2} \qquad (4.5)$$

From this expression, changing the limits of integrations, it is possible to obtain the classical formula of the Bouguer correction; this contains only one inverse trigonometric term, faciliting the computer work; last, but not least, if the sign of x_1 and x_2 are different (y-axis is crossed), for instance, the prism is not divided, as in the well known Nagy's formula (1966) where the integral is separately calculated from 0 to x_1 and 0 to x_2 and finally they are summed, because the signs of x's and y's are automatically taken care of by the algorithm.

With the same heights and algorithm we have also computed the isostatic reduction, at present (August 1988) until 166,75 km. We have used the Airy hypothesis with depths of compensation of 20, 30 and 40 km and a density difference of 0.6 between the crust and the upper mantle.

The results of the gravity reductions are summarized in Table 2.8 are shown the results of the regression analysis where the gravity anomaly (free-air, Bouguer, isostatic) is represented by a linear regression equation of the kind:
anomaly = $A+B \cdot H$, where A is the intercept, B is the regression coefficient or the

gravity gradient (the rate of change of the anomaly with elevation H), H is the elevation.

4.4. PRELIMINARY INTERPRETATION

The results of the gravity reductions are summarized in Table 2.8. Correlations of gravity anomalies (free air, Bouguer, isostatic) are also shown: this approach is usually performed in terms of regression analysis where the anomaly is represented by means of a linear regression of the kind: *anomaly* =A+B·H, where A is the intercept, B is the regression coefficent or gravity gradient or the rate of change of the anomaly with elevation H. Also calculated is the coefficient of correlation R which indicates the degree of linear dependence of gravity on elevation. The basic assumption of the isostasy is that if a region is in isostatic equilibrium the Bouguer anomaly should vary linearly with elevation (the larger the correlation coefficient the greater is the degree of compensation). On the other hand a low value of B for free-air anomaly is also considered a basis of a fully compensated region because the anomaly is roughly zero in this case. Recently, theoretical studies (Murthy et al., 1986) have been performed to assess the parameters concerning the status of isostatic equilibrium: these are mainly the BAE (the ratio of average Bouguer anomaly to average elevation over the entire topography) that is equal to -.1037 mGal/m for a fully compensated topography and the degree of isostatic compensation is calculated from the expression: D= -1·(BAE/.1037)100 (D = 0 for a fully compensated region).

The FAE and IAE ratios of average free-air and, respectively, isostatic anomalies to average elevation measure also the degree of isostatic compensation. Nevertheless the limited area of study and the presence of local anomalies due to shallow geological structure limit, in our case, the considerations on the nature and degree of isostatic compensation. The results of the regression analysis are summarized in table 2.7. Considering the several orientations of the profiles (Fig. 4.22), the different tectonic units involved (see geological map) have been taken into account. The data of the overall survey (Fig. 2.10-2.12) and the data of each profile (Fig. 2.13-2.16) (circles denote the general regression line; crosses, the trend of the profile) are shown. From Fig. 2.17 to Fig. 2.24 we present the relative anomalies. Remarkable differences are observed. Each profile has a different numerical aspect not only as intercept but also as gravity gradient (factor B) and correlation coefficent (factor R). Finally, we remark that local anomalies are identified with a confidence proportional to the accuracy of the estimates of the heights, for which we refer to sect. 3.

Table 2.8. Results of regression analysis.

FAYE ANOMALY					
	FAE FAYE AVERAGE ELEV.	A	B	R	NUMBER STATIONS
GENERAL	-0.0286	-370.20	.074	.75	73 BSN
PROFILE 1	-0.0298	-346.92	.073	.95	16 BSN
PROFILE 2	-0.0113	-547.08	.118	.86	20 BSN
PROFILE 3	-0.0240	-787.01	.179	.91	13 BSN
PROFILE 4	-0.0257	-66.83	-.009	-.14	15 BSN

BOUGUER ANOMALY					
	BAE BOUGUER AVERAGE ELEV.	A	B	R	NUMBER STATIONS
GENERAL	-0.1271	-312.05	-.048	-.63	73 BSN
PROFILE 1	-0.1280	-293.45	-.049	-.80	16 BSN
PROFILE 2	-0.1204	-453.96	-.013	-.21	20 BSN
PROFILE 3	-0.1317	-602.86	.024	.29	13 BSN
PROFILE 4	-0.1337	-82.61	-.113	-.80	15 BSN

ISOSTATIC ANOMALY					
	IAE ISOST. AVERAGE ELEV.	A	B	R	NUMBER STATIONS
GENERAL	-0.0205	71.25	-.038	-.74	73 BSN
PROFILE 1	-0.0182	96.65	-.044	-.89	16 BSN
PROFILE 2	-0.0206	54.48	-.034	-.59	20 BSN
PROFILE 3	-0.0244	-307.15	.055	.63	13 BSN
PROFILE 4	-0.0285	293.98	-.103	-.89	15 BSN

A= intercept; B= regression coefficent; R= correlation coefficent

Profile 1. The profile 1 starts from st. 4, located on the Yarkand river between the Bazar Dara river and the confluence of the Surukwat in the Yarkand, to st. 22, on the Surukwat river at the north side of the Aghil pass. It has a direction NE-SW and concerns the axis of the Surukwat.

According to the geological map (Fig. 4.22) this profile interests these tectonic units: Bazar Dara slates, Surukwat thrust sheets, Aghil Dara granodiorite, an area separated by thrust or faults and consisting of a great variety of lithologies. The anomaly profiles are shown in Fig. 2.15-2.16. The Bouguer profile suggests the presence of two important features: the first, from st. 5 to st. 13 with an amplitude of 16 mGal on 10 km with an inflection point located near the st. 11 (at the confluence of Surukwat and Aghil Dara, where the geologists put the limit between Bazar Dara slates and Surukwat thrust sheets, the other from st. 12- 13 to st. 21 with an amplitude of 20 mGal on 15 km with an inflection point between the st. 18-19, located roughly at the confluence of the Aghil Dara river with the river coming from Aghil pass, can be correlated with the crossing Surukwat thrust sheets and Aghil Dara granodiorite. According to Nettleton (1976) and Sheriff (1978) a simple model of fault can be considered in terms of thin semi-infinite slab in which the inflection point indicates the position of the thrown and is calculated with a relation which connects the amplitude of the anomaly and the density contrast. According to this scheme, in the first case the depth is 1.35 km and in the second is 2.1 km. The thrown is, respectively, roughly 1.5 and 1.8 for a density contrast of .25. The verticality of the contact is possible because the half widths have similar values in both cases. The isostatic anomaly reflects the shape of the Bouguer anomaly and lowers the gravity amplitude. The free-air anomaly is quite correlable with elevation (R=.95). Few points (st. 5 and st. 8) are uncorrelated with altimetry, but this is likely to be due to a near topography situation.

Profile 2. The profile 2 begins at st. 22, north side of Aghil pass, crosses this pass and the axis N-S of the Shaksgam river until the beginning of the Gasherbrum glacier. Geologically it meets the Aghil Dara granodiorite and the Shaksgam Sedimentary Belt. The free-air anomaly shows a sharp (30 mGal on 8 km). A sudden anomaly (st. 27-29-31) located in the south side of Aghil pass can be correlated to Bdongo-la slates of Jurassic age.

The stations 22 to 27-30 denote a gradient different from the other points (31 to 43): this is seen in Fig. 2.12, Bouguer anomaly vs. elevations. These five points are located above the cross line uncorrelated with the other values. The explanation of this behaviour is mainly due to the different nature of the tectonic unit, on the other hand from st. 31 to 43 the gradient is constant, with slight oscillation (37-39)

due to very local condition. Applying the same procedure as above the fault parameters indicate a depth equal 6.0 km and the thrown for a density contrast .20 of 3.6 km. The amplitude of the anomaly is 30 mGal with an extension of 28 km. The lack of tectonical structures in both geological maps and the constant gradient suggests another possible interpretation: a deepening of the unit with an angle of about 7°, with a density contrast .20, that corresponds a lowering of 3.7 km to 28 km.

Profile 3. The profile 3, comprised from st. 47 to st. 59, with direction E-W interests the Shaksgam sedimentary belt with these units: Shaksgam Formation, Aghil Limestone, Tek-ri Formation.

Observing Fig. 2.13, anomalies vs. elevation, one can see the presence of two separate groups of points that justify the high B parameter of free-air vs height, the direct correlation between Bouguer and isostatic anomalies vs elevation; these two groups are related respectively to st. 47 until st. 51, following the general trend also as values, and the other from st. 52 to st. 59. These features are depicted also in the profiles of Fig. 2.19-2.20, in which, as shown above, there is, after a flat distribution of five points (st. 47 to st. 51), a jump (st. 51-53) of 16 mGal in 3 km, then the anomaly increases with constant gradient, except for st. 56. This jump with a depth of roughly 1 km, can be associated to the passage between the above described units of the Shaksgam Sedimentary Belt.

Profile 4. The profile 4, from st. 59 to st. 73, concerns the Shaksgam Sedimentary Belt, the Sughet Granodiorite, Sarpo-Laggo-K^2 metamorphics. Relations between anomalies and elevation (Fig. 2.14) denote the presence of 6 points (st. 68 to 73) which have a different behaviour from the others (mainly in the free-air vs. elevation, explaining the low value of B). The Bouguer anomaly shows a negative uniform trend interested by a jump after st. 66: this feature with an amplitude of 35 mGal can be related with the Karakorum fault zone. The depth is 1.6 km and the feature is located near st. 67 on the contact between Sughet Granodiorite and Sarpo-Laggo-K^2 metamorphic.

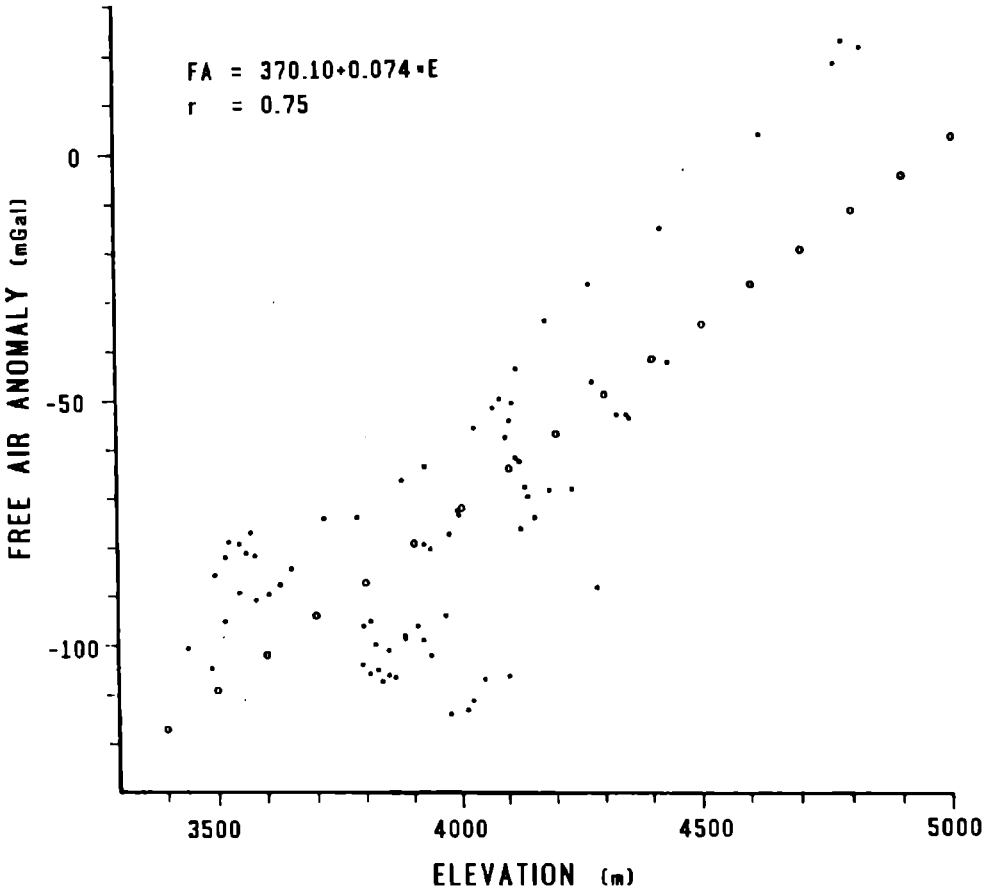

Fig. 2.10. Relationship between the free air anomalies and the elevations of all gravity stations.

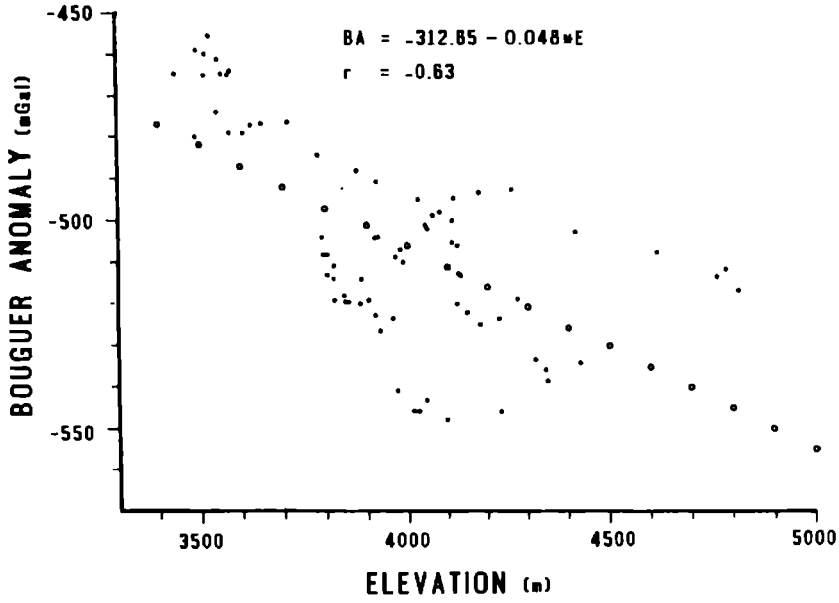

Fig. 2.11. Relationship between the Bouguer anomalies and the elevations of all gravity stations.

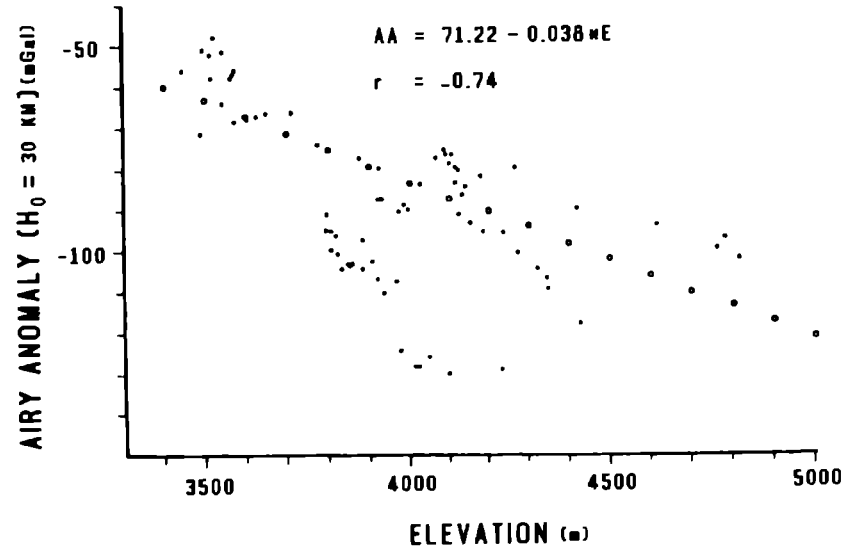

Fig. 2.12. Relationship between the isosastic anomalies and the elevations of all gravity stations.

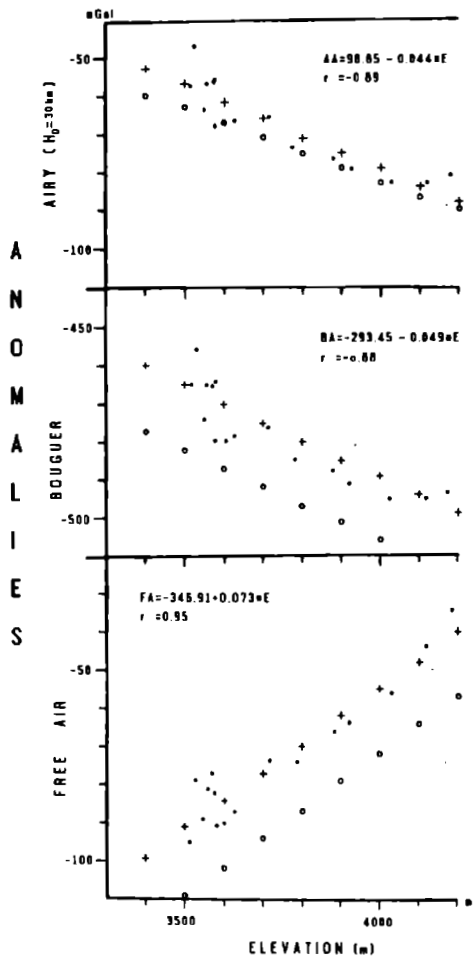

Fig. 2.13. PROFILE 1 - Relationship between free air - Bouguer isostatic anomalies and elevations for Profile 1.

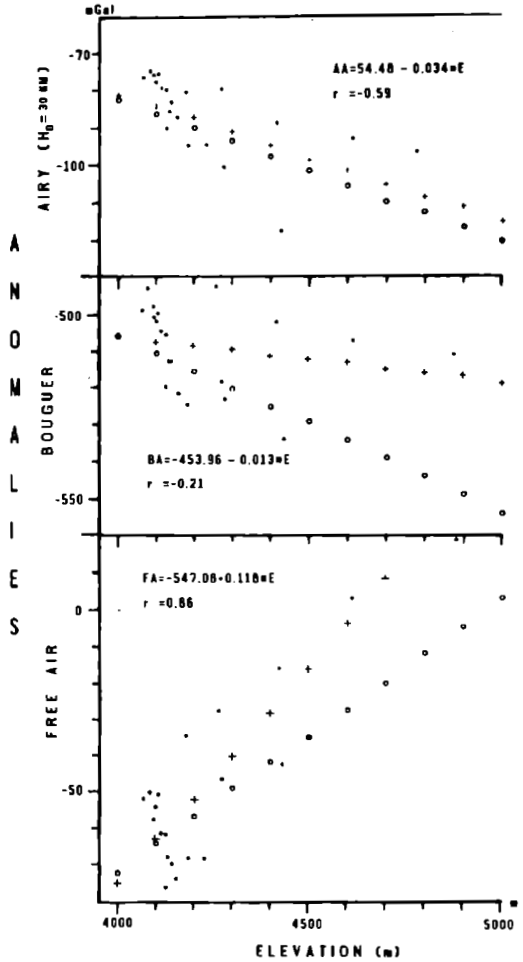

Fig. 2.14. PROFILE 2 - Relationship between free air - Bouguer isostatic anomalies and elevations for Profile 2.

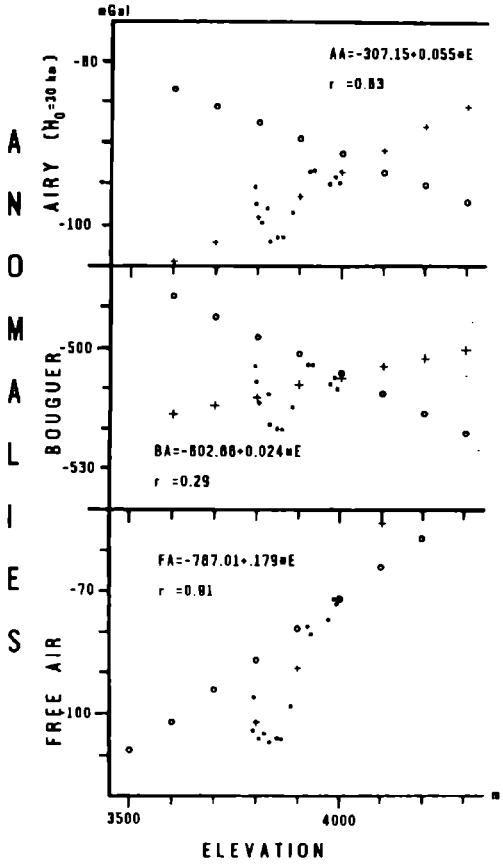

Fig. 2.15. PROFILE 3 - Relationship between free air - Bouguer isostatic anomalies and elevations for Profile 3.

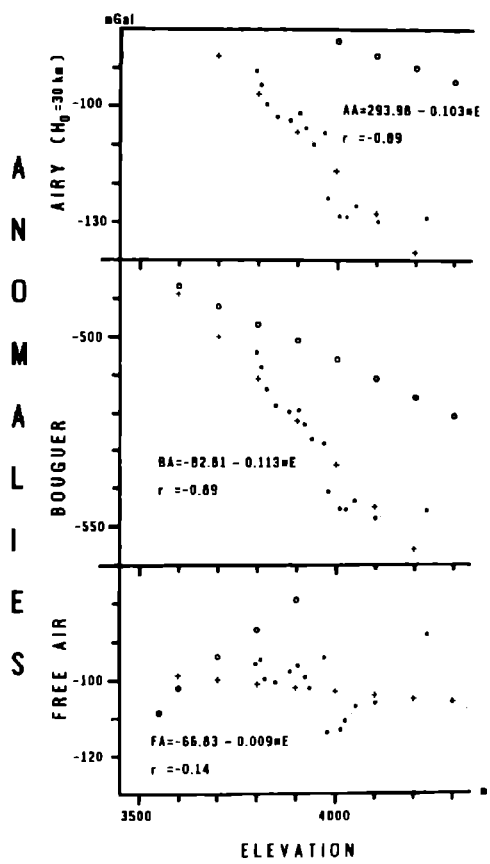

Fig. 2.16. PROFILE 4 - Relationship between free air - Bouguer isostatic anomalies and elevations for Profile 4.

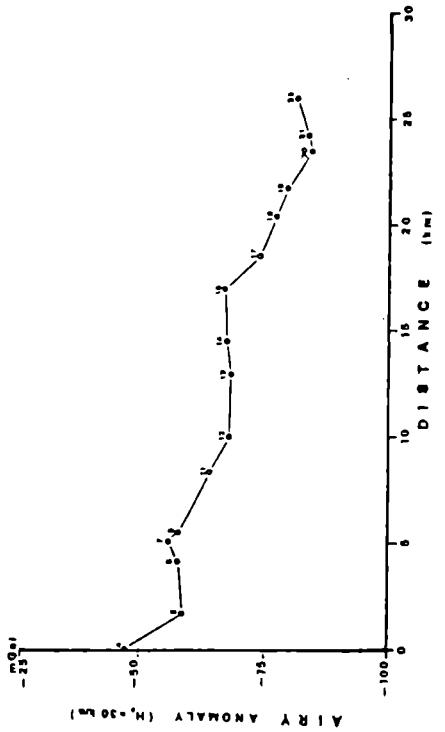

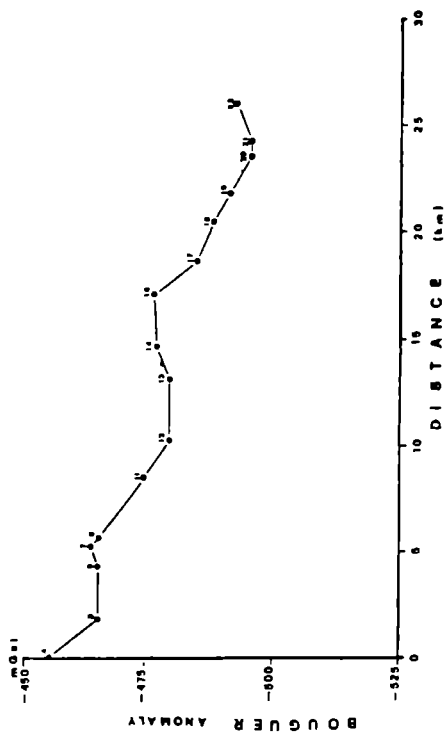

Fig. 2.18. PROFILE 1 (from st. 4 to st. 22) Bouguer and isostatic anomalies profiles.

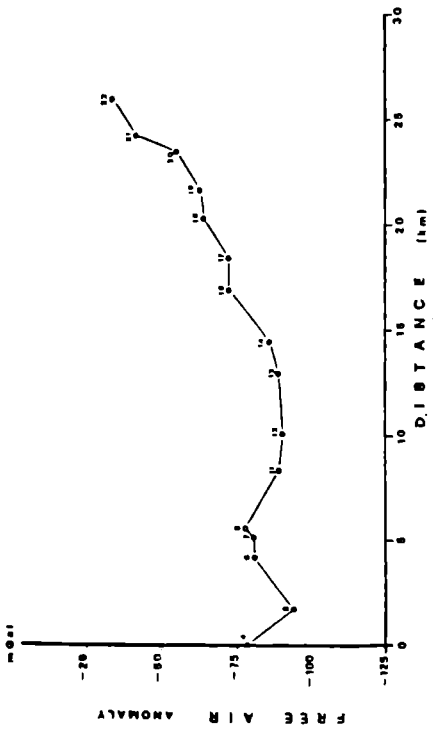

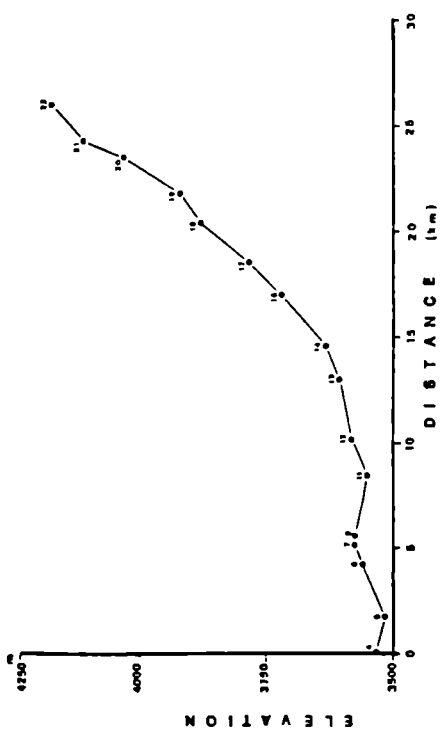

Fig. 2.17. PROFILE 1 (from st. 4 to st. 22) Altimetric and free air anomaly profiles.

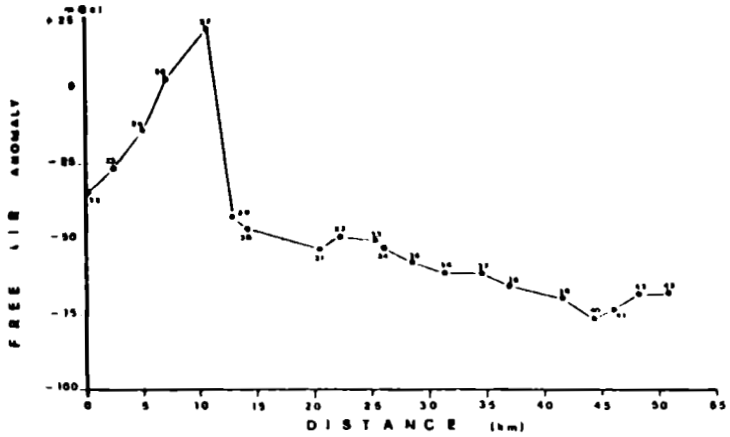

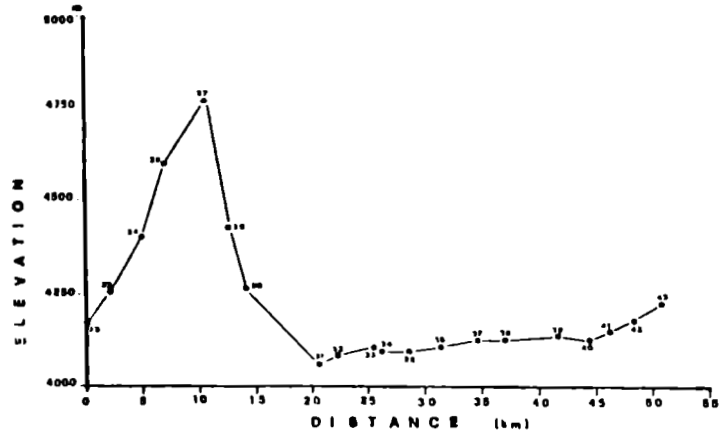

Fig. 2.19. PROFILE 2 (from st. 22 to st. 43) Altimetric and free air anomaly profiles.

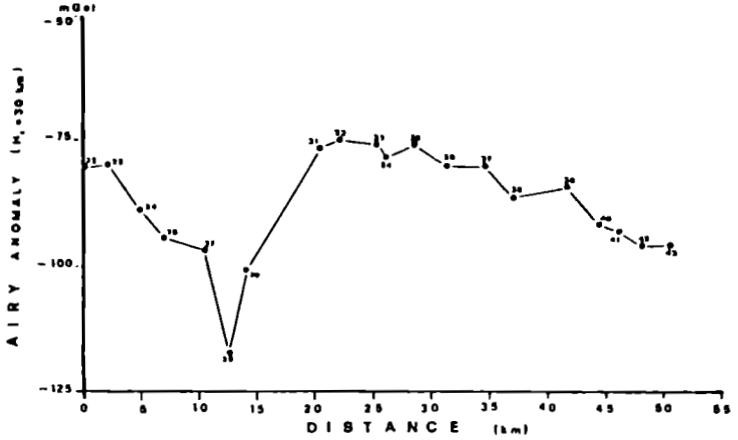

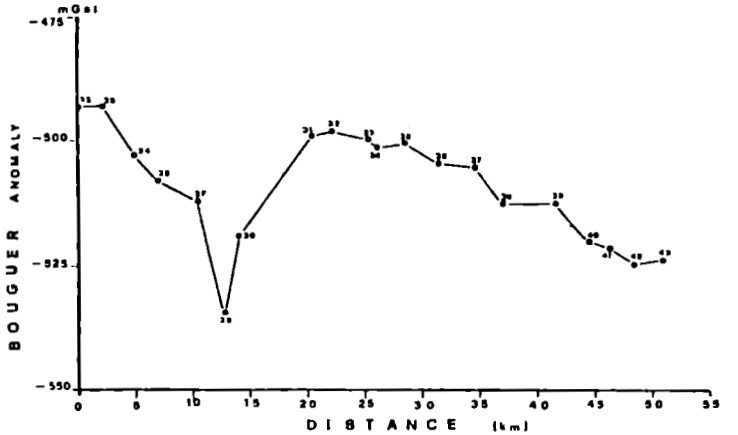

Fig. 2.20. PROFILE 2 (from st. 22 to st. 43) Bouguer and isostatic anomalies profiles.

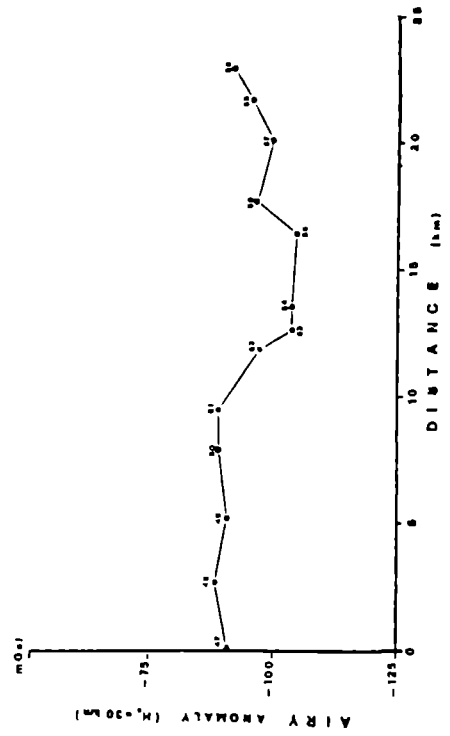

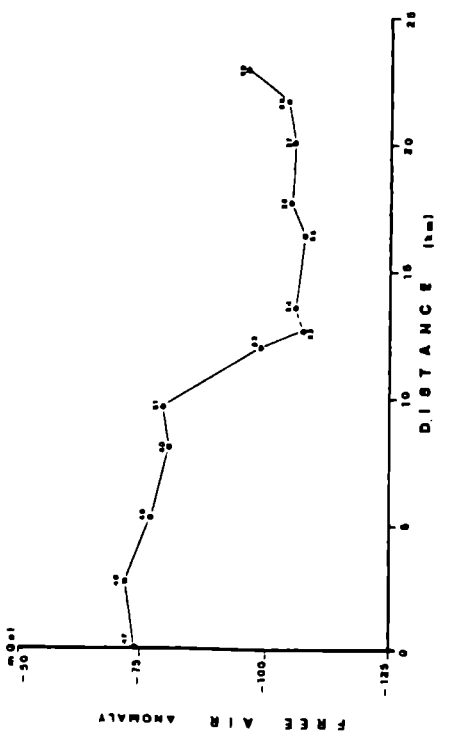

Fig. 2.21. PROFILE 3 (from st. 47 to st. 59) Altimetric and free air anomaly profiles.

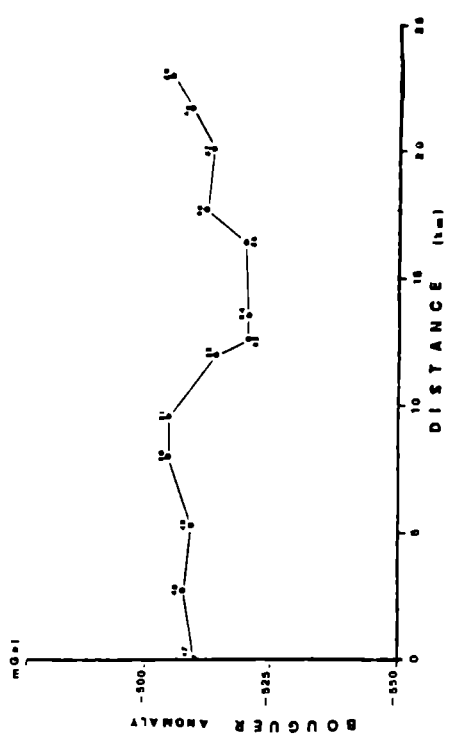

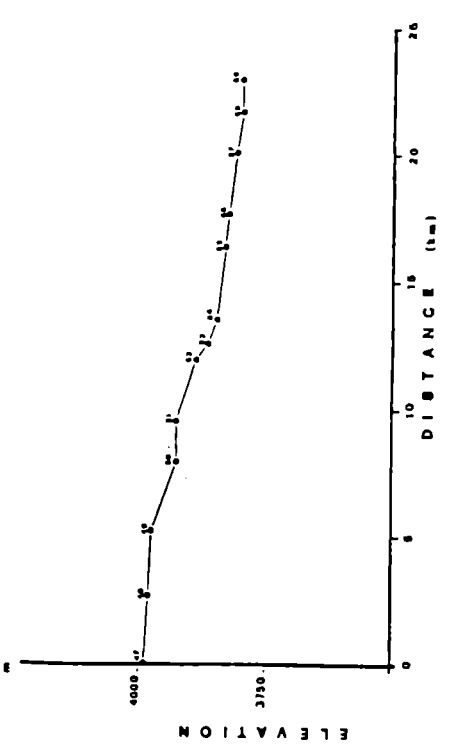

Fig. 2.22. PROFILE 3 (from st. 47 to st. 59) Bouguer and isostatic anomalies profiles.

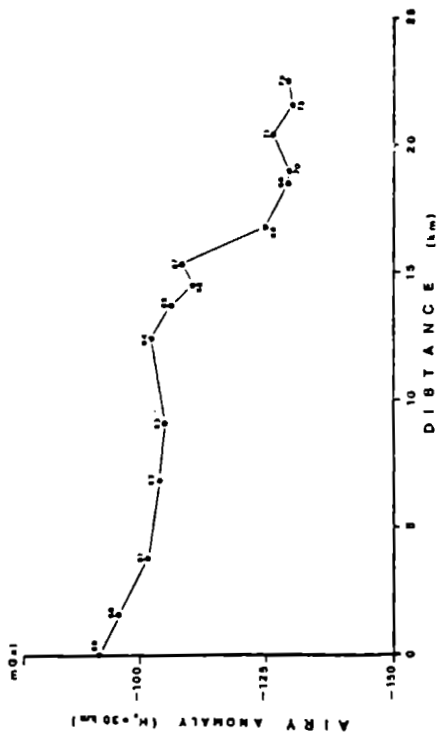

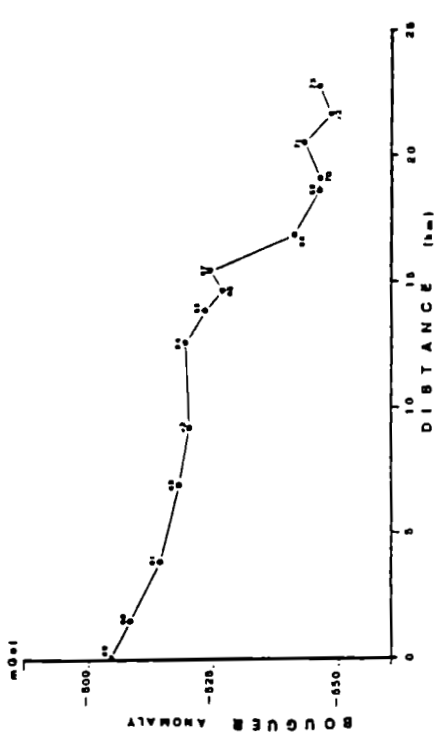

Fig. 2.24. PROFILE 4 (from st. 59 to st. 73) Bouguer and isostatic anomalies profiles.

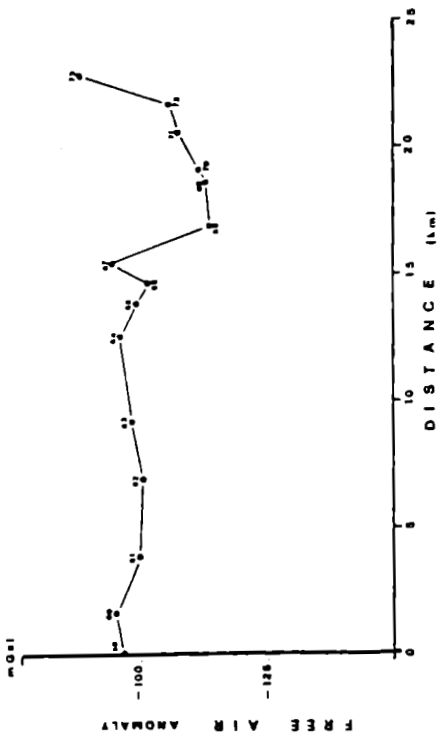

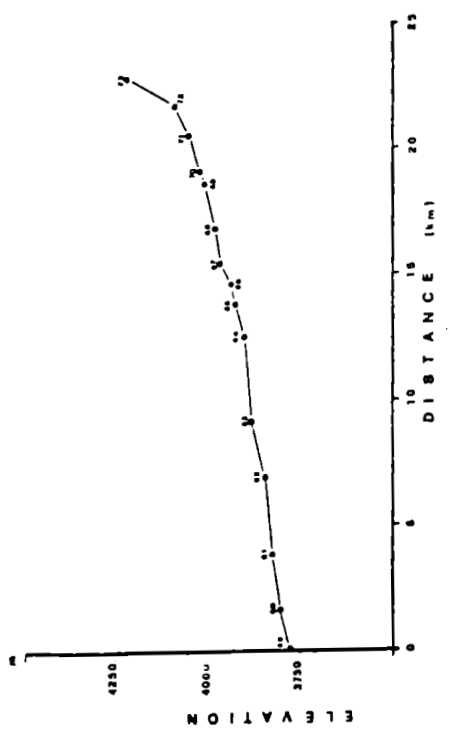

Fig. 2.23. PROFILE 4 (from st. 59 to st. 73) Altimetric and free air anomaly profiles.

APPENDIX A

Tables of Gravity and Gravity Anomalies in Karakorum

Table 2.9. Control gravity stations established during the Ev-K²-CNR 1988 Expedition.

		GRAVITY VALUES	
	STATION	IGSN71	POSTDAM SYSTEM
	PAKISTAN		
1	RAWALPINDI (PEARL CONTINENTAL)	979333.3	979347.17
2	RAWALPINDI (GATT HOTEL ROOM 27)	979331.68	979345.49
3	BATHAGRAM	979224.08	979237.89
4	BESHAM	979276.66	979290.47
5	QILA	979253.83	979267.64
6	GILGIT (CHENHAK HOTEL)	979112.88	979126.69
7	GILGIT AIRPORT	979113.39	979127.20
8	SLIDE NEAR GILGIT	979015.78	979029.59
9	EN 390 TO K. PASS	978989.80	979003.61
10	GULMIT REST HOUSE (UP)	978809.27	978823.08
11	GULMIT REST HOUSE (DOWN)	978809.43	978823.24
12	GULMIT (SHOE HOTEL)	978809.70	978823.51
13	BRIDGE 1 KM TO ENYHAR	978797.78	978611.59
14	BRIDGE GJASHGUL	978588.55	978602.36
15	KHUNJERAB PASS	978451.29	978465.10
16	KHUNJERAB PASS (BORDER)	978451.26	978465.07
	CHINA		
17	TASH KURGHAN (HOTEL PAMIR 206)	978922.01	978935.82
18	LAKE	978882.48	978896.29
19	KASHGAR (EXT)	979531.23	979545.04
20	KASHGAR (ROOM 306)	979528.95	979542.76
21	KM 1500	979459.60	979473.41
22	CHA YECHENG	979392.27	979406.08
23	KM 273 (ROAD NR. 229)	979176.31	979190.12
24	PASS HEIGHT 3200 AQ-KORAM	978964.77	978978.58
25	KM 157 (ROAD N. 219)	978952.96	978966.77
26	PASS HEIGHT 3000	978471.12	978484.93
27	MAZAR	978645.45	978659.26
28	BAZAR DARA BRIDGE	978670.71	978684.52

Table 2.10. Gravity values in the Aghil and Shaksgam area. All values refer to the IGSN 71 System.

ANOMALIES											
N	ST. NAME	LONG.	LAT.	OBS. G	HEIGHT	NORM. G	F. AIR	BOUG.	AIRY		
									H=20	H=30	H=40
1	P.BAZ.D.	76° 48' 20"	36° 23' 45"	978684.52	3545	979853.30	-79.20	-461.00	-22.88	-51.86	-79.63
2	MUR.SOST	76° 46' 30"	36° 23' 20"	978675.28	3490	979852.70	-104.73	-480.19	-41.73	-70.59	-98.30
3	OMET. 01	76° 44' 40"	36° 24' 15"	978695.33	3442	979854.02	-100.74	-464.65	-27.21	-56.01	-83.63
4	OMET. O2	76° 44' 10"	36° 24' 30"	978691.14	3529	979854.38	-78.57	-455.50	-18.70	-47.46	-75.03
5	ST 6 OM. 03	76° 43' 10"	36° 24' 20"	978678.08	3517	979854.14	-95.08	-465.28	-29.02	-57.66	-85.16
6	OM. 04	76° 41' 50"	36° 23' 40"	978678.52	3558	979853.18	-81.09	-464.87	-28.96	-57.29	-84.58
7	ST 7	76° 41' 25"	36° 23' 15"	978671.78	3576	979852.58	-81.70	-463.76	-27.47	-55.72	-82.97
8	ST 8 EX	76° 41' 20"	36° 23' 0"	978677.84	3569	979852.22	-77.43	-464.97	-28.44	-56.68	-83.94
9	CASA ILICA	76° 41' 20"	36° 23' 20"	978688.80	3519	979852.70	-82.31	-460.19	-23.84	-52.09	-79.34
10	C. B. 2/ILICA	76° 41' 0"	36° 23' 20"	978691.37	3497	979852.70	-86.49	-459.37	-23.05	-51.27	-78.50
11	ST 9	76° 41' 10"	36° 21' 10"	978669.72	3548	979849.58	-89.37	-473.83	-35.41	-63.67	-91.02
12	ST 10	76° 40' 35"	36° 20' 30"	978657.80	3579	979848.63	-90.82	-478.69	-39.86	-68.11	-95.46
13	ST 11	76° 39' 10"	36° 19' 40"	978650.18	3603	979847.43	-89.87	-478.86	-39.59	-67.75	-95.05
14	ST 12	76° 38' 0"	36° 19' 30"	978644.52	3629	979847.19	-87.31	-477.46	-38.75	-66.85	-94.12
15	ST 13 GPS	76° 37' 10"	36° 19' 45"	978641.52	3650	979847.55	-84.22	-476.55	-38.21	-66.28	-93.51
16	ST 14	76° 36' 10"	36° 19' 20"	978630.80	3715	979846.95	-74.38	-476.21	-37.88	-65.84	-92.99
17	C. B. 3	76° 36' 0"	36° 18' 20"	978608.22	3784	979845.51	-74.33	-484.51	-45.50	-73.49	-100.67
18	ST 15	76° 35' 5"	36° 17' 50"	978586.51	3878	979844.79	-66.46	-487.78	-48.83	-76.80	-103.96
19	ST 16	76° 34' 50"	36° 17' 10"	978574.23	3923	979843.83	-63.97	-490.77	-51.51	-79.49	-106.66
20	ST 17	76° 34' 20"	36° 16' 20"	978548.70	4029	979842.64	-55.76	-495.12	-55.54	-83.55	-110.75
21	ST 18	76° 34' 20"	36° 15' 50"	978533.00	4116	979841.92	-44.03	-494.69	-54.86	-82.93	-110.16
22	ST 19	76° 33' 45"	36° 15' 15"	978522.14	4179	979841.08	-34.71	-493.08	-53.12	-81.20	-108.45
23	ST 20 C. B. 4	76° 34' 5"	36° 14' 10"	978501.75	4264	979839.52	-27.45	-492.56	-51.55	-79.76	-107.10

Table 2.11. Gravity values in the Aghil and Shaksgam area. All values refer to the IGSN 71 System.

				ANOMALIES							
N	ST. NAME	LONG.	LAT.	OBS. G	HEIGHT	NORM. G	F. AIR	BOUG.	AIRY		
									H=20	H=30	H=40
24	ST 21	76° 35' 20"	36° 13' 15"	978464.74	4418	979838.21	-15.88	-502.73	-60.74	-89.16	-116.64
25	ST 22	76° 35' 50"	36° 12' 15"	978422.25	4614	979836.77	-3.23	-507.57	-64.98	-93.55	-121.14
26	ST 23 GR.S.	76° 37' 10"	36° 10' 50"	978388.94	4762	979834.73	-17.38	-513.90	-70.02	-98.92	-126.72
27	ST 24 PS. A.	76° 37' 5"	36° 10' 45"	978387.68	4780	979834.62	-21.75	-511.72	-67.95	-96.86	-124.68
28	VERT. CIN.	76° 37' 0"	36° 10' 40"	978375.73	4815	979834.50	-20.66	-516.71	-73.01	-101.92	-129.73
29	ST 25	76° 37' 5"	36° 9' 45"	978429.25	4430	979833.18	-42.67	-534.56	-88.68	-117.74	-145.70
30	ST 26 GR.MS.	76° 37' 35"	36° 9' 5"	978472.64	4273	979832.22	-46.52	-518.97	-71.66	-100.88	-128.95
31	ST 27 C.B. 5	76° 38' 50"	36° 6' 15"	978525.81	4069	979826.16	-51.92	-498.85	-47.23	-77.05	-105.54
32	ST 41	76° 39' 10"	36° 5' 30"	978521.77	4086	979827.08	-49.67	-497.63	-45.29	-75.25	-103.84
33	C. B. 6 D. JN	76° 39' 45"	36° 3' 55"	978512.48	4105	979824.81	-50.86	-500.12	-46.27	-76.44	-105.18
34	ST 40	76° 39' 30"	36° 3' 30"	978510.13	4100	979824.21	-54.14	-502.01	-47.95	-78.15	-106.90
35	ST 39	76° 40' 10"	36° 2' 30"	978506.86	4095	979822.78	-57.52	-501.05	-46.06	-76.40	-105.25
36	ST 38	76° 41' 0"	36° 1' 15"	978495.13	4114	979820.99	-61.63	-505.02	-49.09	-79.56	-108.50
37	ST 37	76° 42' 10"	36° 0' 5"	978488.23	4129	979819.32	-62.26	-506.38	-49.49	-80.10	-109.15
38	ST 30 GPS 4	76° 42' 20"	35° 58' 50"	978479.52	4134	979817.53	-67.65	-512.91	-55.46	-86.15	-115.27
39	ST 31	76° 45' 1"	35° 57' 25"	978473.38	4140	979815.50	-69.92	-513.21	-53.49	-84.40	-113.72
40	ST 32	76° 46' 0"	35° 56' 20"	978468.90	4129	979813.95	-76.23	-520.29	-59.69	-90.67	-120.07
41	ST 33	76° 46' 25"	35° 55' 35"	788463.47	4151	979812.87	-73.83	-522.48	-61.84	-92.78	-122.16
42	ST 34	76°47' 0"	35° 54' 35"	978456.44	4187	979811.44	-68.38	-524.91	-64.23	-95.17	-124.56
43	ST 36 CB7 GPS	76° 48' 15"	35° 53' 50"	978441.75	4232	979810.37	-68.19	-523.84	-64.48	-94.92	-123.98
44	GPS 1	76° 45' 12"	35° 53' 48"	978419.90	4382	979810.32	-53.77	-538.60	-78.25	-109.22	-138.57
45	GPS 2	76° 45' 22"	35° 52' 12"	978427.50	4321	979808.03	-52.78	-533.82	-72.88	-103.89	-133.28
46	GPS 3	76° 44' 7"	35° 53' 55"	978421.69	4348	979810.49	-52.76	-536.04	-75.95	-106.94	-136.29
47	ST 42	76° 37' 50"	36° 7' 25"	978529.94	3992	979829.83	-73.10	-510.02	-60.01	-89.57	-117.90
48	ST 43	76° 36' 20"	36° 7' 55"	978534.11	3983	979830.55	-72.41	-507.16	-58.45	-87.65	-115.74

Table 2.12. Gravity values in the Aghil and Shaksgam area. All values refer to the IGSN 71 System.

ANOMALIES											
N	ST. NAME	LONG.	LAT.	OBS. G	HEIGHT	NORM. G	F. AIR	BOUG.	AIRY		
									H=20	H=30	H=40
49	ST 44	76° 34' 40"	36° 7' 50"	978532.15	3974	979830.43	-77.01	-508.51	-61.00	-89.92	-117.81
50	ST 45	76° 33' 5"	36° 7' 45"	978541.57	3931	979830.31	-80.68	-504.13	-57.87	-86.56	-114.31
51	ST 46	76° 32' 5"	36° 7' 0"	978544.11	3926	979829.23	-78.59	-504.48	-58.44	-87.05	-114.72
52	ST 47	76° 30' 45"	36° 6' 20"	978536.54	3884	979828.28	-98.11	-514.38	-68.65	-97.08	-124.62
53	C. B. 8	76° 30' 24"	36° 6' 19"	978535.47	3860	979828.25	-106.52	-519.99	-74.36	-102.77	-130.29
54	ST 48	76° 29' 50"	36° 6' 20"	978538.87	3850	979828.28	-106.22	-519.92	-74.57	-102.94	-130.42
55	ST 49	76° 27' 55"	36° 6' 55"	978543.97	3833	979829.11	-107.17	-519.47	-75.97	-104.07	-131.35
56	ST 50	76° 27' 10"	36° 7' 45"	978550.87	3821	979830.31	-105.15	-510.91	-68.40	-96.35	-123.50
57	ST51	76° 25' 55"	36° 8' 20"	978555.43	3806	979831.15	-106.4	-513.13	-71.52	-99.28	-126.27
58	ST 52	76° 25' 5"	36° 9' 5"	978561.77	3795	979832.22	-104.14	-507.83	-67.00	-94.68	-121.58
59	ST 53	76° 24' 20"	36° 9' 10"	978569.64	3796	979832.34	-96.08	-503.81	-63.32	-90.98	-117.84
60	C. B. 9 GPS	76° 24' 25"	36° 8' 20"	978565.42	3809	979831.15	-95.12	-508.27	-67.26	-94.98	-121.89
61	ST 54	76° 23' 50"	36° 7' 20"	978555.16	3822	979829.71	-99.96	-514.21	-72.67	-100.50	-127.48
62	ST 55	76° 24' 5"	36° 5' 50"	978543.73	3849	979827.56	-100.95	-517.91	-75.13	-103.18	-130.32
63	ST 56	76° 24' 25"	36° 4' 45"	978535.74	3881	979826.01	-97.57	-520.17	-76.16	-104.47	-131.79
64	ST 57	76° 23' 20"	36° 3' 10"	978527.23	3906	979823.74	-96.14	-518.83	-73.77	-102.40	-129.89
65	ST 58	76° 23' 0"	36° 2' 35"	978518.72	3921	979822.90	-99.20	-522.91	-77.69	-106.46	-134.03
66	ST 59	76° 22' 40"	36° 2' 15"	978510.08	3937	979822.42	-102.45	-526.93	-81.59	-110.41	-138.01
67	C. B. 10 GPS	76° 22' 26"	36° 2' 0"	978507.87	3969	979822.06	-94.48	-523.50	-78.19	-107.04	-134.65
68	ST 60	76° 22' 6"	36° 1' 10"	978483.81	3979	979820.87	-114.28	-541.28	-95.43	-124.45	-152.14
69	ST 61	76° 21' 40"	36° 0' 25"	978473.82	4012	979819.79	-113.06	-545.67	-99.39	-128.55	-156.31
70	ST 61B	76° 21' 35"	36° 0' 20"	978471.81	40.25	979819.68	-110.97	-545.82	-99.51	-128.68	-156.43
71	ST 62	76° 20' 50"	35° 59' 40"	978466.30	4050	979818.72	-106.85	-542.98	-96.56	-125.83	-153.61
72	ST 63	76° 20' 35"	35° 59' 10"	978450.97	4103	979818.00	-106.19	-547.64	-101.18	-130.49	-158.29
73	ST 64	76° 20' 10"	35° 58' 40"	978428.11	4233	979817.29	-88.43	-546.20	-99.97	-129.35	-157.16

Table 2.13. Gravity values in Karakorum from previous expeditions. (Courtesy of Prof. Giorgio Poretti). Anomalies refer to T=30 km. All values refer to the Potsdam System.

GRAVITY ANOMALIES OF THE KARAKORUM RANGE												
ST. NAME	*LAT.*	*LONG.*	*ELEV.*	*OBS.G*	*NORM.G*	*RED*	*PLATE*	*TOP.*	*RED*	*F.AIR*	*BOUG.*	*AIRY*
GILGIT AIRP.	35° 55'	74° 20'	1418	979127.2	979823.6	437.5	277.5	33.3	430.5	-258.9	-385.6	11.6751
BUNJI	35° 39'	74° 38'	1358	979111.7	979801	419	265.7	33.3	438.8	-270.2	-390.2	15.3752
RAMGHAT PUL	35° 35'	70° 40'	1186	979100.0	979795.2	365.9	232	46	456	-329.2	-417.2	-7.2753
MAGDOIAN	35° 33'	74° 43'	1557	978944.4	979792.4	480.4	304.8	43.9	458.5	-367.5	-499.3	-84.7754
MUSHKIN	35° 31'	74° 45'	1669	978944.4	979789.6	515	326.8	54.2	471.3	-330.2	-464.2	-47.1755
HARCHU	35° 27'	74° 48'	2041	978999.1	979783.8	629.8	399.9	37.7	458.5	-254.9	-447.1	-26.3756
ASTOR	35° 22'	74° 52'	2318	978899.1	979776.8	715.2	454.4	35.4	464.7	-162.3	-387.8	-41.5757
BULAN	35° 20'	74° 51'	2399	978881.7	979774	740.2	470.3	30.6	462.9	-152	-391.3	41758
GERAK	35° 17'	74° 51'	2322	978900.5	979769.6	716.5	455.1	25	458.9	-152.6	-388.9	45759
PAKORA	35° 15'	74° 54'	2551	978866.2	979766.8	787.1	500.2	34.7	471.4	-113.5	-365.6	71.1760
KHUME	35° 12'	74° 56'	2656	978847.4	979762.4	819.5	520.9	29.7	465.6	-95.6	-364.4	71.5761
CHASHMA	35° 10'	75° 0'	2909	978800.7	979759.6	897.6	570.8	25.8	463.9	-61.4	-362.3	75.8762
KHIRIM	35° 08'	75° 02'	3069	978870.1	979757	946.9	602.4	21.4	461.3	-39.8	-363	76.9763
DASH	35° 05'	75° 04'	3265	978745.7	979752.6	1007.4	641.1	13.9	456.3	.5	-351.9	90.5764
CHELAM	35° 02'	75° 06'	3316	978755.7	979748.4	1023.2	651.1	12.2	457	30.5	-329.3	115.5765
5 ML F.	35° 01'	75° 11'	3808	978665.7	979747	1175	748.4	7.8	427.1	93.7	-325	94.3766
CHACKAR PASS	35° 00'	75° 14'	4163	978611.1	979745.6	1284.5	818.7	1.1	436.6	150.1	-314.6	120.9767
CHUND CUT	35° 00'	75° 20'	4005	978625.7	979745.6	1235.7	787.4	.5	451.5	115.9	-332	119768
BAWI RIV. BR.	35° 02'	75° 24'	3737	978649.1	979748.4	1153.1	734.4	.8	452.6	53.9	-364	87.8769
5 ML F.	35° 04'	75° 28'	3904	978627.9	979751.2	1204.6	767.4	1.4	455.1	81.3	-354.4	99.3770
9 ML TO SATPORA	35° 06'	75° 31'	4166	978578.4	979754.2	1285.4	819.3	2	453.9	109.7	-354.4	97.5771
4 ML TO SATPORA	35° 06'	75° 37'	3671	978638.9	979757	1132.7	721.3	20.5	476.4	14.7	-376.2	79.7772
SATPORA	35° 12'	75° 38'	2873	978783.4	979762.4	886.5	563.7	30.9	481.4	-92.6	-384.5	66773

Table 2.13 (continued).

ST.NAME	LAT.	LONG.	ELEV.	OBS. G	NORM. G	RED	PLATE	TOP.	RED	F. AIR	BOUG.	AIRY
LAKE SATPORA	35°14"	75° 39'	2664	978827.9	979765.4	822	522.5	24.4	474.1	-115.5	-390.6	59.1774
SKARDU R. H.	35° 17'	75° 38'	2237	978915.2	979769.6	690.2	438.4	10.9	457.3	-164.1	-404.1	41.3775
SKARDU P. S.	35° 17'	75° 38'	2229	978923.9	979769.6	687.1	436.5	10.9	457.3	-148.5	-398.3	48.1776
SKARDU AIRP.	35° 17'	75° 38'	2245	978917.2	979769.6	692.7	440	10.9	457.3	-159.7	-401.5	44.9776
THURGON	35° 18'	75° 46'	2246	978913.7	979771	693	440.2	14.5	466.4	-164.2	-402.6	49.3777
5 ML F.	35° 21'	75° 48'	2256	978912.6	979775.2	696.1	442.2	16.4	461.2	-166.5	-404.1	50.7778
GOL	35° 15'	75° 52'	2238	978889.4	979766.8	690.5	438.6	21.4	481.5	-186.8	-417.4	42.7779
SHAYOK BR.	35° 14'	75° 55'	2320	978894.2	979765.4	715.8	454.8	14.5	475.6	-155.4	-401.9	59.2780
50 KM ML. STONE	35° 12'	75° 59'	2380	978884.4	979762.4	734.3	466.6	29.9	494.5	-142.7	-381.6	83781
SHAGARI	35° 11'	76° 02'	2352	978874.2	979761.2	725.7	461.1	30.8	496.2	-161.2	-395	70.4782
GYUTA	35° 11'	76° 07	2438	978853.9	979761.2	752.2	478	24	492.3	-154.9	-405.2	63.1783
YUGU	35° 11'	76° 11'	2467	978841.7	979761.2	761.2	483.7	20.5	490.4	-158.2	-415.2	54.7784
20 KM ML. STONE	35° 14'	76° 13'	2470	978829.0	979765.4	762.1	484.3	17.9	489.6	-174.3	-434.2	37.5785
OPP. YOUSKILL	35° 13'	75° 15'	2479	978832.1	979764	764.9	486.1	17.4	490.5	-166.9	-428.4	44.7786
MOMIMPA	35° 11'	76° 18'	2476	978799.2	979761.2	764	485.5	16.8	491.6	-197.9	-459.6	15.2787
KHAPALU	35° 10'	76° 20'	2484	978811.7	979759.6	766.4	487	17.5	494.1	-181.5	-443.4	33.2700
GILGIT	35° 55'	74° 18'	1418	979127.2	979823.6	437.5	277.5	33.3	430.5	-258.9	-385.6	11.6701
HENZAL OMAIN	35° 58'	74° 13'	1568	979093.6	979828	483.8	306.9	41.4	445.2	-250.4	-385.9	17.9702
GULAPUR	35° 58'	74° 05'	1717	979065.6	979828	529.8	336.2	42.6	449	-232.5	-383.5	22.9703
SINGAL	36° 04'	73 '53'	1763	979062.9	979836.6	544	345.2	44.5	450.1	-229.7	-383.9	21.7705
GAKUCH	36° 11'	73° 47'	1858	979073.4	979846.6	573.3	363.9	28.5	424.9	-199.8	-380.7	15.7711
DAMAS	36° 12'	73 '44'	1880	979072.7	979848	580.1	368.2	29	436.8	-195.1	-378	29.8712
YANGAL	36° 15'	73° 36'	2086	979012.0	979852.2	643.6	408.7	44.5	440	-196.6	-387	8.5713

Table 2.13 (continued).

ST. NAME	LAT.	LONG.	ELEV.	OBS. G	NORM. G	RED	PLATE	TOP.	RED	F. AIR	BOUG.	AIRY
GUPIS	36° 14'	73° 27'	2181	979010.6	979850.8	672.9	427.4	37.4	432.9	-167.2	-375.4	20.1714
JULIAL	36° 12'	73° 16'	2366	978989.2	979848	730	463.8	35	431	-128.7	-359.9	36.1715
PINGAL	36° 10'	73° 06'	2534	978949.5	979845.2	781.9	496.9	43.1	439.1	-113.8	-355.6	40.4716
FULDAR	36° 10'	72° 57'	2940	978883.1	979845.2	907.1	576.9	32	439.9	-54.9	-353.1	54.8717
TERU	36° 11'	72° 46'	3202	978827.4	979846.6	988	628.6	23.3	416.6	-31.1	-367.2	26.1
LANGAR	36° 07'	72° 38'	3483	978777.9	979840.8	1974.7	684.1	19.5	412.6	11.7	-359.3	33.8719
SHANDUR PASS	36° 05'	72° 34'	3735	978729.2	979838	1152.4	734	9.2	399.9	43.7	-365.5	25.2720
HARCHIN	36° 07'	72° 29'	2782	978882.5	979840.8	858.4	545.8	29	418.9	-99.9	-385.5	6.4721
GAST	36° 11'	72° 28'	2592	978887.2	979846.6	799.8	508.3	53.7	442.8	-159.6	-397.3	-8.2722
MASTUJ	36° 17'	72° 31'	2331	978943.9	979855.2	719.2	456.9	34.2	421.9	-192	-420.1	-32.4723
SHANOGAR	36° 18'	72° 24'	2270	978951.2	979856.6	700.4	444.9	33.1	418.9	-205	-427.4	-41.6724
MIRAGRAM	36° 15'	72° 22'	2247	978955.1	979852.2	693.3	440.4	43.2	428.8	-203.8	-413.5	-27.9725
AWI	35° 16'	72° 20'	2152	978973.1	979853.6	664	421.7	35.6	419.9	-216.5	-423.2	-38.9726
KURAGH	36° 13'	72° 10'	1934	979031.7	979849.4	596.7	378.8	31.3	417.1	-221	-407.6	-21.8727
PARPISH	36° 08'	72° 04'	1813	979034.1	979842.2	559.4	355.1	36.6	420.3	-248.7	-416.4	-32.7728
MORELAST	36° 00'	71° 59'	1706	979067.7	979830.8	526.4	334	40.7	420.2	-236.7	-388.3	-8.8729
KOGOSHI	35° 56'	71° 56'	1655	979070.9	979825.2	510.7	324	42	419.7	-243.5	-388.2	-10.5730
ROGH	35° 55'	71° 53'	1574	979077.6	979823.6	485.7	308.1	42	416.9	-260.3	-395.8	-20.9731
CHITRAL	35° 54'	71° 47'	1527	979107.2	979822.2	471.2	298.9	35	406.9	-243.8	-381	-9.1710
IMIT	36° 30'	73° 54'	2239	978916.2	979873.8	690.8	438.8	37.1	458	-266.8	-481.7	-60.8708
SHONAS	36° 25'	73° 51'	2108	978963.6	979866.6	650.4	413	35.1	450.4	-252.5	-454.8	-39.5907
CHATORCHAND	36° 21'	73° 51'	2073	978992.6	979861	639.6	406.2	36.4	447.8	-228.6	-425.7	-14.3706
HASIS	36° 17'	73° 46'	1928	979033.2	979855.2	594.9	377.7	40.4	447.7	-227.1	-403.9	3.4704

Table 2.13 (continued).

ST. NAME	LAT.	LONG.	ELEV.	OBS. G	NORM. G	RED	PLATE	TOP.	RED	F. AIR	BOUG.	AIRY
SILPI	36° 11'	73° 47'	1853	979072.2	979846.6	571.7	362.9	28.5	430.3	-202.6	-382.9	189800
GILGIT AIRP.	35° 55'	74° 20'	1418	979127.2	979823.6	437.5	277.5	33.3	430.5	-258.9	-385.6	11.6802
HUNZA RIV. JCT	35° 58'	74° 21'	1459	979109.6	979828	450.2	285.5	37.7	436.1	-268.1	-395	3.4803
JUTAL	36° 03'	74° 18'	1551	979083.2	979835.2	478.6	303.6	40.8	446.9	-273.3	-407.5	-1.4804
GARESH	36° 09'	74° 19'	1636	979044.2	979843.6	504.8	320.3	58.1	467.6	-294.6	-421	-11.5805
CHALT	36° 13'	74° 19'	1721	979000.0	979849.4	531	337	55.1	466.7	-318.4	-457.4	-45.8806
NILT	36° 15'	74° 24'	1936	978974.7	979852.2	597.4	379.2	48.8	466.3	-280.2	-449.5	-32807
GULMIT	36° 14'	74° 30'	1975	978950.7	979850.8	609.4	386.9	53.5	473.2	-290.7	-459.7	-40808
MURTAZABAD	36° 16'	74° 34'	2069	978906.7	979853.6	638.4	405.4	57.9	484.8	-308.5	-483.7	-56.8809
GANESH	36° 19'	74° 39'	2161	978884.2	979858	666.8	423.5	57.8	492.1	-307	-492.5	-58.2810
MUHAMMADABAD	36° 18'	74° 45'	2398	978841.2	979856.6	739.9	470.1	58.8	497.4	-275.5	-486.5	-47.9811
BURI HARAR	36° 18'	74° 51'	2370	978812.5	979856.6	731.3	464.6	60.3	499.2	-312.8	-519.2	-80.3812
ANDARE	36° 24'	74° 52'	2423	978826.2	979865.2	747.6	475	46.2	490.9	-291.4	-518.8	-73.1813
PASU	36° 28'	74° 54'	2454	978840.9	979871	757.2	481.1	31.2	476.4	-272.8	-417.7	-72.5814
JCT KKH	36° 32'	74° 50'	2597	978826.5	979876.8	801.3	509.3	36.7	485.6	-248.9	-504.2	-55.3815
MORKHUN	36° 37'	74° 52'	2715	978798.2	979883.8	837.7	532.6	42.1	490.8	-247.9	-511	-62.3816
KHUDABAD	36° 42'	74° 49'	2785	978818.6	979891.2	859.3	546.4	21.5	473.7	-213.1	-504.6	-52.4817
2 RIVERS BR.	36° 47'	74° 52'	2829	978764.6	979898.2	8722.9	555	32.8	489.8	-260.7	-545.7	-88.7818
2.2 ML FURTHER	36° 50'	74° 58'	3211	978718.0	979902.6	990.8	630.4	33.9	492.7	-193.7	-520.2	-61.4819
AT KM 247	36° 52'	75° 05'	3470	978678.1	979905.4	1070.7	681.6	29.5	493.7	-156.6	-516.2	-52820
26 KM TO K.P.	36° 51'	75° 14'	3883	978608.7	979904	1198.1	763.3	26	501.6	-97.2	-506.1	-30.5821
7 KM TO K.P.	36° 49'	75° 22'	4380	978538.2	979901.2	1351.4	861.7	14.7	487.8	-11.4	-486.5	-13.4822
BORDER STATION KP	36° 51'	75° 27'	4740	978464.1	979904	1462.5	9383.1	3.5	482.3	22.7	-503.2	-24.4101

Table 2.13 (continued).

ST. NAME	LAT.	LONG.	ELEV.	OBS. G	NORM. G	RED	PLATE	TOP.	RED	F. AIR	BOUG.	AIRY
SKARDU R. H.	35° 17'	75° 38'	2237	978915.0	979769.6	690.2	438.4	8	432.4	-164.3	-408.1	16.3102
HOTO	35° 22'	75° 30'	2279	978907.0	979776.8	703.2	446.7	16	449.6	-166.5	-407	26.6103
AYUB BRIDGE	35° 27'	75° 26'	2253	978915.7	979783.8	695.2	441.6	22	455.3	-172.9	-404.5	28.8106
BAYCHA	35° 35'	75° 20'	2117	978922.7	979795.2	653.2	414.8	25	465.3	-219.3	-432.7	7.6109
RONDU	35° 36'	75° 10'	1967	978953.0	979796.6	606.9	385.3	23	457.4	-236.7	-435.3	-.9113
MALUPAH	35° 38'	74° 59'	1864	978927.9	979799.4	575.1	365.1	47	483.1	-296.4	-459.4	-23.3116
SHENGUS	35° 43'	74° 49'	3322	978686.5	979806.6	1025	652.3	26	441.3	-95.1	-441.8	-26.5121
ALAM BRIDGE	35° 47'	74° 34'	1188	979134.1	979812.2	366.6	232.4	37	457.3	-311.4	-408.6	11.7128
KURCHUNG	35° 42'	75° 02'	2544	978835.2	979805.2	785	498.9	42	467.3	-185	-429.1	-3.8128
CHUTRUN	35° 43'	75° 13'	3560	978656.6	979806.6	1098.4	699.4	44	487.6	-51.6	-406.6	37
GANTO-LA	35° 40'	75° 21'	4482	978476.2	979802.4	1382.9	881.9	65	497.5	56.8	-379.2	53.3142
DASSO	35° 43'	75° 31'	2442	978784.7	979806.6	753.5	478.8	29	476.8	-268.5	-514.2	-66.4148
HOTO	35° 41'	75° 44'	2804	978695.1	979803.8	865.2	550.1	33	496.2	-243.4	-525.5	-62.3157
KOROPHON	35° 41'	75° 59'	3094	978666.6	979803.8	954.7	607.3	33	503.6	-182.4	-496.8	-26.2164
PAJU	35° 40'	76° 06'	3402	978583.2	979802.4	1049.7	668.1	22	498.9	-169.4	-529	-52.1168
URDUKAS	35° 44'	76° 16'	4031	978452.7	979808.2	1243.8	792.6	27	512.8	-11.6	-535.8	-50169
BALTORO GLACIER	35° 45'	76° 31'	4633	978319.6	979809.4	1429.5	911.9	23	532.9	-60.2	-554.8	-44.9170
K^2 BASE CAMP	35° 51'	76° 31'	4978	978267.7	979817.8	1536	980.4	24	525.7	-14.2	-545.7	-44172
KUSHAMUL	35° 35'	75° 35'	2315	978839.0	979795.2	714.3	453.8	22	472.2	-241.9	-480.4	-30.2175
HASHUPA	35° 31'	75° 41'	2319	978861.2	979789.6	715.5	454.6	19	464.2	-212.8	-454.8	-9.6179
SHIGAR	35° 25'	75° 45'	2284	978890.9	979781	704.7	447.7	15	461.3	-185.4	-427.5	18.8185
FAQUIRS HUT	35° 20'	75° 48'	2288	978898.6	979774	706	448.5	27	460.3	-169.3	-399.8	33.5187
SHAYOK	35° 13'	75° 55'	2300	978888.6	979764	709.7	450.8	20	460.1	-165.6	-404.5	35.6191

Table 2.13 (continued).

ST. NAME	LAT.	LONG.	ELEV.	OBS. G	NORM. G	RED	PLATE	TOP.	RED	F. AIR	BOUG.	AIRY
MANTHOKA	35° 06'	75° 59'	2340	978895.2	979754.2	722	458.7	24	468.5	-136.9	-376.2	68.3192
TOLTI	35° 02'	76° 06'	2423	978853.6	979748.4	747.6	475	19	468.6	-147.1	-400.7	48.9195
BAGHICHA	34° 55'	76° 11'	2499	978820.2	979738.4	771.1	490	47	483.5	-147.2	-381.3	55.2306
SHERGARH	34° 24'	71° 54'	383	979413.6	979695	118.2	74.8	1	164.5	-163.1	-205.5	-42307
MALAKAND	34° 33'	71° 58'	826	979329.5	979707.6	254.9	161.5	1	185.8	-123.1	-215.5	-30.7310
KHAL	34° 49'	71° 50'	838	979372.0	979730.2	258.6	163.8	4	221.3	-99.6	-190.3	27313
DIR	35° 13'	71° 52'	1405	979220.7	979764	433.5	274.9	10	298.4	-109.7	-258.3	30.1314
LAWARI PASS	35° 21'	71° 48'	3145	978890.0	979775.2	970.4	617.4	15	318	85.1	-252.9	50.1317
DROSH	35° 33'	71° 49'	1359	979192.4	979792.4	419.3	265.9	25	358.9	-180.6	-309	24.9319
CHITRAL	35° 54'	71° 47'	1508	979107.9	979822.2	465.3	295.2	30	399.1	-249	-389.1	-20323
KHOGOZI	35° 56'	71° 56'	1694	979064.9	979825.2	522.7	331.7	18	418.1	-237.5	-410.5	-10.4328
RESHUN	36° 09'	72° 06'	1931	979020.2	979843.6	595.8	378.2	36	426.2	-227.6	-409.1	-18.9334
MASTUJ	36° 17'	72° 31'	2331	978943.2	979855.2	719.2	456.9	29	436.8	-192.7	-426	-18.2336
BREP	36° 27'	72° 38'	2481	978904.5	979869.6	765.5	486.5	33	453.8	-199.5	-445.5	-24.7340
GAZIN	36° 39'	72° 56'	2958	978811.2	979886.8	912.7	580.5	38	470.4	-162.9	-457.1	-24.7342
LASHT	36° 47'	73° 01'	3239	978772.7	979898.2	999.4	635.9	26	461.1	-126.1	-463.6	-28.5345
BAROGHIL PASS	36° 53'	73° 22'	3890	978675.7	979906.8	1200.3	764.6	12	454.5	-30.9	-454.5	-12347
DARKHOT PASS	36° 45'	73° 25'	4614	978518.7	979895.2	1423.6	908.1	45	483.5	47.1	-423.4	15.1351
YASIN	36° 23'	73° 20'	2395	978951.4	979863.8	739	469.5	30	451.9	-173.4	-412.9	9354
HAIM	36° 14'	73° 43'	1905	979068.6	979850.8	587.8	373.1	52	468.3	-194.4	-357.1	59.2356
SINGAL	36° 06'	73° 53'	1824	979062.2	979839.2	562.8	357.2	33	446.3	-214.3	-386.8	26.5357
GULAPUR	36° 04'	74° 05'	1737	979064.7	979836.6	536	340.1	39	458.2	-235.9	-392.7	26.5358

Table 2.13 (continued).

ST. NAME	LAT.	LONG.	ELEV.	OBS. G	NORM. G	RED	PLATE	TOP.	RED	F. AIR	BOUG.	AIRY
HENZAL OMEIN	35° 58'	74° 12'	1542	979096.6	979828	475.8	301.8	47	453.3	-255.5	-382.4	23.9359
GILGIT	35° 55'	74° 18'	1418	979127.2	979823.6	437.5	277.5	28	429.4	-258.9	-390.9	10.5363
RAKHIOT BR.	35° 30'	74° 36	1300	979120.6	979788.2	401.1	254.4	55	451.5	-266.4	-358.1	38.4366
CHILAS	35° 25'	74° 06'	1191	979242.1	979781	367.5	233	19	387.3	-171.4	-286.9	81.4369
BABUSAR PASS	35° 09'	74° 03'	4150	978606.1	979758.2	1280.5	816.1	14	367.3	128.4	-322	31.3371
BATTAKUNDI	34° 56'	73° 45'	2665	978867.6	979739.8	822.3	522.7	28	432.2	-49.9	-321.5	82.7373
KAGAN	34° 56'	73° 32'	2064	978983.2	979739.8	636.8	404.4	26	328.2	-119.8	-326.2	-24376
BALAKOT	34° 32'	73° 21'	1011	979228.2	979706.2	311.9	197.7	12	263.6	-166	-268.2	-16.6381
HARIPUR	33° 59'	72° 56'	528	979361.7	979660	162.9	103.2	0	166.5	-135.3	-195.1	-28.6389
CHARSADDA	34° 09'	72° 45'	329	979416.1	979674	101.5	64.3	0	147.9	-156.3	-193.6	-45.7390
SHAHBAZGARHI	35° 14'	72° 19'	320	979438.4	979765.4	98.7	62.5	1	238.1	-228.3	-263.5	-26.4392
BARIKOT	34° 40'	72° 14'	799	979326.7	979717.4	246.5	156.2	3	206	-144.2	-231.6	-28.6393
SAIDU SHARI	34° 45'	72° 22'	940	979302.1	979724.4	290	183.8	3	224.5	-132.3	-235.5	-14395
FATEHPUR	35° 04'	72° 30'	1300	979290.0	979751.2	401.1	254.4	10	297.8	-60	-196.8	91398
RAMET	35° 17'	72° 36'	1521	979186.2	979769.6	469.3	297.7	46	370.5	-114.1	-239.7	84.8400
KALAM	35° 32'	72° 35'	2017	979065.4	979791	622.3	395.1	16	367.7	-103.2	-314.4	37.3
BESHAM QILA	34° 56'	72° 52'	577	979286.7	979739.8	178	112.7	24	302.6	-275.1	-316.4	-37.8604
_	35° 01'	72° 52'	638	979271.2	979747	196.9	124.7	38.4	317.3	-278.9	-312.7	-33.8606
_	35° 03'	72° 56'	861	979267.4	979749.8	265.7	168.3	36.7	342	-216.7	-277.3	28608
_	35° 05'	72° 59'	911	979304.9	979752.6	281.1	178.1	15.1	324.9	-166.6	-254.5	55.3611
_	35° 06'	73° 00'	911	979323.2	979754.2	281.1	178.1	29.7	320.7	-149.8	-223.1	67.9612
PATAN	35° 08'	73° 04'	952	979331.4	979757	293.7	186.1	44.5	362.8	-131.8	-194.9	123.4614
_	35° 10'	73° 06'	973	979322.9	979759.6	300.2	190.3	58.7	381.8	-136.5	-187.8	135.3615

Table 2.13 (continued).

ST. NAME	LAT.	LONG.	ELEV.	OBS. G	NORM. G	RED	PLATE	TOP.	RED	F. AIR	BOUG.	AIRY
PATAN	35° 12'	73° 08'	941	979319.9	979762.4	290.3	184	68.4	391.1	-152.2	-190.2	132.5616
_	35° 14'	73° 10'	814	979327.1	979765.4	251.2	159.1	57.1	401.3	-187.1	-222	122.2617
_	35° 16'	73° 14'	818	979326.6	979768.2	252.4	159.9	47.8	380	-189.2	-233.9	98.3618
_	35° 19'	73° 12'	857	979319.0	979772.6	264.4	167.5	42.4	392.1	-189.1	-243.6	106.1620
_	35° 21'	73° 12'	888	979299.9	979775.2	274	173.6	54.7	396.5	-201.4	-247.1	94.7621
DUGA	35° 23'	73° 12'	931	979290.7	979778.2	287.3	182	65	408.2	-200.1	-240.3	102.9622
_	35° 30'	73° 22'	962	979267.5	979788.2	296.8	188.1	42.9	383.7	-223.8	-289.6	51.26243
_	35° 31'	73° 25'	980	979260.2	979789.6	302.4	191.6	35.1	373.7	-226.9	-302.6	36625
_	35° 32'	73° 30'	992	979264.0	979791	306.1	194	27.7	378.8	-220.8	-305.2	45.9627
_	35° 32'	73° 36'	1000	979279.7	979791	308.6	195.6	26.1	378.2	-202.6	-289.5	62.6628
_	35° 31'	73° 43'	1042	979283.6	979789.6	321.5	203.8	20.9	372.8	-184.4	-281.2	70.7630
_	35° 30'	73° 48'	1020	979284.5	979788.2	314.7	199.5	21.1	379.2	-188.9	-283.1	75631
_	35° 29'	73° 52'	1042	979282.7	979786.6	321.5	203.8	31.7	388.3	-182.4	-268.4	88.2632
_	35° 29'	73° 56'	1048	979271.2	979786.6	323.4	205	27.2	385.6	-192	-283.2	75.2634
_	35° 26'	74° 01'	1066	979254.5	979782.4	328.9	208.5	26.5	388.3	-199	-292.9	68.9635
_	35° 25'	74° 04'	1051	979250.2	979781	324.3	205.5	28.4	390.2	-206.5	-296.9	64.9637
CHILAS	35° 24'	74° 07'	1164	979236.2	979779.6	359.2	227.7	25.3	388	-184.2	-290.4	72.3638
638	35° 24'	74° 10'	1099	979235.2	979779.6	339.1	214.9	31.3	407.7	-205.3	-298.1	78.3640
640	35° 24'	74° 13'	1056	979233.2	979779.6	325.8	206.5	31.5	409.3	-220.5	-308.4	69.4642
642	35° 24'	74° 18'	1105	979203.5	979779.6	340.9	216.1	37.1	416.6	-235.1	-322.8	56.7643
643	35° 24'	74° 20'	1101	979172.7	979779.6	339.7	215.3	38.9	423.2	-267.2	-325.6	31.7645
645	35° 24'	74° 26'	1081	979150.2	979779.6	333.5	211.4	41.2	430.4	-295.8	-376.8	12.4646
645	35° 24'	74° 26'	1081	979150.2	979779.6	333.5	211.4	41.2	430.4	-295.8	-376.8	12.4646

Table 2.13 (continued).

ST. NAME	LAT.	LONG.	ELEV.	OBS. G	NORM. G	RED	PLATE	TOP.	RED	F. AIR	BOUG.	AIRY
646	35° 27'	74° 24'	1139	979142.5	979783.8	351.4	222.8	44	437	-289.8	-374.5	18.5648
648	35° 28'	74° 33'	1117	979113.9	979785.2	344.7	218.5	54.1	457.6	-326.7	-398.7	4.8650
650	35° 34'	74° 37'	1205	979093.6	979793.8	371.8	235.7	41	446.2	-328.4	-423.5	-18.3652
652	35° 40'	74° 37'	1247	979128.7	979802.4	384.8	244	34.7	442.4	-288.9	-395	127653
653	35° 42'	74° 37'	1249	979116.9	979805.2	385.4	244.4	32.2	449.4	-302.9	-411.7	5.5654
654	35° 44'	74° 37'	1280	979120.0	979808.2	394.9	250.4	34	451.9	-293.1	-403.6	14.3655
655	35° 48'	74° 34'	1296	979117.2	979813.6	399.9	253.6	42.6	458.5	-296.6	-400.3	15.6656
656	35° 51'	74° 31'	1346	979110.5	979817.8	414.4	262.8	47.3	458	-292.9	-397.2	13.5657
657	35° 52'	74° 26'	1431	979114.2	979819.4	441.5	280.1	41.8	452.1	-263.6	-383.3	27658
658	35° 54'	74° 22'	1445	979109.1	979822.2	445.9	282.8	42.8	455.6	-267.1	-387.4	25.4662
662	35° 36'	74° 39'	1390	979083.2	979796.6	428.9	272	39.2	442.7	-284.6	-402.2	1.3663
RAMGHAT PUL	35° 35'	74° 39'	1320	979073.0	979795.2	407.3	258.3	45.4	448.2	-314.9	-418.5	-15.7666
666	35° 56'	74° 21'	1417	979126.6	979825.2	437.2	277.3	37.9	449.2	-261.2	-383.2	28.1667
667	35° 58'	74° 21'	1440	979104.5	979828	444.3	281.8	40.8	455.4	-279.1	-400.8	138668
668	36° 00'	74° 18'	1513	979082.5	979830.8	466.8	296.1	45.7	460.1	281.4	-406.4	8669
669	36° 03'	74° 17'	1503	979082.2	979835.2	463.8	294.2	45.7	466.8	-289.1	-413	8.1670
670	36° 07'	74° 18'	1610	979040.5	979840.8	496.8	315.2	62.7	480.3	-303.5	-422.4	-4.8671
671	36° 12'	74° 18'	1595	979023.2	979848	492.1	312.2	56.7	485.9	332.6	-455.8	-26.6

APPENDIX B

PLATES

Plate 1.

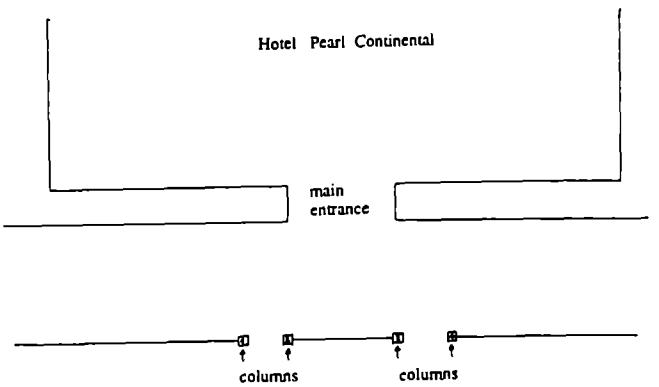

Fig. 1.
Gravity Station N. 0188 PAK; September 1988; Pakistan-Punjab-Rawalpindi; Lat. 33°35', Long. 73°07'; Potsdam Syst. 979347.17; IGSN71 979333.36.
The station is located in the inner court of the Pearl Continental. This hotel has a front porch, supported by four columns, in correspondence of the entrance. The measurement was performed between the first and second column (20 cm apart from the second) starting from the left.

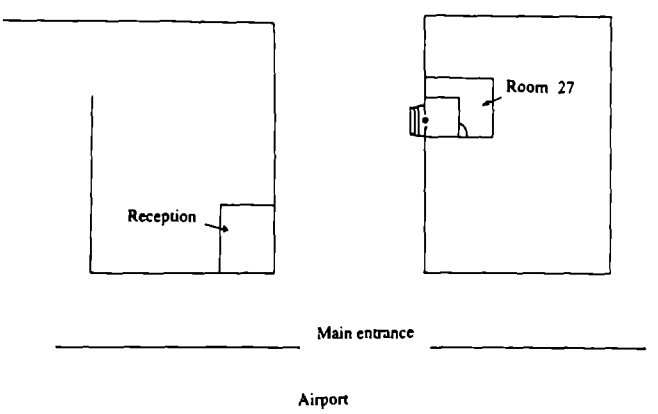

Fig. 2.
Gravity Station N. 0288 PAK; October 1988; Pakistan-Punjab-Rawalpindi; Lat. 33°35', Long. 73°03'; Potsdam System 979345.49; IGSN71 979331.68.
The station is located in front of the room N. 27 of the Gatmell's Hotel. The plate is positioned between the two walls at the same level of the room.

Plate 2.

Fig. 1.
Gravity Station N. 0388 PAK;
September 1988;
Pakistan-NW Frontier Prov.-Batagram;
Lat. 34°41′, Long. 73°02′; Potsdam System 979237.89; IGSN71 979224.08.
The station is located 1 m apart, near lamp of the petrol pump of Pakistan State Oil.

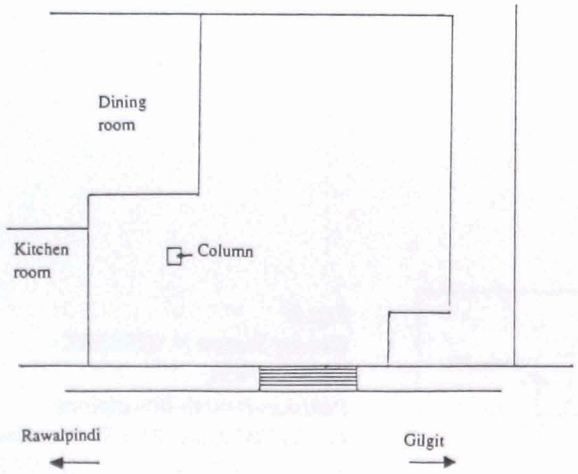

Fig. 2.
Gravity Station N. 0488 PAK;
September 1988;
Pakistan-NW Frontier Prov.-Besham;
Lat. 34°55′, Long. 72°50′; Potsdam System 979290.47; IGSN71 979276.66
The station is located in the inner court of the Prince Hotel. On the left side there is a dining room, a kitchen and, in front of them, a square column. The plate is positioned behind that column.

Fig. 3.
Gravity Station N. 0588PAK;
September 1988;
Pakistan-NW Frontier Prov.-Chilas;
Lat. 35°24′, Long. 74°07′; Potsdam System 979267.64; IGSN71 979253.83.
The station is located on the step door, left side of the main entrance of a restaurant, after the city of

Plate 3.

Fig. 1.
Gravity Station N. 0688 PAK; September 1988; Pakistan-Northern Territory-Gilgit; Lat. 35°55′, Long. 74°20′; Potsdam System 979126.69; IGSN71 979112.88.
The station is located in front of room N. 3 of the Chinnar Hotel. The plate is positioned about 1 m aside of the fourth step.

Fig. 2.
Gravity Station N. 0788 PAK; September 1988; Pakistan-Northern Territory-Gilgit; Lat. 35°55′, Long. 74°20′/Alt. 1418 m; Potsdam System 979127.20; IGSN71 979193.39.
The station is located at ground level of the control tower in Gilgit's airport.

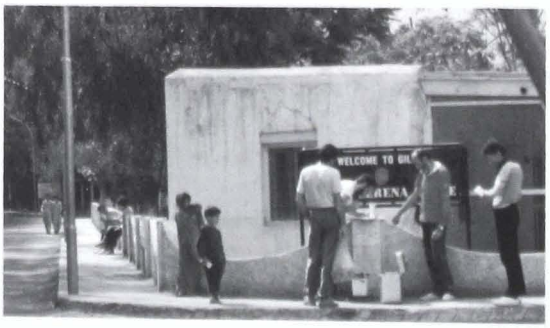

Fig. 3.
Gravity Station N. 0888 PAK; September 1988; Pakistan-Northern Territory-Gilgit; Lat. 35°55′, Long. 74°20′; Potsdam System 979127.21; IGSN71 979113.40.
The station is located on the pavement, at the fork in front of the entrance of Gilgit's airport.

Plate 4.

Fig. 1.
Gravity Station N. 0988 PAK; September 1988; Pakistan-Northern Territory-Km 390 KKH; Lat. 36°11', Long. 74°18'; Potsdam System 979003.61; IGSN71 978989.80.
The station is located on the road 1 m from the marker indicating km 390 of the KK H, roughly 1 km after the Jaglotgah slide.

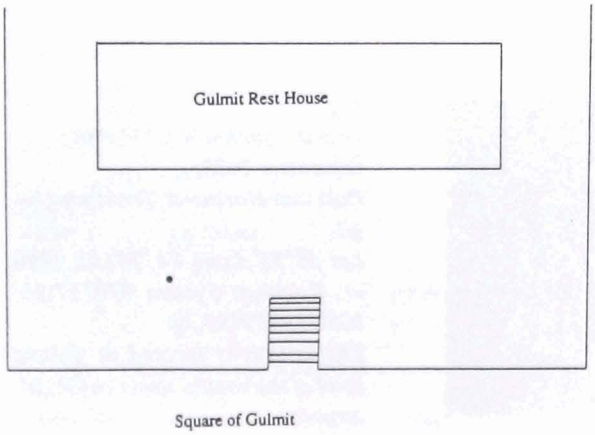

Fig. 2.
Gravity Station N. 1088 PAK; September 1988; Pakistan-Northern Territory-Gulmit; Lat. 36°22', Long. 74°52'; Potsdam System 978823.08; IGSN71 978809.27.
In the garden of the Gulmit Rest House there is a benchmark of the Pakistan Geodetic Institute. The plate is positioned at the top of this benchmark.

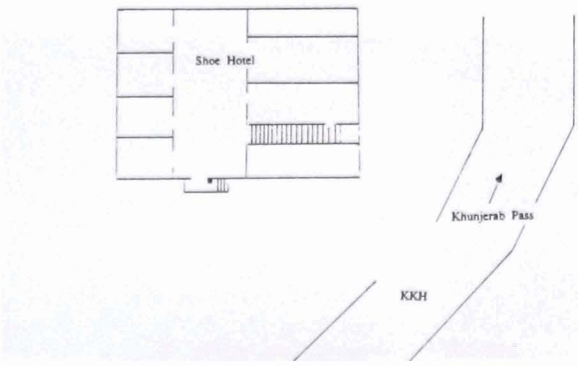

Fig. 3.
Gravity Station N. 1188 PAK; September 1988; Pakistan-Northern Territory-Gulmit; Lat. 36°22', Long. 74°52'; Potsdam System 978823.51; IGSN71 978809.70.
The station is located on the door step of the main entrance of Shoe Hotel.

Plate 5.

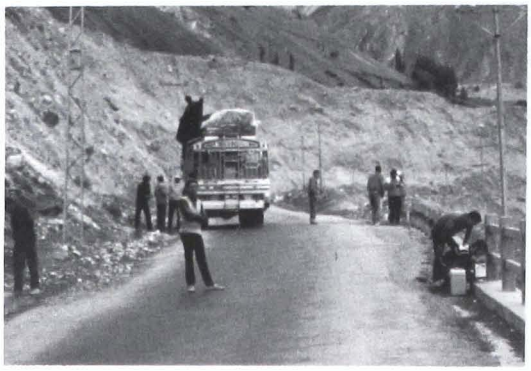

Fig. 1.
Gravity Station N. 1288 PAK;
September 1988;
Pakistan-Northern Territory-Khybar;
Lat. 36° 33′, Long. 74° 47′; Potsdam System 978811.59; IGSN71 978797.78.
Along the KKH, 1.5 km before the little town of Khybar, there is a bridge. The station is located, on the right side of the road, on the bridge, in correspondence with the last upright.

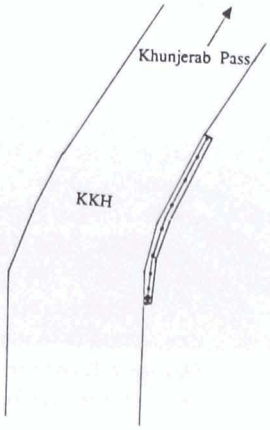

Fig. 2.
Gravity Station N. 1388 PAK;
September 1988;
Pakistan-Northern Territory;
Lat. 36° 52′, Long. 75° 12′;
Potsdam System 978602.36; IGSN71 978588.55.
Along the KKH, roughly 25 km before the Khunjerab Pass, there is the Goashul bridge. The station is located on the right side of the road, on the bridge, in correspondence with the first upright.

Fig. 3.
Gravity Station N. 1488 PAK;
September 1988;
Pakistan-Northern Territory-Khunjerab Pass;
Lat. 36° 51′, Long. 75° 27′; Potsdam System 978465.07; IGSN71 978451.26.
The station is located at the border Pakistan-China, Khunjerab Pass, in correspondence with the marker.

Plate 6.

Fig. 1.
Gravity Station N. 0188 CHI;
September 1988;
China-Xinjiang Uigur-Kashgar;
Lat. 39°32′, Long. 76°00′, Alt. 1313 m; Potsdam System 979545.04; IGSN 979531.23.
The access to Hotel Xinjang of Kashgar is by way of two symmetrical ramps. The front wall of the ramps is covered by small coloured square tiles. The measurement was carried out in correspondence with the vertical purple band.

Fig. 2.
Gravity Station N. 0288 CHI;
September 1988;
China-Xinjiang Uigur;
Lat. 38°24′, Long. 76°19′, Alt. 1235 m; Potsdam System 979473.41; IGSN71 979459.60.
The station is located on road 315 (Kashgar-Yecheng), in correspondence with the marker indicating km 1500.

Fig. 3.
Gravity Station 0388 CHI;
September 1988;
China-Xinjiang Uigur-Yecheng;
Lat. 37°22′, Long. 77°20′, Alt. 1320 m; Potsdam System 979406.08; IGSN71 979392.27.
The station is located 20 cm from the right column of the entrance of the headquarters of Xinjiang Yecheng Mountaineering Association.

Plate 7.

Fig. 1.
Gravity Station N. 0488 CHI; September 1988; China-Xinjiang Uigur; Lat. 37°31', Long. 77°19', Alt. 2090 m; Potsdam System 979190.12; IGSN71 979176.31.
The station is located on road 219 (Yecheng-Mazar-Tibet) in correspondence with the marker indicating km 73.

Fig. 2.
Gravity Station N. 0588 CHI; September 1988; China-Xinjiang Uigur-Aq-Koram; Lat. 37°08', Long. 77°08', Alt. 3200 m; Potsdam System 978978.58; IGSN71 978964.77.
The station is located on road 219 (Yecheng-Mazar-Tibet) in correspondence with the pass at a height of 3200 m. The Plate is positioned on the right side of the road in an open space.

Fig. 3.
Gravity Station N. 0688 CHI; September 1988; China-Xinjiang Uigur; Lat. 36°46', Long. 77°07', Alt. 2850 m; Potsdam System 978966.77; IGSN71 978952.96.
The station is located on road 219 (Yecheng-Mazar-Tibet) in correspondence of the marker indicating km 157.

Plate 8.

Fig. 1.
Gravity Station N. 0788 CHI;
September 1988;
China-Xinjiang Uigur-Mazar pass (Cirag Saldi);
Lat. 36°28', Long. 77°05', Alt. 4800 m; Potsdam System 978484.93; IGSN71 978471.12.
The station is located on road 219 (Yecheng-Mazar-Tibet) in correspondence with the Mazar Pass. The plate is positioned on the left side of the road, in an open space.

Fig. 2.
Gravity Station N. 0888 CHI;
September 1988;
China-Xinjiang Uigur-Bazar Dara;
Lat. 36°23'45", Long. 76°48'20", Alt. 3545 m; Potsdam System 978684.52; IGSN71 978670.71.
The station is located on the bridge of Bazar Dara. The plate is positioned at the beginning of the left parapet, going towards Aghil Pass.

III. TOPOGRAPHICAL REPORT (1)

1. Introduction

The area covered by this research is represented by maps where the Pakistan territory is more accurately defined than the Chinese territory. In short, the work is based on the following topographic maps:

a) Italian Geographic Expedition in Karakorum (the result of the work carried out by the Duke of Abruzzi, the Duke of Spoleto and Prof. A. Desio, 1929, scale 1:75,000);
b) Survey of India, scale 1:253,440;
c) R.C.F. Schomberg, 1936, scale 1:200,000;
d) Parts of Great Karakorum and Aghil Mountains surveyed by Michael Spender and colleagues on the Shipton's Expedition 1937;
e)Baltoro Glacier, survey by Cpt. F. Lombardi (Desio expedition) 1954, scale 1:100,000;
f) K^2, survey of Cpt. Lombardi (Desio expedition) 1954, scale 1:12,500;
g) Series AMS-U502, 1963, scale 1:250,000;
h) NI-43/NE (Survey of Pakistan), 1986, scale 1:500,000.

For purposes of comparison, support and integration of the project and within the framework of the programme of the geophysical and geodetic group, auxiliary astronomics observations, altimetric measurements and terrestrial photogrammetrical surveys were carried out with instruments supplied by firms operating in the topographical field, namely:

a) Th2 precision theodolite and Eldi 2-Zeiss-Salmoiraghi distimeter;
b) Aneroid barometer, model FA Wallace-Pianimpianti;
c) Rolleyflex 6.006-Geotop metric camera.

---

(1) Luigi RAMPINI, *Regione Lombardia, Milano.*

2. Astronomic observations

While the expedition was moving towards the Gasherbrum camp and when proceeding from there to the Tek-ri camp we applied ourselves to perfecting the secondary astronomy programme, prepared in collaboration with the Astronomic Observatory of Merate/Brera (Prof. F. Mazzoleni and Prof. P. Conconi), for the planimetric and orientative determination of a point with the system of elevation lines observing, with the theodolite, the passage of 43 stars (Magnitude from 3.6 to 6.0) at 30° zenith at a given moment of sideral time, but which, for objective reasons, was limited to solar time.

The elevations above the horizon were not below 15° nor over 70°.

The chronometers were synchronized with the signals transmitted by Radio RWM Moscow to eliminate any risk of errors in time; azimuthal directions differ by approx. 60 from one another, i.e. approximately 3 hours; when reading we took into account the index error of the vertical circle of the instrument.

The elevations observed were corrected as follows:

a) atmospheric refraction $r'' = 21.7 \frac{\text{mmHg pressure}}{273 + \text{temperature}}$ zenithal tg (Stanwell-Ball);

b) Sun's semidiameter from the Ephemerides;

c) parallax of the elevation of the Sun=8",8 x cos elevation.

The measurements have been inserted in the known formulas:

$\cos Z = \sin Y . \sin S + \cos Y . \cos S . \cos H$; $\text{sen } A = \cos S \frac{\text{sen} H}{\text{sen} Z}$; $H = RA \pm TSL$ where:

Z=zenithal; A=azimuth; Y=latitude of the location; S=star declination; RA=right ascension of a star; H=hour angle; TSL=local sideral time.

The longitude found takes into account the convergence of the meridians at the Poles with:

$$\lambda_1 = \lambda + \frac{X}{\cos Y_m}.$$

The position of the station, situated on the moraine on the left side of the North Gasherbrum glacier and coinciding with that obtained with GPS, was determined after three Sun observations obtaining the following coordinates: Y= 3553'20"N, λ_1=7644'28"E; while the direction of astronomic north was calculated through 4 collimations of the Sun's edges. The results, which were fairly close to the values obtained by Prof. Caporali using the main astronomy programme and GPS, confirm the limited accuracy of the method.

Table 3.1. Programme for astronomic observation of stars at Y=36°N.

STAR	Mg	AR(b)	S(°)	Azimut) h(°)	Sideral time (h m)	H
1508	4.5	19.471111	24.643611	103.2	17 18.7	2.159277
1535	5.8	20.481944	36.419722	77.9	17 59.3	2.494397
580	5.4	15.623611	40.3911	290.1	18 09.7	2.537519
595	5.0	15.958333	54.783056	319.6	18 14.3	2.280662
635	4.9	17.080833	12.756389	224.6	18 29.2	1.495414
782	4.6	20.751389	57.542778	34.2	18 38.9	2.102328
1558	4.3	21.283056	39.350278	72.0	18 45.2	2.529811
608	3.9	16.323056	46.341667	302.0	18 50.9	2.525895
783	3.6	20.751111	61.798611	23.0	19 07.2	1.630450
701	6.0	18.603056	65.481944	362.2	19 13.7	0.625087
768	4.0	20.544722	11.266111	140.8	19 17.6	1.251921
685	5.0	18.230278	64.396389	346.2	19 18.1	1.071011
1565	4.8	21.490833	23.591667	105.6	19 22.6	2.113402
804	4.3	21.359722	19.758333	115.0	19 26.5	1.918819
1469	4.7	17.992500	16.751044	236.0	19 43.3	1.729643
831	3.8	22.108333	25.292500	101.7	19 55.3	2.186121
852	4.8	22.646111	38.994722	72.7	20 07.2	2.526579
725	5.0	19.288056	11.575556	220.3	10 34.4	1.285801
1604	5.7	23.121111	49.237500	52.1	20 38.5	2.479107
1503	5.1	19.407222	11.920833	221.6	20 43.8	1.322280
1477	4.2	18.324444	36.061389	281.4	20 48.8	2.488728
1488	4.8	18.760278	26.651389	261.4	21 00.0	2.238900
1619	4.2	26.664444	44.274722	62.1	21 07.4	2.541555

Table 3.1 (continued).

STAR	Mg	AR(b)	S(")	Azimut) h(")	Sideral time (h m)	H
1622	5.0	23.758333	46.360833	57.9	21 14.0	2.525685
711	4.0	18.916667	43.933889	297.2	21 27.6	2.542863
855	3.6	22.681944	10.774722	142.8	21 29.2	1.195570
726	5.4	19.280833	53.350833	316.5	21 37.8	2.348972
1629	4.7	23.953333	25.081944	102.1	21 46.5	2.177529
768	3.8	20.544722	11.266111	219.2	21 47.8	1.251921
733	3.9	19.490278	51.708889	313.0	21 54.1	2.411410
885	4.7	23.476667	12.701111	135.6	22 04.6	1.4001231
1021	4.4	0.820278	41.020556	68.6	22 16.8	2.540881
758	4.3	20.219167	56.536667	323.5	22 23.7	2.175579
1023	5.6	0.954167	28.934444	93.6	22 38.2	2.317625
757	3.9	20.221389	46.710278	302.8	22 44.6	2.521641
1040	5.0	1.450000	45.351389	60.0	22 54.9	2.535080
16	4.2	0.539722	62.871944	19.6	23 05.8	1.442484
57	4.2	1.716389	50.634444	49.2	23 16.3	2.444384
826	5.5	22.009444	13.067778	225.6	23 26.7	1.434727
1570	5.1	21.620833	19.270000	243.7	23 30.7	1.890547
1565	4.8	21.490833	23.591667	254.4	23 36.3	2.113402
1054	5.0	2.026111	54.435278	41.2	23 43.7	2.298567
855	3.6	22.681944	10.774722	217.2	23 52.7	1.195570
Polar	2.1	2.348333	89.213611			

Latitude y=36° Zenithal Z=30"

N.B. Basic programme prepared by the Astronomical Observatory of Merate-Brera for the astronomical observation of stars at latitude = 36° N and zenithal distance 30° on the basis of the FK4 catalogue "Fundamental Catalogs n. 4", whereas for the Sun, reference was made to its position on the date of observation taken from "The Astronomical Almanac".

3. Altimetric measurements

The simultaneous observation of the pressure, temperature and relative humidity of the air at 2 p.m. Pakistan time (9 a.m. GMT) from 17th to 26th September 1989 between Gasherbrum camp and the meteorologic observatory of Gilgit and Skardu airports (distance 120 km) in Pakistan and between these and the Tek-ri camp on September 30th gave the following results referred to the altitudes of the camps:

Meteorological observation.

Date	Pressure Reading mmHg			Temperature °C			Humidity %			Camp altitude refered to		Camp note
	Camp	Gilgit	Skardu	Camp	Gilgit	Skardu	Camp	Gilgit	Skardu	Gilgit	Skardu	
Camp Gasherbrum 17.9	457,9	636,88	581,60	14,5	22,2	23,6	26	27	32	4.295,36	4.243,20	overcast
18.9	455,0	640,02	585,04	10,0	14,4	25,3	26	35	51	4.328,06	4.340,55	overcast
19.9	460,8	639,20	584,90	24,0	11,1	26,7	30	22	30	4.259,95	4.278,97	clear
20.9	458,5	633,35	582,79	19,0	21,1	28,9	40	27	28	4.251,01	4.284,08	overcast
21.9	457,9	635,0	581,44	24,0	10,1	28,3	40	53	24	4.255,25	4.288,83	partly overcast
22.9	456,5	635,98	581,89	13,0	15,3	21,1	60	38	56	4.266,29	4.259,65	overcast
23.9	455,5	634,10	583,54	9,0	14,4	25,6	60	30	28	4.236,01	4.306,73	overcast
24.9	459,5	636,35	585,27	0,0	14,4	11,7	80	39	100	4.156,59	1.184,81	snow
25.9	460,2	636,20	588,05	2,0	16,1	13,9	80	26	62	4.159,79	4.223,49	snow
26.9	454,0	634,33	588,05	13,0	20,8	21,7	30	17	38	4.320,01	4.398,69	clear
Camp Tek-ri 30.9	481,0	637,78	585,80	9,3	10,8	20,6	10	73	41	3.816,59	3.851,33	partly overcast
Altitude of airport station of: Gilgit=1,460m, Skardu=2,18m												

The measurements were inserted in Laplace- Ramond's formula, taking into account the influence of temperature on the barometric reading at the camp:

$$d = 18.393\ m \cdot \log \frac{P1}{P2}\ 1 + \left[\frac{2(T1 + T2)}{1.000}\right]$$

where:
P1=lower station pressure (Gilgit and Skardu airports);
P2=upper station pressure (base camp);
T1=bottom station temperature (Gilgit and Skardu airports);
T2=top station temperature (base camp).

Correction coefficients were also taken into account owing to the variable atmospheric humidity (n) and latitude (0.2), following the Tadini tables based on the Ruhlmann-Wild formula and on the V-wind affecting and reading with $e = \frac{V^2}{2g}$ but as the instruments were protected from the wind and as the wind at that time was not greater than 20 km per hour, error (e) was taken as zero.

The final difference in height was therefore: d'=d+n+0.2·n.

Analysis of the results, with the value applied to the respective GPS stations (difference in height determined with the theodolite), the following averages were obtained:

a) Gasherbrum camp and GPS=4,405 m taking into account all the observations of Gilgit, the average of the values was 4,400.93 m (-4.07 m), while for Skardu the average value was 4,429.00 m (+24.00 m); eight observations were considered (i.e. excluding those made on 18th and 24th September), for Gilgit the average value was 4.383.13 m (-21.87 m), whereas for Skardu the average value was 4.406.82 m (+1.82 m).

b) Tek-ri camp and GPS=3,829 m; only one observation is available (on 30th September) which gaves a value referring to Gilgit of 3,816.5 m (-12.41 m) and to Skardu of 3,851.33 (+22.33 m).

The measuring instruments were subjected to testing prior to departure and on return to ascertain any differences in reading. The tests proved negative.

The conclusions which can be drawn are of an evaluative and qualitative nature, confirming the validity of the method applied to a subject which is so difficult to define, since in the limited observation period, the results obtained were very close to the values determined with the GPS.

IV. GEOLOGICAL REPORT

1. Geological Transect from Kun Lun to Karakorum(1)

1.1. FOREWORD

The 1988 Ev-K^2-CNR Italian Expedition to the northern side of K^2 and Gasherbrums carried out a four week geological reconnaissance in the poorly known area north of the main Karakorum range, from the Shaksgam valley to the Yarkand valley at the foot of the Kun Lun range (Fig. 4.1). The area is mostly unhabited, with very few Khirgiz herdsmen driving their flocks along the Yarkand valley and its tributary Surukwat river. Instead the Shaksgam valley is totally barren.

The exploration of the area was firstly done when British ruled India (Younghusband, 1896). The 1913-1914 De Filippi Expedition walked down the Yarkand valley to face Ilik. Unfortunately, they weren't able to cross the Yarkand river and to reach the Shaksgam (De Filippi, 1924). The expedition geologists-geographers (Dainelli and Marinelli) moreover didn't reach Mazar. De Terra (1932) crossed the Yarkand further east. Also Norin in 1935 visited the area further east, and passing near Mazar he observed the very thick slates cropping out in the area. He named them "Kilian Facies" in the 1946 report, on a supposed affinity with slates cropping out on the northern side of the Kun Lun. Consequently, in the old times, no geologists visited the lower Surukwat area. Expeditions starting from Sinkiang preferred to turn more eastwards.

The Shaksgam valley itself was attained only by three geographical and geological parties, all coming from the south and ultimately starting their journey from Srinagar. They were:

1) the Desio team in 1929, within the expedition of the Duke of Spoleto, who

---

(1) Maurizio GAETANI and Guido GOSSO, *Università di Milano. Dipartimento di Scienze della Terra;* Ugo POGNANTE, *Università di Torino. Dipartimento di Scienze della Terra.*

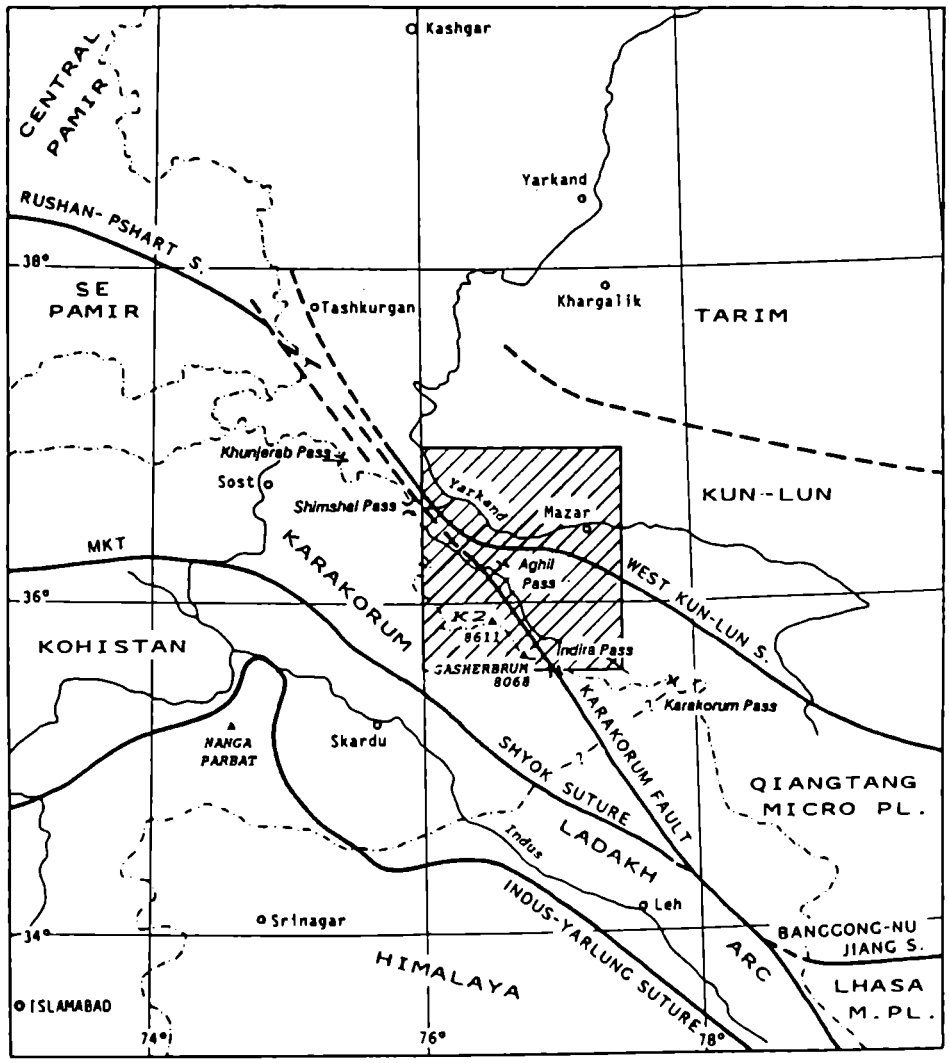

Fig. 4.1. Index map with the main tectonic sudvisions. Connection of the Aghil range to the western termination of the Qiangtang microplate is only tentative. The square with oblique lines indicates the area detailed in Fig. 4.2.

reached the Shaksgam through the Baltoro, (East Muztagh pass), and Sarpo Laggo glaciers and explored most of the valley up to the Kyagar glacier.

2) the Wyss expedition in 1935, who arrived from the Karakorum pass, entered the Shaksgam from the east, but their geologists weren't able to cross the Singhiè glacier. Only a small geographical party arrived to the Gasherbrum glacier snout (Mason, 1948).

3) The Shipton and Auden expedition in 1937, who reached the Shaksgam from the south, via Baltoro and Sarpo Laggo, and travelled further north till Aghil pass and the upper reaches of the Surukwat (named by them Zug Shaksgam, meaning the wrong Shaksgam) and of the Aghil Dara (named by them Surukwat).

The geological and paleontological reports on the data obtained by these expeditions were published over a large span of years. (Desio, 1930a, 1930b, 1936; Merla, 1934; Auden, 1938; Wyss, 1940; Norin, 1946; Ciry, 1965; Fantini Sestini, 1965 a, b; Desio, 1979, 1980). Auden itself didn't publish too much, except the 1938 preliminary report. Some of his observations are, however, incorporated in the Desio's 1980 book. Since our goal was mostly the Shaksgam and Sarpo Laggo geology, we refer to the Desio monograph (1980) for a more complete history of these pioniering researches .

Chinese geologists considered only the main features of these remote areas, including them in general geological maps. Two of them (Chinese Academy of Geological Sciences, 1975, 1976) give a very broad and rough picture of the region. The other two are the 1:1.500,000 Geological Map of Tibet (1980), which appears to be mostly based on satellite imagery for the area here considered (the Shaksgam valley is largely unmapped because of snow) and the Metamorphic Map of China (Cheng et al., 1986), in which the Yarkand, Surukwat and Shaksgam valleys are considered from the metamorphic point of view, the main granitic bodies mapped and their age indicated. However, the low-very low grade metamorphics found in the Aghil Dara are not mentioned and most of the Shaksgam valley is considered of low metamorphic grade also where unmetamorphosed sediments are present. Very general informations are also given in Yang et al. (1986). The Academia Sinica organized since 1986 geological expeditions in the area between Kun Lun and Karakorum, especially in the Yarkand valley, but results are not yet available (Sun, pers. comm., 1990). Very recently, a joint research project between the French CNRS and the Academia Sinica started in 1989, with the geotraverse Yecheng-Shiquanhe. Preliminary results have discussed during the "Colloque Kun lun–Karakorum 90", held in Paris June 1990.

This was the first foreign geological party allowed to study the geology of

Shaksgam since it is under Chinese administration. A preliminary account has been recently published (Gaetani et al., 1990b).

1.2. MAIN GEOLOGICAL FRAMEWORK

Across the N-S traverse from Yeh Chen to the Shaksgam valley (NE slopes of K^2 and Gasherbrum peaks), the following tectonic units have been recognized on field evidence and SPOT satellite imagery (Fig. 4.2) :

1) Kun Lun Crystalline and associated sediments.
2) Bazar-Dara Slates and associated granitoids.
3) Surukwat Thrust Sheets.
4) Aghil Dara Granodiorite.
5) Shaksgam Sedimentary Belt.
6) Sughet Granodiorite.
7) Sarpo Laggo - K^2 Metamorphics.

These units are separated by syn-late-metamorphic thrusts or post-metamorphic faults. We shall discuss here mostly units 2 to 7.

1) Kun Lun Crystalline and associated sediments.

Leaving the Tarim Depression, the road from So-che (Yarkand) and Yeh Chen (Kargalikh) penetrates the gravel fans of the Kun Lun, then the sedimentary belt to the north of the range. Along the Yeh Chen-Mazar road, the Kun Lun Crystalline crops out from the Aq-Koram pass (3475 m) in the north (toponymy after Norin, 1946) where it is bordered by very-low-grade epidote bearing slates (considered as Kilian Slates by De Terra, 1932, and Norin, 1946), to just north of the Cirag Saldi pass (5010 m), immediately north of Mazar, in the south. Close to the northern boundary, the Kun Lun Crystalline chiefly consists of migmatic gneisses and minor amphibolites, while a sequence of granitoids and orthogneisses is widespread elsewhere. The highest grade and originally deeper-seated rocks seems to be mostly located in the northern areas, while southwards, near the main divide, a large granitoid complex crops out.

The granitoid complex is bounded to the south by a fault zone. The area north and south of the Cirag Saldi pass consists of squeezed subvertical slices of terrigenous rocks (10 m thick grey dark conglomerate beds with crystalline pebbles, sandstones and siltstones) and thrusted granitoid slabs. They are bounded to the south of the pass by a faulted contact, vertical or steeply dipping to the north, with the Bazar Dara Slates. This fault zone is considered as the western prosecution of the Altin Tagh Fault (Matte et al., 1990a).

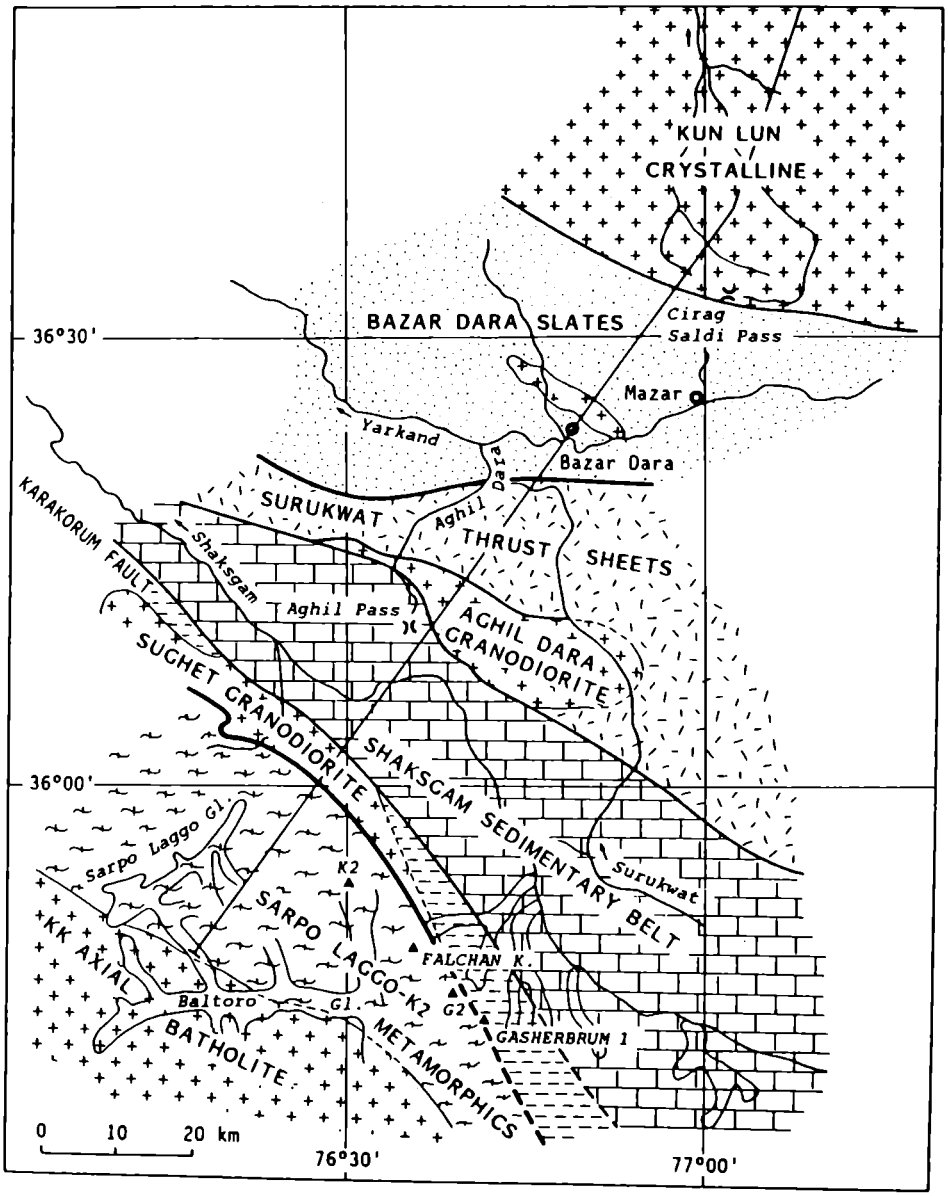

Fig. 4.2. The tectonostratigraphic units described in the text.

2) Bazar Dara Slates and associated granitoids.

The valley of the Yarkand river is carved into a monotonous sequence, several thousand meters thick, of grey to dark slates, siltstones and fine sandstones. Bedding is thin to medium, never graded, with very rare parallel laminations. Composition is litharenitic to sublitharenitic. The Bazar Dara Slates are unmetamorphosed or very low-grade rocks characterized by at least two phases of ductile folding: the first phase formed isoclinal folds with steeply dipping axial planes (Pl. 1, Fig. 1), whilst the second phase formed open folds with gently dipping axial surfaces. Decametre- to kilometre-sized bodies of biotitic granites and rare shoshonitic to ultrapotassic sills and dykes, several decimetres thick, occur within the slates (Pl. 2, Fig. 1). On the metamorphic map of China (1986), the granitoid body near Bazar Dara is considered as belonging to the Variscan cycle. Preliminary K-Ar biotite cooling age obtained on a single sample collected along the road between Mazar and Bazar Dara give a younger, Jurassic age (171.5 ± 5.4 MY; Le Fort, 1990, pers. comm.). On the same map, the slates are attributed to the greenschist facies, whilst we found only anchimetamorphic imprint, between Mazar–Bazar Dara and the Surukwat. The geological map of Tibet (1980) assignes an Ordovician-Silurian age to the slates, in which we didn't found any fossil. If a Triassic-Jurassic age for the intrusive granitic bodies will be confirmed, also a younger age for the Bazar Dara Slates could not be ruled out. We had no time to study in detail the granite/slates deformation relationships: at the mesoscopic level no pervasive and metamorphic deformations were observed in the granodiorites.

3) Surukwat Thrust Sheets (STS).

A complex sequence of metamorphic and non-metamorphic thrust sheets (STS) occurs between the Surukwat–Aghil Dara confluence and a fault located north of the Aghil pass. It is separated from the Bazar Dara Slates by a subvertical to south dipping fault with WSW-ENE strike (Pl. 1, Fig. 2). On the satellite imagery this straight fault seems to be a sinistral strike-slip, which displaces the major suture. This fault is also connected to a gravimetric discontinuity (profile 1, p. 59). We interpret this tectonic lineament as a part of the W Kun Lun Fault (Cheng et al., 1986) or Akhsae Chin Fault (Desio, 1979). It may be also regarded as the western extension of the Lighten Lake Cryptic Suture of Baud (1989) and of the Hongshanhu–Qiaoertianshan Structural Zone of Pan & Wang (1990).

From north to south, the STS start with non-metamorphic slices of coarse to fine red greywackes interbedded with grey-dark fine-bedded wackestone-mudstones boudinaged within anhydritic bodies (Pl. 2, Fig. 2). This anhydrite-limestone boudinaged unit forms a continous belt from the Aghil Dara towards the

Surukwat and may be followed for at least 10 km. It desappears southwestwards against the big vertical fault.

Bodies of metadiorites follow further south and are thrusted on the red sandstones (Pl.2, Fig.3). The metadiorites are intercalated with felsic rocks, mylonitic micaschists with minor marbles, biotite-bearing gneisses and meta-conglomerates, and, finally, strongly foliated biotite-bearing metapelites alternating with mylonitic orthogneisses. This metamorphic slab represent a new finding and it will be described petrologically in the following section (Pognante, p. 142). An increase in the metamorphic grade from unmetamorphosed to very low-grade assemblages in northernmost areas to the low-grade assemblages southwards was observed within this composite unit. All the stacked slabs tend to dip southwards, with an increasing dip of foliation.

4) Aghil Dara Granodiorite.

To the south, out of the gorges, the Aghil Dara opens in a small plain carved in low-grade metapelites. This is the last term of the STS, which is bounded to the south by a sharp fault contact with an intrusive body that we name Aghil Dara Granodiorite (Fig. 4.3). Near the contact, several gneissic layers probably derived from original granitic dykes are present in the metapelites, but they are not in direct relationships with the main graniodioritic body, from which they are separated by a cataclasite (Pl.

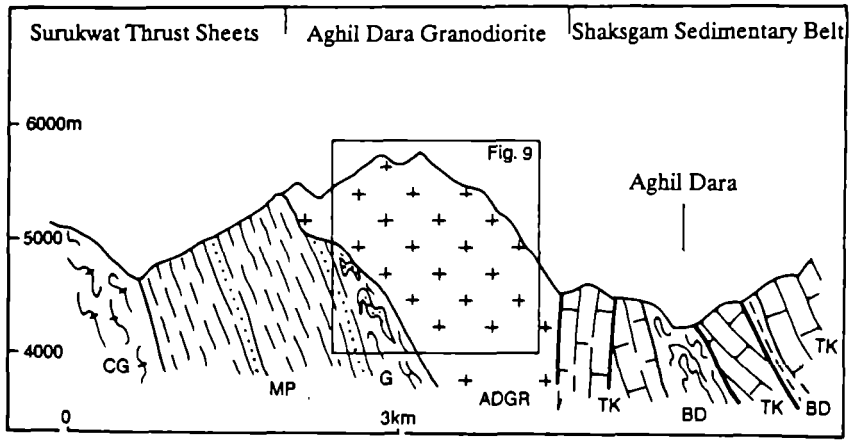

Fig. 4.3. Relationships between STS-Aghil Dara Granodiorite and Shaksgam Sedimentary Belt along the right bank of the upper Aghil Dara. 1 - CG = Conglomeratic gneiss; 2 - MP = metapelites; 3 - G = gneiss dykes; 4 - ADGR = Aghil Dara Granodiorite; 5 - TK = dark-grey oncolitic poorly bedded limestones (Tek-ri Fm., Middle Jurassic); 6 - BD = Dark-grey bedded limestones with chert nodules and marls intercalations (top of the Tek-ri Fm., and Bdongo-la Fm., Middle Jurassic).

3, Fig. 1). The Aghil Dara Granodiorite forms a large body consisting of prevalent horneblende biotite-bearing granodiorites with minor porphyritic granites, quartzodiorites and gabbros. The porphyritic granites rich in large poikylitic K-feldspar intrude these lithologies near the Aghil pass. The Aghil Dara Granodiorite is weakly deformed and altered into sericite, chlorite and epidote associations. According to the metamorphic map of China (1986), this granodiorite belongs to the Yanshanian cycle.

5) Shaksgam Sedimentary Belt.

At the end of the small plain at 4000 m altitude, before the track turn southeast to the Aghil pass, another tectonic boundary is crossed, between the Aghil Dara Granodiorite and the Skaksgam Sedimentary Belt (Pl. 3, Fig. 2). The track along the northern side of the Aghil pass mostly follow this contact, which has been already sketched by Auden (1938) and Desio (1980). The fault is characterized by decametre-thick cataclasites, and is vertical to steeply dipping to the north. Only southeast of the Aghil pass, the granodiorite seems to be thrusted over the sedimentary series (Pl. 4, Fig. 1). This fault coincides with the significant change in density occurring at this level, evident in the gravimetric profile 2 (Palmieri, p. 61).

The Shaksgam valley is mostly carved in a sedimentary belt, 15 - 20 km wide. The sedimentary sequence is at least 3 km thick and extends, where proved by fossils, from Permian to Jurassic. The existence of Carboniferous and Cretaceous rocks is doubtful. The sequence is reported in Fig. 4.4 and here summarized. For a more comprehensive report, refer to Gaetani (p. 124). The sedimentary succession is displaced in a open fold system, faulted, thrusted and stacked toghether. It appears that large folds represent the initial deformation of the sedimentary sequence. They were followed by faults with vertical or subvertical throw, that disrupted the folds and tend to emphasize an antiform structure on both sides of the valley from the Aghil to the Gasherbrum and Staghar glacier snouts (Figs. 4.5 and 4.6). Also minor strike-slip faults with subhorizontal throw were observed (Pl. 4, Fig. 2).

Finally it should be noted that the gravimetric profiles 2 and 3 show a general lowering trend of the gravity anomaly towards south within the sedimentary belt (Palmieri, p. 61). This fact need a more general interpretation and it will be discussed in the final section.

The base of the sedimentary sequence is always thrust or faulted. It starts with at least 150 m of grey to dark siltstones, fine sandstones and coarser litharenites in a coarsening-upward sequence of submerged shelf and deltaic sandy bars. At the top, the marine ingression is characterized by sandstones containing fossil fragments. The following Shaksgam Formation, more than 200 m thick, may be easily sub-

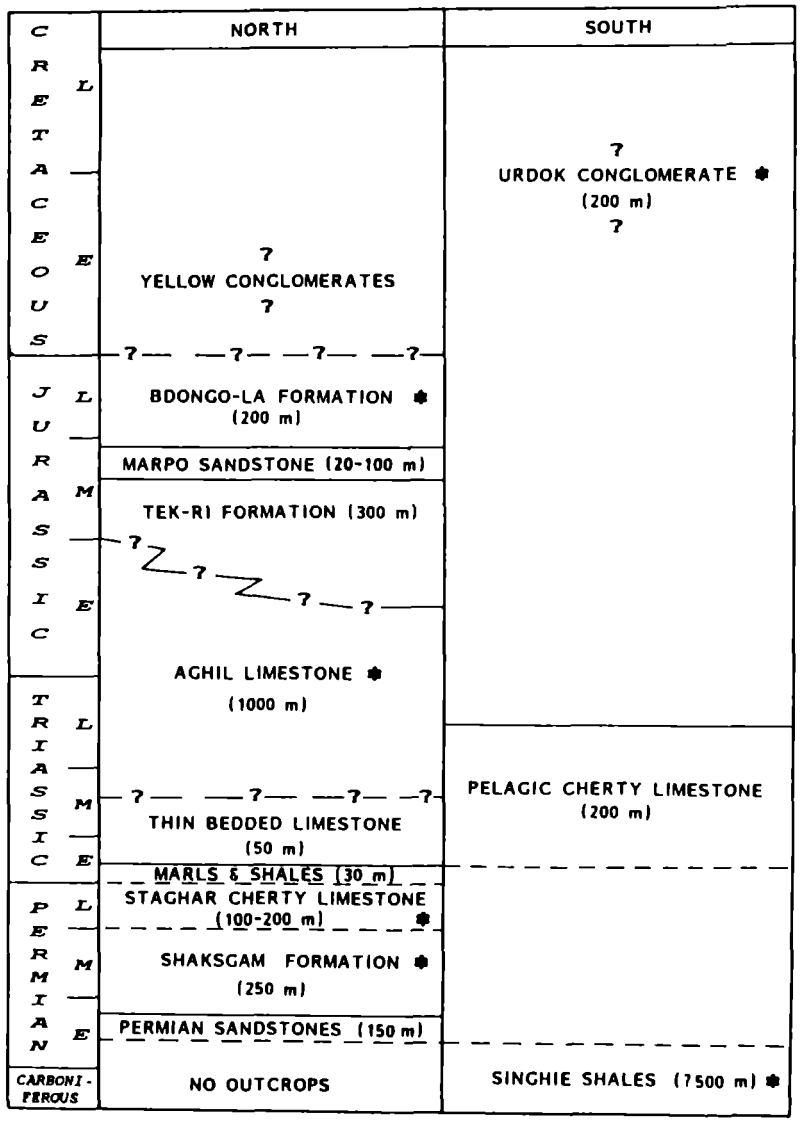

Fig. 4.4. Stratigraphic terminology for the Shaksgam Sedimentary Belt. Units with asterisk were used or introduced by Desio (1980). The others were introduced by Gaetani et al. (1990b).

divided in three members. Top to bottom, they are: C) grey well bedded limestones with marly intercalations; B) quartzarenites, litharenites, hybrid sandstones, with minor carbonate intercalations; A) skeletal shallow water limestones. Age: Artinskian-?Murgabian. Environment: shallow-water carbonate ramp with cyclic clastic inputs, slightly deeper towards the top.

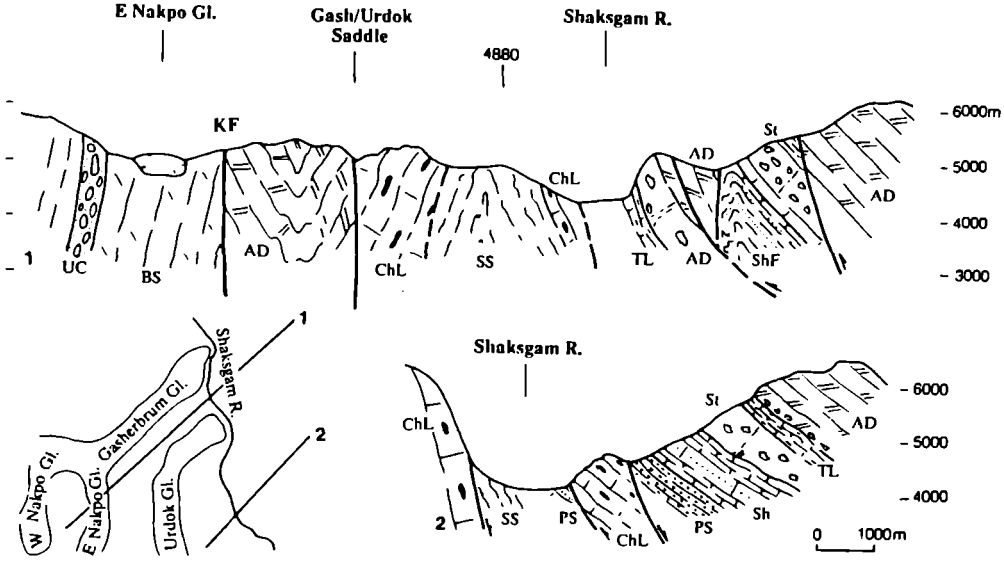

Fig. 4.5. Cross-sections through the Shaksgam valley. To note the broad antiform structure, with older rocks at the center of the valley and the southward change of fault dipping. AD= Aghil Dolomite; ShF = Shaksgam Fm., TL = Thin Bedded Limestones (Triassic), StF = Staghar Fm, including resedimented breccia bodies, ChL = Cherty Limestone, PS = Permian Sandstones, SS = Singhie Shales, UC = Urdok Conglomerate, KF = Main alignment of the Karakorum Fault Zone.

Then, with the Staghar Limestone (at least 100 m thick), the deepening is emphasized. Grey dark well bedded wacke stones to mudstones with dark cherty nodules form the bulk of the unit. Upwards, the pelagic limestones are increasingly polluted by graded calciruditic to calcarenitic beds, with shallow-water carbonates. At the top, one (or two) huge calciruditic well-amalgamated calciruditic horizons, up to 50-100 m thick, follow. Age: Murgabian-Djulfian.

The deep water sedimentation continued through the topmost Permian until the "Thin bedded limestones" (thickness 50 m). These are thin bedded grey-dark mudstone/wackestones, without chert, with thin clay marly interbeds. A few m above the base a Spathian age was proved.

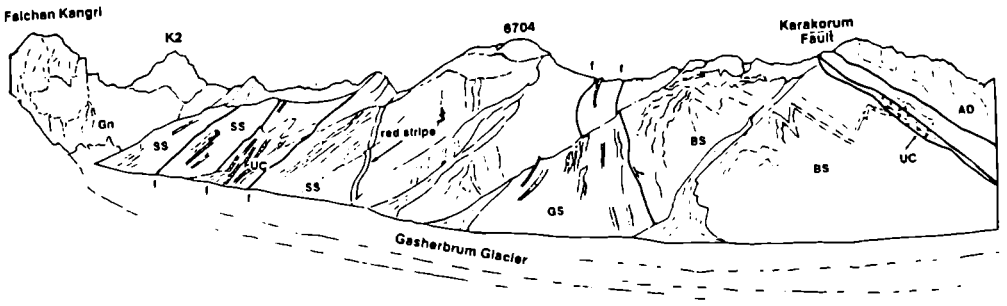

Fig. 4.6. The left bank of the Gasherbrum glacier as seen from the right bank the Gasherbrum. UC = Urdok Conglomerate, BS = Black slates, perhaps correlative with Singhiè Shales, AD = Aghil Dolomite, SS = Singhiè Shales, GS = Grey Sandstone, Gn = K^2 Gneiss. A very good detail of the KFZ is figured in Desio (1980, pl. XXII, fig. 1).

The sequence evolves into a huge polygenetic brecciated body, including boulders from the thin-bedded Triassic limestones, totally dolomitized. Thickness may reach more than 200 m. This event allowed the return to shallow-water conditions, as indicated by the following very thick dolomitic unit, reaching 1000 m in thickness, forming the bulk of the Aghil Limestone. Cyclothemic peritidal sequences with megalodontids represent the most characteristic facies, locally coarsely dolomitized. Well-bedded peritidal sequences grade laterally into massive walls, lining the middle part of the Shaksgam valley. Age: Late Triassic -Early Jurassic.

The shallow-water carbonate complex evolves upwards, but it may also be laterally equivalent to the Aghil Limestone open platform, in a more protected and organic-rich unit, the Tek-ri Formation, at least 300 m thick. This unit consists of bedded grey dark mudstone/wackestones, with rare dark cherts. In the middle and upper part, oncolitic limestones associated with bioclastic packstones are widespread. The benthic Foraminifera suggest a Middle Jurassic age, possibly Bathonian for the top of the Tek-ri Formation.

The carbonate platform development is interrupted by the Marpo Formation, which consists of red sandstones and siltstones, up to 100 m thick east of the Aghil

pass, but usually between 20 and 40 m in the middle part of the valley. Their base is prograding on the Tek-ri Formation. Westwards, the unit starts with alternating grey marls and red siltstones, followed by polymict conglomerates. It ends with red shaly sandstones. Eastwards in contrast, the sequence is thicker and consists almost exclusively of red fine sandstones and siltstones. From east to west, the interfingering of an alluvial plain with coastal lagoons is recorded.

Another marine ingression with the following Bdongo-la Formation is recorded. At the base there are 10 m bed of dark slightly metamorphosed limestone with corals of Middle Jurassic age (Fantini Sestini, 1965b). Above, grey shales and siltstones, with minor sandstones intercalations showing rare convolute and parallel laminations suggest a possible distal turbidite deposition, in a deeper environment. The top of the sedimentary sequence is represented by yellow polymict conglomerate. They contain sedimentary pebbles, derived almost exclusively from the Mesozoic rocks.

In the southeast corner of the visited region, in the Skyang–Gasherbrum–Urdok glaciers area, a partially different sequence crops out, mostly disrupted by faults.

The base might be constituted by the Singhiè Shales. They are black, splintery shales and occasionally siltstones. Thickness should be of several hundreds meters, especially on both sides of the middle Gasherbrum glacier. Along the ridge between the Skyang and Gasherbrum glaciers, the shales seems to pass to sandstones with brachiopod fragments very similar to the basal marine sandstone of the Permian of the Northern Zone. If this is true, the Singhiè Shales would lie below the Permian Sandstone sequence. Consequently an Early Permian or Late Carboniferous age should be inferred. To the south a clear equivalent of the Shaksgam Formation was not observed and most of the carbonate rocks consist of cherty thin-to thick-bedded grey limestones. Their maximum measured thickness is 200 m. The youngest fossil recognized are conodonts of Carnian age. Consequently we have here a more persistent pelagic sequence and more distal than the previously described northern Permo-Triassic sequence.

Finally, we have a puzzling unit, the Urdok Conglomerate. It crops out between the Gasherbrum and Urdok glaciers (Fig. 4.6), south of the main alignement of the Karakorum Fault Zone (KFZ) (Molnar & Tapponnier, 1975). It forms slabs of some hundred meters, tectonically embedded in a shaly, non metamorphic, dark unit, which we are not able to separate from the Singhiè Shales. It consists of m-beds with scoured base of polymict conglomerate, with clasts up to 50 cm, fairly rounded and often poorly sorted, in a red matrix. Clasts are mostly derived from sandstones, whilst carbonates are rarer. Metamorphic pebbles are also present (about 15 %). For reasons

that will be fully developed at p. 106, the evidence seems to be against the Middle Triassic age suggested by Desio (1980) for the Urdok Conglomerate.

6) Sughet Granodiorite.

A body of weakly deformed and relatively well preserved biotite-bearing granodiorite occurs in the lower (northern) part of the Sarpo Laggo valley, near Sughet Jangal. The sharp contact with the Shaksgam Sedimentary Belt is defined by a fault zone a few tens of m thick and directed NW-SE, which we ascribe to the main alignement of the KFZ (Fig. 4.7). Brittle deformation and incipient alteration without

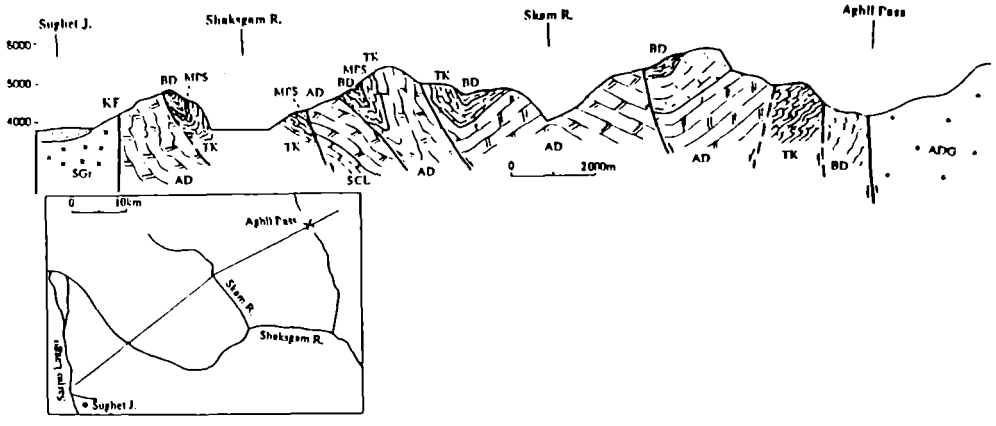

Fig. 4.7. Structure of the Shaksgam Sedimentary Belt near the contact with the Sughet Granodiorite. North dipping isoclinal folds are vertically truncated by the main aligment of the Karakorum Fault. SGr = Sughet Granodiorite, KF = Karakorum Fault, AD = Aghil Dolomite, BD = Bdongo-la Fm., MPS = Marpo Sandstone, TK = Tek-ri Fm, ADG = Aghil Dara Granodiorite.

formation of a new metamorphic fabric occur in the fault zone. Approaching the KFZ, the Aghil Dolomites are deformed and heavily recrystallized, while the Megalodontid fossils are heavily strained. On the contrary, the tectonic contact with the Sarpo Laggo-K^2 Metamorphics is defined by a mylonitic belt associated with a very low-grade recrystallization and including slices of strongly foliated carbonatic slates, marbles and metaconglomerates (Fig. 4.8). In the gravimetric profile 4 p. 62,

measured along the Sarpo Laggo valley, a more significant discontinuity was observed at this boundary than at the KF itself.

According to the metamorphic map of China (1986), this granodiorite belongs to the Yanshanian cycle. One sample K-Ar biotite age of the Sughet Granodiorite give an age of 94.8 ± 3.2 MA (Cretaceous) (Le Fort, 1990, pers. comm).

Lithologies comparable to the Sughet Granodiorite are frequent in the moraine of the northern Gasherbrum glacier, but they are characterized by more pervasive deformations and recrystallization. This suggests that a more or less continuous body of weakly more deformed granodiorites is interposed between the Shaksgam Sedimentary Belt and the Sarpo Laggo-K^2 Metamorphics.

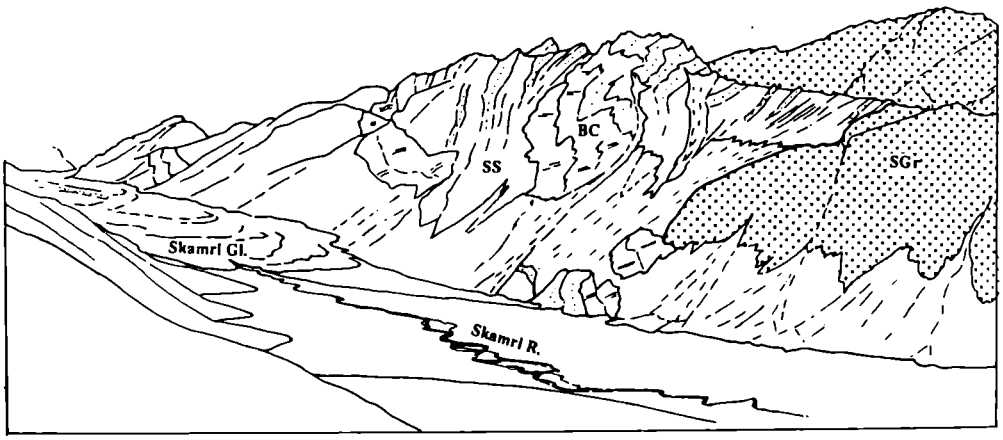

Fig. 4.8. The Sarpo Laggo-K^2 Metamorphics and the Sughet Granodiorite form a south dipping surface on the left bank of the Skamri glacier and the Sarpo Laggo valley. SS = Sandstones beds, BC = Brown Carbonates, SGR = Sughet Granodiorite.

7) Sarpo Laggo-K^2 Metamorphics.

These form a unit of strongly deformed low-to medium-grade metamorphics which crops out in the Sarpo Laggo valley, in the K^2 area and possibly extends to the SE at the head of the northern Gasherbrum valley. The metamorphics include biotite-muscovite bearing ortho- and para-gneisses, impure marbles and pegmatoids, characterized by a pervasive low-grade recrystallization. The complicated tectonic

setting of this unit and the existence of large scale transpositions are recorded by the frequent isoclinal folds characterized by steeply dipping axial planes.

On the left side of the Sarpo Laggo glacier near its snout, and at the stream confluence Skamri–Sarpo Laggo, a less-to non-metamorphosed sedimentary faulted sheet crops out. In this sheet, fusulinid-rich hybrid sandstones (Early Permian) and cherty limestones similar to the Permian of the Shaksgam Sedimentary Belt. If this is true, the Late Permian are still identifiable. The sketch map of Desio (1936) gives further details on the spot and it is more correct than the following interpretation (1980), influenced by the Auden's 1937 survey. The sedimentary belt continues up in the lower reaches of the Skamri glacier, forming also the Crown peak. Abundant garnet-staurolite-andalusite bearing slates and high-grade migmatized gneisses occur in the moraine of the Sarpo Laggo glacier, derived from the upper reaches of the glacier (Desio, 1980).

1.3. POST-METAMORPHIC DYKES

Units 2, 5, 6 and 7 are crosscut by some post-metamorphic porphyritic dykes of high-K calc-alkaline, shoshonitic and ultrapotassic affinity (p. 14). They include dacites, andesites, trachytes and lamprophyres characterized by abundant phologopite and amphibolephenocrysts. These dykes intrude the sedimentary, igneous and metamorphic foliations, but are in turn crosscut by the post-metamorphic faults linked to the KFZ. Comparable dykes have been described on the southern side of K^2-Gasherbrum range (Baltoro glacier) by Desio and Zanettin (1970). Biotites from these dykes give K-Ar ages around 22 MA (Searle et al., 1989).

2. Sedimentary rocks (1)

2.1. INTRODUCTION

Sedimentary rocks are present in four of the tectonic zones recognized during the 1988 geological reconnaissance from the Kun Lun to Karakorum. Most of them are cropping out in the Shaksgam Sedimentary Zone, and consequently major attention will be payed to this zone.

---

(1) Maurizio GAETANI.

2.2. BAZAR DARA SLATES

The valley of the Yarkand river is carved into a monotonous sequence, several thousand meters thick, of grey to dark slates, siltstones and fine sandstones. Bedding is thin to medium, never graded, with very rare parallel laminations. Due to large folding, it was impossible to ascertain if the fine sandstones are prevalent in the lower part of the unit, and if there is a meaning or a logical repetition in the shale/sandstone alternance, each sheet of them several hundred meters thick. The composition is litharenitic to sublitharenitic, poor in matrix, with siliceous cement. The Bazar Dara Slates are unmetamorphosed or very low-grade rocks.

2.3. SURUKWAT THRUST SHEETS (STS)

Within the complex sequence of metamorphic and non-metamorphic thrust sheets of the Surukwat (STS), very peculiar are red sandstones with anhydrite and limestones intercalated bodies. The non-metamorphic slices crop out in the northern part of the tectonic zone and the geometrical base of the stacked slabs. See Pl. 2 and the geological map.

The sequence consists of coarse to fine red volcanic litharenites interbedded with grey-dark fine-bedded wackestone-mudstones boudinaged within anhydritic bodies. A 300 point counting on sandstones, made by L. Angiolini (Milano), indicates the monocrystalline quartz, sometime with magmatic corrosion rim, as the most spread component (42%-69%), followed by compound quartz (4%-16%). Strongly altered volcanic fragments, both felsic both microlithic, represent the 15%-36%, while feldspars (max 1.9%), oxides (usually rare, but in finer samples up to 11%) and matrix (till 3%), are subordinated. Cement is invariably siliceous, forming the 10%-15% of total rock.

Associated with the anhydrite bodies are well bedded gray mudstones, with very few poorly preserved ostracods.

2.4. SHAKSGAM SEDIMENTARY BELT

The Shaksgam valley is mostly carved in a sedimentary belt, 15 - 20 km wide. The sedimentary sequence (Fig. 4.9) is at least 3 km thick and extends, where proved by fossils, from Permian to Jurassic. The existence of Carboniferous and Cretaceous rocks is doubtful.

The sequence has a single development in its broad lines, but in detail several lateral facies changes occur from the Permian to Jurassic. However, our preliminary visit did not have sufficient time to unravel these lateral variations. Moreover, we

were not able to really study the sedimentary sequence along the Gasherbrum glacier, to the southeast of the Karakorum Fault. I will start to describe the sedimentary units northeast of the Karakorum Fault, and subsequently some discussion will dealt with the other rock units. The base of the sedimentary sequence is everywhere thrusted or faulted.

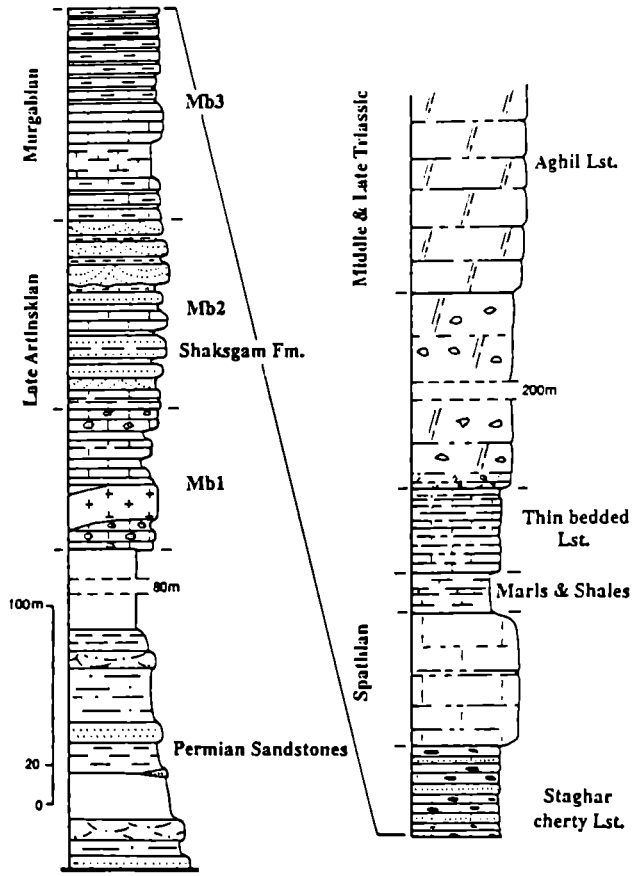

Fig. 4.9. A diagrammatic sketch of the Permo-Triassic succession in Shaksgam valley.

2.4.1. *SINGHIÈ SHALES.*

Name. It was introduced by Desio (1963) and extensively discussed in Desio (1980). In this paper however, I keep distinct the sandstone–shale alternance (here called Permian Sandstones), lying possibly above the main shale–siltstone unit, to which only I applie the name Singhiè Shales.

Lithology. Black splintery shales, siltstones, and rare fine sandstones, poorly bedded, forming a monotonous sequence several hundred meters thick. The fine sandstones are litharenite- sublitharenites, with abundant matrix, locally bioturbated. The black shales cropping out south-west of the main alignement of the Karakorum Fault are here considered separately from the Singhiè Shales. More work is needed on this subject.

Occurrence. The Singhiè Shales crop out on the left side of the Shaksgam valley, from SW of Gasherbrum Jilga eastwards.

Age. No fossils were found in this unit and it is not possible to substantiate the previous claiming for a Carboniferous age. On the ridge between the Gasherbrum and Skyang glacier snouts, the Singhiè Shales seem to underlie, without faults, the Permian Sandstones. If this is true, the supposed Carboniferous age could be correct, as well an earliest Permian.

In the Lingzi Thang area (westernmost Tibet), Norin (1946) described the Horpatso Series, equally not constrained with fossils and referred to the Carboniferous-Early Permian. Also there the sequence evolves from shales and siltstones to sandstones, eventually passing to Permian marine carbonates. Gergan & Pant (1983) introduced for the area south of the Karakorum pass the Saser Brangsa Formation, consisting mostly of shales. In the intercalated sandstone and limestone horizons, they quote a brachiopod fauna of Carboniferous-Permian age. The presence of a coarsening-upwards terrigenous prism in the Late Carboniferous and Early Permian of the Karakorum and surrounding areas seems to be widely accepted in the scanty literature on this matter.

2.4.2. *PERMIAN SANDSTONES.*

Name. Informally proposed in Gaetani et al. (1990b) to designate the sandstone/slaty succession, lying below the Permian marine carbonates. Desio (1980) included it in the Singhiè Shales. I prefer to keep these sandstones independant, because of the coarser lithology and the possibility that the two units are not stratigraphically surimposed.

Lithology. It consists of at least 150 m of grey to dark siltstones, fine sandstones and coarser litharenites in a coarsening-upward sequence of deltaic to submerged

shelf sandy bars. Gray to green bioturbated siltstones may occur in the lower part of the unit. At the top, the marine ingression is characterized by sandstones containing fragmented brachiopods and bryozoans. On the right bank of the Shaksgam river, facing Gasherbrum Jilga, the upper part of this unit consists of black shales with dm-arenaceous concretions.

From the petrographic point of view, the sandstones are quartzarenite to sub-litharenites, dominated by subrounded to well rounded monocrystalline quartz, altered lithics and oxides. Amongst the bioclasts, ammonoids, gastropods, brachiopods, bryozoans, and echinoderms fragments may be recognized. In the upper part of this unit the prevailing cement is carbonatic. The Permian Sandstones record the transgression of a subtidal shelf in which sandy waves accumulated in flat or lens bodies, within a prevailing muddy to silty bottom. The upward cleaner quartzarenites testifye to an increasing of bottom energy towards the top.

Occurrence. This unit was recognized from the right bank of the Shaksgam facing Gasherbrum Jilga, eastwards, on both side of the valley.

Age. The fossil content of the upper part is fairly abundant, but fragmentary. Due to the Artinskian age of the base of the overlying Shaksgam Fm., and supposing a stratigraphical continuity, an Early Permian age is inferred.

2.4.3. *SHAKSGAM FORMATION.*

Name. This term was introduced by Auden (1938) to designate most of the Permo-Carboniferous rocks of the area. Desio (1980) restricted the term to the prevailing carbonate succession of Permian age, capped by the Urdok Conglomerate or the Chikchi-ri Shales (Desio, 1980, p. 87). Here the term Shaksgam Fm. is used, mostly according to Desio, to designate the well-bedded grey carbonates without cherts, interbedded in their middle part with cross-bedded sandstones.

Lithology. The Shaksgam Formation, more than 200 m thick, consists of shallow-water limestones, litharenites and hybrid sandstones, and grey nodular well-bedded limestones with marly intercalations. It may be easily subdivided into three members (Fig. 4.10). The lower one is formed by crinoidal or bioclastic well bedded limestone, in metric packages separated by shales. Thickness from 50 to 80 m, with apparently a greater development in front of the Staghar glacier snout. Conversely, on the right bank of the Shaksgam, facing Gasherbrum Jilga, the sequence is more polluted by clay. A strongly altered sill was observed within this member. The second member is mostly arenitic with high-angle cross-bedded festooned litharenites to quartzarenites, in m thick lenticular bodies. Between the banks, there are m-thick well bedded dark grey packstone to wackestones. This

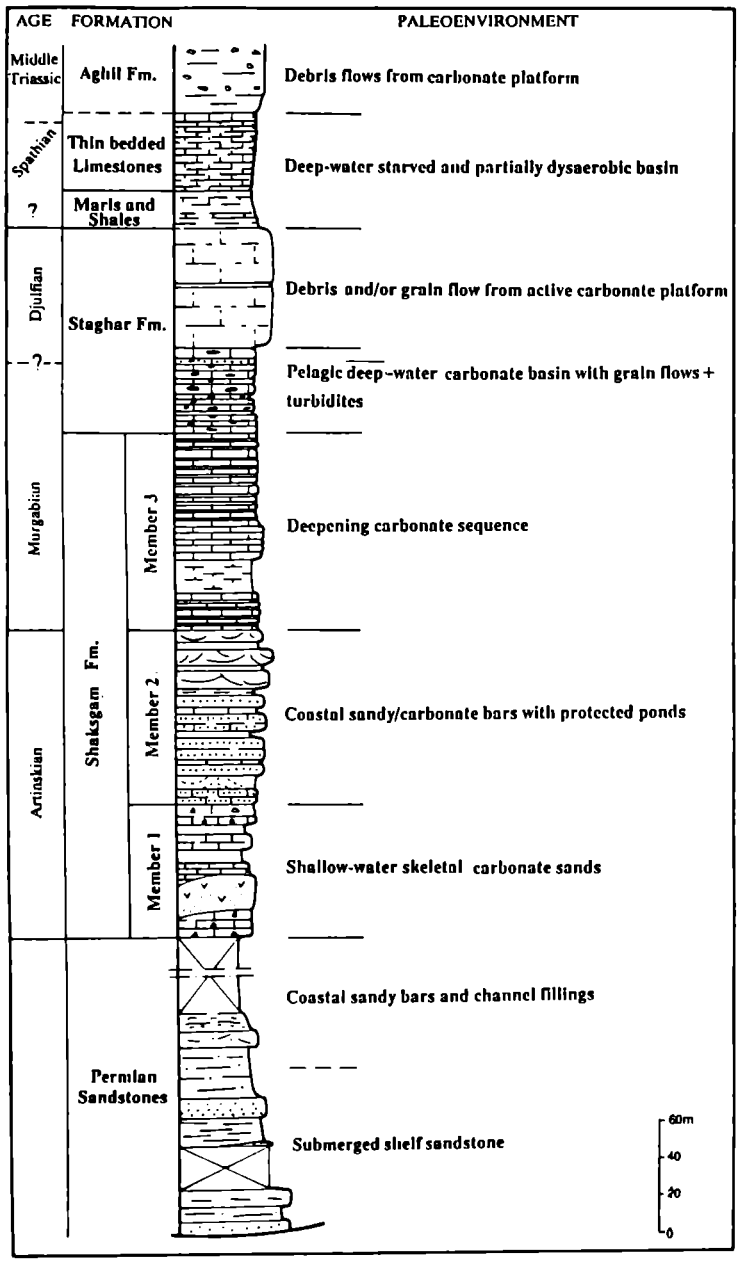

Fig. 4.10. The section of Urdok Doors.

member may be extremely rich in fusulinids. The total thickness seems to vary from 60 to 90 m and the sandy content seems to increase northwards along the Shaksgam valley, from the Urdok Doors section to Gya river. The third member consists of well bedded grey nodular limestone and marls in m thick intercalations. Thickness from 50 to 80 m, at least.

Occurrence. The Shaksgam Fm. is widely distributed from the area in front of Durbin Jangal up in the valley (Fig. 4.11, Pl. 5, Fig. 1). The areas around the Aghil pass and the Tek-ri hillock, mapped as Shaksgam Fm. in Desio (1980), belong instead to the Tek-ri and Bdongo-la Fm. of Jurassic age.

Fossil content and microfacies. This unit is the richest, from the fossil point of view, encountered during the expedition, both in macrofauna and especially in microfauna.

Member 1. Bioclastic packstone with micritic matrix recrystallized in micro- and pseudospar. The bioclasts consist of fenestellid bryozoans, crinoids and other echinoderms, ostracods and brachiopods, calcareous porifera. Amongst the algae the following have been recognized (by L. Angiolini): *Gymnocodium* sp, dasycladacean fragments and some microproblematica like *Tubiphytes obscurus* Maslov and *T. carinthiacus* Flügel. The small foraminifera are also abundant, whilst fusulinids are very rare. The following forms have been recognized: *Agathammina pusilla* Neumayr, *Archaeodiscus* sp., *Lasiodiscus* sp., *Calcitornella* sp., *Ammovertella* sp., *Tuberitina* sp., *Nodosaria* sp., *Geinitzina* sp., *Globivalvulina* sp., *Dunbarula* sp.. Flügel (1990) identified at the base of this member the following solitary Rugosa: *Verbeekiella australis* (Beyrich), *Lophophyllidium (Lophbillidium) martini* (Schouppé & Stacul). In the Staghar section, which probably represents an upwards extension of the calcarenites of the Member 1, Flügel (1990) recognized: *Allotropiochisma (? Allotropiochisma) biseptata* Flügel, *Amandophyllum* (?) sp., *Petraphyllum columnum* Flügel, *Paracaninia* sp. B, *Euryphyllum* sp.. To be noted that all are solitary Rugosa and most are new species. The brachiopod assemblage is dominated by abundant *Enteletes* sp.

The Staghar section shows a larger development of the crinoidal sand facies, with marly intercalations in which a rich macrofauna occurs. Very peculiar are large oncoids. Their centre is made by an *Enteletes* brachiopod or a *Sulcoretepora* bryozoan, coated by *Archaeolithoporella, Tubiphytes obscurus,* and *Eridopora.* Amongst other fossils, small foraminifers are represented by species of *Hemigordius, Tuberitina, Geinitzina, Climacammina, Globivalvulina, Tetrataxis* and *Lasiodiscus.* The rare fusulinids are represented by *Minojapanella wutuensis* (Kuo). The conodont *Merillina* aff. *oertli* Merriam was also found. (det. A. Nicora). The very rich

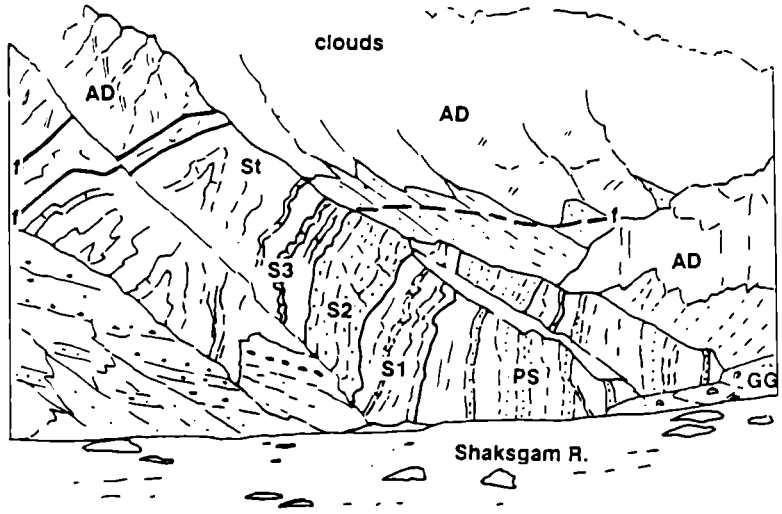

Fig. 4.11. The Permian succession in front of the Gasherbrum glacier (GG). PS = Permian Sandstones. S1, S2, S3 = Shaksgam Formation, respectively members 1, 2, 3. St = Staghar Formation. AD = Aghil Formation, f = fault.

brachiopod locality of the Staghar glacier described by Desio (1936, 1980) and Fantini Sestini (1965a) should belong to this member, according to its position on the Desio' (1936) topographic map. However, probably for a subsequent flooding, I was unable to retrace this locality.

M e m b e r 2 . The arenaceous input which characterizes this member considerably varies through this unit, but it is always present. Arenaceous bioclastic packstones are interbedded with hybride arenites. The quartzarenitic end member seems not to be reached. Peloids, small surficial micritized oolites and wackestone clasts with bivalves are also recorded. The fossil content is less abundant than the previous member, but for the fusulinids, which reach their maximum abundance in this unit. The fossil content consists of: Algae, *Gymnocodium* sp., *Epimastopora* sp., and other Dasycladacean fragments; *Archaeolithoporella* oncoids are also present. Microproblematica like *Tubiphytes obscurus*. Small foraminifers with *Agathammina pusilla, Hemigordius* sp., *Calcitornella* sp., *Tuberitina* sp., *Ammovertella* sp., *Cribroge-*

nerina sp., *Clymacammina* sp., *Geinitzina* sp., *Globivalvulina* sp., and *Tetrataxis* sp.. Amongst the fusulinids were identified (det., M. Pasini, Siena) *Monodiexodina* sp., *Parafusulina japonica* Ozawa, *Boultonia willsi* (Lee). In the fusulinid limestone at the top of Member 2 of the Gya section the following foraminifera have been found: *Monodiexodina caracorumensis* (Merla), *M. wanneri* (Schubert), *Parafusulina japonica* Ozawa, *Parafusulina* sp., *Pseudofusulina shaksgamensis* Reichel, *Chalaroschwagerina* sp. Calcareous sponges with an *Uvanella*-like genus and fragments of Rugosa, Brachiopoda, and crinoids. Bryozoan fenestellids and the genus *Dybowskiella*.

Member 3. Wackestone/packstone with micritic matrix recrystallized in microspar. The quartz content is here lacking and the fossil content is much more reduced. The algae are represented by rare *Epimastopora*. The small foraminifers are represented by the genera *Clymacammina, Geinitzina, Pachyphloia, Nodosaria, Tuberitina, Agathammina* and *Hemigordius*. Amongst the fusulinids the genus *Dunbarula,* have been recognized. Brachiopods are rare, with Martiniid clusters and sparse fragments. Bryozoan fenestellid and Cystoporida are also present, together with echinoderms fragments. The brachiopod locality of Gasherbrum Jilga (Desio, 1936, 1980; Fantini Sestini, 1965a) might be referred to this member.

Age. The age of the Shaksgam Formation is mostly Artinskian because of their Fusulinid (*Minojapanella, Monodiexodina, Parafusulina, Boultonia*) and Conodont content (*Merillina* aff. *oertli* Merriam) in Member 1 and 2. The age of Member 3 remains instead ill-defined. How long it enters in the Kubergandian or already in the Murgabian is presently unknown.

Comparisons. The three-fold subdivision is also present in Hunza (Panjshah Fm. of Gaetani et al., 1990a). Similar lithologies were recorded by Dainelli (1933) and Merla (1934) around the Karakorum pass, whilst such a Permian shallow-water carbonate sequence is scarcerly depicted in the Gergan & Pant report (1983) on the same area. The major volcanic outpourings around the Karakorum pass Chhongtash and Ak Tash Formation have here a poor counterpart in the single sill found in the Urdok Doors area (for its petrography refer to Pognante, this volume).

2.4.4. *STAGHAR LIMESTONE*.

Name. The need for a separate unit was already considered by Desio (1980) introducing the informal term "Cherty Limestones" or "Kyagar Cherty Limestone" as in Desio (1963), later abandoned. Here, a part of the previous "Cherty Limestones" is inserted in the stratigraphic scheme, named from the Staghar glacier in front of which a belt of this unit is developed.

Lithology. Grey dark wackestones to mudstones with dark or grey-dark cherty nodules, thinly bedded and thickening upwards. Thickness of this part more than 100 m. The cherty limestones are increasingly polluted upwards by graded calciruditic to calcarenitic beds, containing shallow-water carbonate fragments. At the top, one (or two) huge calciruditic well-amalgamated calciruditic horizons, up to 50 - 100 m thick, follow. They contain also carbonate clastic from a nearby living carbonate platform.

The cherty limestones, as already noted by Desio (1980), may belong to different horizons. I exclude from the Staghar Formation the well bedded cherty limestones with white to grey cherts in lens and beds, forming the Urdok Doors and their extension towards the Marpo-la. Southwest of this alignment, the sequence seems to pass from the Permian Sandstones straight to cherty limestones and to continue throughout up to the Late Triassic (Carnian). They will be considered separately.

Occurrence. The Staghar Limestone extends from the mountain facing Durbin Jangal up to the Staghar glacier and eastwards, according to Desio (1980). A partial section may also be observed in the middle Shaksgam valley, on the Korkun ridge.

Fossil content and microfacies. The basal cherty limestones are rather poor in fossils, limited to sponge spiculae and Radiolaria. Much richer are the reworked parts, consisting of bioclastic packstone, more rarely grainstone, containing mostly foraminifera and echinoderms. The matrix is recrystallized in micro/-pseudospar. The algae are represented by *Gymnocodium* sp., *Atractyliopsis* sp., and by dasycladacean fragments. Microproblematica are also present (*T. obscurus*). Amongst the small foraminifers, the following forms are recognized : *Agathammina pusilla, Tuberitina* sp., *Lasiodiscus* sp. *Cribrogenerina* sp., *Climacammina* sp., *Pachyphloia* sp., *Dagmarita* sp., *Globivalvulina voenderschmitti* Reichel and *G.* sp.. The fusulinids are represented by *Codonofusiella* sp., *Neoschwagerina simplex* Ozawa and *Dunbarula nana* Devidé and Ramovš, *Triticites* sp. forming mixed-age assemblages due to the resedimentation. Brachiopods, bryozoan fenestellid and echinoderm fragments are also present. A conodont assemblage with *Gondolella bitteri* Kozur vs. *Gondolella liangshanensis* (Z. Wang) was found in the upper part of the unit. These shallow-water dwellers indicates that nearby to the deep-water trough of the cherty limestones, a shallow-water carbonate ramp or platform was contemporary active.

Age. Murgabian to Djulfian are represented in this unit, on the base of fusulinids and conodonts.

Comparisons. A drowning from shallow-water carbonates and hybrid arenites to deep-water cherty limestones (from Panjshah to Kundil Fms.) was also observed in Hunza, though later in time (Midian) (Gaetani et al., 1990a).

2.4.5. *MARLS AND SHALES AND THIN BEDDED LIMESTONES.*

Name. I informally designate this part of the sequence, which need to be worked out with much more detail.

Lithology. With the term "Marls and Shales" I indicate the about 20 m of soft sediments capping the last megabreccia body in front of the Urdok glacier snout, on the right bank of the river. I saw them, but I was unable to hammer them, because of the heavy snow-falling (24-25 September) that stopped our work at the Gasherbrum base camp. This unit is missing in the middle Shaksgam, on the Korkun ridge.

The conodont *Neospathodus homeri* Bender and the foraminifer *Meandrospira pusilla* (Ho) of Spathian age (Early Triassic) were found. However, most of the rocks seem made of barren mudstones.

Occurrence. This marly and thin bedded limestones seems to be missing at northwest. According to Desio (1980), a Triassic soft rocks units will be more spread at southeast (Chikchi-ri Shales).

2.4.6. *CHERTY LIMESTONES.*

Most of the sedimentary sequence returned to shallow-water conditions probably during the Middle Triassic. To the southwest instead, there are pale grey limestones in thin beds, with light to grey cherts in nodules or even in thin beds. They contain floatstone bodies, up to 20 m thick, or thinner calcarenitic to calciruditic horizons, with Permian clasts supported by a pelagic matrix. The maximum measured thickness of this cherty limestones is about 200 m. In the lower part of the sequence a single specimen of the conodont *Gondolella tethydis* Huckriede was collected, indicating a Triassic age. In the floatstones, a latest Permian fauna was found, with foraminiferal species of *Pachyphloia, Geinitzina, Tuberitina, Nodosaria, Luisettita, Bradyina, Agathammina, Baisalina, Climacammina, Hemigordius, Khalerina,* and the species *Globivalvulina voenderschmitti* Reichel and *Dagmarita khanachiensis* (Reytlinger). The genus *Tubiphytes,* with *T. obscurus* and *carinthiacus* is also present, as well *Archaeolithoporella.* This fact indicates that elsewhere the shallow-water carbonates continued throughout most of the Late Permian. The youngest fossil recognized has been the conodont *Gondolella polygnathiformis* Badurov and Stefanov of Carnian age. Consequently we have here a more persistent pelagic sequence (up to the Carnian) and more distal than the previously more northern and eastern described Permo-Triassic sequence, in which, however, reworked latest Permian debris were laid down.

Occurrence. I put in this paper-basket unit all the cherty limestones I was unable to better constrain. Their main occurrence is in the area of the Gasherbrum-Urdok glacier snouts, south of the fault running just north of the Urdok Doors and through

the Marpo-la. However, it should be noted that, along strike to the middle Shaksgam (Korkhun ridge), the cherty limestones seem to desappear.

2.4.7. *AGHIL FORMATION.*

Name. Auden (1938) introduced the term "Aghil Series" for all the Triassic-Jurassic carbonate rocks forming the peaks around the Shaksgam valley. Desio (1980) substantially followed this usage, with more lithological details and introducing the spelling Aghil Limestone. I prefer use the term formation, because the unit is often dolomitic and non calcareous.

Lithology. The sequence consists at the base of a huge polygenetic brecciated body, including boulders from the thin-bedded Triassic limestones, totally dolomitized. It thickness may reach more than 200 m. This event is followed by a dolomitic unit, reaching at least 1000 m in thickness, forming the bulk of the Aghil Formation. Cyclothemic peritidal sequences with meter thick fenestral horizons and subtidal lime mud with megalodontids represent the most characteristic facies, locally coarsely dolomitized. Well-bedded peritidal sequences grade laterally into massive walls, lining the middle part of the Shaksgam valley (Pl. 5, Fig. 2). In a huge boulder in front of Staghar glacier I observed a coral-sponge boundstone, with large solitary and colonial Scleractinia, several sponges, including an *Uvanella*-like genus, encrusting foraminifera and involutinids, worm tubes, dasycladaceans and solenoporaceans. Also here the inferred age is Late Triassic.

Between the Skam river and the Aghil pass, the Aghil Formation is capped by unbedded yellow-brown dolomitic limestones (wackestones) with bryozoans, sponges, serpulids and corals.

Occurrence. The Aghil Formation is the most spread unit of the Shaksgam Sedimentary Belt, also because it reacts as more competent during the deformation. In the middle Shaksgam (Korkhun ridge), the Aghil Fm. might lies directly on the Permian units. In this case, a gap should be hypothetized.

Age. Possibly it starts in the Middle Triassic, but I have no evidence. The Late Triassic is suggested by Megalodonts and by Involutinids; probably extends into the Early Liassic.

Comparisons. The Aghil Formation and its equivalent shallow-water Late Triassic carbonates are wide-spread in Karakorum and SE Pamir.

2.4.8. *TEK-RI FORMATION.*

Name. Introduced informally in Gaetani et al. (1990b), to designate the dark grey well-bedded limestones, lateral equivalent of the topmost part of the Aghil

Formation.

Lithology. The Tek-ri Formation, at least 300 m thick, consists of 20-50 cm thick beds of grey dark mudstone–wackestones, with rare dark cherts. In the middle and upper part, oncolitic limestones associated with bioclastic packstones are widespread and distinctive. Dark shaly interbeds and thin beds may occur, especially in the upper part. Sponges, gastropods and ostreids are randomly diffused, whilst in the uppermost part foraminifera occur (*Lenticulina, Protopeneroplis, Haurania, Mesendothyra, Dentalina*).

Age. The foraminifer assemblage suggests a Middle Jurassic age, possibly Bathonian for the top of the Tek-ri Formation.

2.4.9. *MARPO FORMATION.*

Name. Informally introduced in Gaetani et al. (1990b).

Lithology. The carbonate platform development is interrupted by red sandstones and siltstones, up to 100 m thick east of the Aghil pass, but usually between 20 and 40 m in the middle part of the valley. Their base is prograding on the Tek-ri Formation. Westwards, the unit starts with alternating grey marls with ostracods and red siltstones, followed by polymict conglomerates, with well rounded platy pebbles of sedimentary origin. It ends with red shaly sandstones. Eastwards in contrast, the sequence is thicker and consists almost exclusively of red fine sandstones and siltstones. The sandstone petrography shows a volcanic litharenite, dominated by monocrystalline quartz with magmatic corrosion rim, and with subordinated altered volcanic grains. The 300 point-counting merge these sandstones with the red sandstones of the Surukwat Thrust Sheets. From east to west, the interfingering of an alluvial plain with coastal lagoons is recorded.

Occurrence. The red sandstones occurs through out all the part of Shaksgam valley we visited.

Age. Being interposed between a Middle Jurassic foraminifer fauna at the top of the Tek-ri and the Coral fauna described by Fantini Sestini (1965b) at the base of the following Bdongo-la Fm., the age is sufficiently well constrained to the upper part of the Middle Jurassic.

2.4.10. *BDONGO-LA FORMATION.*

Name. It was informally designated by Desio (1980) as the "Jurassic Fossiliferous Beds of Bdongo-la". Here this unit is more formally considered, including also the shales and the sandstones that contain the fossil bed of Bdongo-la.

Lithology. At the base, a 10 m bed of dark slightly metamorphosed limestone

delivered the coral fauna of Middle Jurassic age studied by Fantini Sestini (1965b). Above, grey shales and siltstones, with minor sandstones intercalations showing rare convolute and parallel laminations suggest a possible distal turbidite deposition, in a deeper environment. Litharenite petrography slightly shift in comparison to the Marpo Sandstone towards a more orogenic field.

Occurrence. The Bdongo-la Fm. crops out in the middle Shaksgam valley and around the Aghil pass. Due to the black weathering of the shales, at distance reconnaissance should be careful. In Auden (1938) and Desio (1980) these shales are mapped as Singhiè Shales around the Aghil pass.

Age. The coral fauna described by Fantini Sestini (1965b) was considered of Callovian age. We have no further data on the top part of the unit.

2.4.11. *YELLOW CONGLOMERATES.*

The top of the sedimentary sequence is represented by yellow polymict conglomerate in 5-15 cm-sized well rounded and medium sorted pebbles, in m-thick beds, with a yellow-brown weathering. I observed only sedimentary pebbles, derived almost exclusively from the Mesozoic rocks. Rounded dolomite pebbles are dominant. The matrix is scarce and no fossils were observed.

These conglomerates are cropping out in the core of the Bdongo-la syncline and of the syncline south of the Skam river. The conglomeratic beds are less folded that the underlying rocks. Large boulders of this conglomerate are sparse on the Shaksgam valley floor, down from the Gasherbrum glacier snout.

2.4.12. *URDOK CONGLOMERATE.*

Name. Desio (1980) introduced the term Urdok Conglomerate (p.113) to designate the red conglomerate cropping out at the head of the Urdok valley. In the map, however, he included also other conglomerates that here are considered as belonging to the Marpo Sandstones. The Middle Triassic age of Desio (1980) was based on a supposed stratigraphic position of what I now call Marpo Sandstones within a series interpreted as continuous, but that now the micropaleontology better constrains and reveals to be tectonically disrupted.

Lithology. I maintain the first designation of Desio (1980, p.113) considering as Urdok Conglomerate the red massive banks cropping out between the Gasherbrum and Urdok glaciers, south of the main alignement of the Karakorum Fault Zone (KFZ) (Fig. 4.6). It forms slabs of some hundred meters, tectonically embedded in a shaly, non metamorphic, dark unit. It consists of m-beds with scoured base of polymict conglomerate, with clasts up to 50 cm, fairly rounded and often poorly

sorted, in a red matrix, with a siliceous cement. Finer sandstones are rarer. Clasts are mostly derived from sandstones, whilst carbonates are rarer. Metamorphic pebbles are also present (about 15 %). Noteworthy are two kind of clasts: a) sandstones with altered volcanic grains, which recall the Marpo Sandstones of Jurassic age; b) biotite-muscovite-Kfeldspar foliated gneisses, in clasts up to 10 cm, similar to the gneisses found in the K^2-Sarpo Laggo metamorphics. If the gneisses are equivalent to the K^2 Gneiss, whose crystallization age is Early Cretaceous (Searle et al., 1990), the Urdok Conglomerate age would be at least Late Cretaceous, if not later. Correlation with the K^2 Gneiss may be disputed, but the affinity to the Marpo sandstones is striking. Consequently, this unit should be post-Middle Jurassic, at least.

I was unable to reach the best oucrops on the left side of the Gasherbrum glacier (Fig. 4. 6). From the large boulders on the morains, I get the impression that the Urdok Conglomerate was deposited in an alluvial environment.

Very thick red conglomerates have been reported around the Karakorum pass trail, southeast of Shaksgam. Gergan & Pant (1983) claim to have found marine Cretaceous foraminifera in their "Chizil Lunghar Conglomerate". According to Dainelli (1933), the Qizil Lungur Conglomerate lies on Norian brachiopod-bearing limestones. Also in Hunza, a similar very thick conglomerate was observed (Tupop Conglomerate in Gaetani et al., 1990a), and it was attributed to the Mid Cretaceous event. However, in Hunza, crystalline rock boulders were not observed.

2.5. PALEOENVIRONMENT EVOLUTION

Summarising, the Permian sedimentary trend is very typical for a transgression on a passive continental margin. The basal litharenitic sandstones of deltaic to shallow marine environment evolve to shallow water carbonates and hybride arenites. Significant subsidence causes the downwarping to deep marine environment, with pelagic carbonates and resedimented bodies, fed by active fault scarps affecting also the neighbouring shallow-water carbonate platforms. The deep water environment continued until the Middle Triassic (or later to the south), when the combination of low sea-level, high carbonate productivity and possibly local movements connected with faults, allowed the return from the pelagic environment to the shallow water carbonate platform complex, which continued into the Jurassic. The shallow water carbonate platform persisted for at least 100 MY until the Middle Jurassic, when a clastic wedge, derived from a neighbouring area with increasing deformation, produced the first terrigenous episode linked to an orogenic event. The progressive

deformation on the accretionary prism produced a fore-arc flyschoid sequence of which the Bdongo-la Fm. represents the distal part. The yellow conglomerates testify a deformation episode closer to the Shaksgam valley, in which the sedimentary covers were mostly involved. Subsequent deformations caused large-scale folds, recumbent toward SW, which were later truncated and stacked by subvertical faulting.

2.6. SARPO LAGGO - K^2 METAMORPHICS

These form a unit of strongly deformed low-to medium-grade metamorphic rocks which crop out in the Sarpo Laggo valley, in the K^2 area and possibly extends to the SE at the head of the northern Gasherbrum valley. They include ortho- and para-gneisses, impure marbles and pegmatoids. The complicated tectonic setting of this unit and the existence of large scale transpositions are recorded by the frequent isoclinal folds characterized by steeply dipping axial planes.

At the confluence Skamri-Sarpo Laggo, a less-to non-metamorphosed sedimentary faulted sheets crop out, in which fusulinid-rich (*Monodiexodina*) hybrid sandstones (Early Permian) and cherty limestones of Late Permian are still identifiable. The sketch map of Desio (1936) gives further details. The sedimentary belt continues up in the lower reaches of the Skamri glacier and would reach the belt between Shimshal village and Shimshal pass, where the sedimentary rocks of the Sost Unit where followed from Hunza (Gaetani et al. 1990).

3. The Crystalline Rocks of the Kun Lun–Karakorum (1)

3.1. INTRODUCTION

A variety of crystalline rocks has been found during the Ev-K^2-CNR 1988 Geological-Geophysical Expedition organized by Prof. A. Desio in the remote and very little known area of northern Karakorum located between Kun Lun and Shaksgam valley (Sinkiang, China). In the seven tectonic units distinguished by Gaetani et al. (1990b and this vol.) along this geological transect (Fig. 4.12), the crystalline units include metamorphites, plutonites, post-metamorphic lamprophyric dykes and rare extrusive volcanics. The following descriptions and discussions are

---

(1) Ugo POGNANTE.

based on field and petrographic observations and, for the magmatic rocks, on mineral and whole-rock chemical data.

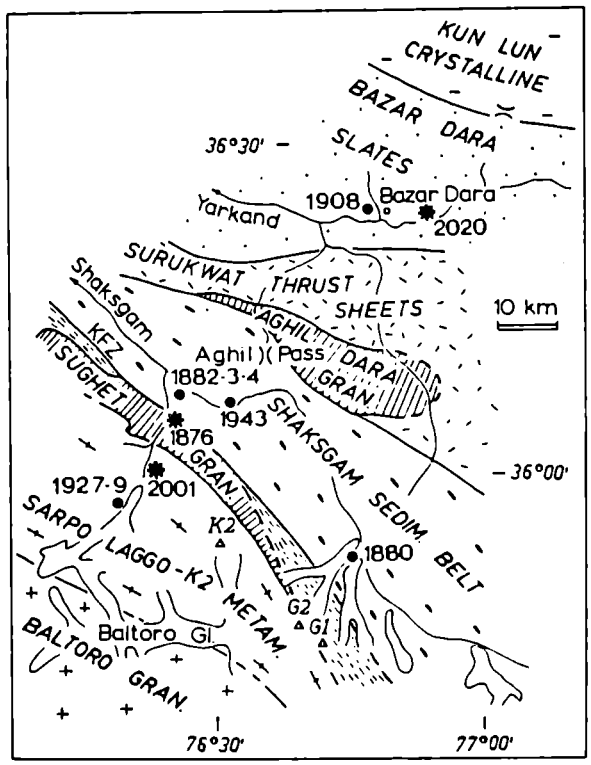

Fig. 4.12. Tectonic map of the northern Karakorum area located north of K^2- Gasherbrum range (after Gaetani et al., 1990b and this vol.). The dashed zone NE of the Gasherbrums (G1 and G2) corresponds to a faulted area linked to the Karakorum Fault Zone (KFZ) and including unmetamorphosed slates and conglomerates. The map also indicates the location of the analyzed Jurassic-Cretaceous granitoids (asterisks) and post-metamorphic dykes of Neogene age (dots). See Table 4.1 for samples description.

The *metamorphic rocks* outcrop in the northern part of the Kun Lun Crystalline, in the Surukwat Thrust Sheets and in the Sarpo Laggo-K^2 Metamorphics, while incipient recrystallizations linked to ductile deformation have been observed also in unmetamorphosed or very-low-grade metamorphic slates from the Bazar Dara Slates and the Shaksgam Sedimentary Belt. The *plutonites* form most of the basement of the Kun Lun Crystalline, while kilometer-sized bodies occur within the Bazar

Dara Slates and form the Aghil Dara Granodiorite and the Sughet Granodiorite. The *post-metamorphic dykes* have been observed in the Bazar Dara Slates, Shaksgam Sedimentary Belt, Sughet Granodiorite and Sarpo Laggo-K^2 Metamorphics. The rare *extrusive volcanics* have been discovered in the Shaksgam Sedimentary Belt.

Owing to the relatively short time required for the expedition and to other logistic difficulties in a remote and very little-known area, the following should be considered as preliminary results and only further detailed investigations will give more reliable conclusions on the evolution of the crystalline rocks. Such uncertainties are still more obvious for the metamorphic rocks occurring south-west of the Shaksgam valley in an area largely covered by glaciers or snow and located at very high elevation (from 4000 m up to the 8616 m of the K^2); in fact, bad weather conditions prevented us from studying and sampling this area in detail.

3.2. Previous Geological Surveys

The few geological works available on the crystalline rocks of the investigated area of northern Karakorum, concern data obtained before the II World War (e.g. Desio, 1980; and references therein) or reported in the Geologic Map of Tibet (1980) and the Metamorphic Map of China (Cheng et al., 1986). The most detailed geological surveys and maps are restricted to the Shaksgam valley area (Auden, 1938; Desio, 1980) and to more southerly sectors of Karakorum (Desio and Zanettin, 1970; Rex et al., 1988; Searle et al., 1989).

On the basis of the previous surveys, notably the Desio monograph and map (1980), Gaetani et al. (1990b and this vol.) obtained new geological data and introduced more detailed subdivisions. However, as already stressed in section 3.1, the available data are not sufficient and further investigations also in adjacent areas are necessary in order to understand the geological setting and history of northern Karakorum.

3.3. Field Relations and Petrography of the Metamorphic Rocks

3.3.1. *Kun Lun Crystalline.*

Following the Yeh Chen-Mazar road, the Kun Lun Crystalline outcrops from the Aq-Koram pass (3475 m) to the north, till the Cirag Saldi pass (5010 m) to the south. The study of the Kun Lun Crystalline was not among the purposes of the expedition and consequently only sampling of a few lithologies has been done along the road just south of the Aq-Koram pass. These rocks include migmatitic gneisses and amphibolites.

The *migmatitic gneisses* are medium-grained rocks showing a granoblastic texture and a compositional layering defined by quartz-rich and amphibole-rich layers. They consist of: quartz; plagioclase rich in rounded inclusions and veinlets of quartz; porphyroblasts of alkali feldspar (microcline) including plagioclase and minor quartz; green-brown hornblende partly transformed to biotite or chlorite; and rare biotite replaced by chlorite. Coarse-grained concordant leucosomes of quarzo-feldspathic composition occur in these rocks.

The *amphibolites* are fine- to medium-grained rocks characterized by a granoblastic texture. They consist of: plagioclase partly replaced by sericite and epidote; brown-green hornblende partly replaced by chlorite; minor colourless clinopyroxene partly transformed to pale green amphibole; and accessory opaques.

3.3.2. *BAZAR DARA SLATES.*

The Bazar Dara Slates outcrop in the Yarkand valley till the confluence between the Surukwat and the Aghil Dara rivers (south of Ilik). They are very fine-grained unmetamorphosed or very low-grade rocks which preserve rare sedimentary structures (i.e. bedding, parallel laminations) and display litharenitic to sub-litharenitic compositions.

The most pervasive foliation of the slates is of tectonic origin and grades from fabric domain to crenulation cleavage. In the fabric domain very fine-grained sericite, chlorite and opaques displaying a strong preferred orientation, anastomose around lenticular domains rich in quartz and/or carbonate.

3.3.3. *SURUKWAT THRUST SHEETS.*

From north to south, the metamorphic rocks of the Surukwat Thrust Sheets include: bodies of metadiorites; mylonitic micaschists; a thick sequence of gneisses; and metapelites.

The *metadiorites* with rare enclaves of melanocratic plutonites have been found just south of the confluence of the Surukwat and the Aghil Dara rivers, till the Aghil Dara gorges. The frequent relics of magmatic granular textures and minerals indicate that these rocks derive from fine-to coarse-grained (quartz-) diorites consisting of andesinic plagioclase and green-brown hornblende, with accessory Fe-Ti oxides, apatite and, in a few samples, quartz. Rare metabasics of uncertain origin, but possibly derived from cumulite layers, consist of plagioclase, euhedral clinopyroxene, opaques and large biotite flakes. The metamorphic foliation is not very pervasive and is defined by the flattening of the magmatic minerals or by neoblastic amphiboles and biotites. Although the magmatic minerals are partly to completely replaced by

metamorphic minerals, only in the ductile shear zones the magmatic texture is completely obliterated.

In the more northerly sectors, the metamorphic mineralogy of the metadiorites is typical of the very low-grade metamorphism: plagioclase is replaced by sericite, epidote and minor prehnite; hornblende is replaced by Fe-rich chlorite, Fe-epidote colour less amphibole; metamorphic veins consisting of prehnite, carbonate and epidote crosscut the foliation. In contrast, to the south, metamorphism produced more pervasive low-grade assemblages: plagioclase is transformed to sericite and epidote-clinozoisite; hornblende transforms to actinolitic amphibole and green biotite; and Fe-Ti oxides are pseudomorphed by aggregates of rutile, ilmenite and sphene. In the southern sectors, intercalations of leucocratic gneisses are frequent within the metadiorites. The gneisses consists of quartz, plagioclase, alkali feldspar and fine grained green biotite defining the etamorphic foliation.

The *mylonitic micaschists* outcrop in the Aghil Dara gorges and form a sheet a few tens of metres thick. They show a marked schistosity defined by muscovite and also consist of quartz, albite and minor Fe-carbonate. Quartz occurs in deformed porphyroclasts and in fine-grained recovered or recrystallized grains. Metre-thick intercalations of marbles have been found within these rocks. On the basis of their fabric and tectonic setting, the mylonitic micaschists may define a major syn-metamorphic ductile shear zone between metadiorites and gneisses.

The *gneisses* form a body a few kilometres thick. They are medium to coarse-grained rocks characterized by a pervasive foliation defined by prevalent brown biotite and minor muscovite. Derivation from conglomerates is implied, for at least part of these rocks, by the presence of centimeter- to decimeter-sized pebbles of quartz and granitoids. The mineralogy of the gneisses includes also plagioclase, alkali feldspar, minor chlorite and accessory apatite and allanite.

The *metapelites* outcrop north of the Aghil pass. They are fine-grained rocks consisting of quartz, brown biotite and minor plagioclase of oligoclase composition. Biotite defines the pervasive schistosity and a few intrafolial folds. Layers of mylonitic leucocratic gneisses, possibly derived from the transposition of original aplitic dykes, are interposed within the metapelites. Elongate quartz and plagioclase grains, flattening of alkali feldspar porphyroclasts and fine-grained muscovite derived from larger deformed flakes, define the schistosity of the gneisses.

3.3.4. *SHAKSGAM SEDIMENTARY BELT.*

In this unit consisting chiefly of unmetamorphosed rocks the only lithologies showing textures which can be ascribed to a syn-tectonic ductile recrystallization are

the Singhiè Shales and the Urdok Conglomerate (Gaetani et al.,1990b and this vol.). In the Singhiè Shales the ductile recrystallization is recorded by the preferred orientation of very fine-grained muscovite in a matrix of quartz, carbonate and albite. In the Urdok Conglomerate, a few clasts of foliated gneisses recall the or- thogneisses of the Sarpo Laggo-K^2 Metamorphics (section 3.3.5). The gneisses show a metamorphic foliation defined by muscovite and biotite.

3.3.5. *SARPO LAGGO-K^2 METAMORPHICS.*

Rocks belonging to this unit have been sampled in the Sarpo Laggo valley and include a series of ortho- and para-metamorphites with a complex internal structure characterized by isoclinal folds and large scale transpositions. The metamorphic rocks include orthogneisses, paragneisses, impure marbles and quartzo feldspathic pegmatoids associated with the paragneisses. In the Desio map (1980) this unit comprises approximately the "K^2-Falchan Gneisses" and the "Muztagh Tower-Sarpo Laggo Gneisses".

The *orthogneisses* are medium- to coarse-grained rocks rich in quartz and showing a marked schistosity defined by biotite and minor muscovite. The schistosity anastomoses around perthitic porphyroclasts of alkali feldspar. The latter includes blasts of plagioclase and quartz and displays myrmekitic textures at the contact with plagioclase. Plagioclase is slightly zoned with compositions ranging from albite to oligoclase and is characterized by inclusions of muscovite. Brown biotite occurs in two generations: large flakes are deformed and chiefly predates deformations; small syn-tectonic biotite defines the schistosity. Minor pale green amphibole, garnet and rare clinopyroxene, along with accessory sphene, apatite, allanite and zircon, complete the mineralogy of the orthogneisses. Among these minerals, garnet is partly replaced by chlorite, muscovite and opaques, while clinopyroxene forms corroded relics within amphibole. The mineralogical and chemical composition (section 3.7.2.) along with the local preservation of magmatic granular textures, point to derivation of the orthogneisses from original granodiorites and granites.

The *paragneisses* are medium- to fine-grained lithologies showing a foliation defined by brown biotite and muscovite and, in a few samples, by a compositional layering. These rocks consist also of quartz, albitic plagioclase and subordinate porphyroclasts of alkali feldspar partly transformed to albite. Less abundant minerals include green hornblende, garnet and rare clinopyroxene partly transformed to hornblende.

The *impure marbles* show a decimeter-thick compositional layering defined by

the presence of quartz and probably also by different proportion between calcite and dolomite. These rocks also include tremolite.

The quartzofeldspathic *pegmatoids* are coarse-grained foliated rocks consisting of quartz, alkali feldspar, plagioclase, muscovite, garnet and minor brown biotite.

Near he contact with the Sughet Granodiorite a complex mylonitic zone including slices of marbles, slates and metaconglomerates occurs. The mylonitic rocks show a rather pervasive foliation parallel to the contact and defined by neoblastic fine-grained muscovite chlorite. This foliation is also present in the ortho- and paragneisses where asymmetric S-C fabrics develop.

3.4. Field Relations and Petrography of the Plutonic Rocks

3.4.1. *KUN LUN CRYSTALLINE.*

South of the metamorphites described in section 3.3.1, the Kun Lun Crystalline consists of prevalent granitoids which contain lenses and discontinuous layers a few metres thick of basic rocks. The granitoids have been ascribed to the Paleozoic by the Geologic Map of Tibet (1980). In a few outcrops both granitoids and basic rocks display a pervasive foliation and are crosscut by basic dykes; all these lithologies are deformed by open folds. Unfortunately it was not possible to sample these interesting rocks.

3.4.2. *GRANITOIDS ASSOCIATED WITH THE BAZAR DARA SLATES.*

The plutonites forming decameter- up to kilometer-sized bodies within the Bazar Dara Slates are biotite monzogranites which give Jurassic cooling age (see section 3.7.2. and Table 4.5 for whole-rock chemistry and geochronology). They are medium-grained rocks consisting of quartz, plagioclase, alkali feldspar, brown biotite and accessory apatite, allanite and zircon. Plagioclase has albitic rims and andesinic cores and is slightly altered to saussurrite and sericite. Alkali feldspar (microcline) includes plagioclase and often shows myrmekitic textures at the contact with plagioclase. Biotite is partly transformed to chlorite.

3.4.3. *AGHIL DARA GRANODIORITE.*

The plutonites occurring in the upper part of the Aghil Dara valley till the Aghil pass are bounded by sharp faults and include prevalent granodiorites with tonalite and quartzdiorite enclaves. Near the Aghil pass the granodiorites intrude bodies of gabbros and are intruded by porphyritic granites and minor leucogranites. The granitoids have been already reported in the Auden map (1938) and have been

attributed to the Cretaceous magmatism by the Geological Map of Tibet (1980).

The *granodiorites* are medium-grained rocks consisting of quartz, zoned plagioclase, poikilitic alkali feldspar, brown biotite, rare green amphibole and accessory apatite, zircon and allanite. Plagioclase has normal or oscillatory zoning with oligoclase rims (An=10-15 mol%) and andesine cores (An=35 mol%). It is partly altered to saussurrite and sericite. Poikilitic alkali feldspar includes plagioclase. Biotite is partly transformed to chlorite, epidote and sphene.

The *tonalites* and *quartz diorites* are medium- to fine-grained rocks consisting of plagioclase (oligoclase-andesine), anhedral quartz, brown biotite, green amphibole, minor poikilitic alkali feldspar and accessory sphene, apatite and opaques.

The *gabbros* are medium- to coarse grained rocks showing a sub-ophitic texture and consisting of plagioclase, colourless augitic clinopyroxene and skeleton Fe-Ti oxides. Plagioclase has a prevalent andesinic composition but the cores altered to saussurrite sericite suggest derivation from more Ca-rich compositions. Augite is partly to completely transformed to chlorite.

The *porphyritic granites* are coarse-grained rocks consisting of poikilitic alkali feldspar, quartz, plagioclase and brown biotite. The very coarse-grained alkali feldspar is perthitic and includes plagioclase and biotite. Plagioclase shows slight normal zoning, has an oligoclase composition and is partly altered to sericite and saussurrite. A few samples show a cataclastic texture.

3.4.4. *SUGHET GRANODIORITE.*

This plutonic body occurs in the lower part of the Sarpo Laggo valley and is bounded to the south by a very low-grade thrust (section 3.3.5) and to the north by a cataclasite a few tens of metres thick trending NW-SE. The plutonites include prevalent granodiorites with enclaves, quartz diorites and leucogranites. In the Desio map (1980) these rocks have been considered "K^2- Falchan Gneisses" like the Sarpo Laggo-K^2 Metamorphics described in section 3.3.5. Indeed the Sughet Granodiorite and the orthogneisses of the Sarpo Laggo-K^2 Metamorphics have comparable whole rocks chemistry and similar Cretaceous age (section 3.7.2.). However, the two lithologies display different textures with prevalent magmatic textures in the former and metamorphic fabrics in the latter; additionally, the Sarpo Laggo-K^2 orthogneisses show intimate association and folding with paragneisses and marbles.

The *granodiorites* and the rare tonalites consist of zoned plagioclase, quartz, poikilitic alkali feldspar, brown biotite muscovite and accessory apatite, zircon and allanite. They have a medium-grained granular texture but, in a few samples, include

large biotite flakes and coarse-grained plagioclase. The cataclastic varieties occurring close to the brittle fault zones show strongly deformed quartz grains and are crosscut by pumpellyite veinlets. Plagioclase shows oscillatory zoning with andesine cores (An = 40-45 mol%) and oligoclase rims (An = 10-15 mol%). They include also corroded relics richer in Ca and are partly altered to sericite and saussurrite. Alkali feldspar is perthitic and poikilitic, including plagioclase and biotite. Myrmekitic textures occur between alkali feldspar and plagioclase. Biotite is partly altered to chlorite epidote. Muscovite occurs both in larger primary crystals and in smaller flakes replacing biotite.

The *enclaves* observed within the granodiorites are often foliated and include: quartz-diorites and amphibolic gneisses consisting of quartz, plagioclase, colourless amphibole and brown biotite; and fine-grained (para?) gneisses rich in biotite and plagioclase.

The *quartz diorites* are fine- to coarse-grained rocks consisting of andesinic plagioclase partly altered to epidote, albite and sericite, abundant green amphibole, brown biotite post-dating amphibole, quartz and accessory allanite. Corroded and altered relics of Ca-rich composition occur in the plagioclase cores.

3.5. Field Relations and Petrography of the Post-Metamorphic Dykes and of the Volcanic Rocks

3.5.1. *Post-metamorphic dykes.*

Location of the post-metamorphic lamprophyres observed during the expedition are reported in Fig. 4.12. The dykes are preferentially oriented NW-SE, inject the unmetamorphosed sedimentary and plutonic rocks and crosscut also the schistosity of the metamorphic rocks in the Sarpo Laggo valley. However, they are dislocated by faults trending NW-SE near the Shaksgam valley. The dykes show a porphyritic texture with a very fine-grained groundmass and abundant phlogopite and minor feldspars, amphibole and quartz phenocrysts. They are often altered with formation of chlorite and carbonate after the mafic minerals and of sericite and carbonate after the feldspars or in the groundmass. Carbonate veinlets are common in a few samples.

On the basis of the mineral proportion the lamprophyres are classified as: *minettes* consisting of phlogopite, alkali feldspar, green-brownamphibole, colourless clinopyroxene ± quartz phenocrysts; *kersantites* and *spessartites* consisting of plagioclase, phlogopite, brown amphibole, quartz clinopyroxene. The very fine-grained groundmass consists of alkali feldspar, albite, phlogopite, apatite, opaques ± quartz ± amphibole.

A detailed petrologic study, including mineral and whole-rock chemistry, has been completed on the dykes reported in table 4.1 (Pognante, 1990). Representative microprobe analyses (ARL-SEMQ microprobe; C.S. Stratig. e Petrog. Alpi Centrali, C.N.R., Milano) of the main minerals are reported in Tables 4.2, 4.3 and 4.4, while the whole-rock chemistry is discussed in section 3.7.2. and reported in Table 4.6.

Colourless clinopyroxene occurs chiefly as phenocrysts and is augite with rims slightly depleted in Mg and enriched in Fe relative to cores. In a few samples augite is rimmed and partly replaced by green-brown aegirine-augite. Amphiboles are relatively frequent as phenocrysts but also occur in the groundmass. According to the IMA classification (Leake, 1978), they are magnesian hastingsites, magnesian hastingsitic hornblendes or edenitic hornblendes with relatively high K contents and rims enriched in Fe and Ti relative to cores. A very fine-grained green-blue riebeckitic amphibole partly replaces augite and/or aegirine-augite in some dykes. Phlogopite phenocrysts show marked zoning with rims strongly enriched in Fe and Ti relative to cores. Plagioclase phenocrysts show normal and oscillatory zoning and are labradorites or andesines (Ab = 32-61 mol%). Albite compositions have been determined in the groundmass or in rims bordering alkali feldspar. Alkali feldspar is perthitic or microperthitic and shows variable albite contents (Ab = 0-25 mol%).

3.5.2. *VOLCANIC SILL IN THE SHAKSGAM SEDIMENTARY BELT.*

A volcanic sill of possible Permian age has been observed in the Shaksgam Formation which is part of the Shaksgam Sedimentary Belt (Gaetani et al., 1990b and this vol.). The volcanic rocks are strongly altered with formation of abundant chlorite, while the only corroded relics are phenocrysts of plagioclase and quartz.

3.6. ROCKS FROM THE MORAINES OF THE SARPO LAGGO, GASHERBRUM AND SKYANG GLACIERS

Owing to logistic difficulties and to the bad weather, during the expedition it was not possible to reach the upper part of the valleys located south of the Shaksgam river. Consequently a few lithologies have been sampled in the moraines of the Sarpo Laggo, Skyang and Gasherbrum glaciers.

Table 4.1. Location and mineralogy of the northern Karakorum rocks analyzed in this paper (see also Fig. 4.12). Secondary minerals are in brackets. Asterisk: minerals completely altered.

SAMPLE	LOCATION	MINERALOGY
	POST-METAMORPHIC DYKES	
1880	BETWEEN GASHERBRUM AND URDOK GLACIERS (4800m)	Phl,Pl*,Qz,(Cc),(Ms)
1882	BDONGO-LA (4400m)	Pl,Hbl,Aug,Qz,Phl,Kfs, (Chl),(Ms)
1883	BDONGO-LA (4400m)	Pl,Hbl,Kfs,Qz,(Chl),(Ms)
1884	BDONGO-LA (4400m)	Phl,Kfs,Pl,Qz,(Cc), (Ms),(Chl),Ap
1908	WEST OF BAZAR DARA	Kfs,Phl,Hbl*,Ab,Ap,(Bi)
1927	SARPO LAGGO VALLEY (4600m)	Pl,Hbl,Phl,Kfs
1929	SARPO LAGGO VALLEY (4600m)	Phl,Kfs,Aug,Ab,Qz,Agt,Ap, (Cc),(Ms)
1943	SHAKSGAM VALLEY (3800m)	Hbl,Phl,Pl,Kfs,Aug,Qz,Ap
	TRACHYTE	
1970	MORAINE OF THE N. GASHERBRUM GLACIER (4400m)	Kfs,Qz,Pl,Ap,(Cc)
	GRANITOIDS	
1876	LOWER SARPO LAGGO VALLEY, BETWEEN SUGHET JANGAL AND TEK-RI (3900m) [SUGHET GRANODIORITE]	Pl,Qz,Kfs,Bi,(Chl),(Ms), (Ep),Ap,Zr,Op,All
2020	YARKAND VALLEY, BETWEEN BAZAR DARA AND MAZAR [BAZAR DARA SLATES]	Qz,Pl,Kfs,Bi,(Chl),All,Ap, Zr,(Ms),(Ep)
2023	SOUTH OF THE KHUNJERAB PASS (PAKISTAN)	Qz,Pl,Kfs,Bi,(Chl),(Cc), (Ms),Ap,All,Zr
	ORTHOGNEISS	
2001	SARPO LAGGO VALLEY, SW OF SUGHET JANGAL (4200m) [SARPO LAGGO-K^2 METAM.]	Qz,Pl,Kfs,Ms,Bi,(Chl), (Ms),Ap,Zr

ABBREVIATIONS. Ab: albite, Agt: aegirine-augite, All: allanite, Ap: apatite, Aug: augite, Bi: biotite, Cc: carbonate, Chl: chlorite, Ep: epidote, Hbl: hornblende, Kfs: alkali feldspar, Ms: muscovite or sericite, Op: opaques, Phl: phlogopite, pl: plagioclase, Qz: quartz and Zr: zircon.

Table 4.2. Representative microprobe analyses of clinopyroxenes from the post-collisional dykes of northern Karakorum.

	AUGITES				SODIAN AUGITE 1929	AEGIRINE AUGITE 1929
	1943 CORE	1943 RIM	1882 CORE	1882 RIM		
SiO_2	53.30	53.30	52.67	52.57	53.04	51.74
TiO_2	0.29	0.32	0.18	0.18	0.09	0.55
Al_2O_3	1.83	2.04	1.01	0.84	0.71	1.16
Cr_2O_3	0.00	0.02	0.02	0.03	0.06	0.02
FeO_{tot}	7.70	7.98	11.52	12.62	12.85	18.66
MnO	0.27	0.28	0.26	0.35	0.74	0.42
MgO	16.93	16.62	13.23	12.47	9.68	5.81
CaO	19.61	19.72	21.37	21.16	17.63	13.79
Na_2O	0.19	0.25	0.20	0.24	4.10	5.97
K_2O	0.00	0.00	0.00	0.01	0.01	0.00
TOT	100.12	100.53	100.46	100.47	98.91	98.12
Si	1.958	1.953	1.974	1.980	2.037	2.048
Al^{IV}	0.042	0.047	0.026	0.020	0.000	0.000
Al^{VI}	0.037	0.041	0.019	0.018	0.032	0.054
Ti	0.008	0.009	0.005	0.005	0.003	0.016
Cr	0.000	0.001	0.001	0.001	0.002	0.001
Fe_{tot}	0.237	0.245	0.361	0.398	0.413	0.618
Mn	0.008	0.009	0.008	0.011	0.024	0.014
Mg	0.927	0.908	0.739	0.700	0.554	0.343
Ca	0.772	0.774	0.858	0.854	0.726	0.585
Na	0.014	0.018	0.015	0.017	0.305	0.458
K	0.000	0.000	0.000	0.001	0.001	0.000
TOT	4.003	4.005	4.006	4.005	4.097	4.137

Structural formulae are on the basis of 6 oxygens. See Table 4.1 for sample location and description.

Table 4.3. Representative microprobe analyses of amphiboles and phlogopites from the post-collisional dykes of northern Karakorum.

	MAGNESIAN HASTINGSITE	HASTINGSITIC HORNBLENDES		EDENITIC HORBLENDE	PHLOGOPITES	
	1943 CORE	1943 CORE	1943 RIM	1927 CORE	1929 CORE	1929 RIM
SiO_2	41.21	42.52	42.43	45.26	40.83	37.65
TiO_2	2.36	2.39	1.65	1.98	2.36	4.59
Al_2O_3	13.52	13.13	12.71	10.51	12.59	13.18
Cr_2O_3	0.00	0.00	0.00	0.01	0.47	0.07
FeO_{tot}	15.17	13.81	17.35	12.19	5.67	13.09
MnO	0.20	0.21	0.35	0.14	0.08	0.19
MgO	11.16	12.01	9.66	14.44	22.70	15.90
CaO	11.42	11.20	11.08	10.62	0.00	0.03
Na_2O	1.73	1.75	1.57	1.84	0.08	0.21
K_2O	1.54	1.39	1.43	0.40	10.66	9.74
TOT	98.31	98.41	98.23	97.39	95.44	94.65
Si	6.143	6.269	6.365	6.616	2.925	2.820
Al^{IV}	1.856	1.731	1.635	1.384	1.063	1.164
Al^{VI}	0.520	0.550	0.613	0.427	0.000	0.000
Ti	0.265	0.266	0.186	0.218	0.127	0.259
Cr	0.000	0.000	0.000	0.001	0.027	0.004
Fe_{tot}	1.891	1.702	2.177	1.490	0.340	0.820
Mn	0.025	0.027	0.044	0.018	0.005	0.012
Mg	2.481	2.639	2.160	3.145	2.424	1.775
Ca	1.825	1.769	1.781	1.663	0.000	0.003
Na	0.500	0.500	0.456	0.520	0.011	0.031
K	0.293	0.261	0.274	0.075	0.974	0.931
TOT	15.800	15.714	15.691	15.557	7.896	7.819

Structural formulae are on the basis 23 oxygens for amphiboles and 11 oxygens for phlogopites. See Table 4.1 for sample location and description.

Table 4.4. Representative microprobe analyses of feldspars from the the post-collisional dykes of northern Karakorum.

	PLAGIOCLASES					ALKALI FELDSPARS	
	1943 CORE	1943 RIM	1882 CORE	1882 RIM	1882 MATRIX	1943 MATRIX	1943 MATRIX
SiO_2	52.17	55.43	55.13	57.17	67.72	65.17	64.91
TiO_2	0.00	0.00	0.02	0.02	0.00	0.00	0.00
Al_2O_3	31.04	28.90	29.52	27.56	20.15	19.22	18.84
Cr_2O_3	0.02	0.00	0.02	0.03	0.02	0.00	0.00
FeO_{tot}	0.32	0.34	0.32	0.30	0.58	0.18	0.13
MnO	0.03	0.00	0.00	0.00	0.00	0.00	0.00
MgO	0.09	0.03	0.05	0.03	0.33	0.00	0.00
CaO	13.17	11.04	11.63	9.71	0.41	0.51	0.00
Na_2O	3.58	4.89	4.66	5.55	10.92	2.81	0.30
K_2O	0.56	0.49	0.45	0.66	0.41	12.39	16.09
TOT	100.98	101.12	101.80	101.03	100.53	100.28	100.27
Si	2.350	2.475	2.449	2.546	2.955	2.968	2.988
Al	1.648	1.521	1.545	1.447	1.036	1.032	1.022
Ti	0.000	0.000	0.001	0.001	0.000	0.000	0.000
Cr	0.001	0.000	0.001	0.001	0.001	0.000	0.000
Fe_{tot}	0.012	0.013	0.012	0.011	0.021	0.007	0.005
Mn	0.001	0.000	0.000	0.000	0.000	0.000	0.000
Mg	0.006	0.002	0.004	0.002	0.021	0.000	0.000
Ca	0.636	0.528	0.554	0.464	0.019	0.025	0.000
Na	0.313	0.424	0.401	0.479	0.924	0.249	0.027
K	0.032	0.028	0.025	0.037	0.023	0.720	0.945
TOT	4.999	4.991	4.992	4.988	5.000	5.001	4.987

Structural formulae are on the basis of 8 oxygens. See Table 4.1 for sample location and description.

3.6.1. *SARPO LAGGO MORAINE.*

Along with the rocks described in section 3.3.5, the moraine of the Sarpo Laggo glacier includes blocks of migmatitic gneisses and of andalusite-bearing black slates. Additional informations on the geological constitution of the Sarpo Laggo valley are reported by Desio (1980) and Desio and Zanettin (1970). According to Desio maps, the Sarpo Laggo valley consists of "K^2-Falchan Gneisses", "Muztagh Tower Gneisses" (roughly corresponding to the Sarpo Laggo-K^2 Metamorphics of this paper) and, in the upper part of the valley, of "Baltoro Black Shales and Slates", "Peribatholitic Gneisses" and "Baltoro Granites". The "Baltoro Black Shales and Slates" and the "Peribatholitic Gneisses" may correspond, respectively, to the andalusite-bearing black slates and to the migmatitic gneisses described in this section.

The *andalusite-bearing black slates* are very fine-grained rocks of sedimentary origin characterized by the peculiar presence of andalusite porphyroblasts several centimeters long. The most pervasive foliation (S1) is defined by very fine-grained brown biotite and by the preferred orientation of andalusite. S1 is often crenulated with the local formation of a crenulation cleavage S2 defined principally by the limbs of the tighter crenulations. The andalusite porphyroblasts show the cruciform pattern of inclusions typical of the chiastolite variety. Although an internal foliation is usually lacking within andalusite, this mineral is probably coeval with formation of S1 and biotite. In contrast, andalusite is deformed by S2 crenulation and in S2 hinges it is replaced by white mica. In other samples andalusite is transformed to chlorite, quartz and biotite, suggesting a polyphase replacement for this mineral.

The other minerals of the black slates are abundant quartz, opaques, Mg-Fe chlorite, garnet and plagioclase. Chlorite form flakes overgrowing S1, while garnet occur as small idioblastic grains. Additionally, two types of pseudomorphs have been observed in these rocks. A first type is a prismatic aggregate of white mica and overgrows S1; it may hypothetically derive from a first generation of andalusite or of another l-rich prismatic mineral. The second type is overgrown by andalusite and forms millimeter-centimeter long lenses consisting of very fine-grained biotite, opaques and quartz; it might represent strongly deformed and recrystallized clay balls.

The *migmatitic gneisses* show frequent decimeter-thick quartzo feldspathic leucosomes and convolute folds. They are medium- to coarse-grained rocks consisting of quartz, plagioclase, alkali feldspar, biotite and minor muscovite and sillimanite. Brown biotite defines the main foliation, while muscovite chiefly post-dates biotite and partly replaces sillimanite.

3.6.2. *GASHERBRUM AND SKYANG MORAINES.*

Along with the lithologies described in section 3.3.4, the moraines of the northern Gasherbrum and Skyang glaciers consist also of porphyritic rocks, trachytes, granodiorites, granophyres, gneisses, black slates and talc-bearing marbles. In the Desio map (1980), the upper part of the northern Gasherbrum valley consists of "K^2-Falchan Gneisses", of marbles, of quartz-diorites and of dykes.

The *porphyritic rocks* consist of plagioclase, colourless au gite, green acmite, phlogopite, amphibole ± quartz ± apatite. These rocks show a very fine-grained groundmass and include centimeter-sized elements of quartz-rich volcanics.

The *trachytes* are microcrystalline rocks lacking mafic minerals and chiefly consisting of euhedral alkali feldspar, which includes corroded relics of plagioclase, and of minor euhedral quartz. Whole-rock composition of one trachyte sample is reported in table 5.

The *granodiorites* are medium- to fine-grained rocks consisting of quartz, zoned plagioclase, large poikilitic alkali feldspar, brown biotite (Bi1) and green hornblende with accessory allanite, apatite and zircon. Plagioclase composition ranges from oligoclase rims (An = 15-20 mol %) to andesine cores (An=35-40 mol %). Corroded relics of colourless clinopyroxene locally occur within hornblende. A few deformed samples show a foliation defined by elongated and deformed quartz grains and by a very fine-grained biotite (Bi2). They are characterized by decimeter-sized inclusions of foliated biotite-gneisses and of foliated clinopyroxene-bearing quartz diorites. The granodiorites have a composition similar to the Sughet Granodiorite (section 3.7.2.) but are more deformed and show more pervasive foliations and recrystallizations.

The *granophyres* are cataclastic rocks consisting of quartz, alkali feldspar and plagioclase with veins of chlorite and carbonate. Quartz and alkali feldspar show intimate micrographic intergrowths.

The *black slates* are very fine-grained rocks similar to the andalusite-bearing black slates found in the Sarpo Laggo moraine. They show a pervasive metamorphic foliation defined by fine- grained brown biotite and are characterized by the existence of aggregates of white mica, biotite and quartz probably replacing original andalusite.

3.7. DISCUSSION

3.7.1. *P-T CONDITIONS OF METAMORPHISM.*

The metamorphic rocks investigated during the 1988 expedition are charac-

terized by metamorphic assemblages formed in a wide range of P-T conditions. On the basis of the observed mineral assemblages and of the equilibria reported in Fig. 4.13, the following P-T estimates are proposed for the metamorphic recrystallization of the various metamorphic units. As already emphasized in section 1, field work and sampling of the metamorphites was done during a reconnaissance expedition in a very little known area and was often accompanied by bad weather; additionally a detailed petrologic investigation involving mineral chemistry and geothermobarometry is not yet completed. Consequently the following estimates should be consid ered as preliminary rather than conclusive results.

a) Kun Lun Crystalline.

In the Kun Lun Crystalline the existence of quartzofeldspathic leucosomes of presumably anatectic origin in the migmatic gneisses, the apparent instability of muscovite + quartz assemblages and the plagioclase - hornblende ± clinopyroxene assemblages observed in the metabasics, all suggests a high-grade recrystallization at temperatures higher than 600-650° C (Fig. 4.13). Unfortunately, the available data do not furnish constraints for reliable pressure estimates. A polyphase history, perhaps related to a retrograde trajectory, is suggested by the replacement of clinopyroxene by pale-green amphibole.

b) Surukwat Thrust Sheets.

The metadiorites from this unit show incipient very low-grade assemblages (including sericite, epidote and prehnite) in the more northerly sectors, and more pervasive low-grade assemblages (including green biotite, actinolitic amphibole ± clinozoisite) in the southern sectors. The different degrees of metamorphic recrystallization are probably linked also to gradients in rock deformation with the concentration of ductile shear zones near the southern contact with the mylonitic micaschists. A metamorphic zonation with southward temperature increase from 250-350°C to 350-450°C is then apparent for the metadiorites of the Surukwat Thrust Sheets (Fig. 4.13). The lack of high-pressure minerals like Na-amphiboles or lawsonite and the stability of Ca-amphibole, chlorite, albite prehnite constrain pressures at relatively low values. Low-grade assemblages with green/brown biotite, muscovite and albite-oligoclase characterize also the gneisses and the metapelites.

c) Sarpo Laggo-K^2 Metamorphics.

The rocks from this unit show a very pervasive metamorphic-tectonic character which is recorded by both the metamorphic recrystallizations and the large scale transpositions and infoldings between the main lithologies. The observed metamorphic minerals (i.e. brown biotite, muscovite, albite-oligoclase, green hornblende and garnet in the gneisses) indicate recrystallization in the upper temperature part of the

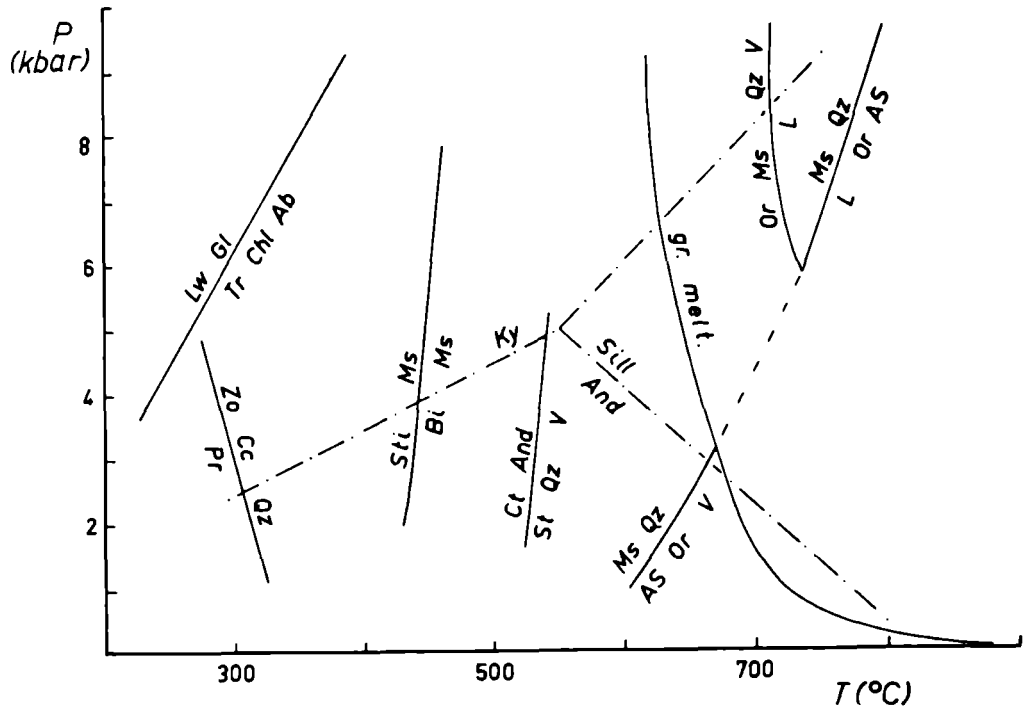

Fig. 4.13. P-T grid showing a few equilibria significant for the studied metamorphites of northern Karakorum. Equilibria are reported from Müller and Saxena (1977, p.183) except: Lw+Gl=Tr+Chl+Ab (Perchuk and Aranovich, 1980), Zo+Cc+Qz= Pr (Perchuk and Aranovich, 1980) and Sti+Ms= Bi+Ms (Winkler, 1974,p.232). Abbreviations. And: andalusite, AS: Al- silicate, Ct: chloritoid, Ky: kyanite, Gl: glaucophane, L: liquid, Lw: lawsonite, Or: orthoclase, Pr: prehnite, Sill: sillimanite, St: staurolite, Sti: stilpnomelane, Tr: tremolite, V: vapor, Zo: zoisite; gr.melt.: beginning of melting in the granitic system. For other abbreviations see Table 4.1.

low-grade or in the lower temperature part of the medium-grade (T = 450-600°C) (Fig. 4.13). A comparable temperature range is given by the impure marbles: for intermediate XCO_2, the tremolite - quartz - calcite assemblages with the apparent lack of diopside point to T = 500-550°C for P = 1 kbar and T = 600-650°C for P = 5 kbar (Winkler, 1974).

d) Metamorphites from the moraine of the Sarpo Laggo glacier.

Among the metamorphic rocks, interesting are the assemblages observed in the andalusite-bearing black slates and in the migmatitic gneisses found in the moraine of the Sarpo Laggo glacier. Unfortunately, the lack of data concerning the field

relationships inhibits the interpretation of the regional significance of these assemblages. For the black slates, the biotite-muscovite-garnet-andalusite assemblages point to relatively low (but not very low) pressures (≤ 4-5 kbar); these assemblages and the apparent lack of staurolite or cordierite are probably indicative of recrystallization in the intermediate/upper temperature part of the low-grade (T = 500-550°C) (Fig. 4.13). More severe high-grade conditions (T ≥ 600-650°C) are suggested for the migmatitic gneisses by the abundance of quartzofeldspathic leucosomes and by the biotite-sillimanite ± alkali feldspar assemblages lacking muscovite (Fig. 4.13).

e) Relations between metamorphism and tectonism.

The data provided by this work indicate that the tectonic setting along the Kun Lun-Karakorum transect is characterized by the association of units which underwent different metamorphic histories with unmetamorphosed units. This suggests the existence of shallow level structural discontinuities. Along the transect, specifically around the Shaksgam valley area, the existence of a recent tectonism is implied by the following evidence:

1) Abundant tectonized and faulted contacts occur not only between the various units but also within each units and at the boundaries of the granitoid batholiths. This tectonism chiefly post-dates metamorphism and ductile deformations which are responsible for the folding observed within some units. It usually occurred under "cold" conditions with the formation of brittle faults and cataclasites like, for example, those occurring between the Sughet Granodiorite and the Shaksgam Sedimentary Belt. These brittle faults have a prevalent NW-SE trend and have been ascribed by Gaetani et al.(1990b and this vol.) to the strike slip Karakorum Fault Zone (KFZ) (Molnar and Tapponnier, 1975). Evidence of ductil deformations under low-grade metamorphic conditions exist within the Surukwat Thrust Sheets and are recorded by the mylonitic micaschists occurring between metadiorites and gneisses (section 3.3.5). Additionally, very low-grade mylonites have been observed also between the Sarpo Laggo-K^2 Metamorphics and the tectonic slices observed near the contact with the Sughet Granodiorite (section 3.3.5). In the Sarpo Laggo-K^2 Metamorphics, this very low-grade recrystallization linked to the tectonic contact, post-dates the main low/medium-grade metamorphism.

2) The lamprophyric dykes of Neogene age (section 3.7.2) post-date the main metamorphism of the Sarpo Laggo-K^2 Metamorphics and are displaced by the NW-SE trending faults linked to the KFZ.

3) Non-metamorphic units are tectonically interposed between the metamorphic units.

4) A few fission-track ages point to very rapid and recent uplift of the

Gasherbrum Diorite (Cerveny et al., 1989).

5) The K^2-Gasherbrum range reaches extremely high elevations exceeding 8000 m.

3.7.2. *GEOCHEMISTRY AND PETROGENESIS OF THE MAGMATIC ROCKS.*

A few representative samples of plutonic and lamprophyric rocks reported in Table 1, have been studied in detail. The whole-rock composition of these samples (Tables 4.5 and 4.6) has been obtained with an emission spectrometer JY70 at the C.R.P.G. (Vandoeuvre) and include determination of major, minor and rare earth elements (REE). Table 4.5 also includes the analysis of one trachyte from the moraine of the Gasherbrum glacier. Additionally, a few minerals have been analyzed using an electron microprobe (Tables 4.2, 4.3 and 4.4; see also section 3.5.1).

a) Plutonites.

The geochemical data indicate an acid peraluminous (sample 1876, 2001 and 2020) or an acid slightly metaluminous composition (2023) for the analyzed granitoids. According to the method of classification of De La Roche et al. (1980) (Fig. 4.14) and in the Q (quartz)-A (alkali feldspar)-P (plagioclase) triangle of

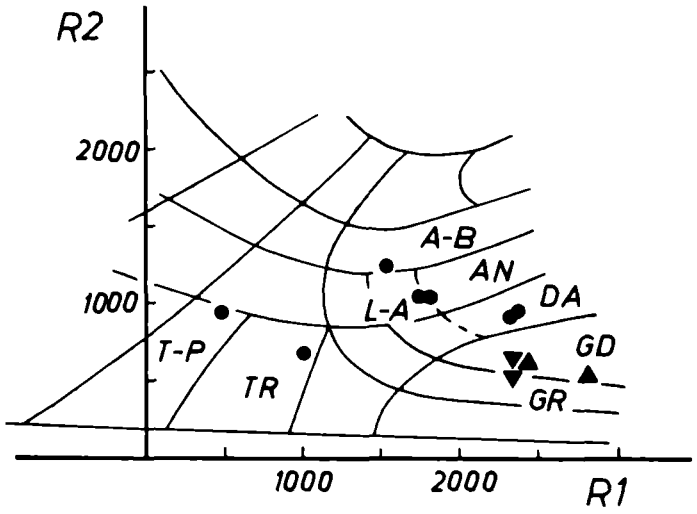

Fig. 4.14. R1-R2 classification diagram of De La Roche et al. (1980) for the analyzed granodiorite 1876 and orthogneiss 2001 (triangles), the monzo-granites 2020 and 2023 (inverted triangles) and the post-metamorphic dykes (dots). Abbreviations. A-B: andesi-basalt, AN: andesite, DA: dacite, GD: granodiorite, GR: granite, L-A: lati-andesite, T-P: trachyphonolite and TR: trachyte.

Streckeisen, the samples from the Sughet Granodiorite (1876) and the Sarpo Laggo-K^2 Metamorphics (2001) plot in the granodiorite field, while a granitoid sampled near the Khunjerab pass along the Karakorum Highway (near the boundary between China and Pakistan) is a monzo-granite (2023). Sample 2020 from the Bazar Dara Slates plots in the granodiorite field following the classification of De La Roche et al.(1980) and in the monzo-granite field in the Q-A-P triangle. The SiO_2 vs $\log_{10}[CaO/(Na_2O+K_2O)]$ diagram of figure 4.15 indicates calc-alkali to slightly calcic characters both for the studied rocks and for the Transhimalayan plutonites. For granodiorites 1876 and 2001, the calc-alkali character is implied also by the scattered crystallization of hornblende and by the association with gabbroic and quartz dioritic enclaves.

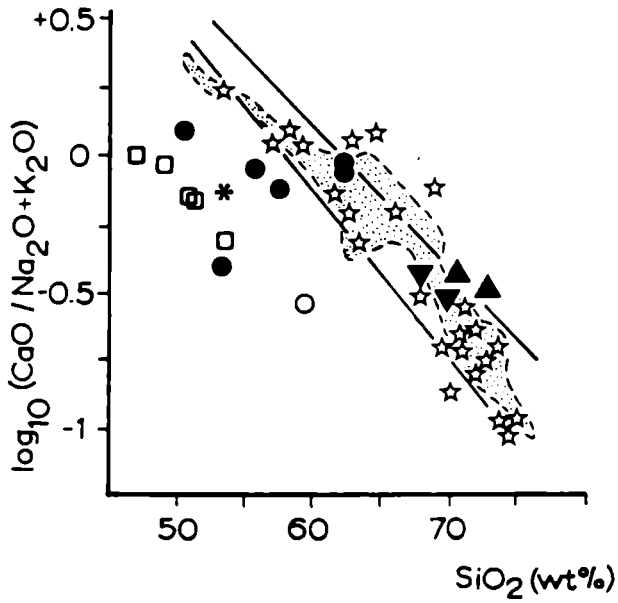

Fig. 4.15. SiO_2 vs $\log_{10}(CaO/Na_2O+K_2O)$ diagram for the analyzed granodiorite and orthogneiss (triangles), monzo-granites (inverted triangles), post-metamorphic dykes (full dots) and trachyte 1970 (circle). Asterisk: Baltoro lamprophyre (Rex et al., 1988); squares: Baltoro lamprophyres (Desio and Zanettin, 1970); stars: granitoids from the Karakorum region (Desio and Zanettin, 1979; Debon et al., 1987; Rex et al., 1988); dotted field: granitoids from the Tibet region (Harris et al., 1988). Solid lines define the field of the Andean andesites (Brown, 1982) and, approximately, of the calc-alkali rocks (Harris et al., 1988).

Table 4.5. Whole-rock compositions of trachyte 1970, monzonitic granites 2020 and 2023 and granodiorites 1876 and 2001.

	1970	2020	2023	1876	2001
SiO_2 (wt%)	59.54	67.81	69.25	70.31	72.67
TiO_2	0.76	0.52	O.30	0.30	0.22
Al_2O_3	13.38	15.21	14.13	15.38	14.83
Fe_2O_{3tot}	3.59	3.66	2.81	2.42	1.67
MnO	0.06	0.07	0.04	0.04	0.03
MgO	2.24	1.46	1.08	0.85	0.48
CaO	2.95	2.62	2.12	2.74	2.11
Na_2O	3.04	2.70	3.02	3.99	3.52
K_2O	7.64	4.75	4.79	3.29	3.12
P_2O_5	0.81	0.22	0.16	0.16	0.17
L.O.I.	5.21	0.90	0.16	0.88	0.67
TOT	99.22	99.92	100.13	100.36	99.49
Ba (ppm)	2933	630	814	965	896
Rb	312	201	168	89	94
Be	3	3.29	2.40	1.1	2.2
Sc	6.5	9	7.19	4.9	3
Co	<5	7	5	<5	<5
Sr 1059	230	361	439	333	
Cr	101	38	23	13	7
Th	50	16	23	6	8
Cu	14	12	12	8	<5
V	40	47	43	34	14
Ga	21	21	12	15	18
Y	19.26	17.49	17.56	8.43	6.67
Nb	45	18	9	6	<5
Zn	60	128	12	24	36
Ni	62	11	6	<5	<5
Zr	397	177	129	112	107
La (ppm)	85.95	38.52	37.64	19.51	26.10
Ce	156.64	85.17	68.55	35.64	51.34
Nd	58.28	31.69	21.78	12.56	18.01
Sm	10.05	6.46	4.31	2.53	3.37
Eu	2.41	1.16	0.92	0.71	1.04
Gd	6.54	4.64	3.31	2.03	2.34
Dy	3.39	2.84	2.56	1.35	1.15
Er	1.49	1.47	1.49	0.75	0.58
Yb	1.15	1.28	1.53	0.65	0.47
Lu	0.26	0.24	0.30	0.14	0.14
K/Rb	101.64	98.09	118.35	153.44	137.77
Ce/Y	8.13	4.87	3.90	4.23	7.70
Zr/Y	20.61	10.12	7.35	13.29	16.04
Nb/Y	2.34	1.03	0.51	0.71	
Ti/Zr	11.47	17.60	13.94	16.05	12.32
La_n/Lu_n	34.06	16.54	12.93	14.36	19.21

Table 4.6. Whole rock compositions of the studied post-metamorphic dykes from northern Karakorum and of the dykes from the Baltoro glacier area (A and B).

	A	B	1880	1884	1908	1943	1882	1883
SiO_2 (wt%)	50.19	52.9	50.46	55.82	53.00	57.57	62.03	62.00
TiO_2	2.13	1.6	0.75	0.85	1.12	0.81	0.70	0.70
Al_2O_3	10.02	10.3	11.66	13.11	13.85	15.71	15.35	15.11
Fe_2O_{3tot}	6.02*	6.9	6.50	6.58	7.25	6.95	5.75	5.50
MnO	0.11	0.1	0.11	0.08	0.10	0.11	0.08	0.10
MgO	7.75	11.1	6.64	6.33	4.47	3.87	2.41	2.32
CaO	7.87	6.0	6.70	4.41	4.33	5.04	4.99	4.74
Na_2O	2.05	1.1	1.33	3.72	1.87	2.12	2.58	2.25
K_2O	8.19	7.9	3.95	1.75	9.28	4.90	3.04	3.62
P_2O_5	0.98	1.7	0.72	0.80	1.37	0.77	0.24	0.25
L.O.I.	4.58		10.83	6.09	2.83	2.51	2.49	3.72
TOT	99.89	99.6	99.65	99.54	99.47	100.36	99.66	100.31
Ba (ppm)	2888	3679	2346	888	1409	1935	852	880
Rb		350	169	63	466	176	87	112
Be			4.59	5.19	4	4.3	2	2
Sc			27.2	22.2	21.2	24.1	19.29	19.2
Co			22	17	11	11	8	8
Sr		1221	708	752	370	1154	389	319
Cr	267	580	444	318	105	37	56	63
Th		8	21	11	41	24	17	16
Cu			24	37	96	17	12	12
V		135	154	148	127	158	107	111
Ga		19	15	15	18	18	17	18

Table 4.6 (continued).

	A	B	1880	1884	1908	1943	1882	1883
Y		34	26.23	30.74	28.86	33.94	29.57	29.55
Nb		46	17	13	26	22	15	15
Zn		153	41	58	229	64	57	56
Ni		403	41	97	36	8	9	11
Zr		692	226	190	365	276	226	234
La (ppm)	114	44.30	33.21	70.23	59.38	41.54	40.68	
Ce		266	88.70	72.82	138.87	115.70	82.40	81.00
Nd	136	36.31	32.14	66.91	49.01	33.09	33.32	
Sm			7.32	7.01	12.74	9.75	6.68	6.76
Eu			1.70	1.55	3.06	2.35	1.48	1.46
Gd		5.73	5.59	8.64	7.50	5.83	5.66	
Dy			4.18	4.67	4.99	5.33	4.60	4.62
Er		2.14	2.54	2.22	2.59	2.45	2.44	
Yb			1.93	2.42	1.80	2.44	2.34	2.36
Lu		0.37	0.42	0.31	0.45	0.40	0.40	
K/Rb		93.69	97.01	115.30	82.66	115.56	145.03	134.16
Ce/Y		7.82	3.38	2.37	4.81	3.41	2.79	2.74
Zr/Y		20.35	8.62	6.18	12.65	8.13	7.64	7.92
Nb/Y		1.35	0.65	0.42	0.90	0.65	0.51	0.51
Ti/Zr		13.86	19.88	26.81	18.39	17.59	18.56	17.93
La_n/Lu_n			12.34	8.15	23.36	13.60	10.70	10.48

Baltoro glacier lamprophyres: A (average of 6 analyses; Desio and Zanettin, 1970) and B (Rex et al., 1988). Asterisk: $FeO+Fe_2O_3$. See Table 4.1 for sample location and description.

The MORB-normalized multi-element patterns (Fig. 4.16) are comparable for all the analyzed granitoids and are typical of the collisional-type magmatism (Pearce, 1982; Pearce and Houjun,1988). However, granodiorite 1876 and 2001 are slightly depleted in most of the analyzed elements reported in Fig. 4.16 relative to monzo-granites 2020 and 2023. Derivation from magmas originated along active continental margins is suggested also by the Rb vs (Y+Nb) diagram of Fig. 4.17; in this diagram the analyzed granitoids plot in the volcanic-arc/post-collisional field, close to the syn-collisional field. The chondrite-normalized patterns for REE indicate an enrichment of light REE relative to heavy REE and an increase of REE content from the granodiorites 1876 and 2001 to monzo-granites 2020 and 2023 (Fig. 4.18).

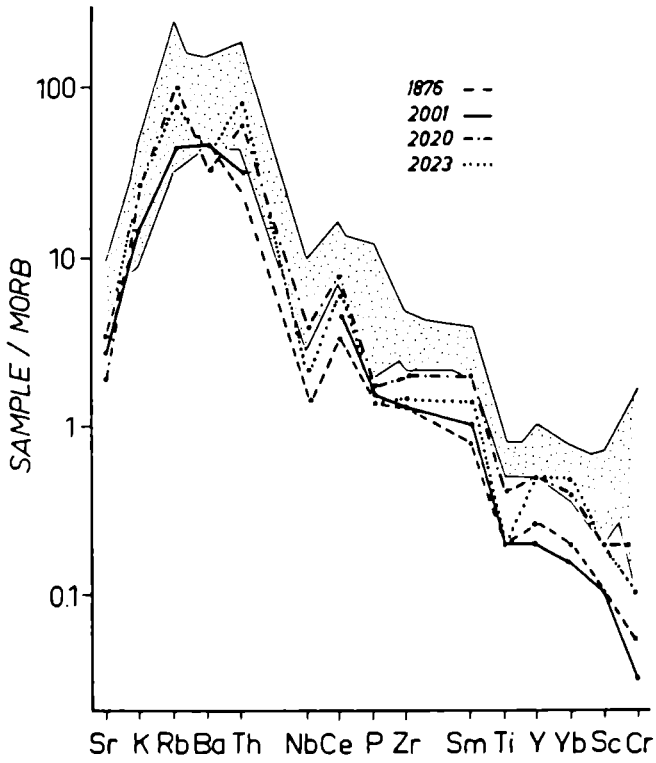

Fig. 4.16. MORB-normalized multi-element patterns for the analyzed granitoids (1876, 2020 and 2023), orthogneiss (2001), post-metamorphic dykes and trachyte 1970 (dotted field).

The monzo-granites also display negative Eu anomalies which are common in the other Transhimalayan plutonites but are lacking in the granodiorites.

These lines of evidence and the different ratios for some hygromagmatophyle elements in the granodiorites 1876 and 2001 relative to monzo-granites 2020 and 2023 (Zr/Y: 14.00-17.83 vs 8.60-11.80; K/Rb: 137.77-153.44 vs 98.09-118.35; Rb/Sr: 0.20-0.28 vs 0.47-0.87: Rb/Zr: 0.79-0.88 vs 1.14-1.30), suggest derivation from sources of different composition.

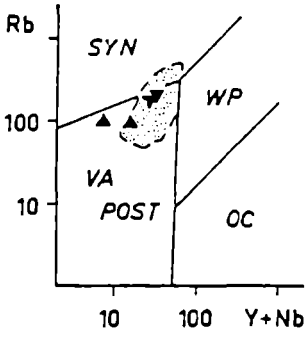

Fig. 4.17. Rb vs Y+Nb (ppm) diagram for the analyzed granitoids of northern Karakorum (symbols as in Fig. 4.15). The field of the syn-collisional granites of upper crustal origin (SYN), of the volcanic arc / post-collisional granites (VA/POST), of the within plate granites (WP) and of the oceanic ridge granites (OC) are after Pearce et al.(1984). Dotted field indicates the Tibetan plutonites reported by Harris et al.(1988).

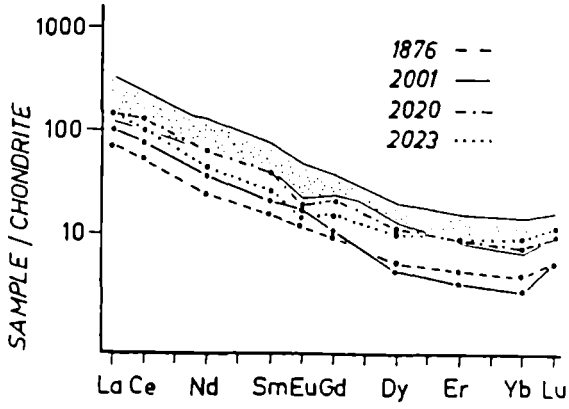

Fig. 4.18. Chondrite-normalized REE patterns for the analyzed granitoids and post-metamorphic dykes (dotted field).

The Sarpo Laggo-K^2 gneissic granodiorite 2001 corresponds to the "K^2 Gneisses" of the upper Baltoro glacier in Pakistan (Desio and Zanettin, 1970) which give U-Pb ages of 115 ± 3 MY (Rex et al., 1988). A geochronological study currently in

progress with P. Le Fort (Grenoble), points to a similar Cretaceous age (94.8 ± 3.2 MY; K-Ar on biotite) also for the Sughet Granodiorite 1876 which may be correlative with the Cretaceous-Palaeocene granitoids of the upper Hunza valley (Debon et al., 1987; Gaetani et al., 1990a). However, in the Sughet Granodiorite, the pervasive metamorphic recrystallization which is typical of the Sarpo Laggo-K^2 Metamorphics, has not been observed. Consequently, the Sughet Granodiorite escaped the Palaeogene metamorphism which followed the Cretaceous Andean-type plutonism (Debon et al., 1987) probably because it was located in a different structural position relative to the granitoids of the Sarpo Laggo-K^2 unit. As regards the monzo-granite 2020 from the Bazar Dara Slates, a Jurassic cooling age (171.5 ± 5.4 MY) is suggested by K-Ar dating of biotite (Le Fort, pers. com.).

b) Post-metamorphic dykes.

Mineral chemistry data concerning the post-metamorphic dykes are reported in Tables 4.2, 4.3 and 4.4 and are summarized in section 3.5.1, whilst whole-rock compositions are reported in Table 4.6. Whole-rock geochemistry indicates prevalent intermediate metaluminous compositions, except for sample 1880 which is a basic metaluminous rock. According to the method of classification of De La Roche et al. (1980), sample 1908 is a trachyphonolite, 1880 is an andesi-basalt, 1884 and 1943 are lati-andesite or andesite, while 1882 and 1883 are dacites (Fig. 4.14). In the K_2O-SiO_2 diagram (Fig.4.19) the dykes plot in the high-K calc-alkaline or in the shoshonite field. Owing to the high K_2O/Na_2O ratios, high K_2O contents and relatively high MgO values, some dykes are considered ultrapotassic rocks. The MORB-normalized multi-element patterns (Fig. 4.16) are similar to those of the post-orogenic magmatism from destructive plate margins (Pearce, 1982; Pearce and Houjun, 1988) and the chondrite-normalized patterns for REE (Fig. 4.18) show an enrichment in light REE relative to heavy REE.

By comparison with the shoshonitic and ultrapotassic lamprophyres of the western Alps (Venturelli et al., 1984), the Tertiary post-collisional volcanics of Tibet (Pearce and Houjun, 1988), or the Neogene lamprophyric dykes of the upper Baltoro glacier (Desio and Zanettin, 1970, Rex et al., 1988), the studied dykes of northern Karakorum show a larger compositional range, are depleted in Mg, Ni, Cr (37-444 ppm), Y, Zr and V, have lower light REE/heavy REE ratios (La_n/Lu_n=8.15-13.60) and are richer in quartz. These differences probably reflect different composition of the sources and/or different degrees of partial melting of comparable source compositions. For the northern Karakorum dykes, the abundance of quartz, the variable Cr content (Fig. 4.20) and the fractionated composition (i.e. relatively rich in Fe and poor in Cr and Mg) of clinopyroxenes, all points to advanced degrees of

fractional crystallization (Pognante, 1990). These petrographic and geochemical characters are unusual for K-rich rocks and probably reflect both advanced fractionation and assimilation of crystal rocks.

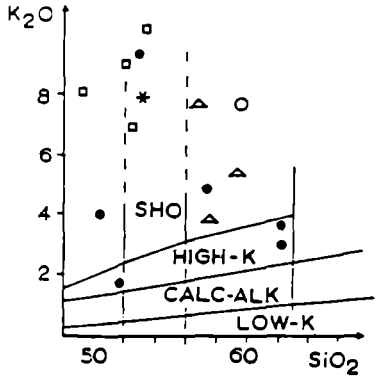

Fig. 4.19. K_2O-SiO_2 (wt%) diagram for the northern Karakorum dykes (dots) and trachyte 1970 (circle) studied here, for the Baltoro lamprophyres (squares: Desio and Zanettin, 1970; asterisk: Rex et al., 1988) and for K-rich Tertiary volcanics of the Tibetan plateau (triangles: Pearce and Houjun, 1988). The fields of the low-K tholeiite (LOW-K), calc-alkaline (CALC-ALK), high-K calc-alkaline (HIGH-K) and shoshonite (SHO) suites are after

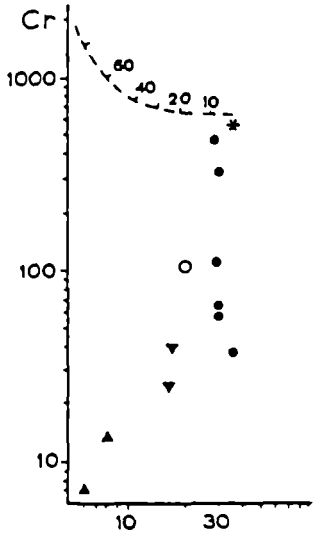

Fig. 4.20. Cr-Y (ppm) diagram for the northern Karakorum rocks. Symbols as in Fig. 4.20. Dashed line and numbers indicate the partial melting trend and the degrees (wt%) of partial melting, respectively, reported by Pearce (1982).

The less primitive geochemical characters relative to the Baltoro lamprophyres, which should have a comparable Neogene age (K-Ar ages of 22 MA have been

obtained on biotite from one Baltoro dyke: Rex et al., 1988), may be interpreted in terms of an early removal of clinopyroxene, phlogopite, plagioclase, garnet ± amphibole followed by precipitation of abundant alkali feldspar ± apatite and eventually accompanied by assimilation of SiO_2 rich rocks (Pognante, 1990). These processes caused: the marked enrichment of light REE relative to heavy REE in the intermediate compositions; and the subsequent depletion of light and intermediate REE, the slight negative Eu anomaly and the depletion in Ba in the silica-rich compositions (like samples 1882 and 1883). The scattered presence of garnet in some primitive lamprophyres of the Baltoro glacier (Desio and Zanettin, 1970) is consistent with the previous considerations.

3.8. Summary and Conclusions

The crystalline rocks observed along the Kun Lun-Karakorum transect include metamorphites, plutonites and post-metamorphic lamprophyric dykes. These rocks occur in different tectonic units separated by syn-/late-metamorphic thrusts and by frequent post-metamorphic faults and cataclasites formed after the main collision between India and Eurasia and during the subsequent post-metamorphic uplift. Ductile syn-metamorphic deformations are common in the high-/medium-grade rocks of the Sarpo Laggo-K^2 Metamorphics and in the very-low-/low-grade rocks of the Surukwat Thrust Sheets. Brittle faults and cataclasites bound most of the intrusive bodies and are frequent in the Shaksgam valley area where they trend NW-SE and have been attributed to the Karakorum Fault Zone (KFZ). The post-metamorphic dykes of probable Neogene age are dislocated by the KFZ.

These lines of evidence along with a few fission-tracks data on the Gasherbrum Diorite (Cerveny et al., 1989) and the extremely high elevation of the K^2-Gasherbrum range which exceeds 8000 m, all point to the existence of a very recent tectonism and uplift along the KFZ. Although the KFZ is usually considered a strike-slip fault (Molnar and Tapponnier, 1975), we have observed also significant vertical throws and consequently it is proposed that the KFZ temporarily behaved as a thrust or a normal fault system. This interpretation provides a mechanism for exhumation of the plutonic and relatively high-pressure metamorphites of southern and central Karakorum with respect to the unmetamorphosed sediments of northern Karakorum. Our observations also indicate that the post-metamorphic lamprophyric dykes are preferentially oriented NW-SE and concentrated near the KFZ, i.e. in the upper Baltoro glacier and in the Shaksgam valley area. Hence it is possible that, during the Neogene, the KFZ reached deep crustal levels, temporarily behaved as

a normal fault and triggered ascent and emplacement of the lamprophyric magma (Pognante, 1990). Later on, further northward migration of India (re)activated a transpressional regime along the KFZ favoring the recent and rapid uplift of the K^2-Gasherbrum range. This is consistent with some geophysical data (Caporali et al., this vol.) which point to the SW dip of the contact between the Sarpo Laggo-K^2 Metamorphics and the unmetamorphosed unit to the North.

As regards the metamorphites, the medium-/high-grade assemblages of the Kun Lun Crystalline have been attributed to the Paleozoic by the Metamorphic Map of China (Cheng et al., 1986) while, by comparison with the assemblages of the southern and central Karakorum (Rex et al., 1988), the low-/medium-grade assemblages of the Sarpo Laggo-K^2 Metamorphics should be of Paleogene age. No geochronological data are available for the very-low-/low-grade assemblages of the Surukwat Thrust Sheets. However, the close relationships between the metamorphic recrystallization and the tectonism linked to the post-collisional history, suggest a Tertiary age for these assemblages.

Among the plutonites, K-Ar data on biotites give Jurassic age (171.5 ± 5.4 MY) for the monzogranites occurring in the Bazar Dara Slates and Cretaceous age (94.8 ± 3.2 MY) for the Sughet Granodiorite. By comparison with U-Pb zircon ages of 115 ± 3 MY obtained for one orthogneiss from the upper Baltoro glacier (Rex et al., 1988), the gneissic granodiorites from the Sarpo Laggo-K^2 Metamorphics should be of Cretaceous age. For the above cited granitoids and the Aghil Dara Granodiorites, a calc- alkaline affinity and derivation from magmas originated in active continental margins, are suggested by the mineralogical and geochemical data. All these lines of evidence suggest that the plutonites of the studied region (except for the Kun Lun Paleozoic granitoids) formed before the India-Eurasia Palaeogene collision in a subduction-related Andean-type setting. The plutonites form bodies elongated approximately NW-SE according to the main tectonic discontinuities. This character should depend on the marked and polyphase post-collisional tectonism of Tertiary age, as implied by the abundance of tectonized and faulted contacts bounding the plutonic bodies. A further possibility is that the elongated shape of the plutonites is a character related to their emplacement during the Mesozoic and hence registers a tectonic influence on magma emplacement in an Andean-type setting.

4. Tectonostratigraphic Framework of the Transect from Kun Lun to Karakorum(1)

4.1. INTRODUCTION

The Kun Lun-Karakorum transect lies between the N Karakorum-Pamir transect to the west (Leven, 1967; Ruzhentsv & Shvolman, 1981; Dronov et al., 1982; Gaetani et al., 1990a) and the Tibetan Plateau transects to the east. On these latter, we have sketchy informations on the westernmost part (De Terra, 1932; Dainelli, 1933; Norin, 1946; Gergan & Pant, 1983; Srimal, 1986; Huang & Chen, 1986; Baud, 1989, Colloque Kun lun-Karakorum 90, 1990), and very scarce data on the west-central part (Tibetan Bureau stratigraphic scheme in Bally et al., 1980; Sun Te, 1983). Instead, detailed studies are available further east, for the Donqiao area (Girardeau et al., 1984; Allègre et al., 1984) and along the road Lhasa-Golmud (Royal Society-Academia Sinica Geotraverse, Chang et al., 1988). A base for correlation are also the Gansser's map (1979), the Geological Map of Tibet 1: 1.500,000 (1980), and the Metamorphic Map of China (1986).

As it may be recognized from the Fig. 4.21, the studied transect lies on the east flank of the "Karakorum promontory". The formation of the Pamir syntaxis, due to the increasing collision in correspondence of the Indian Plate northwest indenter, caused a complex deformation pattern. The transect here discussed crosses a very narrow strip, where several palaeogeographic zones and/or tectonostratigraphic terranes are welded together.

How cylindrical was the original palaeogeographic and tectonic setting, in such a squeezed area? I woud admit fair lateral correlations from SE Pamir to W Tibet, notwithstanding the still inadequate field knowledge. Instead, I found difficult and not established the correlations with the Lhasa-Golmud transect. The possibility that the Lhasa and Qiangtang microplates do not represent original single lithospheric fragments, but an accretion of several terranes should be considered.

4.2. THE WESTERN TERMINATION OF THE KUN LUN MICROPLATE

4.2.1. *THE KUN LUN CRYSTALLINE.*

The Kun Lun Crystalline, with its Late Paleozoic granitoid intrusions (Metamorphic Map of China, 1986;) or pre-Jurassic various granitoid types (Matte et al., 1990a), might be correlated with the Late Paleozoic intrusions of the Kun Lun Range,

---

(1) Maurizio GAETANI.

till the Permo-Triassic plutons near Golmud (Dewey et al., 1988), as it was already stated by the Chinese geological maps and by the Gansser map (1979). The fault system crossed just south of the Cirag Saldi Pass, that may be followed further east on the satellite imagery for several hundreds kilometres, represents the western extension of the Altyn Tagh Fault (Matte et al., 1990a). Westwards, this fault complex turn to northwest, eventually hidden below the Tashkurgan plain deposits.

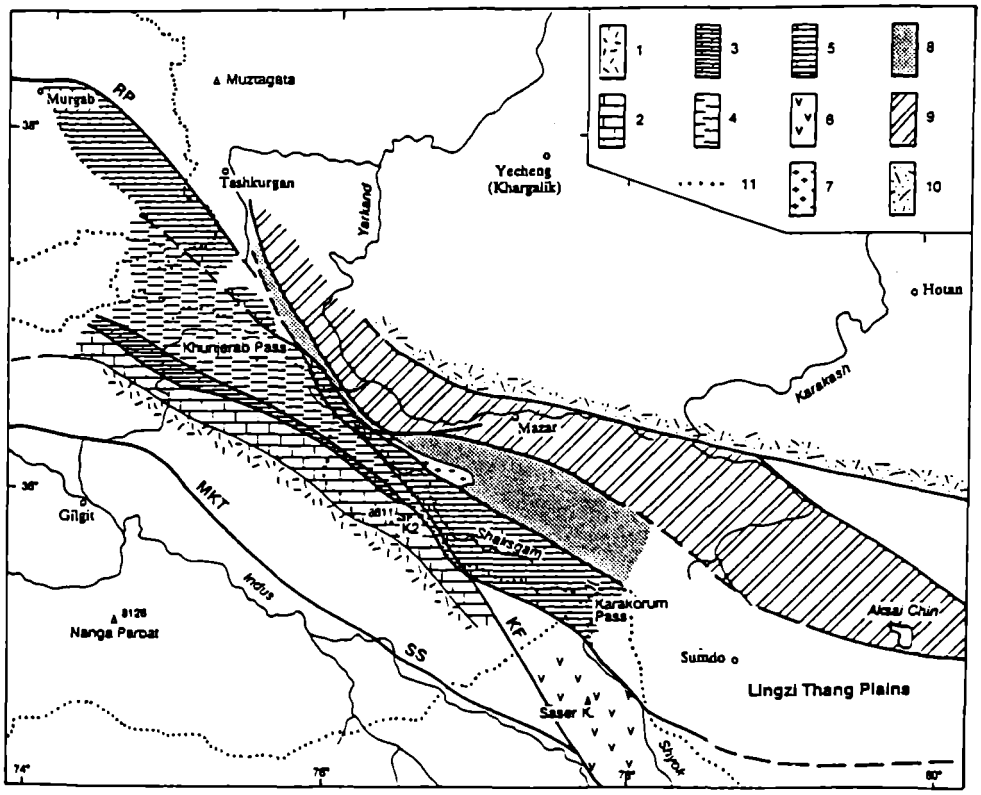

Fig.4.21. General geologic scheme of the area between Karakorum, Pamir, Kun Lun and West Tibet. 1= Karakorum Axial Batholith. 2= Gujhal Unit and its metamorphic derivates in the K^2 area. 3= Sost Unit, mostly non- or very low-grade metamorphic. 4. Misgar Unit black slates, non- to low-grde metamorphic. 5. Sedimentary rocks of SE Pamir (simplified0 and Shaksgam Sedimentary Zone. 6. Saser Kangri Batholith and associated metamorphite. 7. Aghil Dara Granodiorite. 8. Surukwat Thrust Sheets. 9. Bazar Dara Slates and associated granitoids. 10. Kun Lun Crystalline and related sedimentary rocks.

4.2.2. *THE BAZAR DARA SLATES.*

The Bazar Dara Slates, in which we didn't found any fossil, are instead a distinctive unit of the western termination of the Tibetan Plateau. Their age, till present considered as Paleozoic, in my opinion could be reconsidered. The Chinese Map 1:1,500,000 considers them as PT1 (mostly Early Paleozoic), and Baud (1989), following Norin (1946) and De Terra (1932), simply as Paleozoic. Ordovician fossils in slates where found at the Kizil pass on the Akhsae Chin (Dainelli, 1933; Gortani, 1934), but this locality lies southwards of the Bazar Dara Slates belt, according to the Norin's map, in which the slates are named "Kilian Facies". If the age of the granitoid body intruding the slates between Bazar Dara and Mazar, is Late Paleozoic as suggested by the Metamorphic Map of China, a Paleozoic age would be mandatory. If instead the age of the granitoids is younger, as suggested by our preliminary K-Ar cooling ages, also other interpretations could be likely.

Missing a direct age, some inference could be drawn by correlation. According to Matte et al., (1990b), eastwards, this very thick sequence (6000 m) spans from the Cambro-Ordovician to the Permo-Carboniferous (presence of fusulinids) and perhaps to the Triassic. It is intruded by granodiorites with ages around 215 MY.

The lithostratigraphic description matches fairly well with the counturites described south of the Kun Lun along the Lhasa-Golmud transect (Leeder et al., 1988), attributed to the Triassic (Smith & Xu, 1988). At the present state of the knowledge on the Tibetan Plateau this correlation cannot be fully assessed, but in my opinion cannot also be ruled out.

With a "younger" interpretation, the Bazar Dara Slates would represent the western termination of the wide terrigenous apron lining to the south the Kun Lun Microplate, coeval to the beginning of the deformation. In the Desio (1979) and Baud schemes (1989), these slates belongs to the Akhsae Chin Zone.

Following the Bazar Dara Slates on the satellite imagery, they seems to turn north-west, lining the Tashkurgan plain,where they could be seen in distance from the Pirali custom point and along the road further north.

Although a suture defined by ophiolites was not observed, the great fault between Bazar Dara Slates and STS might correspond to the Western Kun Lun Fault (Metamorphic Map of China, 1986), to the Northern Main Suture Zone of Huang & Chen (1986) and to the Lighten Lake Cryptic Suture Zone of Baud (1989).

4.3. THE WESTERN TERMINATION OF THE QIANTANG MICROPLATE

According to recent published tectonic schemes, the area south of the Kun Lun

Microplate and east of the Karakorum Fault should be assigned to the Qiangtang Microplate (Allègre et al., 1984; Montenat et al., 1986; Chang et al., 1986, 1988; Huang & Chen, 1986; Baud , 1989). Recently, Parrish & Tirrul (1989) considered this area as belonging to the Lhasa microplate. In Central Tibet all previously quoted authors agree in defining the Qiangtang Microplate as bounded to the south by the Nujang-Bangong Co Suture Zone and to the north by a suture zone for which different names have been used: Jinsha, Hoh Xil, Litan, Northern Main Suture.

To correlate eastwards this part of our transect is one of the most problematic points. Along the Longmu Co-Bangong Co-transect, Permo-Carboniferous black shales, quartzite and tilitoids (probably Permo-Carboniferous in age) are overlain by basalts and marine Jurassic limestones (Matte et al., 1990b). Along the Lhasa-Golmud transect, in the Qiangtang microplate, Late Permian shallow-water carbonates are unconformably covered by Jurassic alluvial to deltaic terrigenous and evaporitic sediments. A gap corresponding to the Triassic is also depicted in the Tibetan Bureau scheme for the Central Tibet (Bally et al., 1980). A Permian marine sequence with evolution like the Shaksgam Sedimentary Belt has been instead described north of the Bangong Co (Sun Te, 1983), by De Terra (1932) and Dainelli (1933) between the Karakorum pass trail and the Lingzi Thang range and plains. Consequently it appears that there are very different Permo-Triassic sequences between East and West Qiangtang. Is this due to a more intense Jurassic deformation eastwards, eroding the deeper Triassic sediments, or is this because the two area belong to different terranes?

Along our transect, we have only one significant unit of Qiangtang affinity: the red sandstones and anhydrites of the Surukwat Thrust Sheets. Their petrography is similar to the Jurassic Marpo Sandstone of Shaksgam. Very wide spread red sandstones derived during the Jurassic from the newly formed Kun Lun Range, are considered typical for the Qiangtang Microplate (Leeder et al., 1988). Jurassic flora has been described from red sandstones along the Qara Tagh river by Norin (1946, p. 46). This might be a point to consider the STS as an edge of the Qiangtang Microplate.

However, no metamorphic rocks have been so far described eastwards in Western Tibet, belonging to the Qiangtang microplate. The Surukwat Sheets could be related to a basement emergence due to the extreme shortening around the Karakorum promontory. To northwest it is difficult to follow this belt, which seems to be squeezed out towards the Tashkurgan Plain.

4.3.1. *THE AGHIL DARA GRANODIORITE.*

This intrusive body belongs to the Yangshanian, according to the Metamorphic

Map of China (1986). Similar age intrusions are spread all over the Karakorum, both on Pakistani side (Le Fort et al., 1983; Debon et al., 1987; Le Fort, 1988; Rex et al. 1988; Searle et al., 1989; Cerveny et al., 1989) both on the Chinese side (Metamorphic Map of China, 1986). This very wide plutonic activity is related either to the subduction and collision of the Kohistan-Ladakh arc below the Eurasian margin (Rex et al., 1988; Searle et al., 1989) or to a double vergence along both sides of Karakorum (Debon et al., 1987). In any case they cannot be assumed for a Karakorum versus Qiangtang Microplate identification, as instead the Bazar Dara granitoids do for the Kun Lun Microplate.

4.4. THE SE PAMIR-KARAKORUM MICROPLATE

4.4.1. *THE SHAKSGAM SEDIMENTARY BELT.*

The Permo-Triassic internal stratigraphy of the Shaksgam Sedimentary Belt shows closer similarities with the N Karakorum and also with the SE Pamir, as it was already pointed out by Desio (1980). Some Permian events, like the clastic episode in the Late Artinskian-Kubergandian, may be also traced in Chitral (own observations) and in the Central Afghanistan (Wardal) (Termier et al., 1974).

Typical features are the Permian passive margin stage with block faulting and drowning during the Murgabian-Djulfian, and a pelagic stage during the Early and Middle Triassic. A similar evolution, from Permian to the Carnian, may be also recognized through the cumbersome report of Dainelli (1933) in the area from Karakorum trail to Lingzi Thang.

By the Norian, the Shaksgam Sedimentary Belt entered in shallower marine conditions which was tapered by marginal orogenic derived red sandstones and conglomerates in the Middle Jurassic. Similar Jurassic episodes of marginal alluvial sedimentation are recorded both in Afghanistan (Boulin, 1981; Montenat et al., 1986), in SE Pamir (Dronov et al., 1982) in N Karakorum (Gaetani et al., 1990a), and in Lingzi Thang range on the Akhsae Chin plateau. As already discussed in the Sedimentary Formations (Gaetani, this volume), I don't see any cogent datum for a Norian age of the Kizil Lungur Conglomerate, as stated by Dainelli (1933), which according to Gergan & Pant (1983) should even be considered as Cretaceous (Qizil Lungar Conglomerate in their terminology).

After this Middle Jurassic clastic episode, the Shaksgam Sedimentary Belt was gradually involved in the deformation during the Late Jurassic. The Mid Cretaceous transgression, typical for the western part of the Qiangtang Microplate (Norin, 1946; Dainelli, 1933) is missing in Shaksgam, unless it is represented by the Urdok

Conglomerate.

Further east, a wide and thick fan of alluvial to deltaic red sandstones characterizes the Central Tibet (Leeder et al., 1988).

As indicated in the Fig. 4.21, I consider the Shaksgam Sedimentary Belt as the extension of the SE Pamir (Murgab-Aksyi Zone of Leven, 1967; Grunt & Dimitriev, 1973). The SE-Pamir carbonates can be followed on the satellite imagery in the Chinese territory and their very squeezed narrow belt may be observed on both sides of the Pirali custom point. Northwards, the carbonatic complex may be followed on the west side of the Tashkurgan Plain, with the northern boundary exactly corresponding to the spot where the Soviet Authors draw the Rushan-Pshart suture zone till their political boundary. To be noted that this correlation was already considered by Hayden (1915, p.310). This belt would be stirred and eventually crossed by the Karakorum Fault alignment, east of the Khunjerab pass. As a consequence of this interpretation, *the Karakorum Fault doesn' represent a microplate boundary between the Karakorum and Qiangtang microplates*. This boundary, if it exists, should lie eastwards of Shaksgam. The strong gravimetric anomaly changement along the northern contact of the Shaksgam Sedimentary Belt could suggest a possible position. This important density changement may be, however, also accounted with the late tectonic welding of different density rock-units.

4.4.2. *THE SUGHET GRANODIORITE.*

The Cretaceous calc-alkaline Sughet Graniodiorite is correlated with the Cretaceous-Paleocene granitoids occurring within the Misgar Zone in Hunza (Khunjerab/Gyraf granitoids) (Desio & Martina, 1972; Debon et al., 1987; Gaetani et al., 1990a), and in the Chinese territory, from the Khunjerab pass northeast for several kilometers, as well on both sides of Mintaka pass (Hayden, 1915). Along the Sarpo Laggo valley, the sedimentary envelope of this intrusion is cut-away by faults. However, both northwest on the satellite imagery, or southeast along the Gasherbrum glacier (Fig. 4.6), thick black slates appear. I consider these slates as correlated with the Misgar Slates of Hunza (Desio and Martina, 1972; Gaetani et al., 1990 a). This belt would continue in Wakhan, where they were named Sarikol Slates (Hayden, 1915), Khandut Slates (Desio et al., 1968) or Wakhan Fm. (Buchroitner 1979; 1980). Also there, the slates are typically intruded by granitoid bodies. In SE Pamir the black slate belt was also discussed by Norin (1976). If correlation of this belt towards northeast seems to be satisfying, we have no good evidence to trace a possible extension to the southeast.

4.4.3. *THE SARPO LAGGO-K^2 METAMORPHICS.*

Under this collective name we indicate (Gaetani et al.,this volume) several rock-units, including orthogneisses derived from Cretaceous granitoids. Some more specific correlations may be here suggested. The sedimentary belt of the Sost Unit (Gaetani et al., 1990a) can be traced from Sost to Shimshal and then in the upper reaches of the Skamri glacier. Their last outliers, with fusulinid-bearing limestones, are above the Sarpo Laggo-Skamri confluence (see also Desio, 1936). As already observed in Hunza (Gaetani et al., 1990a), metamorphism increases along strike, from northwest to southeast. No data are available for a possible southeast extension of the Guhjal Unit of Hunza. Tentatively we suggest that the andalusite-bearing slates cropping out on the west side of the upper Sarpo Laggo glacier (Sarpo Laggo Slates in Desio, 1980) should be correlated with the Pasu Slates (Desio, 1963; Desio & Martina, 1972) and the equivalent Shimshal Slates (Casnedi & Nicora, 1985). In the upper Baltoro reaches, the metamorphic grade seems to decrease and several stratigraphic units of Shaksgam have been recognized, intruded by granitoids,now gneissified, like the K^2 Gneiss (Desio & Zanettin, 1970; Searle et al., 1991). However, the succession - Shaksgam Formation, Urdok Conglomerate, Aghil Formation - is reported in Baltoro according to a different stratigraphic order with comparison to the type-area.

4.5. THE KARAKORUM FAULT

The following elements seem to characterize the Karakorum Fault Zone (KFZ) in the considered area (Figs. 4.2, 4.21, 4.22).

1) Several subparallel faults disrupt the Shaksgam Sedimentary Belt. However, the fault running from the Indira pass to the lower Sarpo Laggo valley and then along the lower Shaksgam valley is the more continuous and may be considered as the main aligment of the KFZ (for cross-sections see Figs. 4.5 and 4.7).

2) Unmetamorphosed sedimentary and magmatic rocks are located on both side of the fault zone.

3) The Shaksgam sediments are arranged in wide folds, crossed by a younger fault pattern aligned with main KF or forming a very small angle against it.

4) Vertical or steeply dipping faults, with cataclasites and no mylonites associated with metamorphic recrystallization are situated at the contacts.

5) The Permo-Mesozoic sediments of Shaksgam may be correlated with the SE Pamir sediments, thus the KF system cross the same palaeogeographic zone. Consequently, it seems not to coincide with a plate boundary.

6) Several Cretaceous granitoid bodies are cropping out around the Shaksgam valley, on both sides of the KFZ.

7) The lamprophyric dyke system (Pognante, this volume) is faulted along the KFZ. Their equivalent in Baltoro area are Neogene in age (Rex et al., 1988).

8) The gravimetric profiles 2, 3 and 4 (p. 61-62) might indicate a deepening of the Shaksgam Sediments slab below the main Karakorum Range, i.e. in the opposite sense supposed in recent reconstructions (i.e. Rex et al., 1988; Searle et al., 1989).

9) Zircon fission tracks (Cerveny et al., 1989; Carpena & Rutkiewicz, 1989) indicate a latest episode of very recent and rapid uplift in the last 5 MY in the magmatic bodies along the alignment K^2-Gasherbrum IV, which is parallel to the KFZ.

10) The main Karakorum range corresponds to a geoid anomaly (Marussi, 1964; Caporali et al., 1990; this volume), that could be interpreted as a bulge connected with the thrusting of the Main Karakorum range over the Shaksgam.

4.6. CONCLUSIONS

The little-known area north of the main Karakorum range is a very complex zone including a series of sedimentary, magmatic and metamorphic units stacked during the repeated and variously directed collisions between the different microplates existing between India and Eurasia. The previous discussion emphasizes several points.

1) Fairly good correlations may be drawn from the Hunza valley - Khunjerab pass to the Sarpo Laggo valley, including the Sughet Granodiorite and its black slates related sediments. Consequently this part belongs to the Karakorum plate.

2) The Shaksgam Sedimentary Belt during its evolution moves from a "Karakorum style" to a "Qiangtang style", with Middle Jurassic red sandstones. Its intermediate position could reflect an intermediate paleogeographic position between these two domains. But the lack of information east of the Karakorum trail/Lingzi Thang hampers more firm correlations in this direction. Instead, better correlations may be established with the SE Pamir of which the Shaksgam is here interpreted as the SE extension. If we consider the SE Pamir and N Karakorum as connected within a single plate during the Permo-Triassic, also the Shaksgam sediments should belong to this tectonic element. The wide black slate belt, in part surely Paleozoic in age (own unpublished data) (named as Sarikol, Wakhan, Khandut, or Misgar Slates), which is interposed between N Karakorum and SE Pamir, could be interpreted as deposited on a passive margin trough during an extensional

regime.

3) The Bazar Dara Slates and the red sandstones with anhydrites of the STS recall much more the rocks described in the Kun Lun and Qiangtang microplates. Consequently we would assign such affinity to our units.

4) Within the Shaksgam Sedimentary Belt and at the boundary with the Sughet Granodiorite, fault and cataclasites are frequent, forming the KFZ. It does not represent a single discon tinuity, but it should be rather considered a broad "cataclastic" stripe, several km wide. Thrusts or faults with vertical throw of 1 km or more have been observed. The most continuous alignment runs from the contact Sughet Gr./Shaksgam SB in the Sarpo Laggo to the Indira pass at the head of the Urdok glacier. As a whole (Figs. 4.21, 4.22), the KFZ represent the shear-zone between the Tibetan Plateau and the Karakorum-Pamir indenter.

5) The calc-alkaline granitoids of the northern Karakorum Belt form bodies elongated along the structural discontinuities trend NW-SE and which, except for the Sarpo Laggo-K^2 orthogneisses, do not show either pervasive internal deformations, or obvious intrusive relations, but only faulted contacts with the adjacent rocks. Uplift of the granitoids should have occurred in response to the active tectonism along the Karakorum Fault Zone. The existence of a very recent and rapid uplift connected with the KFZ activity is suggested by: a) the ubiquitous presence of tectonized and faulted contacts; b) the frequent faulting of the post-metamorphic porphyritic dykes; c) the zircon fission-track ages measured on the Gasherbrum Diorite and the K^2 Gneiss; d) the extremely high elevation (above 8000 m) of the K^2-Gasherbrum range; e) the geophysical anomalies measured during our expedition.

These observations indicate a multiphase deformation history of the Karakorum Fault Zone. Vertical faulting and dextral shearing were superimposed on the previous folding. Additionally, the existence of Neogene lamprophyres, trending more or less parallel to the KFZ, suggest that the KFZ transiently worked as an extensional fault system, triggering ascent and emplacement of the K-rich magma. A normal fault, parallel to the Karakorum Fault,was also suggested by Rex et al. (1988), Searle et al. (1989, 1990a), and by Parrish & Tirrul (1989) to explain the emplacement of the Baltoro granitoids. The KF is mostly known as a strike-slip fault system. This regime should have more effective to the south (Molnar & Tapponnier, 1975; Liu et al., 1990), whilst north of Karakorum its effects appear to be confined to smaller amplitudes of one or two orders of magnitude (i.e the Misgar Fault in Gaetani et al., 1990a). The present picture for the area here considered is that of a shear-zone, with a certain amount of transpression. After emplacement of the lamprophyric magma, the continuous compression of the Indian Plate should have (re)activated a transpres-

sional regime along this tectonic zone with recent uplift of the Main Karakorum Range and its thrusting over the rocks units of the Shaksgam valley.

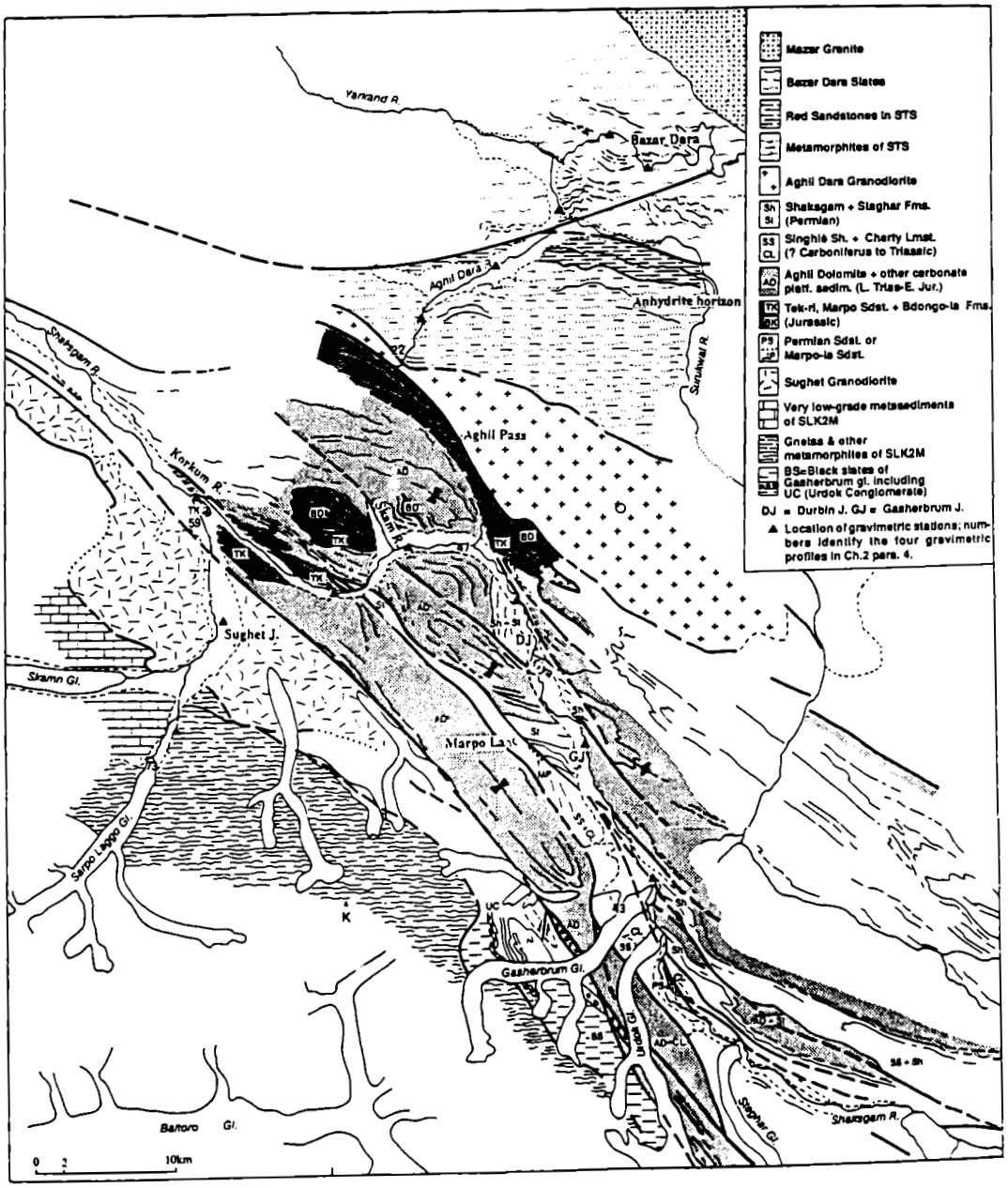

Fig. 4.22. Geological map of the studied area.

PLATES

Plate 1.

Fig. 1. Large fold with vertical axial plane in the Bazar Dara Slates. Right side of the Lower Surukwat, as seen from the confluence Surukwat-Aghil Dara. Height of the mountain slope more than 1500 m.

Fig. 2. Subvertical fault between the Bazar Dara Slates and the sandstones of the Surukwat Trust Sheets as seen from the lower Aghil Dara river. This fault seems to sinistral deplace the W Kun Lun Fault, which divide the Bazar Dara Slates from the Surukwat Thrust Sheets. On the very right, the Red Sandstone unit.

Plate 2.

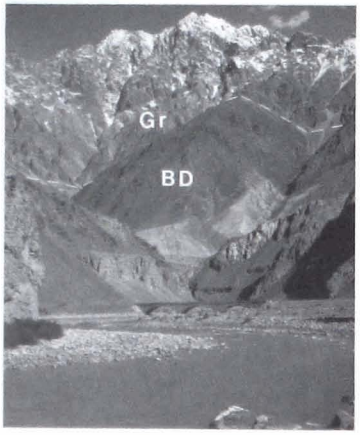

Fig. 1. A granitoid body in the Bazar Dara Slates, dominates the locality of Bazar Dara, which lies at the base of the whitish conoid at the center of the picture. Yarkand river.

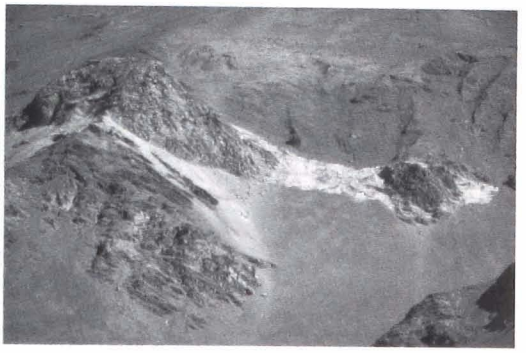

Fig. 2. Boudinaged body of grey dark mudstones and anhydrites within the red sandstones forming the basal sheet of the STS.

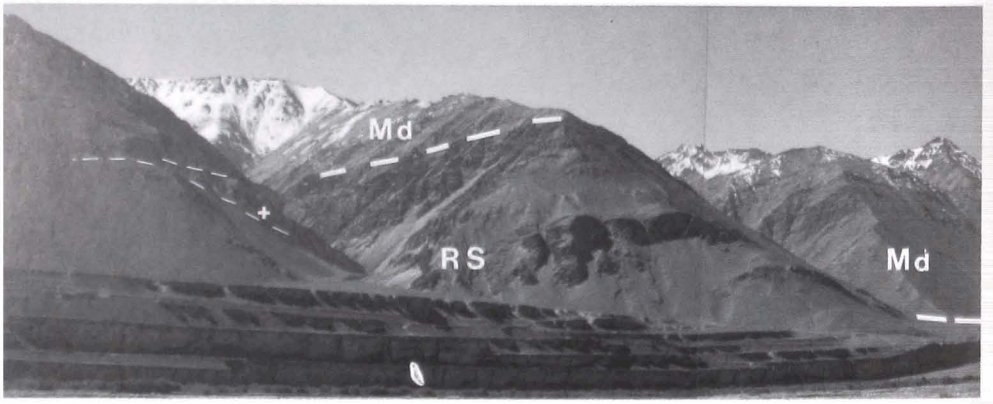

Fig. 3. Surukwat Thrust Sheets. The red sandstones with boudinaged anhydrites and limestones lenses are overthrusted by very low-grade metadiorites (MD). The sandstones show their coarser banks in the upper part of the sequence: consequently an overturning cannot be ruled out. The cross indicates the spot of Pl. 2, fig. 2. Right bank of the Aghil Dara.

Plate 3.

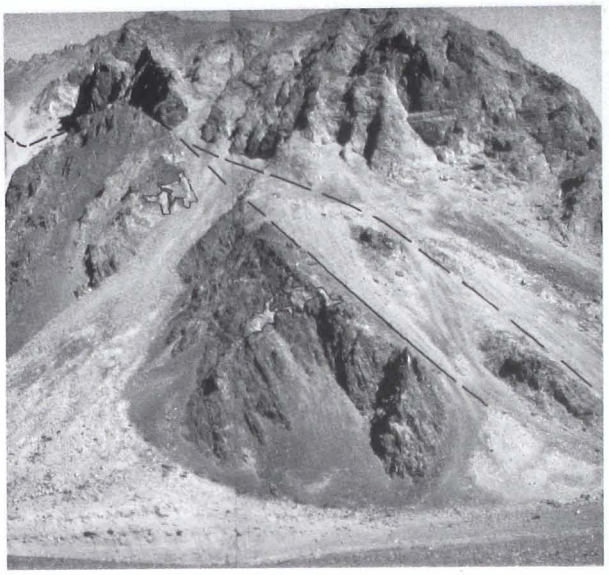

Fig. 1. Detail of the north contact of the Aghil Dara Granodiorite. The metamorphic dykes within the metapelites are not related to the intrusive body. Right bank of the Aghil Dara, before turning up to the Aghil pass.

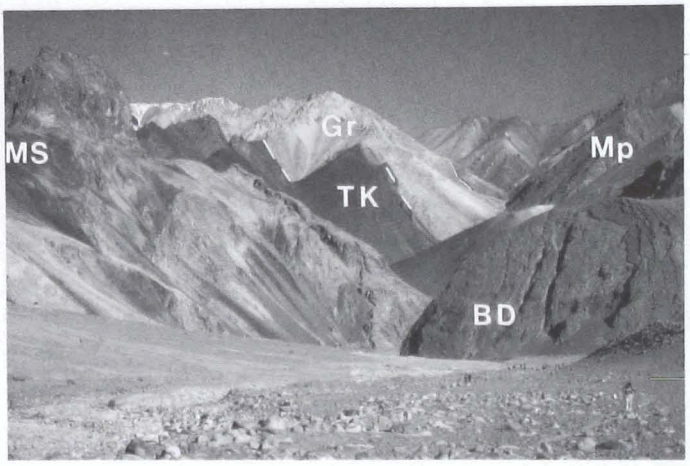

Fig. 2 . The sharp contacts between Shaksgam Sedimentary Belt, the Aghil Dara Granodiorite (Gr) and the metapelites of the STS (Mp), as seen from the trail ascending the Aghil pass. The sediments consist of repeated and stacked slices of Jurassic units (TK = Tek-ri Fm., MS = Marpo Sandstone; BD= Bdongo-la Fm.). Further north the metapelites (MP) of the STS.

Plate 4.

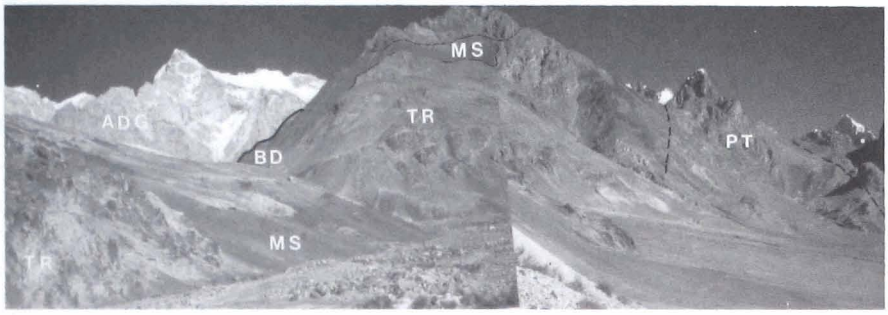

Fig. 1. Composite view of the northern part of the Shaksgam Sedimentary Belt, from the terrace at the foot of the Aghil pass. Compare with the 1937 drawing of Auden, reported in Desio (1980, fig. 16). The Aghil Dara Granodiorite is thrusted on the SSB, which shows large folds with axial planes of various inclination. Folds are cutted by a dense pattern of subvertical faults. ADD = Aghil Dara Granodiorite; BD = ? Bdongo-la Fm. (see only in distance); MP = Marpo Sandstone; TK = Tek-ri Fm.; AD = Aghil Dolomite; P = ? Permian units.

Fig. 2. Subhorizontal strike-slip fault within the Permian Sandstones, right bank of the Shaksgam river, just above the "Urdok Doors" locality .

Plate 5.

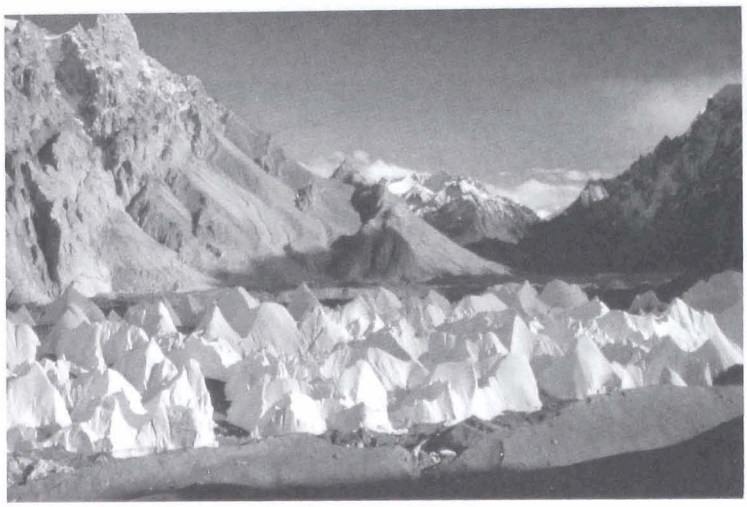

Fig. 1. The area of the Urdok Doors as seen from the Gasherbrum glacier. The Urdok Doors are two hillocks that tend to close the river Shaksgam (white cross) and consists of cherty limestones, mostly of Triassic age. The section Urdok Doors was measured on the right side of the valley.

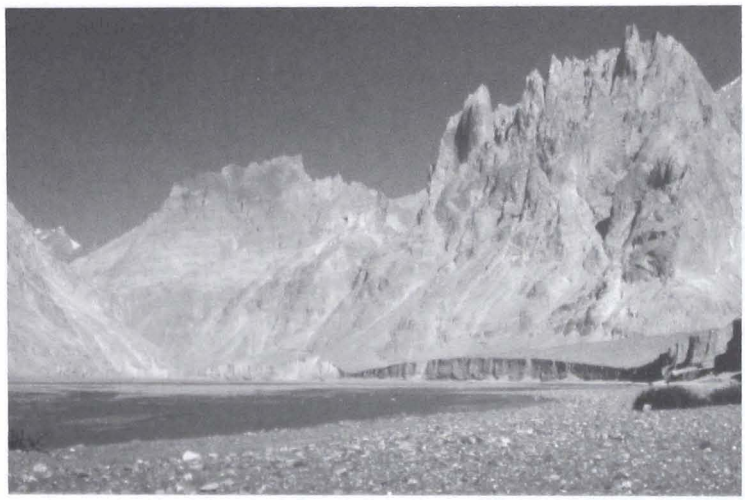

Fig. 2. The "Shaksgam Dolomites" from the Aghil pass valley (opening immediately on the right) and the Skam valley (hidden at the left). The lateral changes from massive yellow limestones on the right, to the well bedded grey limestone may be here appreciated.

Plate 6.

Fig. 1. Metadiorite with melanochratic enclave (Surukwat Thrust Sheets).

Fig. 2. Metaconglomerate (Surukwat Thrust Sheets).

Plate 7.

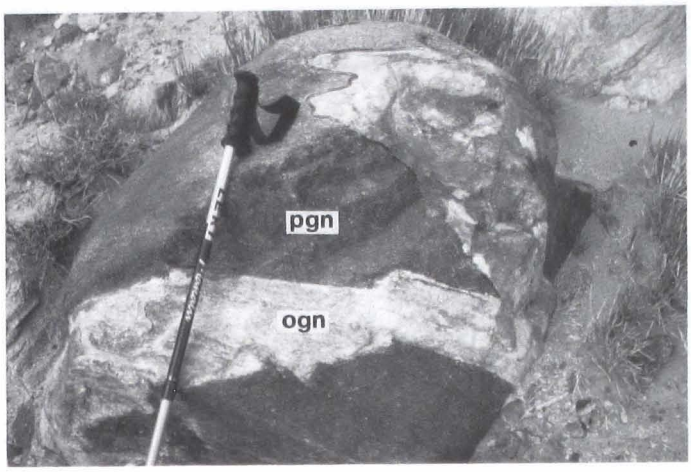

Fig. 1. Paragneiss (pgn) with transposed dyke of orthogneiss (ogn) (Sarpo Laggo-K² Metamorphic).

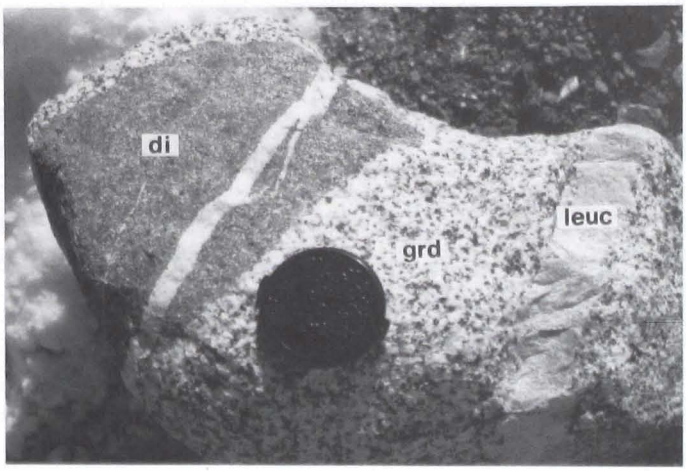

Fig. 2. Granodiorite (grd) with quarz diorite (di) enclave and crosscut by leucogranite (leuc) (Aghil Dara Granodiorite).

V. REFERENCES

ABETTI G., ALESSIO A., ANTILLI C., et al. (1925) - *Astronomia Geodetica, Geodesia e Topografia*. Spedizione Italiana De Filippi nell'Himalaya, Caracorum e Turkestan Cinese (1913-14). Serie 1 - "Geodesia e Geofisica" vol. 1; Zanichelli, Bologna.

ALLÈGRE C.J. and 34 Authors (1984) - *Structure and evolution of the Himalaya-Tibet orogenic belt*. "Nature", vol. 307, pp. 17-22, London.

AMBOLT N. - *Latitude and Longitude Determinations in Eastern Turkestan and Northern Tibet Derived from Astronomical Observations*. "Reports from the Scientific Expedition in the NW Provinces of China under the Leadership of Sven Hedin. The Sino-Swedish Expedition". Publication 6, II Geodesy I., Stockholm.

AUDEN J.B. (1938) - *Geological Results*. In: SHIPTON E. (Ed.), *The Shaksgam Expedition*, 1937, "Geogr. Journ.", vol. 91, pp. 335-336, London.

BALLY A.W, ALLEN C.R., GEYER R.B., et al. (1980) - *Notes on the Geology of Tibet and adjacent areas. Report of the American Plate Tectonics Delegation to the People's Republic of China*. "U.S. Geol. Surv.", Open File Rep., 80-501, 95 pp., Washington.

BANERJEE B., DAS GUPTA S.P. (1977) - *Short note: gravitational attraction of a rectangular parallelepiped*. "Geophysics", vol. 42, pp. 1053-1055, Tulsa.

BAUD A. (1989) - *The western end of the Tibetan Plateau*. In : SËNGOR A.M.C. (Ed.), "Tectonic Evolution of the Tethyan Region", pp. 505-506, Kluwer Ac. Publ., Amsterdam.

BAUERSIMA I. - *Navstar/Global Positioning System (GPS) III"*. "Mitteilungen der Satelliten Beobachtungsstation Zimmerwald n. 12", University of Berne.

BILHAM R., SIMSON D. (1980) - *Indo-Asian Convergence and the 1913 Survey Line Connecting the Indian and Russian Triangulation Surveys*. In: MILLER K.J. (Ed.), "Proc. of the International Conference held at Quaid-i-Azam University,

Islamabad, Pakistan". Vol. 1, pp. 160-170, Cambridge University Press.

BIRARDI G. (1976) - *The Establishment of a Net of Vertical Deflection Points in Italy by Means of a Photo-astronomical Procedure*. "Boll. di Geodesia Sc. Affini", vol. 35, pp. 113-152, Firenze.

BIRARDI G. (1977) - *Combined Use of Doppler and Photo-Astronomical Cameras for the Institution of Vertical Deflection Points*. "Boll. di Geodesia Sc. Affini", vol. 36, pp. 499-503, Firenze.

BOTT M. (1959) - *The use of electronic digital computers for the evaluation of gravimetric terrain corrections*. "Geophysical Prospecting", vol.7, pp.45-54, Leiden.

BOULIN J. (1981) - *Afghanistan structure, Greater India concept and eastern Tethys evolution*. "Tectonophysics", vol. 72, pp. 261-287, Amsterdam.

BOULIN J. (1990) - *Neocimmerian events in Central and Western Afghanistan*. "Tectonophysics", vol. 175, pp. 285-315, Amsterdam.

BROWN G.C. (1982) - *Calk-alkaline intrusive rocks: their diversity, evolution and relation to volcanic arcs*. In: THORPE R.S. (Ed.), "Andesites", pp. 437-461, John Wiley, New York.

BUCHROITHNER M.F. (1980) - *An outline of the geology of the Afghan Pamir*. "Tectonophysics", vol. 62, pp. 13-35, Amsterdam.

BUCHROITHNER M.F., HOLMER K. (1979) - *Notes on the Wakhan Formation of the Great Afghan Pamir and the Eastern Hindu Kush*. "Afghan Journ.", vol. 2, pp. 54-61, Kabul.

BURRARD S.G., HAYDEN H.H. (1933) - *A Sketch of the Geography and Geology of the Himalaya Mountains and Tibet*. Office of the Geodetic Branch, Survey of India, Dehra Dun.

CAPORALI A., CIRAOLO L. (1985) - *Metodi di Elaborazione dei Dati dei Satelliti GPS per Applicazioni Geodetiche*. "Boll. di Geodesia Sc. Affini", vol. 44, pp. 315-332, Firenze.

CAPORALI A., MARZARI F., PALMIERI F. (1990) - *Attività geodetica in Karakorum nell'ambito del progetto Ev-K²-CNR 1988*. "Boll. di Geodesia Sc. Affini", vol. 49, pp. 237-260, Firenze.

CARPENA J., RUTKIEWICZ W. (1989) - *Age traces de fission des apatites et des zircons du sommet du K² (8611 m)*. "Eclogae Geol. Helv.", vol. 82, n. 3, pp. 735-742, Basel.

CASNEDI R., NICORA A. (1985) - *Short notes on the Shimshal Valley geology (Western Karakorum-Pakistan)*. "Riv. Ital. Pal. Strat.", vol. 90 (1984), pp. 463-480, Milano.

CERVENY P.F., NAESER C. W., KELEMEN P.B., et al. (1989) - *Zircon fission-*

track ages from the Gasherbrum Diorite, Karakoram Range, northern Pakistan. "Geology", vol. 17, pp. 1044-1048, Boulder.

CHANG CHENFA et al. (1986) - *Preliminary conclusions of the Royal Society and Academia Sinica 1985 geotraverse of Tibet.* "Nature", vol. 323, pp. 501-507, London .

CHANG CHENFA, SHACKLETON R. M., DEWEY J.F., YIN JIXIANG (Eds.) (1988) - *The Geological Evolution of Tibet. Royal Society – Academia Sinica Geotraverse of the Qinghai-Xizang Plateau.* "Phil. Trans. R. Soc.", vol. A 327, 413 pp., London.

CHENG YUQI, DING SHENBAO, SHEN QIHAN, et al. (1986) - *Metamorphic Map of China 1:4.000.000, with explanatory Text*, Geol. Publ. House, Beijing.

CHEN JIANMING, CROMPTON T.D. et al. (1980) - *The Survey Work of the International Karakoram Project.* In: MILLER K.J. (Ed.), "Proc. of the International Conference held at Quaid-i-Azam University, Islamabad Pakistan." Vol. 1, pp. 124-139, Cambridge University Press.

CHINESE ACADEMY OF GEOLOGICAL SCIENCES (1975) - *Geological map of Asia (1:5,000,000).* Cartographic Publ. House, Beijing.

CHINESE ACADEMY OF GEOLOGICAL SCIENCES (1976) - *Geological Map of Asia (1:4,000,000).* Cartographic Publ. House, Beijing.

COLLOQUE KUNLUN-KARAKORUM 90 (1990) - Abstracts 54 pp., Inst. Physique Globe, Paris.

CROMPTON T.O. (1980) - *The Pakistan to Russia Triangulation Connection: Past and Projected Error Analyses.* In: MILLER K.J. Ed. " Proc. of The International Conference held at Quaid-i-Azam University, Islamabad Pakistan". Vol. 1, pp. 171-185, Cambridge University Press.

CUGIA M. (1936) - *Determinazioni astronomiche di posizione - Determinazioni di magnetismo terrestre.* Aimone d'Aosta, Duca di Spoleto e Prof. Ardito Desio: "La Spedizione Geografica Italiana al Karakoram". pp. III- XXIV. Arti Grafiche Bertarelli, Milano.

DAINELLI G. (1933) *La Serie dei terreni.* In: "Relazioni Scientifiche della Spedizione Italiana De Filippi nell'Himalaia, Caracorùm e Turchestàn Cinese (1913-1914)". II, vol. 2, pp. 458-542, Zanichelli, Bologna.

DEBON F., LE FORT P., DAUTEL D., et al. (1987) - *Granites of Western Karakorum and northern Kohistan (Pakistan): A composite Mid-Cretaceous to Upper Cenozoic magmatism.* "Lithos", vol. 20, pp. 19-40, Amsterdam.

DE CONCINI C., DE FLORENTIS N. (1983) - *Determinazione delle Coordinate Astronomiche dell'Osservatorio di Cima Ekar (Asiago).* "Mem. Acc. Patavina di Sc., Lett. Arti", vol. 95, pp. 175-187, Padova.

DE LA ROCHE H., LETERRIER J., GRANDCLAUDE P., MARCHAL M. (1980) - *A classification of volcanic and plutonic rocks using R1-R2-diagram and major element analysis. Its relationships with current nomenclature.* "Chem. Geol.", vol. 29, pp. 183-210, Amsterdam.

DESIO A. (1930a) - *Itinerari geologici percorsi durante la Spedizione Geografica Italiana nel Karakorum 1929. Appunti geologici e geografici.* "Boll. R. Soc. Geogr. It.", vol. 7, pp. 163-181, 277-300, Roma.

DESIO A. (1930b) - *Geological work of the Italian Expedition to the Karakorum.* "Geogr. Journ.", vol. 75, pp. 402-411, London.

DESIO A. (1936) - *La Spedizione Geografica Italiana nel Karakorum. Storia del Viaggio e Risultati Geografici.* 620 pp. (In coll. con Aimone di Savoia Aosta, Duca di Spoleto). Arti Grafiche Bertarelli, Milano.

DESIO A. (1963) - *Review of the geologic "Formations" of the Western Karakorum (Central Asia).* "Riv. Ital. Paleont. e Strat.", vol. 69, pp. 475-501, Milano.

DESIO A. (1977) - *The Works of Italians in the Scientific Exploration of the Karakorum Range (Central Asia).* Accad. Naz. Lincei, quad. n. 231, pp. 1-22, Roma.

DESIO A. (1979) - *Geologic Evolution of the Karakorum.* In: DE JONG K., SALAM A. (Eds.), "Geodynamic of Pakistan", pp. 111-124, Quetta.

DESIO A. (1980) - *Geology of the Upper Shaksgam Valley, North-East Karakorum, Xizang (Sinkiang).* "Ital. Exped. to the Karakorum (K^2) and Hindu Kush. Prof. A. Desio Leader. Scient. Reports." III, 4, 196 pp., Brill, Leiden.

DESIO A. (1983) - *A Geological Section across the Karakorum and Kashmir Himalaya and its relationship to the seismic profile Punjab-Pamir.* "Boll. Geof. Teor. Appl.", vol. 25, pp. 339-350, Trieste.

DESIO A. (1989) - *Which is the Highest Mountain in the World? Report of the Expedition Ev-K^2-CNR to the Mt. Everest and K^2.* "Mem. Accad. Naz. Lincei", s. 8, vol. 19, pp. 171-194, Roma.

DESIO A., GUJ P., PASQUARE G. (1968) - *Notes on the Geology of Wakhan (North-East Afghanistan).* "Mem. Accad. Naz. Lincei", s. 8, vol. 9, pp. 37-52, Roma.

DESIO A., MARTINA E. (1972) - *Geology of the Upper Hunza Valley, Karakorum, West Pakistan.* "Boll. Soc. Geol. Ital.", vol. 91, pp. 283-314, Roma.

DESIO A., ZANETTIN B. (1970) - *Geology of the Baltoro Basin.* "Ital. Exped. to the Karakorum (K^2) and Hindu Kush. Prof. A. Desio Leader. Scient. Reports." III, 2, 308 pp., Brill, Leiden.

DE TERRA H. (1932) - *Geologische Forschungen im Westlichen K'un-Lun und Karakorum-Himalaya.* 196 pp., Reimer & Vohsen, Berlin.

DOBRIN M.B. (1976) - *Introduction to geophysical prospecting.* McGraw-Hill.

New York.

DRONOV V.I., GAZDIZCKI A., MELNIKOVA G.K. (1982) - *Die triadische Riffe in südöstlicher Pamir.* "Facies", vol. 6, pp. 107-128, Erlangen.

EBBLIN C. (1982) - *Gravity profile along the middle Indus valley, northern Pakistan.* "Boll. Geof. Teor. Appl.", vol. 93, pp. 39-55, Trieste.

EBBLIN C., MARUSSI A., PORETTI G. et al. (1983) - *Gravity measurements in the Karakorum.* "Boll. Geof. Teor. Appl.", vol. 94, pp. 303-316, Trieste.

FANTINI SESTINI N. (1965a) - *Permian Fossils of the Shaksgam Valley.* "Ital. Exped. to the Karakorum (K^2) and Hindu Kush. Prof. A. Desio Leader. Scient. Reports." IV, vol. 1, pp. 149-215, Brill, Leiden.

FANTINI SESTINI N. (1965b) - *Corals from the Upper Jurassic of the Shaksgam Valley.* Ibidem, IV, 1, pp. 219-227, Brill, Leiden.

FLÜGEL H.W. (1990) - *Rugosa aus dem Perm des N-Karakorum und der Aghil-Kette.* "Geol. Paläont. Mitt. Innsbruck", vol. 17, pp. 101-117, Innsbruck.

GAETANI M., GARZANTI E., JADOUL F., et al. (1990a) - *The North Karakorum side of the Central Asia geopuzzle.* "Bull. Geol. Soc. America", vol. 102, pp. 54-62, Boulder.

GAETANI M., GOSSO G., POGNANTE U. (1990b) - *A geological transect from Kun Lun to Karakorum (Sinkiang China): the western termination of the Tibetan Plateau. Preliminary note.* "Terra Nova", vol. 2, pp. 23-30, Oxford.

GANSSER A. (1979) - *Ophiolitic belts of the Himalayan and Tibetan region.* "Geol. Soc. Amer.", Map Ser., MC-33, pp. 12-15, Boulder.

GEOLOGICAL MAP OF TIBET (1980) - 4 sheets at the scale 1,500,000, Chendu.

GERGAN J.T., PANT P.C. (1983) - *Geology and stratigraphy of Eastern Karakoram, Ladakh.* In: THAKUR V.C. & SHARMA (Eds.) - "Geology of Indus Suture Zone of Ladakh", pp. 99-106, Dehra Dun.

GIRARDEAU J., MARCOUX J., ALLEGRE C.J., et al. (1984) - *Tectonic environment and geodynamic significance of the Neo-Cimmerian Donqiao ophiolite, Bangong-Nujiang suture zone, Tibet.* "Nature", vol. 307, pp. 27-31, London.

GODWIN AUSTEN H.H. (1864) - *Geological Notes on part of the North-Western Himalayas; with Notes on the fossil by Messrs. T. Davidson, R. Etheridge and S. P. Woodward.* "Quart. Journ. Geol. Soc.", vol. XX, pt. I., pp. 383-388, London.

GRANT F.S., WEST G.F. (1985) - *Interpretation theory in applied geophysics.* McGraw-Hill. New York.

GRUNT T.A., DIMITRIEV V. J. (1973) - *Permian Brachiopoda of the Pamir.* Ak. Nauk SSSR, Tr. Pal. Inst., vol. 136, 176 pp., Moskva, (in Russian).

GULATEE B.L. (1954) - *The Height of Mount Everest. A New Determination*

(1952-54). Survey of India, "Technical Paper" n. 8, Dehra Dun.

GULATEE B.L. (1955) - *Deviation of the Vertical in India*. Survey of India, "Techn. Paper" n. 9, Dehra Dun.

HARRIS N.B.W., XU RONGHYA, LEWIS C.L.,CHENGWEI J. (1988) - *Plutonic rocks of the 1985 Tibet Geotraverse, Lhasa to Golmud*. "Phil. Trans. R. Soc.", vol. A327, pp. 145-168, London.

HAYDEN H.H. (1915) - *Notes on the geology of Chitral, Gilgit and the Pamirs*. "Rec. Geol. Surv. India", vol. 45, pp. 271-326, Calcutta.

HEISKANEN V.A., MORITZ H. (1967) - *Physical geodesy*. W.H. Freeman, San Francisco.

HUANG J., CHEN B. (1987) - *The Evolution of the Tethys in China and adjacent regions*. Geol. Publ. House, Beijing.

KERTZ W. (1969) - *Einführung in die Geophysik*. Bibliograph Institut, Bd. 275, Mannheim.

KING R.W., MASTER E.G., et al. (1985) - *Surveying with GPS*. Monograph n. 9, School of Surveying. University of New South Wales.

KOBOLD F., HUNZIKER E. (1962) - *Communication sur la courboure de la verticale*. "Bull. Géod.", vol. 65, pp. 265-267, Paris.

LEAKE B.E. (1978) - *Nomenclature of amphiboles*. "Am. Mineral.", vol. 63, pp. 1023-1052, Ann Harbour.

LEEDER M.R., SMITH A.B., YIN JIXIANG (1988) - *Sedimentology, palaeoecology and palaeoenvironmental evolution of the 1985 Lhasa to Golmud Geotraverse*. "Trans. R. Soc.", vol. A 327, pp. 10-143, London.

LE FORT P. (1988) - *Granites in the tectonic evolution of the Himalaya, Karakoram and southern Tibet*. "Phil. Trans. R. Soc.", vol. A 326, pp. 281-299, London.

LE FORT P., MICHARD A., SONET J., ZIMMERMANN J.L. (1983) - *Petrography, geochemistry and geochronology of some samples from the Karakorum axial batholith (Northern Pakistan)*. In: SHAMS F.A. (Ed.) - "Granites of Himalayas, Karakorum and Hindu Kush", pp. 377-387, Institute of Geology, Punjab Univ., Lahore.

LEVEN E.Y. (1967) - *Stratigraphy and Fusulinids of the Pamirs Permian deposits*. "Acad. Nauk SSSR, Tr. Geol. Inst.", vol. 167, 223 pp., Moskva.

LIU Q., AVOUAC J.P., TAPPONNIER P. (1990) - *Holocene movements along the Karakorum Fault*. "Colloque Kunlun - Karakorum 90", pp. 32-33, Paris.

LONGMAN I.M. (1959) - *Formulas for computing thetidal accelerations due to the sun and moon*. "Journal Geophysical Research.", vol. 64, pp. 2351-2355,

Washington.

MARSH J.G., LERCH F.J., PUTNEY B.H., et al. (1988) - *An Improved Model of the Earth's Gravitational Field.* GEM T1, NASA TM 4019, Washington.

MARSON I., FALLER J.E. (1986) - *g-the acceleration of gravity measurement and its importance.* J. Phsys. E: Sci. Instrum., pp. 22-32.

MARUSSI A. (1964) - *Geophysics of the Karakorum.* "Ital. Exped. to the Karakorum (K^2) and Hindu Kush. Prof. A. Desio Leader. Scient. Reports." II, 242 pp., Brill, Leiden.

MARUSSI A. (1983) - *The Pakistani Italian Karakorum Geophysical Project in the Frame of the Pamirs-Himalaya International Project.* "Boll. Geof. Teor. Appl."; vol. 25, pp. 137-142, Trieste.

MATTE PH., TAPPONNIER P., BOURJOT L., et al. (1990a) - *A section through the Paleozoic Kunlun Belt, north of the Altyn Tagh Fault (Western Tibet).* "Colloque Kunlun-Karakorum 90", p. 38, Paris.

MATTE PH., BOURJOT L., TAPPONNIER P., et al. (1990b) - *Tectonics of Western Tibet between the Tarim Craton and the Karakorum Fault.* "Colloque Kunlun-Karakorum 90", pp. 42-43, Paris.

MELCHIOR P. (1978) - *The tides of the planet Earth.* Pergamon Press, Oxford.

MIRONOV V.S. (1977) - *Curso de prospección gravimétrica.* Ed. Reverté. Barcelona.

MOLNAR P., TAPPONNIER P. (1975) - *Cenozoic Tectonics of Asia: Effects of a Continental Collision.* "Science", vol. 189, pp. 419-426, Washington.

MONTENAT C., GIRARDEAU J., MARCOUX J. (1986) - *La ceinture ophiolitique Néo-cimmerienne au Tibet, dans les Pamirs et en Afghanistan. Evolution Géodinamique comparative.* "Sc. Terre, Mem.", vol. 47, pp. 229-252, Nancy.

MORELLI C. (1968) - *Gravimetria.* Del Bianco, Udine.

MORELLI C. et al. (1974) - *The International Gravity Standardization Net.* I.U.G.G.-I.A.G. Pubbl. Spec. n. 4, Paris.

MORITZ A. (1980) - *Geodetic reference system 1980.* The Geodesist's Handbook. I.U.G.G.-I.A.G., pp. 395-371, Paris.

MULLER R.F., SAXENA S.K. (1977) - *Chemical petrology.* Springer Verlag, Berlin.

NAGY D. (1966) - *The gravitational attraction of a right rectangular prism.* "Geophysic", vol. 31, pp. 362-371, Tulsa.

NAGY D. (1966) - *The prism method for terrain correction using digital computers.* "Pure & appl. Geoph.", pp. 31-39, Basel.

NEGGLETON L.L. (1976) - *Gravity and magnetics in oil prospecting.* McGraw-

Hill. New York.

NORIN E. (1946) - *Geological Exploration in Western Tibet.* "Rep. Sc. Exp. Sven Hedin", vol. 29, III, Geology-7, 214 pp., Stockholm.

NORIN E. (1976) - *The "Black Slates" Formations in the Pamirs, Karakoram and Western Tibet.*, In: "Intern. Coll. on the Geotectonics of the Kashmir Himalaya etc., Accad. Naz. Lincei", vol. 21, pp. 245-264, Roma.

PAN Y., WANG Y. (1990) - *Tectonic framework of the geotraverse from Yecheng to Siquanhe.* "Colloque Kunlun-Karakorum 90", pp. 40-41, Paris.

PARRISH R.R., TIRRUL R. (1989) - *U-Pb age of the Baltoro granite, northwest Himalaya, and implications for monazite U-Pb systematics.* "Geology", vol. 17, pp. 1076-1079, Boulder.

PEARCE J. A. (1982) - *Trace element characteristics of lavas from destructive plate boundaries.* In: THORPE R.S. (Ed.) - Andesites. pp. 525-548, John Wiley, New York.

PEARCE J.A., HARRIS N.B.W., TINDLE A.G. (1984) - *Trace element discrimination diagrams for the tectonic interpretation of granitic rocks.* "J. Petrol.", vol. 25, pp. 956-983, Oxford.

PEARCE J.A., HOUJUN M. (1988) - *Volcanic rocks of the 1985 Tibet Geotraverse: Lhasa to Golmud.* "Phil. Trans. R. Soc.", vol. A327, pp. 169-201, London.

PECCERILLO A., TAYLOR S.R - *Geochemistry of Eocene calcalkaline rocks from the Kastaniony area, Northern Turkey.* "Contrib. Mineral. Petrol.", vol. 58, pp. 63-81, Berlin.

PERCHUCK B.D., ARANOVICH B.Y. (1980) - *The thermodynamic regime of metamorphism in the ancient subduction zones.* "Contrib. Miner. Petrol.", vol. 75, pp. 407-414, Berlin.

PERICOLI A. (1973) - *Applicazioni Topografiche.* "Studio e Impianto di Ponti Radio. Collezione Testi Tecnici". Istituto Geografico Militare, Firenze.

POGNANTE U. (1990) - *High-K calc-alcaline, shoshonitic and ultrapotassic post-collisional dykes from Northern Karakorum (Sinkiang, China).* "Geol. Magaz." (in press), Cambridge.

RADHAKRISHNA MURTHY I.V., RAMA RAO P. (1986) - *Some new empirical relations in isostatic studies.* "Boll. Geof. Teor. Appl.", vol. 97, pp. 111-112, 241-249, Trieste.

RAPP R.H. (1979) - *Global Anomaly and Undulation Recovery Using GEOS 3 Altimetry data.* Ohio State University - Report n. 285, Columbus, Ohio.

REX A.J., SEARLE M.P., TIRRUL R., et al. (1988) - *The geochemical and tectonic*

evolution of the central Karakoram, North Pakistan. "Phil. Trans. Royal Soc.", vol. A 326, pp. 229-255, London.

RUZHENTSEV S.V., SHVOLMAN V.A. (1981) - *Tectonics and structure of Pamir metamorphics.* In: SAKLANI P.S. (Ed.), Metamorphic tectonites of the Himalaya. "Hind. Publ. Corp.", pp. 27-41, Delhi.

SAZHINA N., GRUSHINSKY N. (1971) - *Gravity prospecting.* Mir publishers. Moscow.

SCHLAGINTWEIT (von) H.A. and R. (1861) - *Astronomische Ortbestimmungen und Magnetische Beobachtungen in Indien und Hochasien.* "Zeitsch, Allgem. Erdkunde", Berlin.

SCHOMBERG R.C.F. (1947) - *North Karakoram. A Journey in the Muztagh-Shaksgam Area.* "Geogr. Journ.", vol. 109, pp. 94-98, London.

SEARLE M.P., REX A.J., TIRRUL R., et al. (1989) - *Metamorphic, magmatic, and tectonic evolution of the Central Karakoram in the Biafo-Baltoro-Hushe regions of Northern Pakistan.* "Geol. Soc. America - Sp. Pap.", vol. 232, pp. 47-73, Boulder.

SEARLE M., PARRISH R.R., TIRRUL R., REX D.C. (1990) - *Age of crystallization and cooling of the K^2 gneiss in the Baltoro Karakoram.* "J. Geol. Soc.", vol. 147, pp. 603-606, London.

SEARLE M. & TIRRUL R. (1991) - *Structural and thermal evolution of the Karakoram crust.* "J. Geol. Soc.", vol. 148, pp. 65-82, London.

SHERIFF R.E. (1978) - *A first course in geophysical exploration and interpretation.* IHRDC. Boston.

SHIPTON E. (1938) - *The Shaksgham Expedition.* "Geogr. Journ.", vol. 91, pp. 313- 319, London.

SHIPTON E. (1985) - *Blank on the Map.* Reprinted in: The Six Mountains Travel Books. Diadem, London.

SRIMAL N. (1986) - *India-Asia collision: Implications from the Geology of the Eastern Karakoram.* "Geology", vol. 14, pp. 523-527, London.

SUN TE (1984) - *Late Carboniferous - Early Permian strata and fauna in north Ali District, Xizang (Tibet), China.* "Wuhan College J. Geology", vol. 19, London, Beijng.

SURVEY OF INDIA (1922) - *Triangulation of India and Adjacent Countries (Data complete to 1921).* Sheet 52.A. Office of the Trigonometrical Survey, Dehra Dun.

TELFORD W.M., GELDART L.P., SHERIFF R.E., KEYS D.A. (1976) - *Applied Geophysics.* Cambridge University Press.

TERMIER G., TERMIER H., DE LAPPARENT A.F., MARIN PH. (1974) - *Monographie du Permo-Carbonifère de Wardak (Afghanistan Central).* "Doc. Lab.

Géol. Fac. Sc. Lyon", H.S. 2, 167 pp., Lyon.

TOMELLERI V. (1960) - *Procedimento d'Elaborazionee dei Dati di Osservazione nel Metodo delle Altezze Uguali.* "Boll. Geodesia Sc. Affini", vol. 19, pp. 439-463, Firenze.

TORGE W. (1980) - *Geodesy.* Walter de Gruiter ed., Berlin-New York.

TSUBOI C. (1983) - *Gravity.* Allen & Umwin, London.

VANICEK P., KRAKIVSKI E. (1986) - *Geodesy. The concepts.* Amsterdam.

VENTURELLI G., THORPE R.S., DAL PIAZ G.V., et al. (1984) - *Petrogenesis of calc-alkaline, shoshonitic and associated ultrapotassic Oligocene volcanic rocks from the North-western Alps.* "Contrib. Min. Petrol.", vol. 86, pp. 209-220, Berlin.

WALLERSTEIN G. (1987) - The Possible Height of K^2. "American Alpine Journal", vol. 29, pp. 133-135.

WELLS D. (1986) - *Positioning with GPS.* Canadian GPS Associates.

WINKLER H.G.F. (1974) - *Petrogenesis of the metamorphic rocks.* 320 pp. Springer Verlag, Berlin.

WOOLLARD G.P. (1969) - *Regional variations in gravity.* In: The earth's crust and upper mantle. "Am. Geophys. Monogr.", 13, pp. 320-341,

WYSS R.(1940) - *Geologie. Mit Beitraegen von Dr. Carl Renz und Dr. Manfred Reichel.* In: "Wissensch. Ergebn. Niederl. Exped. Karakorum und angr. Geb.", Jhr. 1922, 1925, 1929/30, & 1935, III, Brill, Leiden.

YANG ZUNYI, CHENG YUQI, WANG HONGZHEN (1986) - *The Geology of China.* "Oxford Mon. Geol. Geoph.", vol. 3, 303 pp., Oxford.

INDEX

C

D

E

F

G

H

I

J

K

L

M

N

O

P

Q

R

S

T

U

V

W

X

Y

Z

Composto e stampato
dalla UPSEL s.a.s.
via P. d'Abano 1/a
tel-fax 049/8753090
35100 Padova
— Dicembre 1991 —